2013 | School voor Levenswetenschappen

DOCTORAATSPROEFSCHRIFT

The maternal venous system: the ugly duckling of obstetrics

Proefschrift voorgelegd tot het behalen van de graad van doctor in de biomedische wetenschappen te verdedigen door:

Kathleen Tomsin

Promotor: prof. dr. Wilfried Gyselaers
Copromotor: prof. dr. Louis L.H. Peeters

D/2013/2451/16

Maastricht University | universiteit hasselt KNOWLEDGE IN ACTION

The maternal venous system:

the ugly duckling of obstetrics

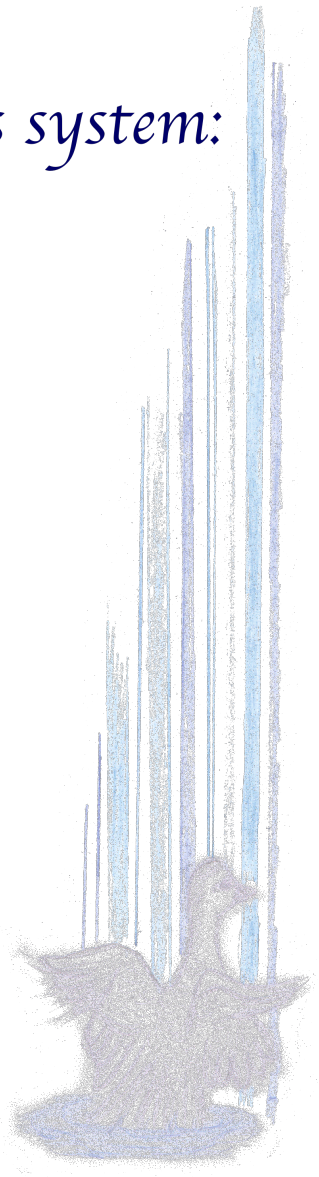

Kathleen TOMSIN

Promotor

W. GYSELAERS, MD PhD

Co-promotor

L.L.H. PEETERS, MD PhD

Jury

I. LAMBRICHTS, DDS PhD (Hasselt University)
E. VAN KERKHOVE, MSc PhD (Hasselt University)
V. SOMERS, MSc PhD (Hasselt University)
E. DE JONGE, MD PhD (Ziekenhuis Oost-Limburg, Genk)
J. NIJHUIS, MD PhD (Maastricht University Medical Center)
C. LEES, MD MRCOG (Cambridge University Hospitals)
O. MOREL, MD PhD (Maternité Régionale Universitaire de Nancy)

Proefschrift voorgelegd tot het behalen van de graad van
Doctor in de Biomedische Wetenschappen

Met dank aan het Bijzonder Onderzoeksfonds van de Universiteit Hasselt en
de Maatschap Verloskunde en Gynaecologie van het Ziekenhuis Oost-Limburg

"I never dreamed of such happiness as this,
while I was an ugly duckling."

The Ugly Duckling *by* Hans Christian Andersen (*1844*)

Voor mama en papa

Contents

Samenvatting

Zowel de maternale vasculaire tonus als de hartfunctie tijdens zwangerschap worden beschouwd als cruciale factoren in de uitkomst van zowel moeder als kind. In dit complex verhaal van maternale hemodynamiek, hetgeen intens beschreven wordt in de huidige wetenschappelijke literatuur, wordt de rol van de maternale venen desalniettemin sterk onderschat.

Tijdens deze thesis ontwikkelden en evalueerden wij een set van meetbare, objectieve parameters die een indicatie zijn voor veneuze functie, namelijk de veneuze impedantie index en de transitietijd van de veneuze pols. Deze parameters blijken onderhevig te zijn aan veranderingen geïnduceerd doorheen de normale zwangerschap en in preeclampsie, hetgeen ons in staat stelt deze te gebruiken in zwangerschapsgerelateerde hemodynamische studies. Uit onze studies besluiten wij dat het veneuze systeem een cruciale rol speelt in het hartminuutvolume, dewelke geschat kan worden door impedantie cardiografie. De introductie van deze niet-invasieve technieken in de verloskunde stelt ons in staat een maternaal cardiovasculair profiel op te stellen die zowel slagaders als aders beschrijft, alsook de maternale hartfunctie.

Het bestuderen van deze cascade aan cardiovasculaire veranderingen doorheen de zwangerschap gebruikmakende van zulke niet-invasieve, gemakkelijk toepasbare en zeer toegankelijke methodes geeft ons de mogelijkheid dit maternaal cardiovasculair profiel toe te passen in meerdere klinische omstandigheden. Het vroege opsporen van laag en hoog risico patiënten, samen met de onderverdeling van de verschillende zwangerschapsaandoeningen, zal ons gidsen in de klinische aanpak van onze zwangere populatie voor zowel preventie als behandeling en opvolging.

Deze thesis illustreert dat het veneuze systeem, zijnde “het lelijke eendje” van de verloskunde genegeerd door de medische wereld, verandert en transformeert tot een mooie zwaan, aanvaard door de verloskundige wereld. We hopen dat de lezer van deze thesis zo overtuigd is als zijn auteur, en dat dit het begin mag zijn van vele studies omtrent het maternale veneuze systeem - een belangrijk puzzelstukje van de zwangerschapsfysiologie.

Abstract

In pregnancy, both maternal vascular tone and cardiac function are considered key players to reach a normal outcome for both mother and child. This complex story of maternal hemodynamics is intensely discussed in current scientific literature, however the role of the maternal veins has been strongly underestimated.

During this thesis, we developed and evaluated a set of measurable objective parameters which give an indication of venous function, i.e. the venous impedance index and the venous pulse transit time. These parameters turned out to be subject to changes throughout normal pregnancy and in preeclampsia enabling their use in gestational hemodynamic studies. From our studies, we concluded that the venous system is a crucial determinant of cardiac output, which can be estimated by impedance cardiography. The introduction of these non-invasive techniques in obstetrics enabled us to create a maternal cardiovascular profile, integrating both arteries and veins, as well as maternal cardiac function.

Studying the cascade of cardiovascular changes throughout pregnancy using such non-invasive, easily applicable, and highly accessible methods gives us the opportunity to apply this maternal cardiovascular profile in several clinical settings. The early discrimination between low and high risk patients, together with the classification of different pregnancy disorders will help us guide the clinical work-up of our pregnant population regarding both prevention and treatment, as well as follow-up.

This thesis illustrates that the venous system, being an "ugly duckling" at first neglected by the medical world, transforms and matures into a beautiful swan, accepted by the obstetric world. We hope that the reader of this thesis is as confident as its author that this is the beginning of many other studies regarding the maternal venous system, an important piece of the gestational physiology puzzle.

Chapter 1

General introduction

Most of you will associate the beginning of life to the birth of a child. However, we are not created in seven days (cfr. Genesis, the Holy Bible)! Most of our fundamental mechanisms are developed during the 40 weeks (or 9 months) of pregnancy, and the intra-uterine environment and the maternal body both have a great influence on this development.

The cardiovascular system of a pregnant woman undergoes a series of profound changes (Chapter 1.1), and a single derangement in this adaptation process can lead to maternal or fetal disease. Studying this cascade of events is necessary to understand the physiology of normal and pathological pregnancies. Therefore, the use of non-invasive, easily applicable, and highly accessible methods for cardiovascular profiling in obstetrics has become increasingly important. Studies at our Department of Obstetrics and Gynecology (Ziekenhuis Oost-Limburg, Genk, Belgium (ZOL)) are

mainly focussed on the maternal venous system (Chapters 1.1.1 and 2). In this thesis, the use of two-dimensional (2D) Doppler ultrasonography in the study of venous tone is discussed (Chapters 2.2, 2.3, 2.4, and 2.5). Furthermore, the opportunity of three-dimensional (3D) Doppler ultrasonography in this research field will be briefly introduced (Chapter 2.6). Finally, the application of impedance cardiography (ICG) (Chapters 3.1, 3.2, and 3.3) is explored to enable global maternal cardiovascular profiling (Chapters 4.1, 4.2 and 4.3), including heart, arteries, and veins.

Maternal vascular tone [1, 2, 3] and cardiac function [4, 5, 6, 7, 8, 9] are key players in both fetal growth (e.g. fetal growth restriction (FGR) or intra-uterine growth retardation (IUGR)) and the development of hypertensive pregnancy disorders such as preeclampsia (PE) (Chapter 1.2) or the HELLP syndrome (Hemolysis Elevated Liver enzymes and Low Platelets). Up till now, the maternal veins, as part of the vascular system, are thought to be merely connected to the heart and arteries, and thus are considered to play a passive role in many cardiovascular diseases. In this thesis, however, we present observational evidence that venous dysfunction actively contributes to the clinical presentation of PE (Chapters 2.1 and 2.7). To date, we can conclude that this role of venous physiology in pregnancy has been strongly underestimated.

This thesis illustrates that the venous system transforms and matures from its own "ugliness" into a beautiful swan, accepted by the obstetric world (Chapter 5). We hypothesize that including venous characteristics into the global maternal cardiovascular profile may be essential to define a risk profile for several pregnancy disorders and will help guiding the clinical work-up of this high-risk population.

1.1 Pregnancy

Maternal physiological changes during normal human pregnancy facilitate the increased metabolic needs of both the mother and growing fetus. The main focus of this thesis is situated on the important changes at the level of the maternal cardiovascular system, more specifically the role of the maternal venous system in pregnancy.

Pregnancy is characterized by a decrease in *peripheral vascular resistance*, which is likely to be one of the first cardiovascular adaptation mechanisms during early gestation [1, 2]. The uteroplacental circulation secretes numerous vasoactive substances that tip the *balance* from vasoconstriction to vasodilation [2, 10, 11], e.g. prostacyclin. This balance, however, is not the sole explanation of the systemic decrease in tonicity during pregnancy [2]. The role of many pregnancy hormones, such as progesterone and estrogen, is also studied extensively [12, 13]. But the most important mediators of vasodilation are the endothelium-derived relaxing factors such as nitric oxide (NO) [2, 13, 14].

Thus, a crucial role in the decrease of this tonicity is played by the endothelium [2]. Especially the integrity of this inner layer is important in the normal gestational adaptation of vascular tone throughout the maternal circulatory system [2, 14].

The fall in systemic vascular tone affects both the arteries and the veins [13]. At the arterial level, this drop induces a decrease in afterload and a decrease of both pre- and postglomerular arteriolar resistance. Therefore, renal blood flow and glomerular filtration rate (GFR) are increased. On top of this, the simultaneous fall in venous tone increases the venous compliance which resets the renine-angiotensin and the osmoregulatory systems, and therefore facilitates volume retention [2, 13, 14]. Baroreceptor resetting and an attenuated response to the pressor effects of angiotensin II also allows for a volume expansion [2, 14, 15].

The increase in preload, due to the plasma volume expansion, induces a reversible remodeling of the maternal heart, i.e. left ventricular eccentric hypertrophy, together with a well-preserved left ventricular systolic function. The latter probably results from enhanced active relaxation of the left ventricle at the start of diastole, most likely due to hormonal influences [9, 16].

When a single derangement occurs in these processes and/or in the maintenance of this specific vascular tonicity, the balance is disturbed [2] and this can lead to maternal

cardiovascular maladaptation, as is seen in pregnancy disorders such as preeclampsia (Chapter 1.2).

1.1.1 The maternal venous system in normal pregnancy

As extensively discussed in Chapter 2, the maternal venous system changes dramatically throughout pregnancy. Venous distensibility is enhanced due to increases in both compliance and diameter [17]. This allows for the augmentation of both venous capacitance and unstressed volume [18]. Together with the observed plasma volume expansion [2, 13, 14, 15], these changes provide a larger buffer to control cardiac output (CO); changes in venular tone will have a much larger impact on venous return in pregnancy than in the non-pregnant state. Therefore, the pregnancy-induced changes in the venous bed ameliorate its ability to regulate CO, which is particularly of value in the third trimester, when the impact of fluctuations in the uteroplacental circulation on the maternal cardiovascular function is greatest [19, 20].

1.2 Preeclampsia

Preeclampsia (PE) is defined as a pregnancy-induced hypertension $\geq 140/90$ mmHg observed on at least two occasions $\geq$ six hours apart, combined with *de novo* proteinuria of > 300 mg/24h [21, 22], however, its pathophysiology is still unknown. This pregnancy disorder affects 7 to 10% of all pregnancies and is characterized by a significant morbidity and mortality for both mother and child [23]. PE can be associated with IUGR (birth weight percentile of ≤ 10), a normal fetal growth, as well as with the birth of macrosomic infants ($\geq 90^{th}$ percentile).

During normal pregnancy, the build-up of shear stress due to volume expansion is counteracted by vasodilation, i.e. adaptive endothelial vasodilatory mechanisms overcome the chronic *vasoconstrictor tone* [24]. Failure of this process is responsible for impaired vasodilation, leading to endothelial dysfunction [24], which causes a vicious cycle to develop.

One of the proposed pathophysiological mechanisms behind this endothelial dysfunction is the inhibition of vascular endothelial growth factor by soluble fms-like tyrosine kinase receptor-1 [25], which is also studied by our research group (Tomsin & Oben, unpublished results) in parallel to this thesis. In addition to the development of hypertension, this mechanism will likely lead to a dysfunctional interaction between the renal podocytes and endothelial cells of the glomerular filtration barrier,

which in turn induces the proteinuria observed in PE. However, further research is necessary to elucidate the tubular protein reabsorption mechanisms [25, 26]. Important to note is the presence of both gestational hypertension without proteinuria and gestational proteinuria in normotensive pregnancies [26]. This indicates the complex pathophysiological nature of hypertensive pregnancy disorders.

Maternal maladaptation of vascular tone allows extremely slight long-term changes in blood fluid volume and CO to change arterial pressure, following the Guytonean model [2]. As is mentioned above, the endothelium plays a crucial role in maternal adaptation. Therefore, dysfunction of this important cardiovascular component is suggested to play a role in the pathophysiology of PE. Next to the production of numerous vasoactive substances as discussed above, the placental unit is able to secrete pro-inflammatory cytokines induced by hypoxia. Hypoperfusion can develop from placental insufficiency due to defective spiral artery remodeling [2, 25, 27]. The following endothelial dysfunction causes the damage of circulating thrombocytes which results in the increased secretion of thromboxane [2], i.e. the antagonist of prostacyclin. But also a maternal inflammatory response to, for instance, obesity is suggested to play a role in placental dysfunction [28]. On top of this, numerous other derangements have been reported to play a role in the defective vasodilatory mechanisms in PE, for instance NO deficiency [29], a restored vessel sensitivity to angiotensin [30, 31], or a state of sympathetic overactivity [32, 33].

In PE, a left ventricular concentric, rather than an eccentric, hypertrophy of the maternal heart is observed [7, 9]. Gestational hypertensive patients with such a concentric hypertrophy are those with pressure overload, but also volume underload and diastolic dysfunction [8]. Diastolic dysfunction in association with raised sympathetic activity has been reported in former PE patients with chronically subnormal plasma volume, a condition which predisposes to hemodynamic maladaptation to pregnancy and recurrence of PE [4].

This indicates the importance of an increased venous capacitance to allow for an adequate volume expansion in pregnancy. Therefore, studies on the maternal venous system, such as the studies presented in this thesis, are urgently needed in order to understand the mechanisms of normal and abnormal cardiovascular adaptation in pregnancy.

1.2.1 The maternal venous system in preeclampsia

The maladaptation of the maternal venous system in PE is the main subject of our research group and will be extensively discussed in this thesis (Chapter 2). Several weeks prior to the onset of clinical PE, plasma volume is diminished and, compared to normal pregnancy, levels of progesterone and aldosterone are increased and decreased, respectively [34]. Also, the pregnancy-induced changes in the venous bed seem to fade, as indicated by reversal of the changes in venous distensibility [18], capacitance [35], and compliance [17]. These responses of the venous compartment suggest a less effective control of venous return and regulation of the amount of stressed volume in response to fluctuations in CO.

Consequently, measurement of cardiovascular function at the maternal-fetal medicine unit is needed to evaluate and score the adaptation mechanisms in pregnant women in order to predict and follow-up the disease process of PE. Therefore, we briefly introduce the different aspects of the circulatory system (Chapter 1.3), with the emphasis on vascular tone, and in Chapter 1.4, we will describe several cardiovascular function tests.

1.3 The circulatory system

The human cardiovascular system integrates several functionalities: the *heart* (Figure 1.1 (A)) pumps blood throughout the body via blood vessels [36]. This complex set of blood vessels can be divided into three main compartments: the arteries, the microcirculation, and the veins [37, 38] (Figure 1.1 (B); from right to left, respectively). This classification of blood vessels is based upon differences in the constitution of both passive and active tension elements that determine the nature and corresponding role of a specific blood vessel. Generally, a blood vessel consists of three layers: (a) tunica intima, (b) tunica media, and (c) tunica adventitia, or the inner, middle, and outer layers respectively [38].

The inner layer of a blood vessel is made up from a heterogeneous set of endothelial cells, which can be considered as a dynamic organ lining the entire vascular system, with different functions depending on its location [38]. Elastin and collagen located in the adventitia are passive tension elements, which contribute to the distensibility of a vessel [37, 39]. This compliance partly influences the response to the active tension that is created by the activation of the vascular smooth muscle cells of the tunica media. Specific pressure-flow relationships can be generated for each vessel depending

on its structure: the arteries act as resistors, the microcirculation as a diffusion and filtration system, and the veins as capacitors [37]. These three main compartments can be further divided into subcompartments.

Conducting *arteries* contain many elastin fibers in the outer layer in order to sustain the force of ventricular contraction. These conducting arteries branch into conduit arteries which direct blood to specific locations of the human body. As part of the microcirculation, the resistance arteries regulate perfusion of tissues by sympathetic (de)activation of the large amount of highly innervated smooth muscle cells [37].

Tissue perfusion occurs at the level of the capillaries of the *microcirculation,* which, in contrast to other vessels, consist of merely one single layer, i.e. a thin and fenestrated endothelium attached to a basal membrane. Here, exchange of oxygen, nutrients, and waste products occurs through diffusion, filtration, and osmosis. Blood is transported from the capillaries to the heart by the venous system, whereafter it can be transferred to the pulmonary circulation for oxygenation [37].

The *veins* are richly innervated by sympathetic nerves and have a 30 times greater compliance than arteries, i.e. a great change in volume causes only a small change in pressure [39, 40]. Consequently, the veins are able to significantly influence the distribution of blood throughout the human body, and they determine most of the vascular capacitance [37]. Normally, approximately 70% of the total blood volume is present in the systemic veins [37, 40]. The venous system acts differently at different sites of the human body: The skeletal muscle veins are poorly innervated and largely depend on the activity of the muscle fibers for their functionality, and the cutaneous veins are mostly controlled by temperature [40]. It is mainly the splanchnic circulation that serves as a site of adjustable resistance and this contains blood that does not participate in the active circulation but merely serves as a reservoir; most of this blood is present in the liver [39, 41].

1.3.1 Vascular tone

Regulation of blood flow throughout the entire cardiovascular system is a complex interaction between different systemic and local subsystems [42]. The balance between vasodilation and -constriction of the vascular smooth muscle cells determines the state of vascular tone. A basal or intrinsic tone can be observed at the arterial side of the circulation, but this has not been illustrated for the veins [43]. Modulation of smooth muscle tone or vascular tone can occur via *direct* stimulation or *indirect*

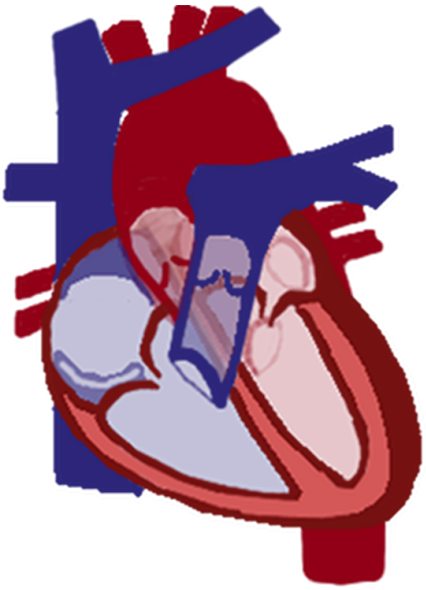

(A) Heart

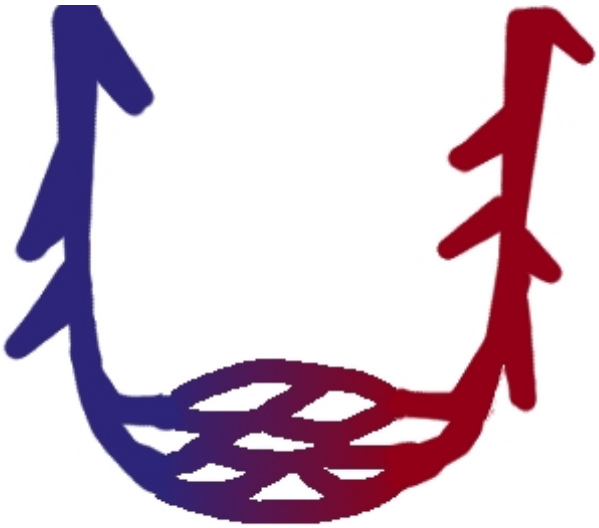

(B) Blood vessels

Figure 1.1: The human cardiovascular system integrates heart (panel A) and blood vessels (panel B). Panel B is a simplified representation of this complex system of blood vessels (not true for the pulmonary circulation): from right to left, it can be divided into three main compartments: the arteries (red), the microcirculation, and the veins (blue).

endothelium-dependent stimulation [44]. The mechanisms involved can be divided into local, neural, and hormonal influences. This enables the control of blood flow rate throughout the peripheral organs by changes in arteriolar tone. These control mechanisms are expressed differently in the venous compartment, where the most important function of venous tone is the peripheral-central distribution of blood volume [43].

After direct or indirect stimulation, the intracellular free calcium level of the vascular smooth muscle cells alters, which is responsible for increased or decreased tension [45]. This results in changes in both the *stiffness* (its resistance to deformation in response to the application of a force) and the *geometry* (the diameter and shape) of a vessel. The balance of both these vascular characteristics guides the net effect of the smooth muscle changes, and is therefore the key regulator of vascular tone [46]. It is important to note that the change in compliance, resulting from vascular tone changes, can potentially occur in concert with an increase, a decrease, or no change in vessel wall stiffness [46]. Arterial stiffness is dependent on both functional and structural changes in the vasculature [38]. For example, an imbalance between elastin and collagen contributes to structural arterial stiffening. This is in contrast to functional arterial stiffness which can be caused by endothelial dysfunction or sympathetic activation [47].

Important to note is that each organ has its own *regulation* of blood flow, and these mechanisms can be roughly divided into *1*) local control mechanisms depending on the metabolic needs of the surrounding tissue, e.g. at the level of the brain and heart, and *2*) systemic control mechanisms resulting from sympathetic activity, e.g. at the level of the kidneys and splanchnic organs. This enables the human body to preserve functionality of important vital organs during cardiovascular distress [43].

Sympathetic nervous system

Direct stimulation occurs through the sympathetic nervous system, which plays a significant role in the reflex control of the global vasculature, for instance the regulation of arterial blood pressure [43]. Moreover, the sympathetic nervous system is the most important vasopressor system in the control of *venous capacitance* [39]. Sympathetic activity is able to mobilize stored blood to the circulation due to venoconstriction [41]. In the presence of minimal sympathetic tone, 60% of total blood volume is hemodynamically inactive and constitutes a blood volume reservoir (unstressed volume) [48], the majority of which is stored in the splanchnic system [39, 41]. The veins, however,

are also susceptible to physical influences, such as compression by a gravid uterus, which passively influences the amount of blood they contain [43].

Parasympathetic nervous system

The parasympathetic nervous system acts only on a small proportion of the resistance vessels and therefore, the effect on total vascular resistance is relatively small. It is, however, capable of depressing the ventricular performance, mainly by counteraction of its antagonist, i.e. the sympathetic nervous system. In this way, it plays a role in the baroreceptor reflex modulation by regulating myocardial performance, in order to maintain normal blood pressure and heart rate [43].

Endothelium

Endothelial cells respond to hormones, neurotransmitters, and vasoactive factors, thereby *indirectly* influencing the underlying vascular smooth muscle cells [38] through release of NO, prostacyclin, thromboxane, endothelin, and hyperpolarization [38, 44]. On top of this, the endothelium can be activated by changes in flow-dependent shear stress. Shear stress is the force applied on a vessel due to the blood flow in that vessel, which is dependent on its diameter, its resistance, and blood viscosity [36]. Endothelial cells activate several intracellular pathways in response to this mechanical force produced by blood flow, which in turn will influence the blood flow by changing vascular tone [49]. The bioavailability of NO and the sensitivity to shear stress seem to be of importance in processes such as aging and cardiovascular disease [50].

Other biological variables

As explained in Chapter 1.3.2, central venous pressure - an important factor in venous capacitance - can be changed by different biological variables of daily life, such as ventilation and position changes. This in turn influences *venous return* [40].

1.3.2 Venous physiology

The vascular function curve (Figure 1.2) describes the functional relationship between the venous return and the right atrial pressure. This relationship depends on critical characteristics of the vascular system independent of the cardiac tissue properties, such as the peripheral resistance (vascular tone), the arterial and venous capacitances, and the blood volume. Any changes in blood and vessel volumes can be expected to alter the mean circulatory filling pressure (e.g. during pregnancy). The mean circulatory (systemic) filling pressure is defined as the pressure measured in the

circulatory system when the heart is suddenly arrested. The mean circulatory filling pressure minus the right atrial pressure represents the pressure gradient (atriovenous pressure difference) for venous return. A marked increase in blood volume will shift the curve to a higher venous return, a higher atriovenous pressure difference and a slower filling phase of the heart. If the vascular tone changes, the vascular function curve changes too [51, 52]. Both structural and functional properties allow the venous system to serve as the main regulator of the circulating blood volume: in case of hypovolemia, reflex-induced venoconstriction mobilizes stored blood from the venular bed (the passive circulation) to preserve venous return to the heart (the active circulation), whereas in case of blood volume expansion (e.g. during pregnancy), most of the surplus volume is retained in the venous compartment [51].

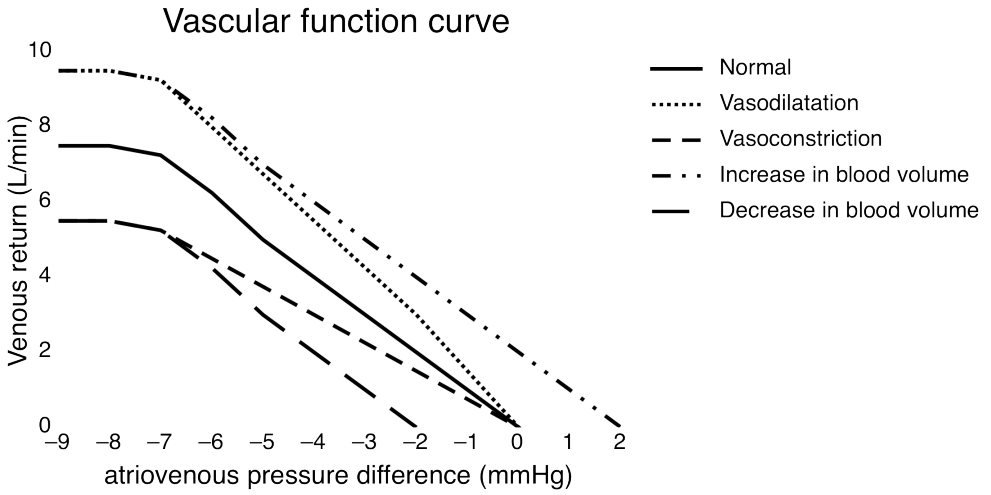

Figure 1.2: Influences of blood volume and vascular tone on the vascular function curve (Adapted from Boulpaep *et al.* [52]).

The driving force of blood flow differs between arteries and veins. In the arterial compartment, the ventricular contraction creates a positive pressure gradient between heart and arterial bed, moving the blood at a certain pressure towards the systemic microcirculation. Conversely, in the venous compartment, relaxation of the heart during diastole creates a negative pressure gradient between the peripheral veins on the one hand, and the central veins and heart, on the other hand. This suction force is one of the most important driving forces for venous return [51, 53].

Many physiologic variables are known to interfere with venous return and the shape of the venous pulse waves. Respiratory movements, particularly the inspiration, are

responsible for raising the venous pulse waves [54, 55]. This may be counteracted by intraluminal obstruction, such as thrombi, or by external compression [54]. An example of this is the gravid uterus, which is responsible for a rise of intravenous pressure of the femoral vein [56]. Orthostasis and gravity tend to reduce venous return, whereas postural change from an upright to a supine position tends to raise venous return temporarily [51, 52]. Veins, surrounded by skeletal muscular tissue, depend largely on contractions of these muscles to accelerate venous flow and to prevent stasis of blood. This is mainly true for the lower extremities, where this muscle pump activity is supported by mechanical compression from stockings for the prevention of deep vein thrombosis in cases of reduced mobility [57]. Several drugs and medications have been studied with respect to direct or indirect activity on venous wall muscular contractility [39].

The lower central venous compartment

The splanchnic bed is the most important blood reservoir of the body, containing up to 25% of the total blood volume [58], most of it located in the liver bed [59]. The blood in the central veins, i.e. the jugular veins, the upper and lower vena cava, the hepatic veins, and the renal veins, flows undisturbed into the right atrium, as there is no interposition of an anatomical or functional valve [60]. As a result, intravascular measurements of venous pressure, flow velocities, and volumes in the central veins mirror right atrium pressure changes [51, 53]. In clinical practice, this principle is commonly used to estimate central venous pressure at the level of the jugular veins using both non-invasive and invasive methods [61]. However, when studying hepatic venous flow, it should be noted that congenital aberrations and intra-hepatic vascular shunts result in a wide inter-individual variation in hepatic vein Doppler patterns, even in healthy subjects [62].

1.4 Cardiovascular function tests

All the properties of the vessel wall, i.e. structural and functional characteristics, determine the velocity at which a flow wave propagates within the vessel, and thus *pulse wave analysis* is useful to non-invasively assess vascular function [47, 63, 64]. This can be done by manometry [65], photoplethysmography [64, 66, 67], echocardiography [68], applanation tonometry [69, 70], and magnetic resonance imaging [71].

Pulse wave analysis includes an augmentation index (AI_x), pulse wave velocity (PWV), and pulse transit time (PTT), which are interrelated indices of arterial stiffness [65, 70, 72, 73]. According to the Moens-Korteweg equation, pulse waves travel faster in stiffer arteries [73], for instance in age-related vessel stiffening [74]. When the PWV of both forward and reflected waves increases, the reflected wave arrives earlier and augments the pressure in late systole, therefore AI_x increases [72]. As a result, the time it takes for the pulse to propagate to the periphery or the PTT is decreased. As there is a site-specific relationship of PTT, the location of PTT measurement is of great importance for interpretation [74]. Pulse wave analysis has many clinical applications, such as arterial stiffness in chronic renal failure [70], pulmonary venous flow reversal in diastolic function testing [75], arterial pressure determination during spinal anesthesia [67], and evaluation of sympatholytic antihypertensive medication in pregnancy hypertension [69].

The hemodynamic assessment of the maternal cardiovascular state using the invasive conventional methods, e.g. pulmonary artery catheterization and thermodilution method, are rarely justified in most pregnant women. As a result, combined ECG-Doppler ultrasonography and impedance cardiography are presented in this thesis as suitable and non-invasive methods to investigate maternal cardiovascular adaptation. Therefore, the principals behind these techniques will be briefly discussed in the following sections.

1.4.1 Doppler ultrasonography

2D-ultrasonography is a non-invasive imaging technique which is based on the transmission and reflection of high frequency (20 kHz) sound waves. The size of the scanned object (e.g. the liver) influences the type of reflection. A red blood cell is smaller than the wavelength and therefore the acoustic wave is scattered in all directions. In a Doppler-unit, ultrasound waves are reflected by the moving interface, i.e. the flowing red blood cells, which changes the wavelengths of these waves. This is called the Doppler-effect. In this way, the profile of the bloodstream throughout vessels (or blood flow) can be imaged and registered [76].

The representative of the right atrial pressure is the jugular venous pulse, as presented in Figure 1.3. The A-wave represents transient venous distention caused by retrograde pressure from the contraction of the right atrium by lack of a valve mechanism between the right atrium and the vena cava. The X-descent, which represents the fast filling of the right atrium during atrial relaxation and the downward movement of the tricuspid valve during ventricular systole, may be interrupted by a small upward deflection (C-wave) at the time of tricuspid valve closure. The V-wave corresponds to passive filling of the right atrium from the systemic veins, when the tricuspid valve is closed. Opening of the tricuspid valve in early diastole allows blood to flow rapidly from the right atrium into the right ventricle; that fall in right atrial pressure corresponds to the Y-descent. After this Y-minimum, venous return slows down again, thus increasing the venous pressure, due to the reduced ventricular filling phase, i.e. diastasis [53, 77]. Comparable Doppler patterns can be found at the level of the maternal liver and kidneys throughout pregnancy, which are described in more detail in Chapter 2.1.

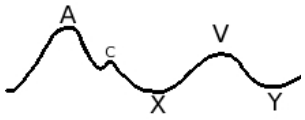

Figure 1.3: Jugular venous pulsations with its typical waveform (A-X-V-Y).

1.4.2 Electrocardiogram

An ECG measures the electrical activity of the heart using electrodes placed on the upper and lower extremities. The ECG apparatus requires particular amplifiers, as the electrodes are attached to the skin, to measure the total electrical activity of the heart. Although electrical filters reduce the electrical noise, artifacts can arise due to movement of the limbs or breathing [78]. The extracellular signals produced by the action potentials moving through the cardiac myocytes can be registered by the ECG device. As such, the ECG provides fundamental information about the origin and conduction of the cardiac action potential within the heart. The ECG-waves (Figure 1.4) represents the fluctuations of the extracellular voltage, each representing a specific polarization change in the heart muscle [78].

The P-wave reflects the depolarization of the right and left atrial muscle. This occurs at the end of diastasis (the period of decreased filling). The atrial contraction immediately follows the P-wave (end of inflow phase). Depolarization of the ventricular muscle is represented by the QRS-complex. Systole starts when the ventricles begin to depolarize. The ventricles contract and the pressure of the ventricles exceeds the pressure of the atria. As a result, the atrioventricular valves close and the semilunar valves open. The T-wave represents the repolarization of both ventricles and this occurs slightly before the closing of the semilunar valves [53, 78].

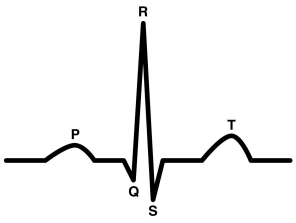

Figure 1.4: A normal ECG pattern including the five characteristic waves (P-QRS-T).

1.4.3 Impedance cardiography

ICG is designed for the safe and non-invasive measurement of cardiovascular parameters on a beat-to-beat basis. Two dual sensors are placed on opposite sides at the base of the patient's neck, and two dual sensors are placed on either side of the thorax at the level of the xiphoid process on the mid-axillary line (Figure 1.5). Each dual sensor consists of both an ICG- and ECG-lead, and contains a stimulating electrode, most distal to the heart, and a measuring electrode, most proximal to the heart. The stimulating electrodes generate an alternating current with a high frequency (60-100 kHz) and a very low amplitude (1 mA). The voltage, which is produced when the current flows through the thorax, is measured by the measuring electrodes, and can be used to calculate the impedance (i.e. resistance against an alternating current, Ω). As an electric current always follows the path of least resistance, the changes of thoracic impedance during the cardiac cycle are most dependent on the changes in size and blood volume of the thoracic aorta. Consequently, ICG enables calculation of the amount of blood ejected from the left ventricle. To measure data of cardiac function, ICG detects pulse-synchronic changes in thoracic electrical bio-impedance between simple surface electrodes, together with a conventional ECG. With each ventricular contraction, there is an increase in the electrical conductance of the thoracic cavity, which results in the bio-impedance waveform. The impedance cardiogram or ICG (dZ/dt) is the first mathematical derivative of the change in thoracic impedance (Z) over time to this alternating current.

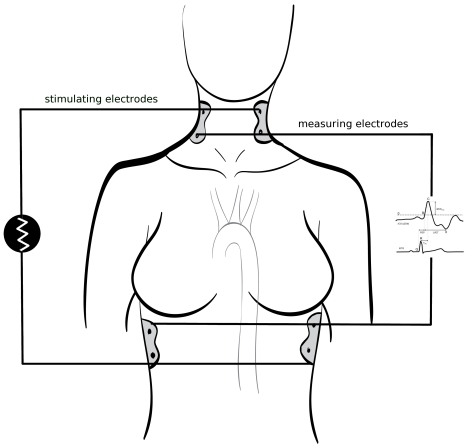

Figure 1.5: Location of the electrodes in impedance cardiography (Adapted from Staelens *et al.* 2013, submitted).

ICG was first introduced by Kubicek *et al.* in 1966 and commissioned by the National Aeronautics and Space Administration who described their method for calculating stroke volume (SV) from the thoracic impedance signal. Kubicek's equation for the calculation of SV, based on a cylindrical model of the chest, incorporates the maximum rate of the first derivative of the impedance waveform (dZ/dt_{max}) in Ohms per second and the left ventricular ejection time (LVET), as follows:

$$SV = \rho \times (\frac{L^2}{Z_0^2}) \times (\frac{dZ}{dt_{max}}) \times \text{LVET} \tag{1.1}$$

where ρ is a constant, L the distance between the receiving electrodes, and Z_0 equals the thoracic impedance [79].

Over the years, both the software and hardware of the ICG-technology have been repeatedly revised and improved, and high correlations are reported with the standard thermodilution technique for CO determination [80]. Today, the equation used for ICG-technology is an adaptation of the Kubicek equation by Sramek and Bernstein [81, 82]. They modified the approximation of the chest to a truncated cone, whereby SV was calculated as follows [81, 82]:

$$SV = \delta \times \frac{(0.17 \times H)^3}{4.25} \times (\frac{dZ}{dt_{max}} / Z_0) \times \text{LVET} \tag{1.2}$$

As is shown, they introduced the patient's weight (δ) and height (H), and thus using a different model in describing the electrical properties of the human chest.

The equations and derivations of the other ICG-parameters are extensively discussed in Chapter 3, more specifically in Chapter 3.3.

1.5 The maternal venous system: the ugly duckling of obstetrics?

From this general introduction (Chapter 1), it is evident that maternal cardiovascular (mal)adaptation is of importance in the development of PE. However, Doppler studies on the resistance and tone regulation at the level of the uterine vessels only characterize the uteroplacental circulation [2, 83, 84], but not the generalized maternal maladaptation. On top of this, vascular resistance in early gestation is sometimes normal or even lower in PE patients [2]. As such, we suggest that studying vessels in different maternal organs by Doppler ultrasonography, together with hemodynamic monitoring of the global cardiovascular system, is more likely to be informative on the cardiovascular adaptation mechanisms in normal and preeclamptic pregnancies. Even more, we believe that the evaluation of the venous system in early gestation may provide more crucial information, as it is the most important blood reservoir and regulator of circulatory volume.

1.5.1 Hypothesis and strategies

We hypothesize that global cardiovascular profiling in pregnancy, including heart, arteries, and veins, might allow defining a risk profile for gestational disorders with placental dysfunction as common denominator and guiding the clinical work-up of this high-risk population.

The main research question in this thesis is: *"Can we ameliorate cardiovascular profiling in pregnancy by including the concomitant information of the dynamics of the maternal venous system?"* . To evaluate this, we divided this study into several subquestions based on three main methodological strategies: *1*) Doppler ultrasonography (Chapter 2), *2*) impedance cardiography (Chapter 3), and *3*) the maternal cardiovascular profile integrating both techniques (Chapter 4):

1. The venous system in pregnancy and preeclampsia: what do we already know and how can we study it?
    - Venous impedance index: does Doppler ultrasonography allow for reproducible measurements in pregnancy (Chapter 2.2)?
    - How does preeclampsia affect venous impedance in the clinical phase as compared with uncomplicated pregnancies (Chapter 2.3)?
    - Venous pulse transit time: is this novel combined electrocardiogram (ECG)-Doppler ultrasonography technique feasible to study venous tone in pregnancy (Chapter 2.4)?
    - Does venous pulse transit time change in preeclampsia as compared with uncomplicated pregnancies (Chapter 2.5)?
    - Can we visualize the venous circulation: a three-dimensional approach (Chapter 2.6)?
2. How can we non-invasively study the heart and arterial system parallel to our venous Doppler evaluation?
    - Impedance cardiography: is it feasible and reproducible (Chapter 3.1)?
    - Can impedance cardiography be used to evaluate cardiac and arterial (mal)adaptation in pregnancy (Chapters 3.2 and 3.3)?
3. Does the venous system contribute to the maternal cardiovascular profile in pregnancy?
    - Can we establish a maternal cardiovascular profile based on a combined cardiac, arterial, and venous assessment (Chapter 4.1)?
    - Do maternal hypertensive disorders present differently in cardiovascular profile (Chapter 4.2)?
    - Does our maternal cardiovascular profile allow for the stratification of preeclampsia based on differences in maternal cardiovascular profile (Chapter 4.3)?
    - Is there a future for this type of maternal cardiovascular profiling in obstetrics (Chapter 5.2)?

Chapter 2

The venous system

2.1 The venous system in normal pregnancy

Doppler assessment of maternal central venous hemodynamics in uncomplicated pregnancy:

a comprehensive review

Wilfried GYSELAERS, Tinne MESENS, ***Kathleen TOMSIN****, Louis PEETERS*

Facts, Views and Visions in Obstetrics and Gynaecology
F, V & V in ObGyn 2009, 1 (3): 171-181

2.1.1 Introduction

Doppler studies on hemodynamics of the cardiovascular system and intra-abdominal organ perfusion in non-pregnant individuals are usually performed by cardiologists and radiologists. Specialists in maternal-fetal medicine are also familiar with cardiovascular Doppler sonography, however, they mostly focus on the fetal [85] or uteroplacental circulation [86, 87, 88]. Recently, several studies have been reported using Doppler assessment to explore the dynamics of the maternal venous compartment, illustrating its feasibility and reproducibility [89, 90, 91, 92, 93, 94]. These studies have shown that the venous compartment is also subject to maternal cardiovascular adaptation during uneventful pregnancy [93, 94]. In gestational diseases, such as PE, some of the observations show promising results with respect to detecting maternal cardiovascular maladaptation [93, 94] and predicting the development of subsequent disease [95]. Therefore, the maternal venous compartment is a new area to be explored in obstetric ultrasound imaging [92], in order to link Doppler observations to known features of gestational (patho)physiology [93, 94] and to the information obtained from other techniques [96].

This paper offers a comprehensive review on Doppler assessment of the maternal venous compartment during uncomplicated pregnancy (UP).

2.1.2 Literature sources

A literature search was conducted to identify all the published observational Doppler studies on maternal venous hemodynamics. Relevant citations in PubMed and Medline were searched using combinations of the keywords: *maternal physiology, Doppler, hepatic veins, renal interlobar veins, pregnancy, venous hemodynamics, venous compartment, central veins, gestational cardiovascular adaptation, review* . The reference list of all known primary and review articles was examined for additional relevant citations. Relevant chapters from handbooks were searched in the Library of Hasselt University and in the author's personal collections.

2.1.3 The venous system

Definition and anatomy of the lower central venous compartment

The venous system is responsible for the return of deoxygenated blood from the organs back to the heart. The central veins are the large single lumen veins, which are anatomically located in the vicinity of the heart. Basically they include the jugular veins, the upper and lower vena cava, the hepatic veins, and the renal veins. The blood in the central veins flows undisturbed into the right atrium, as there is no interposition of an anatomical or functional valve. The anatomical structure known as the valve of the inferior vena cava, first described by Eustachius [60], is a non-occlusive semilunar endocardial fold at the anterior side of the entrance of the inferior vena cava in the right atrium, which directs the oxygenated blood towards the open foramen ovale during fetal life, but degenerates after birth [60]. As a result, intravascular measurements of venous pressure, flow velocities, and volumes in the central veins mirror the right atrium pressure changes [51, 53]. In clinical practice, this principle is commonly used to estimate central venous pressure at the level of the jugular veins using both non-invasive and invasive methods [61].

As illustrated in Figure 2.1 (A), the liver drains blood into the inferior vena cava through the hepatic venous tree, which consists of three main branches: the left, middle, and right hepatic veins (HV). Sometimes, an accessory inferior right HV is found [97]. Right and left HV, respectively, drain the largest and smallest liver volumes [97]. Hepatic veins are the sole exit of blood from the portal vein and hepatic arteries [98].

As illustrated in Figure 2.1 (B), the right renal vein (RV) is located more caudally and is half a long as the left RV, which is the one crossing the midline and draining blood from the left ovarian vein. The left RV is squeezed between the aorta and the superior mesenteric artery, and sometimes this may provoke orthostatic hematuria [99]. This so-called Nutcracker phenomenon may aggravate during pregnancy [100]. Compared to the left side, accessory RV are more frequent on the right side and the proximal RV diameter is larger [101, 102].

The anatomy of the lower central venous system differs widely between individuals, not only because of a high frequency of accessory veins as mentioned above, but also because of asymptomatic congenital variations. These congenital anomalies are found in all segments of the inferior vena cava [103] and have to be taken into account in the pre-operative work-up of liver or kidney transplantation [104, 105]. Next to this, different types of congenital intrahepatic vascular shunts have been observed, such

as arteriovenous connections, arterioportal shunts, and portosystemic fistulas [106]. Both congenital aberrations and intrahepatic vascular shunts are responsible for a wide inter-individual variation in HV Doppler patterns in healthy subjects [62].

Physiology of venous hemodynamics

The venous compartment has an important role in human physiology. It is a large capacitance reservoir, containing 65-75% of the total blood volume, 75% of which residing in small veins and venules [58]. The splanchnic bed is the most important blood reservoir of the body, containing up to 25% of the total blood volume [58], most of it located in the liver bed [59]. The venous walls contain collagen and elastin fibers, together with a circular layer of smooth muscle cells [107]. This structural composition enables physiological properties such as expansion, viscoelasticity, and active contraction [58]. As such, the venous compartment contributes actively to the regulation of CO [51, 52]. Contrary to the arterial system, small changes of intravenous pressure have a major impact on CO [51]. In the control and regulation of CO, the heart and veins cooperate as one functional unit [51]. Both structural and functional properties allow the venous system to serve as the main regulator of the circulating blood volume: in case of hypovolemia (e.g. after hemorrhage), reflex-induced venoconstriction mobilises stored blood from the venular bed to preserve venous return to the heart, whereas in case of blood volume expansion (e.g. pregnancy), most of the surplus volume is retained in the venous compartment.

The driving force of blood flow differs between arteries and veins. In the arterial compartment, the ventricular contraction creates a positive pressure gradient between heart and arterial bed, moving the blood at a certain pressure towards the systemic microcirculation. Conversely, in the venous compartment relaxation of the heart during diastole creates a negative pressure gradient between the peripheral veins on the one hand, and the central veins and heart, on the other hand. This suction force is the most important driving force for venous return [51, 53].

Many physiological variables are known to interfere with venous return and the shape of the venous pulse waves. Respiratory movements, particularly the inspiration, are responsible for raising the venous pulse waves [54, 55]. This may be counteracted by intraluminal obstruction, such as thrombi, or by external compression from intrapelvic masses [54]. An example of this is the gravid uterus, which is responsible for a rise of intravenous pressure of the femoral vein [56]. Orthostasis and gravity tend to reduce venous return, whereas posture change from an upright to a supine position

tends to raise venous return temporarily [51, 52]. Veins, surrounded by skeletal muscular tissue, depend largely on contractions of these muscles to accelerate venous flow and to prevent stasis of blood. This is mainly true for the lower extremities, where this muscle pump activity is supported by mechanical compression from stockings for the prevention of deep vein thrombosis in cases of reduced mobility [57]. Several drugs and medications have been studied with respect to direct or indirect activity on venous wall muscular contractility [39].

2.1.4 How to study the venous system in normal pregnancy?

Study of venous hemodynamics by duplex ultrasonography

Methods to study body venous tone have been reviewed by Pang [58]: they include the measurement of the mean circulatory filling pressure, the constant CO reservoir technique, plethysmography, blood-pool scintigraphy, linear variable differential transformer technique and intravascular ultrasound. These techniques all have limitations and are difficult to perform in a clinical setting, especially during pregnancy. Duplex ultrasonography has been reported to be a simple, non-invasive, and easily-accessible method to study venous hemodynamics, both in non-pregnant [108] and pregnant subjects [89, 91, 109]. Because of high intra- and inter-observer variations reported for Doppler-derived measurements [110, 111], methodological standardization is needed, especially when interfering factors, as mentioned previously, are to be excluded.

A standardized duplex ultrasound examination has been reported, enabling the acquisition of reproducible data of renal interlobar vein impedance index (RIVI) based on maximum and minimum flow velocities (MxV and MnV, respectively), defined as [89, 94]

$$RIVI = \frac{MxV - MnV}{MxV} \tag{2.1}$$

and of hepatic pulse wave velocities [93].

Despite methodological standardization, single measurements of RIVI showed poor intra-observed intraclass correlation (ICC) [92]. Repeatability improved markedly after using the mean value of three consecutive measurements, as this resulted in good to excellent ICC both for RIVI [94] and HV velocities [93].

Figure 2.2 (A and B) shows the intercostal two-dimensional ultrasound image at the craniocaudal midportion of the liver, and Figure 2.3 (A and B) represents the

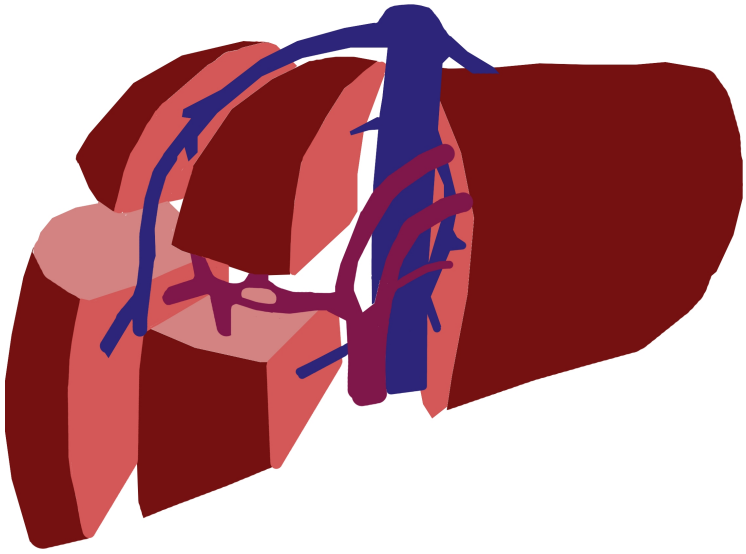

(A) Liver

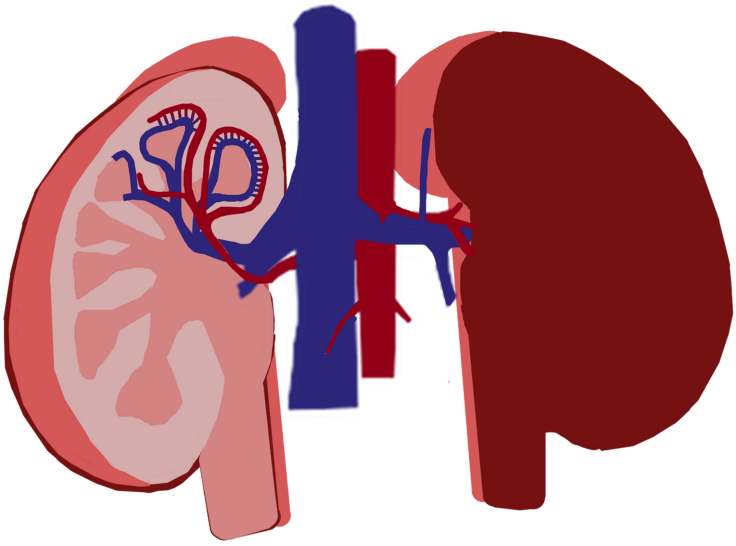

(B) Kidneys

Figure 2.1: Anatomy of the lower central venous compartment from liver to kidneys. As is shown in panel A, there are three HV: left, middle, and right, which are often accompanied by additional branches. Usually, left and middle HV fuse before draining into the vena cava inferior at a few centimeters caudal from the right cardiac atrium. Panel B shows that the right RV is shorter and inserts more caudally into the vena cava inferior then the left RV. Next to this, the right RV has more accessory branches and a wider proximal diameter than the left RV. Also, the left RV is sometimes sandwiched between aorta and superior mesenteric artery (Nutcracker Syndrome) and drains blood from the left ovarian vein.

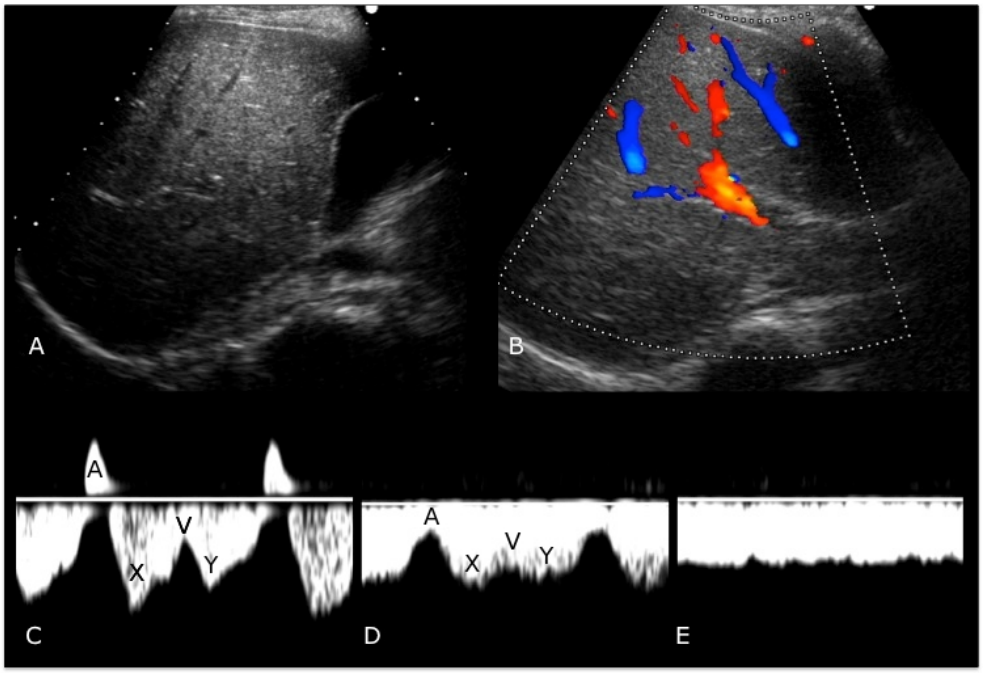

Figure 2.2: Illustrations of 2D-ultrasound and Doppler images of the intrahepatic vascular tree. Panel A shows the standard view of the liver, scanned intercostally at the craniocaudal midportion. Panel B shows the color Doppler image at this level, which enables distinguishing portal branches and hepatic arteries (red) from HV (blue). Panel C illustrates the typical triphasic HV Doppler wave pattern, in which the A-deflection represents backflow of blood from the right atrium into the HV circulation during atrial contraction. This pattern is mostly observed in non-pregnant individuals and during early pregnancy. Panel D illustrates a biphasic pattern, where the A-deflection is not reversed. This pattern is commonly observed during midgestation. Panel E illustrates the flat HV pattern, which is the most common pattern in term pregnancy.

transverse ultrasound section of the kidney at the level just above the hilus. Both figures illustrate the usefulness of color Doppler to distinguish different types of blood vessels in the parenchym and to identify those veins in line with the direction of the Doppler beam in which velocimetry can be performed correctly [110].

Doppler studies of lower central hemodynamics in non-pregnant individuals

As explained above, there are no anatomical valves between the central veins and the cardiac atria. Due to this open communication, the shape of the venous pulse and Doppler waves reflect the cardiac cycle of the right atrium [51, 53]. This is well-known for the pulse wave characteristics of the jugular veins [52], vena cava, and hepatic veins [108]. The typical pulse wave characteristics of hepatic veins are illustrated in Figure 2.2 (C). As is shown, the A-deflection represents central venous backflow away

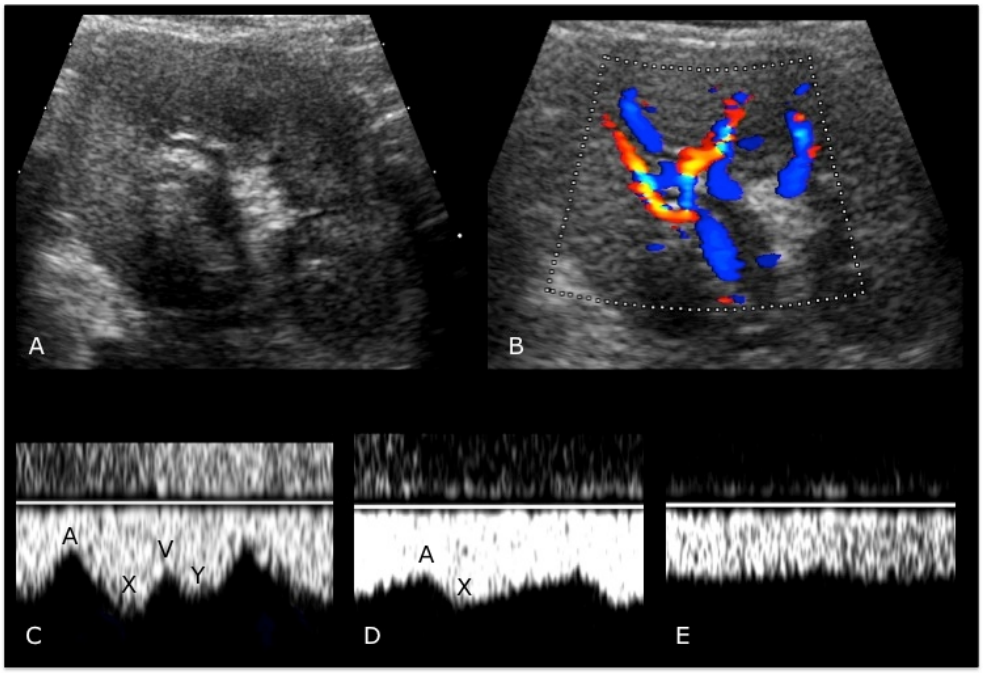

Figure 2.3: Illustrations of intrarenal vascularity, as observed by 2D-ultrasound and Doppler ultrasonography. Panel A shows the standard view of the kidney, scanned in transverse position at the level just above the renal hilus. The intrarenal pyelon can be identified easily. The interlobar vessels are located between the pyelon and the renal cortex. Color Doppler imaging, as illustrated in panel B, allows distinguishing interlobar arteries (red) from veins (blue). Panel C illustrates the typical biphasic pattern of RIV, which is the most common pattern in non-pregnant individuals and during early and midgestation. Panel D shows the monophasic pattern, which is very common in term pregnancies. Panel E illustrates a flat pattern, which is frequently found during urological obstruction.

from the heart during atrial contraction [92], the X-deflection represents forward flow towards the heart following atrial relaxation, which decelerates just before opening of the tricuspid valve (V-deflection). The Y-deflection represents forward flow following ventricular relaxation. Sometimes, a C-deflection is also present shortly after the A-deflection, and this represents the closure of the tricuspid valve. At increasing distance from the heart, the triphasic shape of the venous pulse wave, presented in Figure 2.2 (C), changes gradually towards a biphasic, monophasic, and flat pattern. Biphasic venous pulse waves are the predominant pattern in RIV of non-pregnant individuals (Figure 2.3 (C)). Monophasic waveforms are also observed frequently at the level of RIV (Figure 2.3 (D)) but they are not found in HV. A flat pulse wave is the common pattern observed in the lower extremities [54] and is also frequently observed in RIV during ureteral obstructive disease (Figure 2.3 (E)) [90, 112]. The same types of Doppler waveforms are also found in the venous circulation of the fe-

tus: triphasic patterns are observed at the level of the inferior vena cava and HV, biphasic waveforms are present in the ductus venosus, and flat patterns are found in the umbilical vein [113, 114].

As explained above, anatomical variations and intrahepatic shunts are responsible for a wide inter-individual variation in the presence of tri- or biphasic or flat Doppler waves in the liver of healthy individuals [62]. Besides, these patterns are also strongly influenced by cardiac and liver diseases. Typical patterns of abnormal HV Doppler waveforms have been reported for restrictive and constrictive cardiopathy, pulmonary hypertension, and tricuspid regurgitation [115]. These patterns also show typical variations with respiration. Similarly, an association was reported between mono- and biphasic HV Doppler waveform patterns and histology of liver steatosis [116, 117], whereas the presence of triphasic waves essentially excludes fatty infiltration of the liver [116, 118]. Monophasic patterns in HV have also been reported for impaired liver function due to cirrhosis [119], compression by intra-abdominal or intrahepatic masses [120], or HV thrombosis (Budd-Chiari Syndrome) [119, 120]. In non-pregnant individuals, Doppler studies of RIV are used in obstructive uropathy to distinguish physiological from pathological pyelocaliectasis [90, 112], for non-invasive monitoring of transplant kidneys [121, 122] and in the work-up of RV occlusion [122, 123].

Doppler studies of hepatic veins during pregnancy

As illustrated in Figure 2.2 (C-E), there is a high intra- and inter-individual variation of HV Doppler waves, ranging between triphasic, biphasic, and flat patterns [62, 108]. Roobottom *et al.*, reported that during the course of normal pregnancy, the HV waveforms changed from predominantly triphasic to predominantly flat patterns [91]. The postpartum return from gestational patterns to the prepregnant condition has also been reported [124]. The HV A-deflection, known to represent central venous backflow during atrial contraction, was reported to convert to constantly forward moving flow into the direction of the heart at about 22-24 weeks of gestation [93]. This development with advancing pregnancy mimics the one in plasma volume [56]. Therefore, it was suggested that this phenomenon resulted from dampening of the intermittent backflow during the cardiac cycle by increasing intravascular filling [93]. Consecutive Doppler-derived estimates of hepatic flow in the course of pregnancy suggested a significant rise in hepatic perfusion relative to the non-pregnant state, by 28 weeks. Since hepatic arterial blood flow remains unchanged throughout pregnancy, this effect may reflect a rise in portal venous drainage after 28 weeks pregnancy [125].

Figure 2.4 (B) shows the evolution of HV A-wave velocities, measured at 1-2 week intervals, between 9 weeks and term in one uneventful pregnancy. As is shown, the velocities change from positive towards the liver (triphasic waves) during early pregnancy, to negative into the direction of the heart (biphasic and flat waves) in the second trimester. In this particular case, the shift from tri- to biphasic, and flat Doppler waves occurred at 25-27 weeks, but shortly returned to triphasic again by 32 weeks, and then became biphasic and flat again until term. This reversal illustrates the high intra-individual variation of HV waveforms during the third trimester of pregnancy. In a group of 13 UP, three different types of HV Doppler wave combinations could be identified in the course of the third trimester of pregnancy: *1*) women presenting flat waveforms only, *2*) women having both flat and biphasic waveforms, and *3*) women presenting flat, bi-, and triphasic waveforms [93] .

Doppler studies of renal interlobar veins during pregnancy

As illustrated in Figure 2.3 (C-D), Doppler wave patterns in RIV of pregnant women gradually shift from biphasic to monophasic in the course of pregnancy [92, 94]. Karabulut *et al.* were the first to report lower RIVI values in pregnant women compared to non-pregnant individuals [89]. From the late second trimester onward, they observed that at the right side, RIVI was 10-15% lower than at the left side, and that this difference was inversely related to the diameter of the renal pelvis. This observation was considered to result from increased intrarenal interstitial pressure, due to retroperitoneal compression by the growing pregnant uterus with subsequent dilatation of the renal pelvis, especially on the right side [89, 92]. Sometimes, this can be associated with the presence of flattened RIV Doppler waveforms (Figure 2.3 (E)). As mentioned above, flat RIV Doppler wave patterns are frequently observed during obstructive uropathy [90, 112].

In a cross-sectional study [92] and in a prospective observational study [94], RIVI was found to decrease gradually in both kidneys during the first and second trimester of pregnancy, with only an ongoing decline until 30 weeks at the right side. The change in RIV MxV and MnV with advancing pregnancy mimicked the changes with pregnancy in cardiac stroke volume (SV) and renal GFR [94], suggesting an association with features of maternal gestational cardiac and renal adaptations. Venous flow velocities were consistently higher in the right than in the left kidney, and this was linked to interrenal anatomical differences: as detailed previously, larger diameters and more accessory RV are present on the right side [101, 102, 126], greatly facilitating venous drainage. Influx of ovarian blood and compression between the

superior mesenteric artery and the aorta are likely to reduce flow velocities in the left RV [99, 100]. These anatomical differences also help to explain the lower RIVI values during the third trimester of pregnancy [94].

There appears to be a variation in time for RIVI values in both kidneys. The graphic presentation of serial RIVI measurements at weekly or two-weekly intervals shows a slow oscillating pattern, as illustrated in Figures 2.4 (A) and 2.5 (A-B). The frequency and amplitude of this sinusoidal pattern seems similar in both kidneys but the increasing and decreasing slopes do not occur simultaneously. Figure 2.5 (A) shows that this oscillating pattern is present both in a normal menstrual cycle as throughout pregnancy. Figure 2.5 (B) illustrates a case of reduced oscillation during the third trimester of pregnancy, particularly on the right side where RIVI values are lower than on the left side [92]. This oscillating pattern suggests that the venous vascular wall activity towards maintenance of venous tone and/or distensibility is a dynamic physiological process which is variable in location and time.

2.1.5 Why study the venous system in normal pregnancy?

Towards a link between maternal venous Doppler parameters and known features of gestational cardiovascular physiology

Human pregnancy is subject to major adaptations of the maternal cardiovascular system [11, 56]. These adaptations occur on both the arterial and venous sides of the circulation. Total peripheral resistance decreases to a nadir at midgestation and increases again in the third trimester. As a result, arterial blood pressure is lower in the second trimester than in early or late gestation and venous distensibility is increased [18]. Plasma volume expands to a maximum in the early third trimester and reduces slightly afterwards. These changes coincide with a gradual increase of maternal heart rate throughout pregnancy, an increase of cardiac SV until a maximum at midgestation and an increase of CO to approximately 50% above the prepregnant level at term [13, 56].

Most Doppler studies on gestational hemodynamics focus either on the analysis of maternal uterine artery (UtArt) waveforms or on the evaluation of the fetal and uteroplacental circulations; the wide range of publications on these topics have been reviewed extensively [86, 87, 88]. However, Doppler studies on maternal venous hemodynamics are scarce.

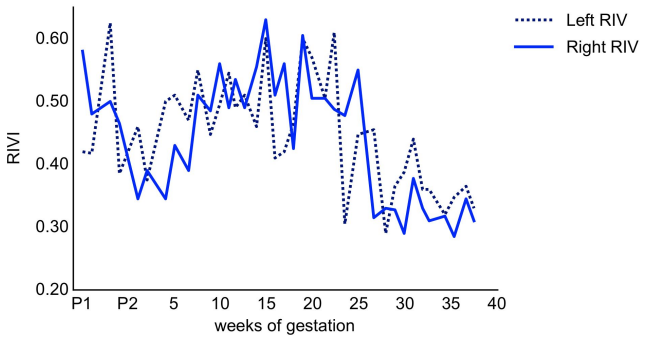

(A) Evolution of RIVI from preconception to term

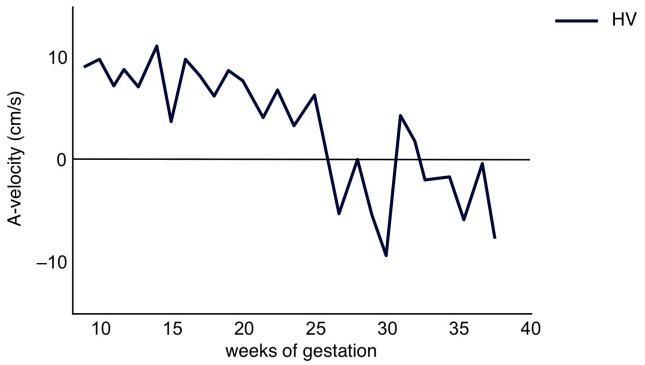

(B) Evolution of HV A-velocity from early pregnancy to term

Figure 2.4: Graphical illustration of serial measurements of RIVI (A) and HV A-velocity (B) at 2-weeks interval from preconception (A) or early pregnancy (B) until term (n=1). As is shown, RIVI measurements of both kidneys show a slow pattern of oscillation with the highest values intermittently observed in the left or right kidney. This oscillation is present both during the normal menstrual cycle, marked as the interval between menstrual period 1 (P1) and menstrual period 2 (P2), as during pregnancy (3 to 37 weeks of gestation). In the course of pregnancy, RIVI decreases and at term, right RIVI values are lower than those from the left kidney. This is presented more clearly in Figure 2.5 (B). Simultaneously, HV A-velocities shift from positive values, reflecting triphasic HV Doppler wave patterns with blood flowing into the direction of the liver during atrial contraction, to negative values, representing biphasic or flat HV Doppler wave patterns with blood flowing into direction of the heart. In this woman, the conversion from backward to forward flow relative to the heart occurs around 26 weeks. She also shows a transient reversal to positive HV A-values, at 32 weeks, which become negative again afterwards. The latter illustrates the intra-individual variation of HV Doppler wave patterns during uneventful third trimester pregnancy.

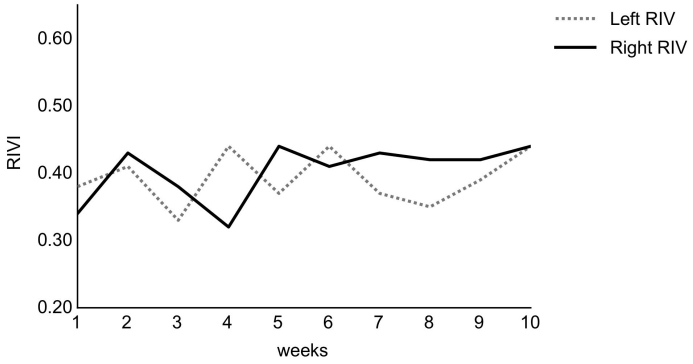

(A) Weekly evolution of RIVI in non-pregnant woman

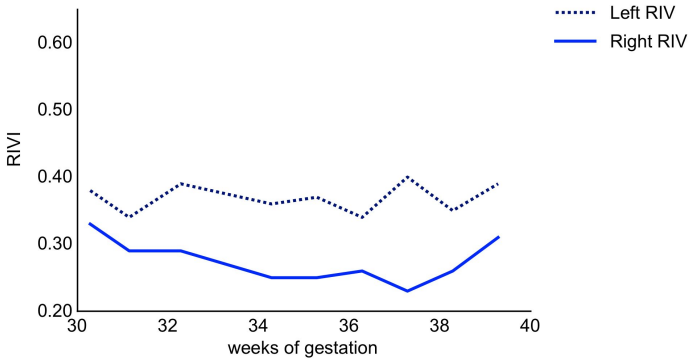

(B) Weekly evolution of RIVI in third trimester UP

Figure 2.5: Illustration of serial measurements of RIVI at weekly intervals in a non-pregnant individual (A; n=1), and during third trimester UP (B; n=1). During the third trimester of pregnancy, right RIVI values are consistently lower than those at the left kidney, and the pattern of oscillation, as illustrated in Figure 2.4 (A), seems to be less pronounced than in the non-pregnant woman.

As explained above, the venous tone and with it, the venous compliance are crucial determinants of CO by their direct impact on central venous pressure and cardiac preload, with the latter regulating SV by way of the Frank-Starling mechanism [52]. Venous compliance, which is much larger than arterial compliance [127], decreases with age, and is influenced by autonomic function, medication, systemic and/or vascular diseases [39], and parity [128, 129]. During uneventful pregnancy, venous compliance and distensibility are raised [18] returning to non-pregnant values in the first three months postpartum [130]. The ability of vessel walls to contract or relax and, as such, modulate compliance can be studied by duplex sonography: MxV and MnV are measured to calculate venous impedance index, which is the venous equivalent of arterial resistivity index (RI), defined as $\frac{MxV-MnV}{MxV}$ (see Equation 2.1) [90]. RIVI decreases with advancing pregnancy, which is consistent with an increase in venous compliance [89, 92, 94]. This observation supports the view that duplex sonography enables indirectly to generate non-invasive information on venous compliance and distensibility, with the RIVI measurement providing more or less quantitative information on tone and with it, resistance in the RIV. In this perspective, the undulating pattern of RIVI values in non-pregnant and pregnant women, illustrated in Figures 2.4 and 2.5, is interesting. The pattern suggests that the physiological process of maintaining venous tone requires a dynamic mechanism which enables achieving a fairly constant steady state, but in the mean time this mechanism is highly variable at different sites of the venous bed. The splanchnic venous bed plays a critical role in the homeostatic responses to changes in the intravascular volume [128]. Up to 33% of the total blood volume resides here, with $\frac{1}{3}$ located in the liver [39, 59]. Therefore, the splanchnic veins are called capacitance vessels [39, 58]. Sympathetic nerve stimulation can mobilize up to 21% of the total blood volume into the circulation [39], thus raising venous return markedly [131]. Again, the contribution of the liver in this process is important [39]. During pregnancy, the properties of the vascular walls of mesenteric veins change allowing the accommodation of a larger intravascular volume at the expense of compliance [129]. Doppler-derived estimations of hepatic flow during pregnancy have shown that hepatic perfusion increases significantly after 28 weeks most likely in conjunction with a rise in portal drainage [125]. This development is associated with dampening of the HV A-wave, indicating that during the second trimester of pregnancy the normal physiological backflow of right atrial blood during atrial contraction into the inferior vena cava and hepatic venous bed, reverses to constant forward moving flow towards the heart [93]. The pattern of change in HV A-velocities with advancing pregnancy mimics the one in plasma volume [93]. Therefore, the presence or absence of the HV A-wave [93], together with the manifestation of tri- or biphasic, and flat HV Doppler wave patterns, provide indirect information

on the hepatic venous filling state. In this context, the large intra-individual variation in types of HV Doppler waves during the third trimester of pregnancy is another interesting observation [93]. This suggests that the liver may be actively involved in the preservation of the circulating volume during the third trimester of pregnancy.

These observations are the basic elements of an interesting hypothesis, in which an active role is attributed to the maternal venous compartment in the regulation and maintenance of the pregnant woman's circulating volume, which is known to be crucial for a normal course and outcome of pregnancy.

Relevance of exploring maternal venous hemodynamics by duplex sonography

From this information summarized in this review, it is clear that data from duplex sonography studies into maternal venous hemodynamics add to the current knowledge of the normal function and adaptation of the venous compartment during pregnancy. Next to this, several papers have been published reporting abnormalities of venous Doppler parameters at the level of RIV or HV during PE [93, 94, 109]. Increased RIVI values and intrahepatic backflow during atrial contraction are more pronounced in early- than in late-onset PE (EPE and LPE, respectively) (see Chapter 2.3) [93, 94]. Even more, in EPE but not in LPE, RIV Doppler abnormalities were observed simultaneously in both kidneys and presented up to several weeks before clinical onset of disease [95]. These studies illustrate that the venous compartment is involved in PE-related maternal cardiovascular maladaptation and that its assessment may provide relevant information on some pathophysiological background mechanisms of gestational hypertensive disease and/or clinical work-up of PE. This particular topic is the subject of another review paper currently in progress (see Chapter 2.7).

2.1.6 Conclusion

The present review of the literature provides evidence for the feasibility of obtaining information on the maternal venous compartment by duplex ultrasonography. The reported results correlate well with known features of gestational cardiovascular physiology. Some of the observations open perspectives to generate and test new hypotheses on the physiological role of the venous compartment in the volume homeostasis during pregnancy. Finally, the resemblance of the maternal and fetal venous circulations [132, 133] suggests that a better insight into dynamic events in the maternal venous circulation may also contribute to a better understanding of fetal venous hemodynamics. Last but not least, ultrasonography is generally accepted as being safe in pregnancy, and it is an examination easily accessible to all pregnant women undergoing obstetric scanning. These arguments are an open invitation for obstetric ultrasonographers to initiate Doppler studies in the "forgotten field" of obstetrics: *the maternal venous compartment.*

2.1.7 Acknowledgements

We acknowledge all co-workers in the project of Doppler study on maternal venous hemodynamics, currently ongoing in our departments: Dr. G. Molenberghs, Center for Statistics at Hasselt University (Diepenbeek, Belgium), Dr. W. Ombelet, Chief of the Department of Obstetrics and Gynecology, Dr. G. Verswijvel and Dr. L. Meylaerts from the Department of Medical Imaging, and Dr. W. Van Mieghem and Dr. P. Vandervoort from the Department of Cardiology, at ZOL. We also thank Mr. E. Van Herck from Laboratory AML (Antwerp, Belgium) and Mr. J. Bollen and Mrs. L. Grondelaers from the Department of Press and Communication (ZOL) for their help with visual presentations.

2.2 Feasibility of the maternal venous impedance index

Reproducibility and repeatability of maternal venous Doppler flow measurements in renal interlobar and hepatic veins

letter to the Editor

Tinne MESENS, ***Kathleen TOMSIN****, Geert MOLENBERGHS, Wilfried GYSELAERS*

Ultrasound in Obstetrics and Gynecology
Ultrasound Obstet Gynecol 2010, 36: 120-125

Many physiological variables are known to interfere with venous return: cardiac contractility, respiration, body position, gravidity, external compression, and morphological and embryological variations [51], and Doppler velocimetry is subject to intra- and inter-observer variation [110]. For these reasons, sonographers tend to refrain from performing venous Doppler velocimetry. While Doppler flow characteristics of maternal RIV and HV have now been described in both UP and those affected by PE [89, 91, 93, 94, 109], some of these studies being performed using a standard protocol with a reported intra-observed ICC of .88 [93, 94], there are no available data regarding the inter-observer correlation and/or reproducibility of this methodology. We therefore evaluated the repeatability and reproducibility of measurements of RIV MxV, MnV, and RIVI (see Equation 2.1), and of HV X-, V-, Y-, and A-velocities, performed by two ultrasonographers (Wilfried Gyselaers; Tinne Mesens) according to a reported protocol [93, 94] at the Department of Obstetric Ultrasonography (ZOL), comparing mean values of three consecutive measurements rather than following convention and relying on a single value.

A set of measurements is said to have compound symmetry if there is constant variance between measurements and the correlations between all pairs of measures are the same. We assumed a compound symmetrical structure among six measurements of the same parameter (three consecutive measurements of each of the two observers), using a linear mixed model with restricted maximum likelihood estimation to calculate intra- and inter-observer ICC, intra-observer repeatability and inter-observer reproducibility coefficients with 95% confidence intervals for measurement differences, coefficients of variation, and mean inter-observer differences with 95% confidence intervals [134]. Appropriate model checking was performed.

Three groups each of 24 women were assessed: *1*) only by sonographer 1, *2*) only by sonographer 2 (Table 2.1), and *3*) by both sonographers 1 and 2 (Table 2.2) . Both intra- and inter-observer ICCs for RIVI and HV A-velocity were $\geq .66$, being consistently higher than those for all other velocity measurements. 95% of confidence intervals for the repeatability and the reproducibility coefficients overlapped, thereby excluding significant systematic intra- or inter-observer differences and allowing for assessment of clinical relevance, as discussed below. Apart from HV A-velocity, the coefficient of variation was < 1 for all measurements, which is indicative for a good model of fit. Mean inter-observer differences were $\leq .02$ for RIVI and the 95% confidence intervals were narrow. This indicates that both sonographers tended to agree without showing a systematic (mean inter-observer difference far from zero) or a random (wide 95% confidence intervals) pattern of variation. For HV velocimetry,

mean inter-observer differences and 95% confidence intervals were smallest for HV A-velocity, but these values were still higher than those for RIV Doppler parameters.

Table 2.1: Intra-observer correlation

	Sonographer 1 (n=24)			Sonographer 2 (n=24)		
	ICC	Repeatability Coefficient 95% Confidence Interval	CV[1]	ICC	Repeatability Coefficient 95% Confidence Interval	CV[2]
Left kidney						
MxV (cm/s)	.60	3.77 (2.34;5.19)	0.23	.79	8.22 (5.63;10.80)	0.39
MnV (cm/s)	.60	2.53 (1.56;3.49)	0.24	.71	5.13 (3.40;6.85)	0.46
RIVI	.76	0.15 (0.10;0.20)	0.16	.83	0.25 (0.17;0.32)	0.23
Right kidney						
MxV (cm/s)	.65	4.82 (3.07;6.56)	0.24	.70	7.39 (4.90;9.88)	0.35
MnV (cm/s)	.63	3.83 (2.10;4.54)	0.25	.60	4.54 (2.86;6.22)	0.40
RIVI	.89	0.23 (0.16;0.30)	0.24	.82	0.31 (0.21;0.40)	0.30
Liver						
A (cm/s)	.93	17.14 (12.10;22.17)	2.38	.87	14.14 (9.93;18.34)	1.99
X (cm/s)	.62	6.74 (4.25;9.23)	0.26	.53	4.23 (2.53;5.93)	0.28
V (cm/s)	.93	11.12 (7.85;14.39)	0.70	.75	8.63 (5.83;11.43)	0.76
Y (cm/s)	.78	8.46 (5.72;11.20)	0.33	.26	2.56 (.78;4.33)	0.30

Table 2.2: Inter-observer correlation (n=24)

	ICC	Repeatability Coefficient 95% Confidence Interval	Difference[3]
Left kidney			
MxV (cm/s)	.33	7.51 (2.72;12.30)	0.37 (-0.61;1.35)
MnV (cm/s)	.32	4.75 (1.45;7.50)	0.14 (-0.47;0.76)
RIVI	.66	0.19 (0.07;0.31)	0.01 (-0.01;0.04)
Right kidney			
MxV (cm/s)	.23	9.77 (5.38;14.17)	-0.29 (-1.37;0.79)
MnV (cm/s)	.23	6.43 (3.34;9.53)	-0.27 (-1.00;0.46)
RIVI	.73	0.30 (0.18;0.42)	0.02 (-0.01;0.05)
Liver			
A (cm/s)	.74	7.97 (1.66;14.28)	0.38 (-0.77;1.53)
X (cm/s)	.33	8.57 (2.98;14.16)	1.44 (0.31;2.57)
V (cm/s)	.56	4.19 (-3.32;11.70)	1.38 (0.49;2.27)
Y (cm/s)	.24	8.52 (3.13;13.92)	1.73 (0.62;2.83)

[1]Coefficient of Variation

[2]Coefficient of Variation

[3]Mean inter-observer difference (95% Confidence Interval)

According to our data, Doppler velocimetry in the HV is much more variable than that in the RIV; this can be explained by the morphology of the hepatic venous tree, which contains three main branches with or without accessory branches, and the presence of intra-hepatic arteriovenous and venoportal shunts. Different patterns of HV Doppler waves have been reported in healthy subjects without liver disease [62].

Our results show that our methodology of Doppler measurement of RIVI and HV A-velocity is repeatable and reproducible within our department. Expansion of this study to more sonographers and centers is logical and mandatory for the evolution of this project. We conclude that we can use this methodology to: *1*) study gestational (patho)physiology of maternal venous hemodynamics, *2*) link maternal venous Doppler parameters to other clinical, biochemical, or ultrasound parameters of gestational disease, and *3*) assess the rationale of introducing this methodology into clinical work-up and prediction of PE [95].

2.3 The venous impedance index in preeclampsia

Maternal renal interlobar vein impedance index is higher in early- than in late-onset preeclampsia

original paper

Wilfried GYSELAERS, Tinne MESENS, ***Kathleen TOMSIN****,*
Geert MOLENBERGHS, Louis PEETERS

Ultrasound in Obstetrics and Gynecology
Ultrasound Obstet Gynecol 2010, 36: 69-75

2.3.1 Abstract

Objectives To test the hypothesis that Doppler characteristics of maternal RIV are different between pregnancies affected by EPE and those affected by LPE.

Methods A gestational age of 34 weeks was considered to differentiate EPE from LPE. All women had a renal duplex scan according to a standard protocol, with known intra-observer ICC (.88). RIV MxV and MnV were measured on two occasions (between 28 and 32, and between 34 and 37 weeks) in 18 women with uncomplicated pregnancy (UP). In women with EPE (n=32) or LPE (n=41), these variables were measured once, within three days following hospital admission. Delta velocity (Δ V) was calculated as $MxV - MnV$ and the RIVI was calculated as $\frac{\Delta V}{MxV}$ (see also Equation 2.1). Data on neonatal outcome and maternal renal function were obtained for UP and those with EPE and LPE, and group-specific means $\pm$ were calculated and compared.

Results Compared with UP, the RIVI of both left and right kidneys was higher in those with EPE (0.49$\pm$ 0.13 vs. 0.36$\pm$ 0.04, P=.0001, and 0.46$\pm$ 0.15 vs. 0.33$\pm$ 0.04, P=.0008) and in those with LPE (0.41$\pm$ 0.07 vs. 0.37$\pm$ 0.06, P=.04, and 0.38$\pm$ 0.12 vs. 0.30$\pm$ 0.05, P=.009). RIVI was higher in pregnancies with EPE than in those with LPE ($P \leq$ .01), and this difference was associated with lower median birth-weight percentiles (22.5 (interquartile range (IQR), 15.0-35.0) vs. 40.0 (IQR, 12.0-55.0), P=.01), higher maternal serum uric acid concentrations (419$\pm$ 84 vs. 374$\pm$ 85 μ mol/L, P=.03) and higher proteinuria (4131$\pm$ 3885 vs. 1190$\pm$ 1133 mg/24h, $P <$ .0001).

Conclusion Maternal vascular adaptation in PE is associated with abnormal Doppler findings in the venous compartment. RIVI is higher in EPE than in LPE pregnancies, and this is associated with lower birth weight percentiles and higher proteinuria.

2.3.2 Introduction

Evidence is growing that EPE and LPE, both characterized by gestation-induced hypertension and proteinuria in the active phase, present different hemodynamic background mechanisms in the latent phase of the disease [135]. Easterling *et al.* reported different types of PE depending on the degree of peripheral resistance: in PE with high total peripheral resistance, delivery was earlier and birth weight percentiles were lower than in PE with low total peripheral resistance [136]. They also reported that low-resistance PE was associated with high maternal CO and delivery near term [137].

Vasoconstrictor agents have been noted to be active much earlier in EPE than in LPE pregnancies [2]. Doppler studies of the uterine artery (UtArt) have shown that abnormal notching of the Doppler waveform, suggestive of increased arterial wall resistance, with or without the combination of angiogenic factors [138], predicts EPE pregnancy much better than it does LPE pregnancy [88, 139].

Maternal cardiac function has also been reported to differ between EPE and LPE pregnancies: at 24 weeks of gestation, maternal CO was lower and total peripheral resistance was higher in the latent phase of EPE compared with LPE pregnancies [135]. In the first trimester of pregnancy, the mean arterial pressure was increased in women subsequently developing PE, as compared to pregnancies with normal outcome, and this was associated with increased CO in the group with normal fetal growth and with increased total peripheral resistance in the group with impaired fetal growth (FGR) [140].

It is still unclear whether EPE and LPE are also accompanied by differences in Doppler blood flow profiles in the maternal venous compartment. The venous impedance index (see Equation 2.1) is considered the Doppler equivalent of the arterial resistance index. A number of recent studies [89, 94, 141] provide evidence for the RIVI to be a reproducible Doppler-derived parameter of intrarenal venous vascular function, both during pregnancy and postpartum. RIVI was found to be higher in PE than in normal pregnancies, and this was associated with fast decelerating forward flow during the last hundred milliseconds of the venous Doppler wave [109]. This phenomenon, the so-called *venous pre-acceleration nadir* (VPAN), was linked to backflow of blood from the heart into the venous circulation during atrial contraction, due to lack of a valve mechanism [92].

This study aimed to compare RIV Doppler parameters between UP and those

with EPE or LPE in relation to parameters of neonatal outcome and maternal renal function.

2.3.3 Methods

Approval of the local ethics committee was obtained before study commencement and all women gave informed consent to participate. Only singleton pregnancies were included of women without known diseases, such as chronic hypertension, thrombophilia, diabetes, and glomerular or rheumatic disease. We evaluated 18 women with UP and term birth of an infant with normal weight. These women were evaluated twice during pregnancy (between 28 and 32, and again between 34 and 37 weeks). We also included 73 women with PE, who were evaluated once shortly after admission at the maternal-fetal medicine unit (ZOL). PE was defined as gestation-induced hypertension $\geq 140/90$ mmHg on at least two occasions combined with proteinuria > 300 mg/24h [21, 22]. We defined EPE as PE diagnosed at a gestational age < 34 weeks and LPE as PE diagnosed at ≥ 34 weeks.

All women were examined according to a standard protocol [94] with a known intra-observer ICC of .88. All examinations were performed by the same ultrasonographer (Wilfried Gyselaers), using a 3.5-7.0 MHz probe (Hitachi EUB 6500, Hitachi Medical Systems, Heverlee, Belgium). The methodology is presented schematically in Figure 2.6. All women were placed in a supine position and both kidneys were scanned in the transverse plane just above the renal hilus. The interlobar arteries and veins were identified using color Doppler flow mapping [141]. The impact of breathing movements on the ultrasound image was demonstrated to every patient and the relevance of breath-holding during Doppler measurements was explained and demonstrated. Once the patient was familiar with the instructions of the ultrasonographer, the examination was performed as follows. *1*) A simultaneous Doppler signal of both interlobar arteries and veins was obtained for unequivocal identification of the examined vessels. *2*) The real-time ultrasound image in combined B-D mode was frozen after visualization of at least two or three similar Doppler flow patterns during interrupted breathing. *3*) As the direction of the Doppler beam was mostly parallel to the examined vessels, adjustment of the beam was rarely needed. If it was, the axis of adjustment was always within $\pm 30\,^{\circ}$. *4*) MxV and MnV were plotted and printed out. Throughout the course of the ultrasound examination, the ultrasonographer was blinded to the results depicted on screen. *5*) For every woman, three consecutive measurements were printed out for each kidney. *6*) After the scan, Δ V ($MxV - MnV$) and RIVI (see Equation 2.1) were calculated.

The mean of three values for each MxV, MnV, Δ V, and RIVI was considered the kidney-specific value and was recorded in the database. The reproducibility of this methodology was evaluated by defining RIVI twice for each kidney in a set of 24 women: the intra-observer ICC was calculated using restricted maximum likelihood estimation for the linear mixed model [134, 142].

The following patient demographics and outcome data were obtained from all women included in the study: maternal age, parity, first-trimester body mass index (BMI), smoking habits, history of fetal loss or gestational hypertensive disorders and/or FGR, current use of antihypertensives or anticoagulation, mode of delivery, gestational age at delivery, birth weight, population-specific birth weight percentile [143], maternal serum concentrations of uric acid, 24h proteinuria, and creatinine clearance. Data were categorized into groups: UP, EPE, and LPE. Because RIV blood flow is reported to change in the third trimester [94, 141], UP-RIV Doppler parameters were also categorized into 30-week and 36-week measurements. PE was categorized into those with and those without infants born small-for-gestational age ($\leq 10^{th}$ percentile, SGA). Student's t-test was used for statistical comparison at the nominal level $\alpha < .05$).

A repeated-measures analysis of covariance (repeated measures ANCOVA) was applied to compare the impact of advancing gestation on RIVI values of both kidneys between UP, EPE, and LPE, using the SAS procedure MIXED with restricted maximum likelihood (SAS/STAT software, version 9.2 (2007), SAS Inst. Inc., Cary, NC, USA) [134, 142].

2.3.4 Results

Table 2.3 lists the patient characteristics of women in the three study groups. The women in the EPE and LPE groups differed from those in the UP one, with lower maternal age and gestational age at delivery, higher BMI, use of medication, and Cesarean section rate. The proportion of SGA neonates was higher in the EPE and LPE groups than in the UP groups. The proportion of infants with birth weight $\geq 90^{th}$ percentile (large-for-gestational age, LGA) did not differ between LPE and UP groups, but none was observed in the EPE group. Compared to neonates of women with LPE, the median birth weight percentile of those of women with EPE was lower and both maternal serum uric acid and 24h proteinuria were higher.

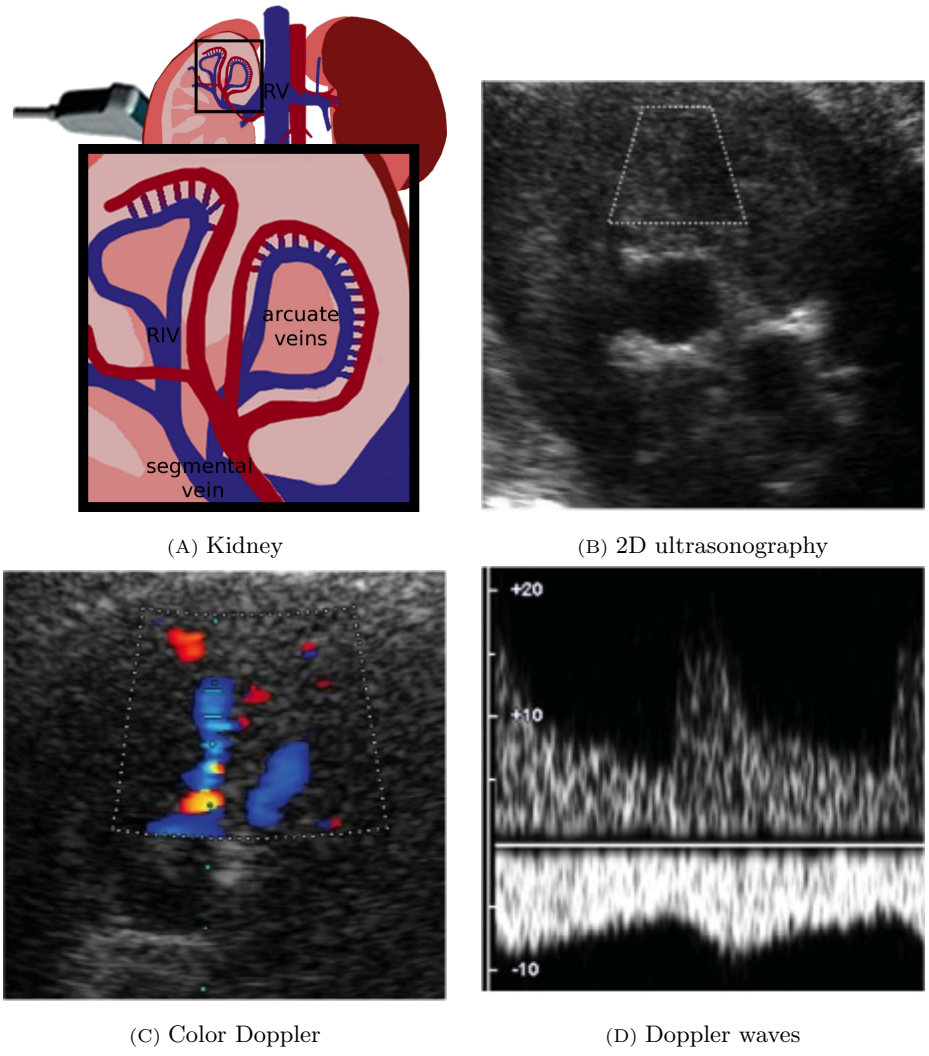

(A) Kidney (B) 2D ultrasonography

(C) Color Doppler (D) Doppler waves

Figure 2.6: Schematic illustration of the methodology used in this study. (A) Anatomy of the intrarenal venous system. The RV collects blood from the segmental veins, which are located at the level of the renal pelvis. The renal arcuate veins are present in the cortex underneath the renal surface and drain their blood into the RIV, which are located between the renal pelvis and the cortex. (Adapted from http://www.nlm.nih.gov/medlineplus/ency/images/ency/fullsize/8817.jpg). (B) Two-dimensional ultrasound image of the kidney, scanned in the transverse plane as illustrated by the Doppler probe in panel (A). The white trapezium marks the area between renal pelvis and cortex, where the RIV are located. (C) Color Doppler image of the renal interlobar vessels. Renal interlobar arteries are red, indicating blood flow towards the Doppler beam, while veins are blue. Note that the direction of the Doppler beam is parallel to the examined vessels, reducing the need for Doppler angle correction. (D) Doppler waves obtained from both renal interlobar arteries (upper waveform) and veins (lower waveform).

In both EPE and LPE groups, RIVI values were not different between pregnancies with and those without infants born SGA (EPE; left kidney: 0.55 ± 0.14 vs. 0.48 ± 0.12, $P = .17$, and right kidney: 0.53 ± 0.14 vs. 0.44 ± 0.15, $P = .20$; LPE; left kidney: 0.40 ± 0.05 vs. 0.41 ± 0.07, $P = .80$, and right kidney 0.35 ± 0.06 vs. 0.38 ± 0.14, $P = .47$).

Table 2.4 shows the intergroup comparison of RIV Doppler parameters between UP (30 weeks), EPE, LPE, and UP (36 weeks) groups. RIVI in EPE pregnancies was approximately 30% higher than it was in UP. This observation was mainly due to the significantly lower MnV values and higher Δ V values in EPE pregnancies. In LPE pregnancies, MnV was also significantly lower than it was in UP, and RIVI was significantly higher; however, this was not associated with a higher Δ V. Both RIVI and Δ V were significantly higher in EPE than in LPE pregnancies.

The equations for linear regression curves of RIVI evolution (Y) according to gestational age (X) in the left kidney were:

$$\mathrm{Y_{UP}} = 0.3059 + 0.0018\mathrm{X}$$

$$\mathrm{Y_{EPE}} = 1.059 - 0.018\mathrm{X}$$

$$\mathrm{Y_{LPE}} = 0.2616 + 0.004\mathrm{X}$$

$$\mathrm{Y_{PE}} = 0.8816 - 0.0128\mathrm{X}$$

For the right kidney, these equations were:

$$\mathrm{Y_{UP}} = 0.495 - 0.0055\mathrm{X}$$

$$\mathrm{Y_{EPE}} = 1.3572 - 0.0292\mathrm{X}$$

$$\mathrm{Y_{LPE}} = 0.4988 - 0.0033\mathrm{X}$$

$$\mathrm{Y_{PE}} = 0.9699 - 0.0163\mathrm{X}$$

As illustrated in Figure 2.8 (A), the evolution of RIVI was significantly different between UP and PE for both left ($P < .0001$) and right ($P = .009$) kidneys, due mainly to the different evolution of RIVI in the EPE group compared with the UP group, which was significantly different for both left ($P = .0016$) and right ($P = .001$) kidneys. The differences between the LPE group and the UP group were not significant ($P \geq .725$ for both kidneys). This is illustrated graphically in Figure 2.8 (B).

Table 2.3: Patient characteristics of the three study groups: UP, EPE, and LPE. Data are given as mean±standard deviation, n (%), or median (IQR). All characteristics are presented as defined at the first antenatal visit, the time of PE diagnosis, or delivery. n.a.=not applicable.

	UP		PE			
			EPE		LPE	
	n=18	P-value[4]	n=32	P-value[5]	n=41	P-value[6]
Maternal characteristics						
Maternal age (years)	31.1±3.5	.02	28.1±4.7	.99	28.1±4.8	.02
Parity	0.7±0.8	.36	0.5±0.7	.07	0.3±0.5	.02
BMI (kg/m^2)	21.2±2.6	.001	25.5±4.8	.75	25.8±5.1	.0006
Smoker (n(%))	0		1 (3.1)	.33	5 (12.2)	
Obstetric history						
Fetal loss (n(%))	7 (38.9)	.48	8 (25.0)	.98	9 (22.0)	.31
PE/IUGR (n(%))	0		4 (12.5)	.90	6 (14.3)	
Medication during pregnancy						
Antihypertensives (n(%))	0		10 (32.3)	.02	3 (7.3)	
Anticoagulation (n(%))	0		3 (9.7)		0	
Pregnancy outcome						
Cesarean section (n(%))	2 (11)	$<$.0001	26 (83.9)	.001	18 (43.9)	.03
Gestational age at delivery (weeks)	39.6±1.4	$<$.0001	31.3±2.9	$<$.0001	37.2±1.6	$<$.0001
Birth weight (g)	3515±352		1456±527		2861±637	
Birth weight (median (IQR))	58 (50;74)	$<$.0001	23 (15;35)	.01	40 (12;55)	.12
Birth weight						
$\geq 90^{th}$ percentile (n(%))	3 (16.7)		0		3 (7.3)	.53
$\leq 10^{th}$ percentile (n(%))	0		6 (18.8)	.78	10 (24.4)	
Renal function						
Maternal serum uric acid (μmol/L)	n.a.		419±84	.03	374±85	
Proteinuria (mg/24h)	n.a.		4131±3385	$<$.0001	1190±1133	
$>$5 g/24h (n(%))			13 (40.6)		0	
Creatinine clearance (mL/min)	n.a.		114.0±39.0	.13	127.9±36.9	

[4] UP vs. EPE
[5] EPE vs. LPE
[6] UP vs. LPE

Table 2.4: Comparison between UP at 30 weeks and at 36 weeks, EPE, and LPE of RIV Doppler characteristics. Data are given as mean± standard deviation.

	UP at 30 weeks		EPE		LPE		UP at 36 weeks
	n=18	P-value[7]	n=32	P-value[8]	n=41	P-value[9]	n=18
Gestational age (weeks)	30.0± 1.9	.37	30.7± 2.8	< .0001	36.7± 1.6	.07	36.0± .5
Left kidney							
MxV (cm/s)	9.2± 1.7	.19	8.5± 1.9	.01	7.4± 1.7	.04	8.4± 1.4
MnV (cm/s)	5.9± 1.2	.0002	4.3± 1.4	.68	4.4± 1.1	.02	5.2± 1.0
Δ V (cm/s)	3.3± 0.6	.02	4.2± 1.5	< .0001	3.0± 0.8	.70	3.1± 0.5
RIVI	0.36± 0.04	.0001	0.49± 0.13	.0006	0.41± 0.07	.04	0.37± 0.06
Right kidney							
MxV (cm/s)	10.3± 2.4	.31	9.6± 2.1	.16	8.9± 2.5	.44	9.4± 1.9
MnV (cm/s)	6.9± 1.6	.0009	5.1± 1.8	.38	5.5± 1.8	.03	6.6± 1.4
Δ V (cm/s)	3.4± 0.9	.02	4.5± 1.9	.01	3.4± 1.8	.19	2.8± 0.8
RIVI	0.33± 0.04	.0008	0.46± 0.15	.01	0.38± 0.12	.009	0.30± 0.05

[7] UP at 30 weeks vs. EPE

[8] EPE vs. LPE

[9] UP at 36 weeks vs. LPE

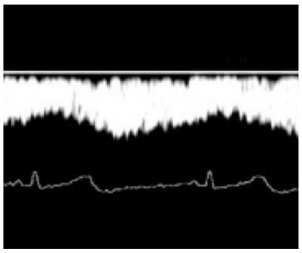

(A) UP

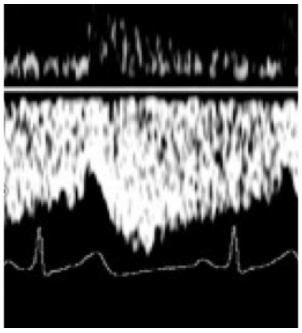

(B) LPE

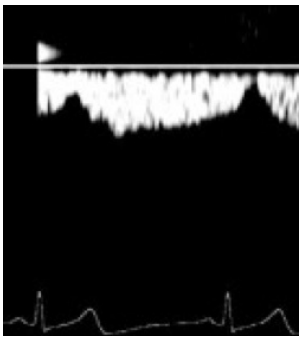

(C) EPE

Figure 2.7: Examples of Doppler waveforms from RIV in UP and PE. Doppler waves are presented together with the maternal ECG-signal, to illustrate the time-relation between the P-wave of the ECG, initiating cardiac atrial contraction, and the sudden sharp deceleration of flow during the last hundred milliseconds of the Doppler wave resulting from backflow of blood into the venous circulation following atrial contraction, which is the so-called VPAN [92]. (A) Uniform Doppler wave in a 28-week UP, with absence of VPAN. (B) Doppler waveform with a small but clearly visible VPAN, as observed frequently in LPE but also in late third-trimester UP. (C) Doppler wave from a pregnancy with EPE, with a deep VPAN.

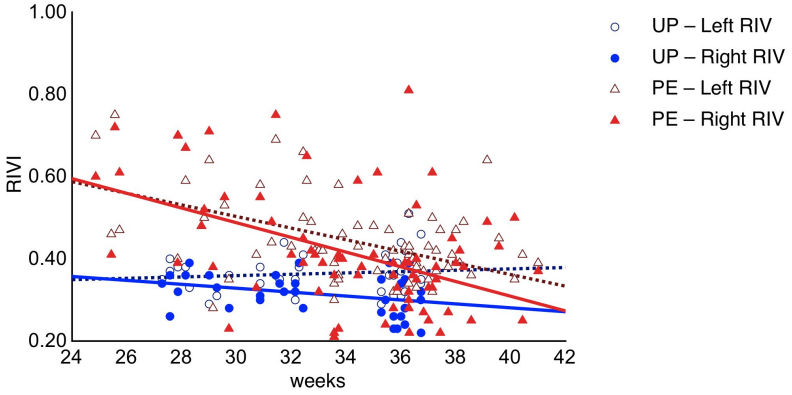

(A) Scatter diagram of RIVI in UP and PE

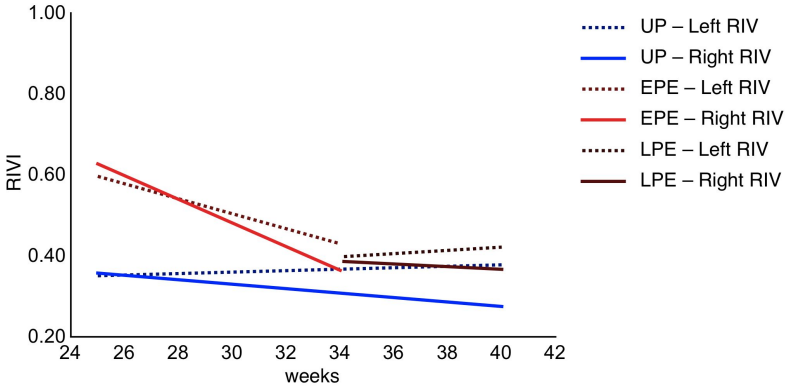

(B) Evolution diagram of RIVI in UP, EPE, and LPE

Figure 2.8: (A) Scatter diagram of measured values of RIVI relative to gestational age for UP in left (blue open circles) and right (blue closed circles) kidneys and for PE in left (red open triangles) and right (red closed triangles) kidneys. Lines show regression. Evolution of RIVI in both left and right kidneys was significantly different between UP and those with PE ($P < .01$). (B) This differing evolution of RIVI can be attributed mainly to its evolution in EPE, which was significantly different from that in UP in both left and right kidneys ($P \leq .001$); the evolution of RIVI was not significantly different between UP and those with LPE. As in (A), blue lines indicate normal left and right kidney regression lines and red lines are those for PE left and right kidneys.

2.3.5 Discussion

Methods to study human venous hemodynamics are complex and often difficult to perform in pregnancy [58]. Doppler measurement of RIVI seems to be a simple non-invasive method to study renal venous blood flow dynamics, both in non-pregnant and pregnant state [89, 94, 141]. We reported previously a high intra-observer correlation coefficient for RIVI measurement, supporting its validity and reproducibility [94]. Using this technique we found increased RIVI in PE diagnosed before 34 weeks [94]. In the present study, we evaluated whether RIVIs in EPE and LPE were associated with different neonatal outcome values and parameters of maternal renal function.

Our results confirm former observations that RIVI is higher in PE than in UP [94, 109]. This can be explained by lower MnV values in both EPE and LPE (Table 2.4). Bateman *et al.* observed in PE a sharp deceleration of forward flow at the end of the RIV Doppler wave and suggested that this could result from a selective increase of downstream resistance [109]. As we have reported elsewhere, there is a time relation between VPAN and cardiac right atrial contraction [92], suggesting that backflow of blood from the heart into the venous circulation during atrial contraction is responsible for this temporary increased resistance against forward venous flow (Figure 2.7). Our current data show that this countercurrent phenomenon is more pronounced in EPE than it is in LPE (Table 2.4): *1*) the differences between UP and EPE are more pronounced than are those between UP and LPE, and *2*) in EPE, but not in LPE, reduced MnV values are associated with increased Δ V values. From our current observations, it is unclear whether this reduction of MnV in PE results from PE-related reduction of intravascular volume [13], from venous distensibility [18], or from both. Our analysis also shows that the impact of gestational age on RIVI measurements is significantly different between EPE and UP, but not between LPE and UP (Figure 2.8).

Our data on neonatal outcome agree with the observations by Easterling *et al.*, who reported lower birth weights in high-resistance PE than in low-resistance PE, due to earlier delivery and lower percentile birth weights for gestational age [136]. As shown in Table 2.3, we observed that gestational age at delivery was approximately 6 weeks earlier in EPE than in LPE, and that median neonatal birth weight percentiles in EPE were significantly lower. Additionally, we found infants with a birth weight $\geq 90^{th}$ percentile in UP and LPE pregnancies, but not in EPE. Contrary to Khaw *et al.*, who reported different vascular characteristics between PE pregnancies with and without FGR [140], we found no difference in RIVI values in PE pregnancies

with and without infants born SGA. It should be emphasized that in this study our observations in PE were not made in the latent phase of the disease but only when hypertension and proteinuria were both manifest.

Our observations also provide evidence for another important aspect of gestational hypertensive disorders. Parameters of maternal renal function, such as serum uric acid and 24h proteinuria, but not creatinine clearance, were significantly more abnormal in EPE than in LPE pregnancies (Table 2.4). It has been reported that in formerly PE women, postpartum persistence of cardiovascular abnormalities are accompanied by impaired venous drainage of the conjunctival microcirculation, reflected in dilated venules and tortuous capillaries [144]. Our data provide evidence for impaired drainage of venous blood from the kidneys during PE. The elevated impedance of RIV and the countercurrent venous flow during atrial contraction in PE provide indirect evidence for impeded venous drainage from the kidneys. Impaired renal venous drainage also occurs in clinical syndromes, such as renal vein thrombosis [123], abdominal compartment syndrome [145], and nutcracker syndrome [100]. These syndromes present with proteinuria, with or without hypertension. Under experimental conditions, a pressure rise in the RV has been reported to provoke proteinuria [146]. It is necessary to further explore the role of increased venous impedance and impaired venous drainage of blood from the kidneys in the pathogenesis of PE-related proteinuria.

We conclude from the current study that Doppler parameters of RIV differ between UP and PE, and that these differences are more pronounced in EPE than in LPE. We are aware that, because several tests were carried out simultaneously, one must be careful not to overinterpret differences found. However, our observation illustrates that the severity of PE-related vascular abnormalities in PE is reflected in Doppler parameters of the venous compartment and relates to neonatal birthweigth percentile and maternal renal function. Our data suggest impaired drainage of venous blood flow from the kidneys during PE, suggesting a need for further exploration of the role of abnormal renal venous hemodynamics in the pathogenesis of PE-related proteinuria.

2.3.6 Acknowledgements

We acknowledge Professor M. Hanssens of the Catholic University of Louvain, Belgium for her useful recommendations towards the initiation of this study. We also thank Mrs. V. De Loenen for assisting in the administration and data collection.

2.4 Feasibility of the maternal venous pulse transit time

Time interval between maternal electrocardiogram and venous Doppler waves in normal pregnancy and preeclampsia:

a pilot study

Kathleen TOMSIN*, Tinne MESENS, Geert MOLENBERGHS, Louis PEETERS, Wilfried GYSELAERS*

Ultraschall in der Medizin/The European journal of Ultrasound
Ultraschall in Med 2010, 31: 1-7

2.4.1 Abstract

Purpose To evaluate the time interval between maternal ECG- and venous Doppler waves at different stages of UP and in PE.

Materials and Methods Cross-sectional pilot study in 40 singleton UP, categorized in four groups of ten according to gestational age: *1*) 10-14 weeks (UP1), *2*) 18-23 weeks (UP2), *3*) 28-33 weeks (UP3), and *4*) $\geq$37 weeks (UP4) of gestation. A fifth group of ten women with PE was also included. A Doppler flow examination at the level of RIV and HV was performed according to a standard protocol, in association with a maternal ECG. The time interval between the ECG P-wave and the corresponding A-deflection of the venous Doppler waves was measured (PA) and expressed relative to the duration of the cardiac cycle (RR), and labeled PA/RR.

Results In HV, the PA/RR is longer in UP4 than in UP1 (0.48 ± 0.15 vs. 0.29 ± 0.09, $P\leq.001$). When all UP groups were compared, the PA/RR increased gradually with gestational age. In PE, the HV PA/RR is shorter than in UP3 (0.25 ± 0.09 vs. 0.42 ± 0.14, $P<.01$) and this difference persisted under antihypertensive treatment (0.28 ± 0.06 vs. 0.42 ± 0.14, $P\leq.01$, $n=6$). Similar results were found in both kidneys. In UP1 but not in UP3 or UP4, the HV PA/RR is shorter in the liver than in the left and right kidney (0.29 ± 0.09 vs. 0.38 ± 0.12, $P<.01$, and vs. 0.36 ± 0.09, $P\leq.01$).

Conclusion The PA/RR is organ-specific and gestation-dependent, and is considered to relate to venous vascular tone and/or intravascular filling. Increased values at advanced gestational stages are consistent with known features of maternal cardiovascular adaptation. Shorter values in PE are consistent with maternal cardiovascular maladaptation mechanisms. Our pilot study invites more research on the relevance of the time interval between maternal ECG- and venous Doppler waves as a new parameter for studying the gestational cardiovascular (patho)physiology of the maternal venous compartment by duplex sonography.

2.4.2 Introduction

Maternal vein hemodynamics is a new area to be explored by duplex sonography [92]. During UP, a decrease of RIVI [89, 141] and flattening of the HV-waveforms [91, 93] are observed. In PE, however, the RIVI is above the normal $95/^{th}$ percentile [94] and HV-waveform flattening is less frequent [93]. PE-related venous Doppler wave abnormalities are more pronounced in EPE than in LPE (see Chapter 2.3) [93, 94, 95, 147]. These observations illustrate that duplex sonography of the maternal venous compartment may help to unravel some of the cardiovascular background mechanisms of PE, and that maternal vein Doppler measurements seem promising for the prediction and clinical work-up of PE [95, 147].

Unfortunately, venous Doppler waves often show atypical patterns, which make it difficult to identify the individual Doppler wave characteristics and measure Doppler parameters correctly [62]. Venous Doppler waves indirectly reflect *right cardiac atrial function,* and wave deflections are identical to the known wave characteristics of the jugular vein [148, 149]: the A-wave is triggered by backflow of blood from the right atrium into the vena cava during atrial contraction [77, 150]. The latter in turn is initiated by the P-wave of the ECG [78]. Since A and P both correspond to right atrial contraction, these parameters are related in time. This is illustrated in Figure 2.9.

The goal of this study was to evaluate whether *1*) the addition of the maternal ECG to duplex sonography would facilitate the interpretation of venous Doppler flow characteristics and *2*) whether the time interval between ECG- and Doppler waves (PA) is subject to change in UP and in PE. If so, this time interval requires further assessment of its role as a potential new parameter for the prediction and work-up of PE.

2.4.3 Methods

A cross-sectional pilot study was performed in a population of randomly selected pregnant women, presenting at the department of obstetric ultrasound or admitted to the maternal-fetal medicine unit (ZOL). Approval of the local ethical committee was obtained before study onset (MEC ZOL reference: 08/049). Singleton pregnancies of women without history or symptoms of renal or liver diseases were included, thus avoiding disease-induced flow changes [151]. UP was categorized into four groups of ten women, according to gestational age at inclusion: *1*) 10-14 weeks or first trimester (UP1), *2*) 18-23 weeks or second trimester (UP2), *3*) 28-33 weeks or third trimester

(UP3), and *4*) ≥ 37 weeks or term (UP4) of gestation. A fifth group of women with PE was also included. PE was defined as gestational hypertension ($\geq 140/90$ mmHg), measured on at least two occasions $\geq$ six hours apart, associated with *de novo* proteinuria ≥ 300 mg per 24 hours [21].

After informed consent, all women underwent a conventional ultrasound scan together with a Doppler flow examination of both kidneys and of the liver, simultaneously with an ECG. All examinations were performed by the same ultrasonographer (Wilfried Gyselaers) using a 3.5-7.0 MHz probe (Hitachi EUB 6500). All women were examined in a supine position, and both kidneys and the liver were scanned in the transverse plane. RIV and HV (left, middle, and right) were identified using color Doppler flow mapping. Doppler signals were obtained between the renal pyelon and cortex at the level just above the hilus and in the craniocaudal midportion of each of the three HV branches. The impact of breathing movements on the ultrasound image and of maternal limb movements on the ECG-signal was demonstrated to every woman and the relevance of breath-holding during Doppler measurements was explained and demonstrated. The examination was performed according to the protocol reported elsewhere [93, 94]. For every woman, three consecutive Doppler flow images of each kidney and of the liver were stored digitally on the hard disk of the scanner for later analysis by the principal researcher (Kathleen Tomsin).

Triphasic and non-triphasic HV Doppler wave patterns were labeled "typical" and "atypical", respectively [62]. Fractions of the atypical patterns were calculated for each group and compared statistically using the t-test at nominal level $\alpha = .05$.

The time intervals between two consecutive Doppler waves were measured as the AA and XX intervals (Figure 2.9 (A and B)). Similarly, the time intervals (ms) between two consecutive ECG-waves were recorded as PP and RR intervals. These time intervals all express the duration of the cardiac cycle (ms). ICC between the corresponding characteristics 'PP and AA' and 'RR and XX' were calculated as explained further. Finally, the time interval (ms) was measured between the ECG P-wave and the Doppler wave A-deflection (PA) (Figure 2.9 (A and B)). To ensure consistency in measurements for every type of Doppler waveform, the PA was measured between the peak of the ECG P-wave and lowest velocity of the Doppler A-wave. As the heart rate (HR) increases with advancing gestation [11], all measured PA intervals were expressed relative to the ECG-wave duration RR, PA/RR.

For statistical analysis, the SAS procedure MIXED was used for linear mixed

Figure 2.9: Venous Doppler waves with simultaneously depicted ECG signals of both (A) a HV and (B) a RIV. Corresponding characteristics of Doppler and ECG waves are marked A and P, respectively. The A-wave represents the backflow of blood into the hepatic veins (signal above the Doppler zero line in panel A) or a deceleration of forward venous flow in the RV (panel B) caused by the contraction of the right atrium. Atrial contraction is initiated by the P-wave of the ECG. The Doppler X-wave indicates fast forward venous flow following atrial relaxation. Atrial relaxation occurs at the same time as ventricular contraction, which in turn is initiated by the ECG R-wave. PA/RR is measured as the time interval (ms) between A and P (indicated with an asterisk), corrected for the changing HR. (C) QD/RR is measured as the time interval (ms) between Q and D at the level of the arcuate branches of the UtArt, corrected for the changing HR. Q and D both represent the start of systole (S). HR is derived from the time interval between two consecutive ECG R-waves

models, with restricted maximum likelihood parameter estimation. All statistical hypothesis tests were conducted using conventional F-tests [134, 142]. To correct for multiple comparisons within the same study population, the nominal level was defined as $\alpha = \frac{.05}{3}$.

2.4.4 Results

A total of 50 women was evaluated, ten in each of the five groups. The mean maternal age of the total study population was 29.0 ± 5.0 years and did not differ significantly between the groups ($P \geq .14$). The mean gestational age for the UP groups (UP1 to 4) was 12.2 ± 0.6 weeks, 20.5 ± 0.9 weeks, 30.3 ± 0.4 weeks, and 37.9 ± 1.1 weeks, respectively. the mean gestational age of the PE group was 33.0 ± 5.1 weeks, which was not significantly different from the normal third trimester group UP3 ($P = .13$).

Correlation between inter-ECG- and inter-Doppler wave time intervals was performed in all groups for each of the three organs and for each gestational stage. The ICC between PP and AA were $\geq .84$.

The frequency of atypical non-triphasic HV Doppler wave patterns for UP1, UP2, UP3, and UP4 were 20% (6/30), 60% (18/30), 87% (26/30), and 93% (28/30), respectively. These fractions differed significantly between UP1 and UP2 ($P = .004$), between UP2 and UP3 ($P = .04$), but not between UP3 and UP4 ($P = .67$). In PE, the fraction of atypical non-triphasic HV Doppler wave patterns was 30% (9/30), which was significantly different from all UP groups ($P \leq .04$), apart from UP1 ($P = .56$). The overall incidence of atypical Doppler waves was 58% (87/150). In these atypical Doppler wave patterns, the ECG facilitated the identification of the individual characteristics of the venous pulse waves as illustrated in Figure 2.10.

Table 2.5 presents numerical values (means and standard deviations) of the ECG-Doppler time interval (PA) and cardiac cycle duration (RR) for each of the three organs and for each of the five groups. Comparison of the PA/RR between different stages of UP, as measured in the liver, is presented graphically in Figure 2.11 (A): compared to UP1, the PA/RR is significantly longer in UP3 ($P < .01$) and UP4 ($P < .001$). As shown, this time interval seems to increase gradually from first trimester to term. Similar results were found in both the left and right kidney (Table 2.5).

Comparison of the PA/RR between both kidneys and the liver at each stage of

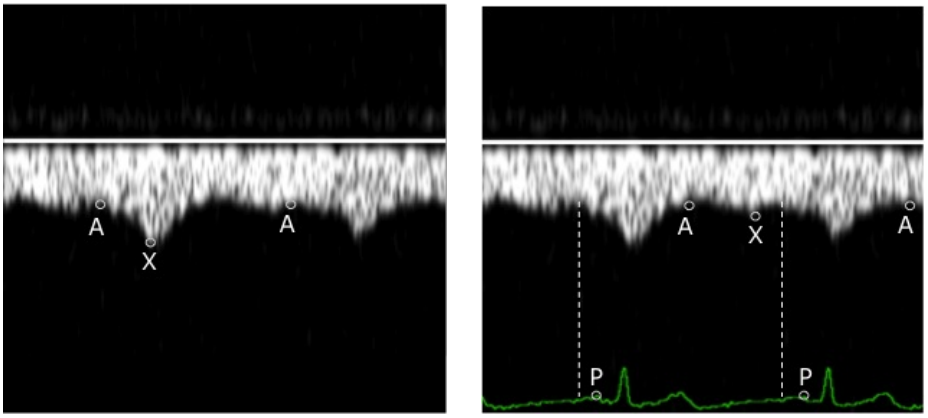

(A) Without ECG: incorrect identification (B) With ECG: correct identification

Figure 2.10: Non-triphasic atypical HV Doppler wave pattern observed near term without accompanying ECG (panel A) and with ECG (panel B). As illustrated, without the ECG as a reference signal, distinct Doppler wave characteristics can easily be misinterpreted: A is the result of atrial contraction, which in turn is initiated by the ECG P-wave. Therefore, A should always present later in time than P. This time relation can only be assessed properly with the simultaneous depiction of ECG and Doppler.

UP is presented graphically in Figure 2.11 (B). In UP1, the PA/RR was significantly shorter in the liver than in RIV ($P \leq .01$). In UP2, this differences was only observed between the liver and the left kidney and was not found in UP3 or UP4. Inter-kidney differences were not significant ($P \geq .04$).

PA and RR measurements in PE are also presented in Table 2.5. Compared to UP3, the PA/RR is significantly shorter in PE at the level of the liver and the right and left kidney ($P < .01$). This difference is due to a combination of shorter PA and longer RR intervals in PE compared to UP. Six of ten women with PE were on antihypertensive treatment when they were examined: α-Methyldopa ($n=4$), Labetolol ($n=3$), and/or Nifedipine ($n=1$). In these small groups, the PA/RR was not different between the women with or without antihypertensive treatment ($P > .05$): 0.40 ± 0.03 vs. 0.35 ± 0.04 for the left kidney, 0.36 ± 0.03 vs. 0.35 ± 0.03 for the right kidney, and 0.23 ± 0.05 vs. 0.28 ± 0.06 for the liver. Compared to UP3, the PA/RR was significantly shorter in PE with antihypertensive treatment at the level of the right kidney ($P=.01$) and the liver ($P < .01$), and also in PE without antihypertensive treatment at the level of the left kidney ($P=.01$) and the right kidney ($P=.01$). Demographic patient data, results from serum and urine analyses and the neonatal outcome of the PE group are provided in Table 2.6.

Table 2.5: Numerical values of the time relation between maternal ECG- and venous Doppler waves. PA is the time in ms between the ECG P-wave and venous Doppler A-wave; RR is the duration in ms of one cardiac cycle in the ECG. Measurements are expressed as means ± standard deviations for four groups of 10 women with UP in first trimester (UP1), second trimester (UP2), third trimester (UP3), and at term (UP4) and for one group of women with PE. For each group, values are presented separately for the left kidney, right kidney, and liver. For the UP groups, all significant differences when compared with UP1 or UP2 are indicated with an $*$ or $\circ$, respectively. Significant differences between PE and UP at corresponding gestational age are indicated in bold.

	Organ	UP1	UP2	UP3	UP4	PE
PA (ms)	left kidney	292 ± 73	330 ± 42	344 ± 33$*$	347 ± 18$*$	326 ± 50
	right kidney	274 ± 56	298 ± 56	330 ± 31$*$	345 ± 25$*\circ$	312 ± 61
	liver	220 ± 47	258 ± 65	297 ± 93$*$	337 ± 74$*\circ$	**213 ± 68**
RR (ms)	left kidney	789 ± 87	790 ± 79	716 ± 112	717 ± 153	**880 ± 124**
	right kidney	771 ± 68	794 ± 84	725 ± 97	713 ± 151	**893 ± 115**
	liver	779 ± 79	796 ± 97	717 ± 115	727 ± 146	**881 ± 125**
PA/RR	left kidney	0.38 ± 0.12	0.42 ± 0.07	0.49 ± 0.08$*$	0.50 ± 0.10$*$	**0.38 ± 0.09**
	right kidney	0.36 ± 0.09	0.38 ± 0.09	0.46 ± 0.05$*\circ$	0.50 ± 0.08$*\circ$	**0.36 ± 0.08**
	liver	0.29 ± 0.09	0.33 ± 0.10	0.42 ± 0.14$*$	0.48 ± 0.15$*\circ$	**0.25 ± 0.09**

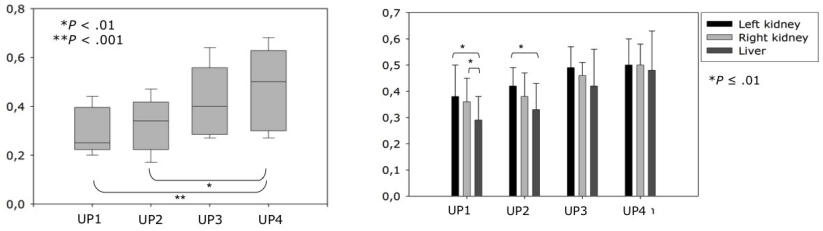

(A) Cross-sectional (B) Inter-organ

Figure 2.11: (A) Graphical representation of the PA/RR in HV at four stages of UP: first trimester (UP1), second trimester (UP2), third trimester (UP3) and at term (UP4). The boxplots represent median values ± 1 standard deviation, and the expansion ranges indicate ± 2 standard deviations. Significant differences at $\alpha = \frac{.05}{3}$ are marked by an asterisk. (B) Graphical representation of means and standard deviation of PA/RR, compared between the left kidney, right kidney and liver at four stages of gestation in UP: first trimester (UP1), second trimester (UP2), third trimester (UP3) and at term (UP4). Significant differences at $\alpha = \frac{.05}{3}$ are indicated by an asterisk.

Table 2.6: Demographic patient data, results from serum and urine analysis (reference values in table legend), medication use, and neonatal outcome are presented for ten women with PE.

	Age	GA[10] at exam	Proteinuria[11]	Uric acid[12]	ASAT[13]	ALAT[14]	Blood platelets[15]	Meds[16]	GA at delivery	Birth weight	
	years	weeks+days	mg/24h	μmol/L	U/L	U/L	$\times 10^3/mm^3$	A[17], L[18], N[19]	weeks+days	g	%
1	36.7	32+6	5666	375	26	13	328	A, L	33+2	1522	15
2	23.0	33+3	6 426	482	23	11	264	A	33+4	1 715	25
3	30.6	24+6	847	339	37	25	144	A	26+2	445	<5
4	22.6	25+5	13 800	482	157	96	86	A, L	25+5	670	10
5	30.6	34+0	3 407	476	26	29	120	L, N	34+0	1 840	15
6	23.6	35+1	763	357	25	10	222	L	35+3	2 690	50
7	38.1	32+0	1 056	274	13	11	295	/	32+1	1 693	35
8	21.7	31+3	5 325	422	15	14	403	/	31+4	1 473	25
9	29.4	39+1	443	339	17	12	126	/	39+1	4 110	95
10	33.3	41+0	1 060	297	18	21	422	/	41+0	3 600	50

[10] gestational age
[11] <140mg/24h with proteinuria diagnosed when ≥ 300 mg/24h
[12] 155-357μmol/L
[13] aspartate aminotransferase: 0-32 U/L with liverdysfunction diagnosed when ≥ 64 U/L
[14] alanine aminotransferase: 0-33 U/L with liverdysfunction diagnosed when ≥ 66 U/L
[15] 150-400$\times 10^3/mm^3$ with thrombocytopenia diagnosed when $<100\times 10^3/mm^3$
[16] antihypertensive medication
[17] α-methyl dopa
[18] labetolol
[19] nifedipine

2.4.5 Discussion

This small cross-sectional study on the time relation between maternal ECG- and venous Doppler waves, provides evidence for four interesting observations:

1. The maternal ECG facilitates the interpretation of venous Doppler wave characteristics.
2. The PA/RR is longer at term than in early pregnancy.
3. In early pregnancy, but not at term, the PA/RR is shorter in the liver than in both kidneys.
4. The PA/RR is shorter in PE than in third trimester UP.

The ECG-signal depicts the standard deflections P, QRS, and T consistently clearly at every cardiac cycle, and the physiology of each of these components is well understood. Venous Doppler waves are also known to show a typical pattern, each of the components reflecting a specific stage of the cardiac cycle in the right atrium [148, 150]. It has been reported that under physiological conditions, venous Doppler waves may present atypical patterns [62]. It has also been reported that atypical patterns, such as flattened HV Doppler waves, occur more frequently at term than in early pregnancy [91, 93]. In our study, we also observed an increasing number of atypical patterns at advanced stages of gestation: in the first trimester the frequency of non-triphasic hepatic Doppler wave patterns was lower than in late pregnancy. Atypical patterns may complicate the visual identification of distinct venous Doppler wave characteristics. This is illustrated in Figure 2.10. Without the presence of the ECG as a reference signal, distinct Doppler wave characteristics would have been easily mislabeled. The high correlation between corresponding time intervals of ECG- and Doppler waves in our study indicates that the simultaneous depiction of ECG and Doppler enables correct measurement of time intervals within and between both signals, even when 58% of the Doppler waves are atypical.

Measurements of the time interval between the ECG pattern and blood flow have been reported in echocardiographic studies on inter- and intraventricular dyssynchrony in non-pregnant cardiovascular patients [152] , but also in studies using arterial photoplethysmography to investigate age-related changes in peripheral pulse timing characteristics [74]. Here, this parameter is considered to indirectly relate to vascular tone, since arterial wall stiffness is age-related [67, 74, 153]. Similar findings were reported for photoplethysmography during spinal anesthesia in pregnant women: the arterial PTT increased after injection of the spinal anesthetics, while the arterial

blood pressure decreased [67].

In our study, the ECG-Doppler wave time interval PA/RR is considered the venous equivalent of the arterial PTT. Our results provide evidence for a PA/RR increase with advancing pregnancy (Table 2.5 and Figure 2.11 (A)). This is consistent with known reduced vascular tone and increased venous distensibility during normal pregnancy in combination with plasma volume expansion [18]. Further studies are necessary to directly link PA/RR to venous compliance and the tone of the vascular wall and to evaluate the role of intravascular filling (see Chapter 4.1).

As is shown in Figure 2.11 (B), the first trimester (UP1) PA/RR is shorter in the liver than in both kidneys. It is likely that this relates to the organ-specific morphology and/or histology [116]. As we reported elsewhere, the venous return from the right kidney is faster than the efflux from the left intrarenal blood [94], due to a different number of primary tributaries, additional renal vein, and inter-renal variations of RV length and diameter [101, 102, 116, 126]. Since the liver is anatomically closer to the heart than the kidneys, its drainage requires a shorter PA/RR than the kidneys. A similar phenomenon was also reported in other studies. The arterial PTT obtained by photoplethysmography were longer at the level of the toes compared to the fingers and were the shortest at the level of the ears [74]. Our results show that this characteristic of normal physiology is gestation-dependent, because the first trimester (UP1) inter-organ PA/RR difference is not observed at term (UP4), which indicates that gestation-induced changes in venous hemodynamics result in the simultaneous efflux of blood from the organs (liver and kidneys), located at different distances from the heart.

As shown in Table 2.5 the PA/RR is significantly shorter in PE than in UP. This observation may relate to the lower filling state of the vascular bed together with sympathetic dominance in the autonomic control of the cardiovascular function, i.e. a primary vasoconstriction or a vasoconstriction secondary to blood volume expansion failure [18, 30, 154, 155]. This phenomenon is also well-known at the arterial side: hypertension during pregnancy resulted in shorter PTT compared to normotensive pregnant women, as measured with a miniature pressure transducer [69]. Both the gestation-dependent increase and PE-related shortening of the PA/RR indicate that, similar to the reported results of arterial applanation tonometry, the PA/RR may be an indirect marker for venous vascular tone and relates to the generalized vasorelaxation during UP, with or without the associated expansion of plasma volume.

We are aware of the limitations of our pilot study: it is a cross-sectional observational pilot study, with small numbers of women in every group, addressing more than one research question. Therefore, our preliminary results need confirmation from larger and longitudinal studies. However, our study illustrates the feasibility of measuring time intervals between maternal ECG and venous Doppler waves in an obstetric ultrasound setting and illustrates that these measurements are organ-specific and gestation-dependent. Different values between UP and PE suggest that PA/RR may be an indirect marker of venous tone and/or intravascular filling. Therefore, the PA/RR may have potential as a new marker to study venous hemodynamics during normal and pathological pregnancies, in particular PE.

2.4.6 Acknowledgements

The authors thank Dr. Leen de Ryck and Dr. Emmy Van Kerkhove of Hasselt University for their useful recommendations during the writing of the first author's Master thesis in Biomedical Sciences on the topic presented in this paper. The authors also acknowledge Mrs. Elize Beckers from the Department of Press and Communication (ZOL) for her kind help with preparing the figures.

2.5 The venous pulse transit time in preeclampsia

Venous pulse transit time in normal pregnancy and preeclampsia

original paper

Kathleen TOMSIN*, Tinne MESENS, Geert MOLENBERGHS, Wilfried GYSELAERS*

Reproductive Sciences
Reprod Sci 2012, 19 (4): 431-436

2.5.1 Abstract

UP (n=16) were evaluated longitudinally and compared to EPE (n=12) and LPE (n=14), assessed once at diagnosis. PTT equivalent to PWV, was measured as the time interval between corresponding characteristics of ECG- and Doppler waves, corrected for HR, at the level of RIV, HV, and arcuate branches of UtArt. ICG was used to measure PTT at the level of the thoracic aorta. In UP, all PTT increased gradually ($P \leq .01$). PTT was shorter in LPE ($P < .05$) and also in EPE, with exception for HV and thoracic aorta ($P > .05$). Our results indicate that PTT is an easy and highly accessible measure for vascular reactivity at both arterial and venous sides of the circulation. Our observations correlate well with known gestational cardiovascular adaptation mechanisms. This suggests that PTT could be used as a new parameter in the evaluation and prediction of PE.

2.5.2 Introduction

Conduction of cardiac signals throughout heart and blood vessels, the so-called PTT, can be measured by echocardiography [152] and photoplethysmography [67, 74]. The anatomical distance from the heart [74, 156] and the organ-specific morphology and/or histology play a role in this signal transmission. On top of this, physiological/pathophysiological and pharmacological conditions influence this conduction, such as aging [74, 153], medication [67], and disease [62]. Here, arterial wall stiffness influences PTT of the arterial pulse [74], and therefore vascular tone is considered to play a role in the conduction of cardiac signals. Until now, PTT has been evaluated extensively in arteries but no data have been reported from the venous side of the circulation. On top of this, current methods of arterial PTT measurements require additional education and equipment not directly available for obstetricians.

Pregnancy is associated with a reduction in total peripheral resistance and increased vascular compliance [11]. PE is a gestational disease with increased vascular resistance, characterized by hypertension and proteinuria [18, 21]. The cardiovascular background mechanisms associated with PE involve both the arterial and venous compartment [92, 94]. We recently reported a cross-sectional pilot study (see Chapter 2.4) using standard Doppler ultrasound in combination with the maternal ECG and observed an increase in the venous ECG-Doppler time interval or VPTT in UP. This parameter was significantly lower in PE [156].

A longitudinal study was initiated for the establishment of a normal range for VPTT throughout UP, as a reference for measurements in PE. Following this, we also evaluated PTT at the arcuate branches of the UtArt using combined ECG-Doppler ultrasound and the thoracic aorta using ICG.

2.5.3 Methods

A longitudinal study was performed in a population of randomly selected pregnant women presenting at the Department of Obstetric Ultrasound or admitted to the maternal-fetal medicine unit (ZOL). Approval of the local ethical committee was obtained before the onset of study (MEC ZOL reference: 08/049). Singleton pregnancies of women without a history of renal or liver disease were included, thus avoiding disease-induced flow changes [151]. UP women were included at six to eight weeks of gestation and were evaluated monthly until six to eight weeks postpartum. A second group of women with PE were also included and classified into EPE and LPE according to gestational age at diagnosis ($<$ and ≥ 34 weeks of gestation, respectively). PE

was defined as gestational hypertension ($\geq$ 140/90 mmHg) measured on at least two occasions $\geq$ six hours apart, associated with *de novo* proteinuria $\geq$ 300 mg/24 hours [21].

After verbal informed consent, all women underwent a conventional ultrasound scan in a supine position together with a Doppler flow examination of both the kidneys, liver, and uterus in the transverse plane, simultaneously with a maternal ECG. All examinations were performed by 2 ultrasonographers (Wilfried Gyselaers; Tinne Mesens) using a 3.5-7.0 MHz probe (Hitachi EUB 6500).

Identification of the RIV and the HV was achieved by color Doppler flow mapping. Doppler signals were obtained between the renal pyelon and cortex at the level just above the hilus and in the craniocaudal midportion of each of the three HV branches (left, middle, and right). The relevance of breath-holding during Doppler measurements and the impact of maternal limb movements on the ECG-signal was explained and demonstrated to every woman (see Chapter 2.4) [156]. Next to this, we also obtained signals at the level of the arcuate branches of the left and right UtArt in the myometrium [157]. For every woman, three consecutive Doppler flow images of each kidney, liver, and arcuate branches of both UtArt were stored digitally on the hard disk of the scanner for later analysis by the principal investigator (Kathleen Tomsin).

For the veins, the time interval between the ECG P-wave and the corresponding venous Doppler A-wave (PA in ms) was measured (Figure 2.9 (A and B)). The time interval (ms) between the ECG Q-wave and the start of the systolic Doppler signal or end-diastolic point D (QD in ms) was measured at the level of the arcuate UtArt (Figure 2.9 (C)). As the HR increases with advancing gestation [11], all measured PA and QD intervals were expressed relative to the ECG-wave duration measured between consecutive R-signals in ms. Venous and arterial PTT were labeled PA/RR and QD/RR, respectively. For UP, three PA/RR and QD/RR intervals measured at each location were calculated and stored in the database.

We also performed ICG measurements on every woman included in the study, using the Non-Invasive Continuous Cardiac Output Monitor (NICCOMO, Software version 2.0, Medis Medizinische Messtechnik GmbH, Ilmenau, Germany). This system non-invasively obtains multiple cardiovascular parameters under physiological and stressed conditions [158, 159, 160]. Two dual sensors are placed on the patient's neck, one to each side, and two dual sensors are placed on each side of the thorax along the midaxillary line. Each dual sensor has one current electrode (most distal

to the heart) and one measuring electrode (most proximal to the heart). The current electrodes pass an alternating current with a high frequency (60-100 kHz) and a very low amplitude (1 mA). The voltage which is produced when the current flows through the thorax is measured by the measuring electrodes. On the monitor two signals are depicted: the ECG and the ICG generated by this system. The location of the curve points on the ICG are derived from the basic waveform averaged over 16 heart cycles. During the measurements, ICG values were recorded every two seconds, and data were exported from the monitor into a database: 30 values of each parameter were eligible for analysis [161]. The pre-ejection period (PEP) measured by this device is the time interval in ms between the Q-wave of the maternal ECG and the start of systolic rise of blood flow velocity in the thoracic aorta. The heart period duration (HPD) is the time interval in ms measured between two consecutive ECG-signals. As such, PEP/HPD can be considered the ICG equivalent of the ECG-Doppler time interval QD/RR. Reproducibility of our methodology was high, as confirmed by ICG measurements in response to postural and diurnal challenge, using mean values of multiple measurements instead of individual measurements for each parameter (see Chapter 3.1) [161]. To ensure consistency throughout the study, all women were examined in the supine position. Mean values of 30 consecutive measurements per minute under standardized conditions comparable to the ultrasound examinations were also stored in the database for later analysis.

To establish the reference curves, a linear mixed model was fitted to the data for each PTT separately [134]. As such, both intra-subject correlation over time and the repeated nature of measurements were accomodated, allowing assessment of a patient-specific profile and evolution over time. To avoid imposing parametric structures on the curve, an unstructured profile was considered. To this end, the data were binned in four-weekly intervals: eight to 36 weeks of gestation, term, and postpartum.

Measurements in PE were obtained in a similar way, and the results were plotted against the normal values (Figure 2.12). When comparing PE to UP, a subject-specific effect was included, i.e. patient-specific location (intercept) and patient-specific evolution over time (slope). Hence, the comparison was done using an F-test on two degrees of freedom. Statistical differences between demographic characteristics was assessed by Fisher's exact test for the categorical variable "nulliparous" and Mann-Whitney U-test for the continuous variables "maternal age", "BMI", "birth weight", and "gestational age".

2.5.4 Results

A total of 16 women with UP, 12 women with EPE, and 14 with LPE were included. Gestational age and birth weight percentiles were lower in PE groups than in UP (Table 2.7). All women with UP were evaluated at gestational age of 8 ± 1, 12 ± 0, 16 ± 0, 20 ± 1, 24 ± 1, 28 ± 1, 32 ± 1, 36 ± 1, 38 ± 1 weeks of gestation, and at 7 ± 1 weeks postpartum. Women with PE were evaluated at the moment of hospital admission, that is EPE at 31 ± 3 and LPE at 37 ± 2 weeks of gestation.

Figure 2.12 represents reference ranges for PTT: PA/RR, QD/RR, and PEP/HPD in UP at different stages of gestation. As is shown, all PTT increased significantly throughout the course of UP ($P<.0001$) and were significantly lower in postpartum as compared to term ($P<.0001$). Postpartum PTT values at the level of the liver and the thoracic aorta were not different from early pregnancy values ($P=.43$ and .19, respectively), wheras all other PTT values were significantly shorter in postpartum than in early pregnancy ($P<.02$).

Comparison between UP and EPE or LPE is shown in Table 2.8. The PTT intervals were significantly shorter in EPE and LPE than in UP at corresponding gestation for both kidneys and arcuate UtArt. At the level of the liver and the thoracic aorta, the PTT was significantly shorter in LPE compared to UP, but this was not true for EPE (Table 2.8, Figure 2.12). For all PTT, the slopes but not the intercepts were significantly different between EPE and LPE (Table 2.8, Figure 2.12).

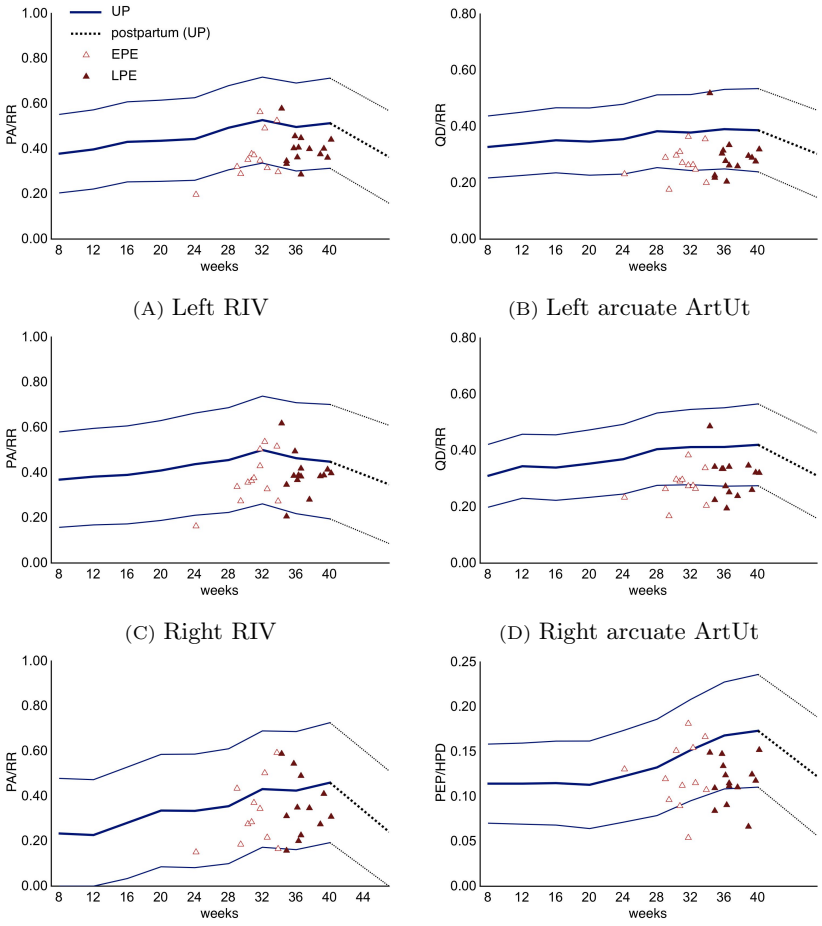

(A) Left RIV

(B) Left arcuate ArtUt

(C) Right RIV

(D) Right arcuate ArtUt

(E) HV

(F) Thoracic aorta

Figure 2.12: Normal reference range of PTT at the level of left RIV, right RIV, HV, left arcuate UtArt, right arcuate UtArt, and thoracic aorta (see Methods for definitions). For each gestational age and for postpartum values, median, 5th, and 95th percentiles were calculated and presented graphically using lines throughout pregnancy and dashed lines for postpartum values. Measurements in EPE and LPE were plotted against the normal values (open and closed triangles, respectively).

Table 2.7: Demographic characteristics and pregnancy outcome of UP, EPE, and LPE. Data are represented as medians (IQR) or numerical values (%). Significant differences at $\alpha = .05$ between UP and PE, and between EPE and LPE are labeled $*$ and $\circ$, respectively. The Fisher's exact test was used for the categorical variable "nulliparous" and the Mann-Whitney U-test for the continuous variables "maternal age", "BMI", and "gestational age at delivery".

	UP	EPE	LPE
	$n = 16$	$n = 12$	$n = 14$
Characteristics at inclusion			
Age (years)	28.8 (26.9;31.5)	29.7 (26.1;30.9)	30.1 (27.4;33.9)
BMI (kg/m^2)	23.4 (21.4;24,3)	26.5 (23.8;30.8)$*$	24.1 (22.8;28.0)
Nulliparous, (n (%))	9 (56.3)	8 (66.7)	11 (78.6)
Pregnancy outcome			
Birth weight (g)	3 380 (3 044;3 668)	1 347 (1 229;1 464)$\circ$	2 528 (2 176;2 886)$\circ$
Birth weight (%)	44 (38;68)	18 (5;28)$*$	14 (5;25)$*$
Gestational age (weeks)	39 (38;40)	32 (31;33)$*\circ$	37 (36;39)$\circ$

Table 2.8: Comparison between UP, EPE, and LPE. Data are represented as medians (IQR). Mann-Whitney U-test was used to compare the gestational ages between the groups. Differences in PTT were assessed using a non-parametric F-test on two degrees of freedom. Significant differences between UP and PE are labeled ∘ for $\alpha = .05$ and • for $\alpha < .001$.

Organ	Parameters	UP n=16 32 (31;32) weeks	EPE n=12 31 (30;32) weeks	LPE n=14 36 (36,39) weeks	UP n=16 36 (36;36) weeks
Left kidney	PA/RR	0.52 (0.49;0.55)	0.35 (0.31;0.41)∘	0.40 (0.36;0.43)∘	0.53 (0.44;0.55)
Right kidney	PA/RR	0.48 (0.44;0.53)	0.36 (0.31;0.45)∘	0.39 (0.37;0.41)•	0.45 (0.42;0.50)
Liver	PA/RR	0.45 (0.34;0.56)	0.28 (0.20;0.40)	0.33 (0.26;0.43)•	0.41 (0.39;0.49)
Left ArtUt[20]	QD/RR	0.38 (0.35;0.40)	0.27 (0.24;0.30)∘	0.28 (0.26;0.31)∘	0.41 (0.35;0.44)
Right ArtUt[21]	QD/RR	0.40 (0.37;0.43)	0.27 (0.26;0.30)∘	0.32 (0.25;0.34)∘	0.41 (0.37;0.50)
Thoracic Aorta	PEP/HPD	0.15 (0.13;0.18)	0.12 (0.10;0.15)	0.12 (0.11;0.13)∘	0.17 (0.14;0.19)

[20] Left arcuate branches of UtArt

[21] Right arcuate branches of UtArt

2.5.5 Discussion

PTT is defined as the time (in ms) needed for a cardiac signal to travel through the vascular tree to distant locations or between two arterial sites [66] and can also be expressed as PWV (in cm/s). Under normal physiological conditions, it is influenced by autonomic nervous activity and therefore reflects vascular reactivity [162]. Reported physiological/pathophysiological conditions with impact on PTT are genetic factors, age, gender, blood pressure, smoking, and diseases such as atherosclerosis, hypertension, diabetes, renal failure, and hypercholesterolemia [163, 164, 165]. Abnormal PTT can be present before clinical manifestation of cardiovascular disease, and for this its value as a biomarker for prediction of cardiovascular disease is currently under investigation [166, 167]. It is influenced by medication and can be used to assess pharmacodynamic effects and efficacy in clinical studies [65, 164, 167, 168]. Methods to measure PTT are applanation tonometry [169, 170, 171, 172], photoplethysmography [66, 162, 173], venous occlusion plethysmography [174, 175], or whole body ICG [176]. However, these methods are not directly available for obstetricians and require additional training. To measure the PTT, we used standard Doppler ultrasound combined with maternal ECG, which has been shown to be highly reproducible [92, 156].

Studies on arterial PTT during normal pregnancy show conflicting results: a slight increase after the second trimester has been reported [177] as well as marginally different values between gestational age groups [64, 172] or a significant decrease throughout normal gestation [175, 178, 179]. These contradictory results were considered to result from other gestational hemodynamic adaptations in the arterial tree, which might mask or compensate the velocity changes and therefore decrease the usefulness of these parameters in the assessment of arterial stiffness in normal pregnancy [64, 172, 177]. As a consequence, considerable inter-individual variation in hemodynamic parameters was observed after 32 weeks of gestation [20, 93]. Throughout pregnancy, we found a significant increase in QD/RR at the level of the arcuate branches of UtArt and of PEP/HPD at the thoracic aorta, with the widest range of variation at 36 weeks of gestation and at term (Figure 2.12 (D, E, and F)). We also found that women with EPE and LPE had significantly shorter uterine PTT than women with UP (Table 2.8), as shown by others [171, 176, 177]. This correlates with the known increase of vascular tone and total peripheral resistance in PE, which induces faster transmission of cardiac signals through the circulation [171, 176, 177].

In normotensive pregnancies, a strong association of arterial stiffness with birth weight percentiles and catch-up growth after birth has been reported [170]. Birth

weight percentiles were lower in PE than in UP in our study (Table 2.7). In addition to these observations at the arterial side of the circulation, we found similar results in RIV and HV. It is well known that the configuration of the venous Doppler waves represent characteristics of right atrial function of the heart [148, 150]. The ECG P-wave and Doppler A-wave are related to the same physiological event: right atrial contraction. Therefore, the time interval between P and A can be used to study the retrograde transmission of cardiac signals in the venous circulation [156]. As shown in Figure 2.12 (A, B, and C), there is an increase in the PA/RR interval during the course of pregnancy, both at the level of HV and RIV. As for uterine and aortic PTT, all venous PTT were significantly shorter for LPE, but for EPE this was not true at the level of HV (Table 2.8). It is likely that this finding relates to the shorter distance from the heart to the liver than to the kidneys. Our results indicate that in PE, autonomic control of vascular hypertonia and pulse transit is not restricted to the arterial vascular tree but also affects the venous side of the circulation. On top of this, all PTT behave significantly different between EPE and LPE, indicating a difference in the maladaptation or constitution of the vascular tree between these two types of the disease [135].

The finding of reduced PTT in PE opens perspectives toward research into the role of the venous system in the etiology of PE. It has been reported that women who had a history of PE have had impaired vasodilatation for several years after delivery [174], and this was associated with higher joint and skin stiffness as compared to normal controls [170]. It has also been suggested that reduced expansion capacity of the venous compartment in early pregnancy could predispose to the development of PE [180]. The combination of these observations suggests that there might be a constitutionally determined connective tissue and/or venous vascular wall disorder, predisposing to the development of PE. Alternatively, there could be a direct compression of the venous system related to increased intra-abdominal pressure. Arterial and venous PTT measurements might be an easy and highly accessible method to investigate these hypotheses.

Changes in PTT throughout pregnancy are consistent with known physiological vascular adaptation mechanisms in normal pregnancy and with vascular hypertonia in PE. These changes occur at both the arterial and venous sides of the circulation and can be measured using a combination of maternal ECG and vascular Doppler. Studies using this technique may improve our knowledge of gestational reactivity of maternal arteries and veins and contribute toward a better understanding of the pathophysiology of PE.

2.5.6 Acknowledgements

The authors would like to thank Prof. Dr. Louis Peeters of the Maastricht University Medical Centre for his kind help and recommendations in our study.

2.6 Feasibility of three-dimensional power Doppler

Validation of 3D power Doppler and VOCAL software in the sonographic assessment of hepatic venous flow

a reproducibility and repeatability study

Jorien CLAESKENS, ***Kathleen TOMSIN****, Geert MOLENBERGHS, Caroline VAN HOLSBEKE, Tinne MESENS, Liesbeth MEYLAERTS, Wilfried GYSELAERS*

Facts, Views and Visions in Obstetrics and Gynaecology
F, V & V in ObGyn 2013 - in press

2.6.1 Abstract

Aim To evaluate the reproducibility of three-dimensional power Doppler ultrasonography (3D-PDU) and the repeatability of Virtual Organ Computer-aided AnaLysis (VOCAL) software in the assessment of HV flow in ten healthy non-pregnant individuals.

Methods Visualization of HV was performed using both intra- and subhepatic approaches; These examinations were repeated twice. Vascular indices were obtained for each examination in a reference point using both small and large volume samples (three times per type of volume sample). ICC and PCC were calculated to assess reproducibility and repeatability, respectively.

Results ICC were more than .60 in small volumes, but variable in large volumes for both approaches. However, re-identification of the reference point failed in 30% using the subhepatic approach. Repeatability was high for all VOCAL analyses (PCC $>$ .98).

Conclusions These results indicate reliable use of intrahepatic small volume samples in clinical application and invite to explore the role of this technology in the assessment of HV hemodynamics.

2.6.2 Introduction

The systemic blood circulation integrates arteries and veins together with the microcirculation. The venous compartment comprises most of the systemic blood [40, 58], with the splanchnic circulation as the most important blood reservoir [41, 58].

Studies of the venous compartment have gained interest in the field of obstetrics and gynecology [144, 181]. Throughout UP, HV flow changes have been observed [92, 181] and these patterns are different in pathologic pregnancies [92, 181]. Non-invasive methods such as ultrasonography are useful to study the venous compartment during pregnancy. 3D ultrasound is more accurate in volume measurements as compared to 2D ultrasound and offers opportunities for clinical application in obstetrics [182, 183, 184]. On top of this, the application of VOCAL software in 3D-PDU volumes allows quantification of vascularity and blood flow, which is currently used in vascularization studies of tumors [185], placenta [186, 187, 188, 189], ovaries and endometrium [190, 191], and fetus [192].

To the best of our knowledge, studies using 3D-PDU and VOCAL in the assessment of hepatic hemodynamics and venous blood flow in particular have not yet been published. In this study, both the use of 3D-PDU and VOCAL software were validated in the sonographic assessment of HV hemodynamics in healthy non-pregnant individuals.

2.6.3 Methods

Study population

Approval of the local ethical committee (MEC ZOL reference: 08/049) was obtained before study-onset. A heterogeneous population of ten healthy, non-pregnant subjects (three male and seven female) was included. After informed consent, each subject was sonographically examined on two separate occasions at least one week apart (exam 1 and 2). Standardization of the clinical conditions in both exams required *1*) an equal time frame between last meal and exam, *2*) examination at the same hour of the day and *3*) after the same amount of physical exercise on both days, and *4*) with identical ultrasound and Doppler settings [193]. Information about weight, blood pressure, and medication use were recorded for each exam.

Sonographic exam

Sonographic exams were performed by a single operator (Kathleen Tomsin), with experience in HV Doppler flow examinations, using a 4.4 MHz probe (RAB4-8-D, Voluson E8 system, GE Healthcare, Austria). Each subject was examined in a supine position and branches of the HV were visualized from two different probe angulations, i.e. *1*) the intercostal or intrahepatic approach and *2*) the subhepatic approach (Figure 2.13). The intrahepatic approach required positioning of the probe in the transverse plane between the ribs (Figure 2.13 (A)), whereas for the subhepatic approach the probe was angled towards the coronal plane underneath the thoracic chest in the right epigastrium (Figure 2.13 (B)). The relevance of breath-hold during 3D-sampling was explained and demonstrated to every subject. For each method, a 2D image of the liver was stored towards definition and identification of the anatomical reference point for measuring the same HV branches on each occasion. Next to this, a 3D color Doppler image was obtained to discriminate between portal veins and HV in each sample. The 3D-PDU image volumes were stored digitally on an external hard disk for vascularization analysis. Four 3D image volumes were collected for each subject, i.e. an intrahepatic and a subhepatic image volume at exam 1, and an intrahepatic and a subhepatic image volume at exam 2.

Volume analysis

After completion of the ultrasound examination, all 3D-PDU image volumes were analyzed using the VOCAL software (4D View Version 10.x, GE Healthcare, Austria). VOCAL allows for analyzing a sphere-shaped volume of the collected 3D-image around a user-defined reference point (Figure 2.14 (A)). Both small and large sphere volume analyses were performed for each 3D image sample by placing the contour points at the smallest (0.1 cm^3) and largest (10.0 cm^3) possible distances from each other, respectively.

For each analysis, a system-specific histogram (4D View Version 10.x, GE Healthcare, Austria) was generated, displaying the vascular indices: vi (%), fi (0-100), and vfi (0-100) (Figure 2.14 (B)). These measured values were expressed per volume unit. All volume analyses were performed three times by the same operator (Jorien Claeskens), each time starting from the original 3D-PDU image. The three consecutive analyses are designated A, B, and C for both the small and large volumes (Figure 2.15 (C)).

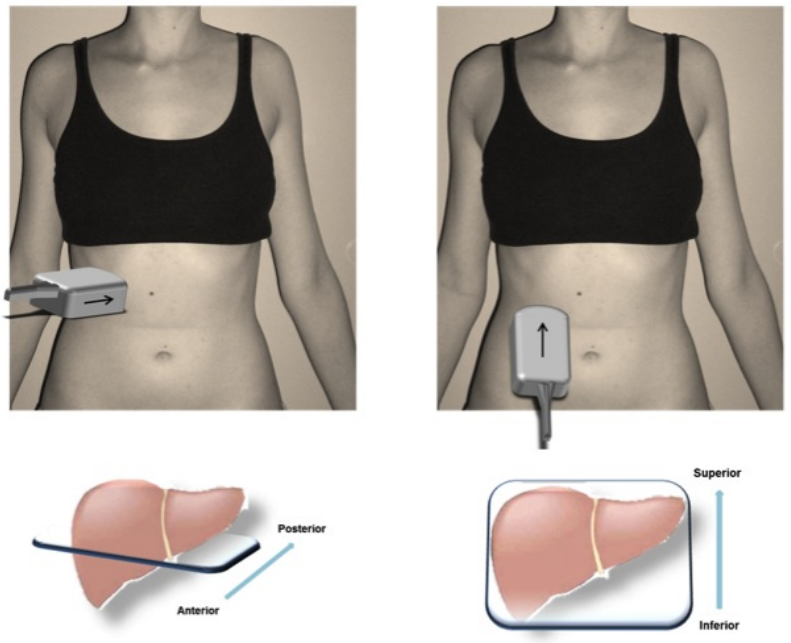

(A) Intrahepatic approach (B) Subhepatic approach

Figure 2.13: Illustration of the intrahepatic (A) and subhepatic (B) approach of the liver for 3D-PDU, with positioning of the probe in the transverse or coronal plane of the liver, respectively.

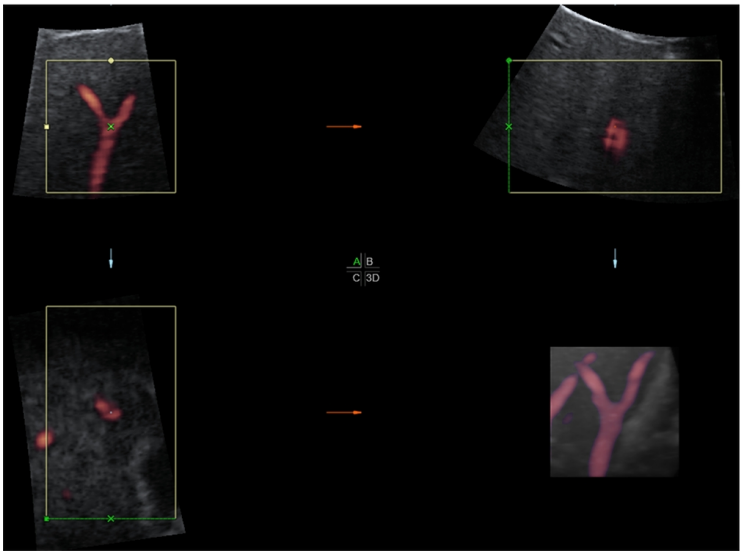

(A) Reference point

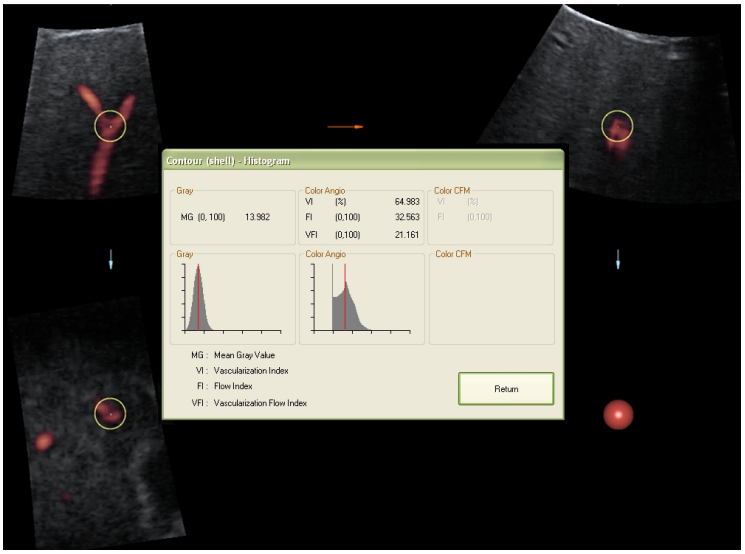

(B) Small sphere volume analysis and histogram

Figure 2.14: Analysis of a sphere-shaped volume in a 3D-PDU image sample around (A) a user-defined reference point (green x in upper left hand corner) with VOCAL software. (B) Small sphere volume analysis with the corresponding histogram showing the values for vi, fi, and vfi.

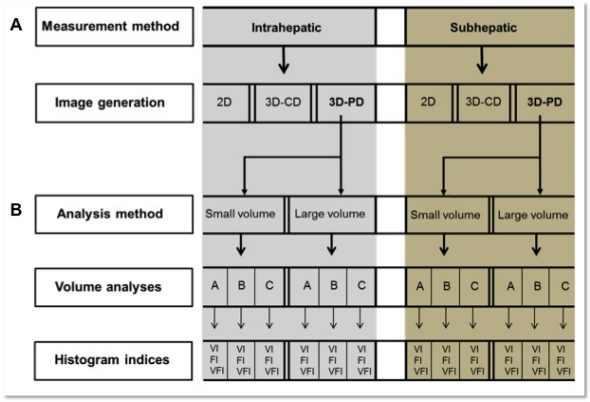

Figure 2.15: Illustration of the study protocol. (a) Intra- and subhepatic approach. Generation and storage of three images within each approach: 2D, 3D-color Doppler (3D-CD) and 3D-PDU images. (b) Volume analysis. Each 3D-PDU image sample was analyzed using both a small and large sphere volume. Each analysis was performed three times (A, B and C) in which vi, fi, and vfi were measured.

Statistical analysis

Repeatability To evaluate the VOCAL software, the three consecutive volume analysis (A, B, and C) within one sonographic volume of the same day were compared using PCC, i.e. A vs. B, B vs. C, and A vs. C. PCC was calculated for each parameter (vi, fi, and vfi).

Reproducibility The 3D-PDU performance, i.e. the ability to reproduce a sonographic volume around a given anatomic reference point, was evaluated using Linear Mixed Models [194] , which is valid even when some measurements are missing, provided the missing depends on observed rather than unobserved information. Such a model allows for population-level covariate effects (fixed effects), as well as person-to-person variation (random effects). For each parameter (vi, fi, and vfi), ICC and standard error between exam 1 and exam 2 were calculated based on three measurements per type of sphere (small and large volumes), per type of approach (intra- and subhepatic methods), and per subject (n=10). PCC and ICC $\geq .80$, $\geq .60$, and $< .60$ were defined high, moderately high, and low, respectively.

To evaluate the most appropriate type of approach and size of volume, repeatability and reproducibility were calculated separately for intra- and subhepatic approach and for large and small sphere volumes.

2.6.4 Results

Repeatability

For all measurements and methods, repeatability of VOCAL-calculations within each exam was high (PCC$\geq$ .98 for A vs. B, B vs. C, and A vs. C).

Reproducibility

Reproducibility results are shown in Table 2.9. For small sphere volumes in the intrahepatic approach, moderately high correlation (ICC between .60 and .75) were found for all parameters (vi, fi, and vfi). This was not true for large sphere volumes, for which ICC were highly variable (ICC between .44 and .71).

Table 2.9: Reproducibility of the 3D-PDU exam. For each parameter, ICC and standard error between exam 1 and exam 2 was calculated using Linear Mixed Models for mean values of three measurements per sphere volume (small and large volumes) per type of approach (intra- and subhepatic methods) per subject.

		Exam 1 vs. Exam 2					
		Small volume[22]			Large volume[23]		
		vi	fi	vfi	vi	fi	vfi
Intrahepatic approach (n=10)	ICC	.64	.60	.62	.58	.71	.44
	Standard error	.20	.21	.21	.22	.17	.27
Subhepatic approach (n=7)	ICC	.75	.70	.75	.11	.70	.13
	Standard error	.19	.20	.20	.45	.19	.45

In the subhepatic approach, identification of the reference point during exam 2 failed in three out of 10 cases (30%), and these data were registered as missing values. For all parameters, correlations were moderately high (ICC between .70 and .75) in small sphere volumes. This was also true for fi in large sphere volumes, but for vi and vfi very low ICC values were found (.11 and .13, respectively).

[22]sample volume of 0.1 cm^3

[23]sample volume of 10.0 cm^3

2.6.5 Discussion

3D-PDU and the corresponding analytic software (VOCAL) are validated in several studies regarding ovarian, endometrial, and placental vascularization [187, 188, 191]. However, the use of this methodology at the level of the liver has not yet been described. In this study, we assessed the reproducibility of 3D-PDU and the repeatability of the VOCAL software in ten healthy, non-pregnant subjects. In addition, we evaluated two types of probe position and sphere volumes.

Repeatability correlations of three repeated analyses within one image volume were used to evaluate the performance of the VOCAL software. These were high for both types of approach and sphere volumes (PCC$\geq$.98). This result is identical to those reported by others [195]. The VOCAL software seems to be a reliable tool for calculating vascular indices within one image volume around a user-defined reference point. These indices may have important clinical applications in the assessment of HV hemodynamics.

The validation of the 3D-PDU-examination was achieved by comparing volume analyses between two independent exams in the same subject under standardized conditions. Reproducibility correlations were moderately high (.60 to .75) within small sphere volumes using the intrahepatic approach. Although the subhepatic correlations were slightly higher (.70 to .75), identification of the anatomic reference point failed in 30% of subjects, whereas there were no failures with the intrahepatic approach. Furthermore, the subhepatic approach caused more discomfort than the intrahepatic approach, and is theoretically even more vulnerable for technical failure in late pregnancy due to the large uterine volume. Therefore, in our study set-up, we consider the intrahepatic approach to be most suitable for hepatic vascularity studies. Next to this, reproducibility of VOCAL analyses within large sphere volume samples resulted in highly variable correlations (.11 to .71). This was not true for small sphere volumes, where all correlation coefficients were $\geq$.60 (Table 2.9).

It is likely that, in large sphere volumes, the amount of vessels captured in the 3D sample can be highly variable between two independent exams depending on the position of the ultrasound probe [183, 196, 197]. Since the reproducibility correlations were lower in comparison to the repeatability correlations, 3D-PDU is more subject to variation than the VOCAL software. This can be explained by the high operator-dependence of the 3D-PDU-assessment [76], which determines image capturing [195]. Therefore, we emphasize that the sonographer's use of the probe is the *"Achilles*

tendon" of quantitative vascularization studies using 3D-PDU.

We conclude that 3D-PDU and VOCAL software can be used to study the HV system in healthy, non-pregnant individuals. In order to obtain acceptable reproducibility and repeatability, an intrahepatic approach using small sphere volumes is preferred.

This study invites to validate 3D-PDU and VOCAL in pregnant women to quantify liver vascularization and hepatic blood flow changes during the course of normal and pathologic pregnancy.

2.6.6 Acknowledgements

The authors would like to thank the Department of Obstetrics and Gynecology (ZOL) for their kind help and support in this study.

2.7 The venous system in preeclampsia

Role of dysfunctional maternal venous hemodynamics in the pathophysiology of preeclampsia:

a review

Wilfried GYSELAERS, Wilfried MULLENS, ***Kathleen TOMSIN****, Tinne MESENS, Louis PEETERS*

Ultrasound in Obstetrics and Gynecology
Ultrasound Obstet Gynecol 2011, 38: 123-129

2.7.1 Abstract

The venous compartment has an important function in regulation and control of CO. Abnormalities of CO have been found in early gestational stages of both EPE and LPE. The venous compartment also maintains the balance between circulating and non-circulating blood volumes and regulates the amount of reserve blood stored in the splanchnic venous bed. It is well known that adaptive regulation of maternal blood volume is disturbed in PE. Abnormal venous hemodynamics and venous congestion are responsible for secondary dysfunction of several organs, such as the kidneys in cardiorenal syndrome and the liver in cardiac cirrhosis. Renal and liver dysfunctions are among the most relevant clinical features of PE.

Doppler sonography studies have shown that the maternal venous compartment is subject to gestational adaptation, and that blood flow characteristics at the level of RIV and HV are different in PE compared with UP. In comparison to LPE, in EPE venous Doppler flow abnormalities are more prominent and present up to weeks before clinical symptoms. This paper reviews the growing evidence that dysfunction of maternal venous hemodynamics is part of the pathophysiology of PE and may perhaps be more important than is currently considered. Doppler sonography is a safe and easily performed method with which to study maternal venous hemodynamics. Therefore, exploring the role of maternal venous hemodynamics using Doppler sonography is an exciting new research topic for those who are interested in cardiovascular background mechanisms, as well as prediction and clinical work-up of PE.

2.7.2 The maternal venous system

Physiology of venous hemodynamics

In human physiology, the venous compartment has two important functions.

1) It serves as a large-volume reservoir for approximately $\frac{2}{3}$th of the total blood volume, 75% of which is located in small veins and venules [58]. The venous compartment comprises "actively moving" blood or "stressed volume" and "passive reserve" blood or "unstressed volume" [48]. The stressed volume serves as venous return to the heart, and this corresponds to CO under normal physiological conditions [52]. The unstressed volume serves as a reserve volume that can be mobilized to become stressed volume in the case of increased demand for venous return or CO [48]. Splanchnic veins are the most compliant vessels of the human body, containing 25% of the total blood volume. Therefore, they comprise the largest blood reservoir of the body [58], the largest fraction being located in the liver [51].

2) The venous compartment contributes both passively and actively to the regulation of CO, by acting in concert with the heart as as single functional unit [40, 51, 53]. The splanchnic veins are densely innervated by sympathetic nerves, indicating their high sensitivity to adrenergic stimulation [40]. As as consequence, a change in splanchnic venous tone has a large impact on the stressed volume and thus on venous return and CO.

The amount of stressed volume can be altered by two mechanisms [40].

1) A change in venous pressure, resulting from a change in venous tone, will lead to a change in the pressure gradient between the central veins and right atrium, which is the driving force for venous return. Contrary to the arterial system, small changes in venous pressure have a large impact on CO [51, 131, 198].

2) Input and output of the venous compartment are under control of both arterioles and the heart. Arteriolar dilatation or constriction may lead to expansion or contraction of the venous compartment by more than 1000 mL without concomitant change in venous return and CO [199]. This is achieved by a shift of blood between stressed and unstressed volumes, followed by restoration of the original condition through fast baroreceptor activity and slow volume-regulatory mechanisms.

Active (venoconstriction) and passive (arteriolar constriction) mechanisms can boost stressed volume by as much as 25% and 75%, respectively [40]. Active mechanisms are more prominent in the liver, whereas passive mechanisms are more prominent in the splanchnic bed [40]. Both structural and functional properties allow the venous system to serve as the main regulator of the circulating blood volume.

Clinical consequences of venous hemodynamic dysfunction

Dysfunction of the venous compartment affects organ function, both in experimental conditions [146, 200, 201, 202, 203] and in clinical syndromes such as RV or HV obstruction/thrombosis, cirrhotic cardiomyopathy, and the cardiorenal syndrome [99, 100, 204, 205, 206, 207]. Impaired organ function results from *a*) increased venous pressure causing microcirculatory congestion, and *b*) compromised organ perfusion due to arteriolar constriction, secondary to raised sympathetic activity. The concept of renal dysfunction as a result of venous congestion being transmitted to the RV and kidneys has been supported by a wide range of studies since the 1930s. In an experimental model with induced hypervolemia, an increase in RV pressure led to renal insufficiency, irrespective of CO and renal blood flow [208, 209]. Other studies indicated that transient RV compression reduced sodium excretion, GFR, and renal blood flow [210, 211, 212]. Also, an increase in central venous pressure has been found to increase renal interstitial pressure, most likely leading to renal hypoxia, resembling congestion and dysfunction of the liver as observed during cardiac failure [213, 214, 215, 216, 217, 218, 219]. In addition to these mechanically induced effects, an increase in venous pressure can activate the renin-angiotensin-aldosterone system [215, 220]. The latter will further reduce effective renal plasma flow and GFR [221, 222, 223, 224, 225, 226]. Another sequel to elevated central venous pressure is the development of visceral edema and ascites, both likely to aggravate dysfunction of the intra-abdominal organs and kidneys [227, 228]. Venous congestion rather than impaired CO has been shown to be the most important trigger for deteriorating renal function in patients with advanced low-output heart failure [207, 229, 230]. In this context it is important to emphasize that renal dysfunction due to venous congestion almost always reverses rapidly after lowering the renal venous pressure or the intra-abdominal pressure as indicated by an immediate recovery of diuresis and GFR [208, 209, 227, 229, 231].

Gestational adaptation of the maternal venous compartment

Normal pregnancy is associated with important adaptations in maternal cardiovascular function and in the venous compartment. During pregnancy, venous distensibility is increased, augmenting venous capacitance and unstressed volume [18]. This returns to prepregnant values in the first three months postpartum [130]. During pregnancy, venous compliance and the inferior vena cava diameter increase by 30% and up to 70%, respectively, relative to prepregnant values [17]. The absence of change in left atrium diameter in early gestation [4, 232] in conjunction with the absence of increase in atrial natriuretic peptide (ANP), facilitates plasma volume expansion during this

period [233]. In contrast, circulating ANP levels tend to increase in the second half of pregnancy [17], which may explain, at least in part, the decreasing trend in plasma volume in the third trimester of pregnancy. Further, after the 28^{th} week hepatic flow increases, presumably because of a higher portal flow due to more drainage from the splanchnic bed [125]. Concerning animal models, pregnant rats differ from their non-pregnant counterparts by a higher filling state of the splanchnic venous bed, accompanied by a higher venous tone and lower venous compliance [234]. The increase in capacity and filling state of the venous compartment during pregnancy provides a larger buffer to control CO; changes in venular tone will have a much larger impact on venous return in pregnancy than in the non-pregnant state. Therefore, the pregnancy-induced changes in the venous bed ameliorate its ability to regulate CO, which is particularly of value in the third trimester, when the impact of fluctuations in the uteroplacental circulation on the maternal cardiovascular function is greatest [19, 20].

Maternal venous hemodynamic maladaptation in preeclampsia

PE is accompanied by absence of the normal maternal cardiovascular adaptation to pregnancy, which is reflected, for example, in a constricted plasma volume compartment [235] and lower CO [236]. Several weeks prior to the onset of clinical PE, plasma volume is diminished and, compared to UP, levels of progesterone and aldosterone are increased and decreased, respectively [34]. Also, the pregnancy-induced changes in the venous bed seem to fade, as indicated by reversal of the changes in venous distensibility [18], capacitance [35], and compliance [17]. In nearly half of the women with a history of PE, subnormal plasma volume persists postpartum [237], along with a low venous capacitance [238] and impaired venular drainage of the conjunctival microcirculation [144]. These postpartum abnormalities are accompanied by a reduced autonomic response to volume expansion [180] and an abnormal cardiovascular response to exercise [239]. Further, these women have a three-fold higher risk of developing recurrent PE in their next pregnancy [240]. When pregnant again, these women respond as if their vascular bed was relatively overfilled, as indicated by an aberrant rise in the left atrial diameter and in ANP release during the first weeks of pregnancy [17]. Together, these data support the view that such women have a chronically reduced venous capacity and a more rigid venous compartment than women who had UP. These responses of the venous compartment are consistent with a subnormal function because of less effective control of venous return and regulation of the amount of stressed volume in response to fluctuations in CO. The latter can be expected to lower the threshold for increased sympathetic activity in the cardiovascular system in

response to, for example, orthostatic stress [17, 40]. Compared to UP, first trimester CO was higher in women who developed PE without FGR [140, 241]. The same difference in early gestational CO was observed between EPE and LPE [135]. EPE is characterized by early-onset sympathetic dominance in the cardiovascular system, elevated circulating markers of endothelial dysfunction, increased UtArt resistance, early-onset of clinical signs which are usually severe, elective preterm birth, and birth of an SGA infant [88, 135, 136]. In contrast, LPE is usually superimposed upon pre-existent maternal conditions with increased cardiovascular or metabolic risk of endothelial dysfunction [242]. This type is characterized by late onset (>34 weeks), normal to relatively high birth weight percentiles, and a clinical presentation which is usually mild [135, 136, 243]. For obese women, high CO and reduced cardiovascular and metabolic reserves in stressed conditions have been reported [244].

2.7.3 Why study the venous system in obstetrics?

Maternal venous hemodynamics in preeclampsia: research questions

The observations described above suggest that the role of the venous compartment in balancing stressed and non-stressed blood volumes, and in controlling CO may be much more important during UP and PE than generally considered today. Even more, the role of the venous compartment in securing a normal course of pregnancy or in the pathophysiology of PE has never been explored. Based on the evidence presented here, three interesting and challenging research questions can be posed with respect to gestational venous hemodynamic (mal)adaptation:

1. What is the role of abnormal venous hemodynamics and drainage of blood from liver and kidneys in the dysfunction of both organs during PE and/or the HELLP-syndrome?
2. Is there a constitutional and/or functional condition of the venous compartment associated with low plasma volumes and sympathetic dominance, predisposing to the development of EPE?
3. What is the role of the venous compartment in maintaining the balance between circulating and stored blood volumes in the third trimester of pregnancy, and how does this relate to maternal intra-abdominal pressure and the development of LPE?

Initiation of this kind of research is important, not only to move towards a better understanding of the background mechanisms of maternal cardiovascular adaptation and maladaptation, but also for the potential implications in the context of prevention, follow-up, and treatment of gestational hypertensive disease.

2.7.4 How to study the venous system in obstetrics?

Maternal venous duplex sonography in uncomplicated pregnancy and preeclampsia

Methods to study venous tone have been reviewed by Pang [58]. The mean circulatory filling pressure technique and intravascular ultrasound imaging have been used under experimental conditions; the constant CO reservoir technique and blood pool scintigraphy require major cardiac surgery and the use of radioactive tracers, respectively. Only plethysmography and the *in vivo* microscopic measurement of dorsal hand vein diameter can be used safely in pregnant women, but these procedures are technically difficult. Duplex ultrasonography has been shown to be a simple, non-invasive, and easily performed method to study venous blood flow velocity patterns, in both non-pregnant [108] and pregnant subjects [89, 91, 109]. Because of high intra- and inter-observed variation reported for Doppler-derived measurements [110, 111], methodological standardization is needed, especially when potentially confounding factors are to be excluded, e.g. respiratory movements, orthostasis, and muscle contractions. A standardized duplex ultrasound examination has been reported, which enables the acquisition of reproducible data for the RIVI [89, 94] and HV pulsed wave velocities [93]. The ICC for single RIVI measurements obtained according to this standard protocol was poor [141]. However, the reproducibility and ICC of RIVI and HV pulsed wave velocity has been improved markedly by using the mean value of three consecutive measurements [93]. The methodology for measuring RIVI and HV velocities has been reported elsewhere [93, 94, 147] and is illustrated in Figure 2.16 and in videoclips. Certain important technical aspects are illustrated in the videoclips: *1*) choice of a vein, draining blood in accordance with the direction of the Doppler beam, as this allows for correct measurement of flow velocities; *2*) depiction of the duplex image during patient's breath hold; and *3*) identification of Doppler wave characteristics under guided assistance of the maternal ECG-signal.

Some aspects of abnormal venous hemodynamics in PE using duplex sonography have been reported previously. Bateman *et al.* were the first to report increased RIVI values in PE compared to UP, which were associated with a sharp drop in forward flow in the late phase of the venous Doppler flow wave [109]. In combined ECG-Doppler examinations, this VPAN was considered equivalent to the biphasic pattern in HV Doppler waves and linked to the opposing forward venous flow during atrial contraction [92, 156]. In EPE this phenomenon was more pronounced in LPE (see Chapter 2.3) [147], and was present in both kidneys weeks before onset of clinical disease [95]. Figure 2.17 (C) illustrates an example of the evolution of weekly RIVI

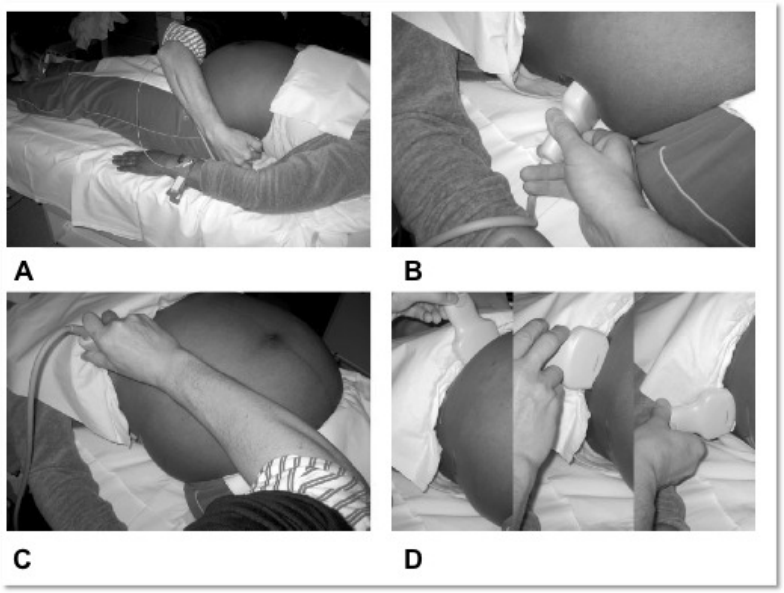

Figure 2.16: Scanning technique used to study HV and RIV flow in pregnant women as reported elsewhere [94, 93, 147]. The woman is examined in the supine position. The ultrasound probe is placed in a transverse position at each loin to capture three measurements per kidney (A, B). Similarly, each of the three main branches of the HV is assessed once, after intercostal positioning of the ultrasound probe at the level of the right epigastrium (C) at 11 o'clock (left HV), 10 o'clock (middle HV) and 9 o'clock (right HV) (D) positions.

measurements in the latent phase of PE. During the month prior to clinical onset of disease, RIVI values were much higher and the oscillation pattern differed markedly from that in the non-pregnant state (Figure 2.17 (A)) and normal third trimester of pregnancy (Figure 2.17 (B)). Total liver flow, which is the combined flow in hepatic arteries and portal veins, is lower in PE with HELLP than in PE without HELLP [245], and this flow reduction precedes the onset of clinical symptoms of HELLP [246]. In addition, hepatic artery resistance to blood flow has been reported to be increased in PE, irrespective of the presence of the HELLP syndrome [247]. Intrahepatic back-flow of blood during atrial contraction and triphasic Doppler waveforms were more common in PE than in UP, and this effect was more pronounced in EPE than in LPE [93]. Ultrasonographic measurement of the left RV diameter also showed increased values in cases of PE compared to UP controls, and again this was more pronounced in EPE than in LPE [248].

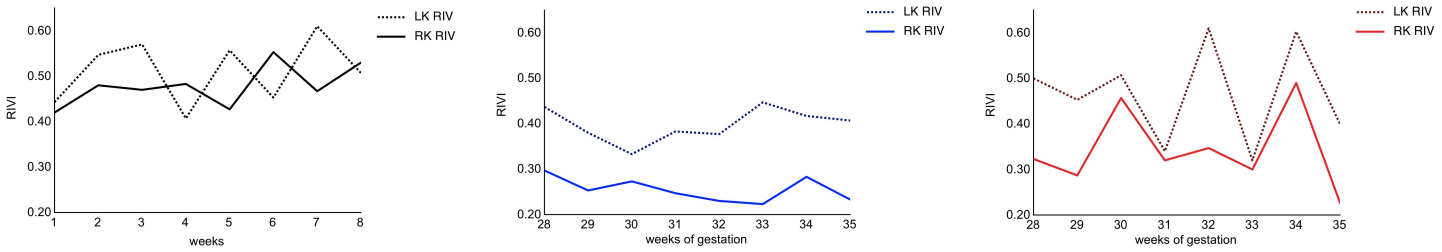

(A) Non-pregnant (B) UP (C) PE

Figure 2.17: Consecutive weekly Doppler measurements of RIVI, (defined as Equation 2.1). In the non-pregnant woman (A), RIVI measurements show a cyclical pattern with peak value variation between left and right kidneys (n=1). This oscillation is also present in third-trimester UP (B), along with RIVI measurements being lower in the right than in the left kidney (n=1). (C) RIVI measurements in a pregnant woman during the 7 weeks before clinical onset of PE (n=1). In addition to each Doppler assessment, the woman's blood pressure was measured and serum as well as 24-h urine collections were analyzed. PE was diagnosed at 35 weeks. RIVI values are higher than in UP, the amplitude of oscillation is larger, and increasing and decreasing slopes are present simultaneously on both sides.

2.7.5 Perspectives for future research

From the inferences elaborated in this review, it is clear that understanding the mechanisms of hemodynamics in both normal and complicated pregnancies is possible only when all aspects of cardiovascular function are considered: the heart, the arterial compartment, the venous compartment, and the mechanisms regulating peripheral organ perfusion. This overview intends to stress the role of a normally functioning venous compartment in enabling the prolonged institution of a *high-flow and low-resistance circulation* during pregnancy. It is a matter of even more interest to explore the functionality of the venous compartment in relation to early gestational low CO, increased vascular tone, and the consecutive evolution toward EPE and, similarly, in relation to early gestational high CO, high intra-abdominal pressure and evolution toward LPE.

The hypothesis that the venous compartment plays an important role in the development of impaired cardiovascular regulation during PE is a new concept with potential implications not only for prediction, diagnosis, and follow-up, but also for clinical management, e.g. the development of strategies aimed to improve the buffer function of the venous compartment.

We think that the time has come to initiate both scientific and clinical studies to further explore the function of the maternal venous compartment during pregnancy. Medical and obstetrics sonographers, having both the equipment and the skills to evaluate *non-invasively* the hemodynamic processes in pregnant women, are in an ideal position to perform this kind of research.

Chapter 3

The heart and the arterial system

3.1 Feasibility of impedance cardiography

Diurnal and position-induced variability of impedance cardiography measurements in healthy subjects

a reliability study

Kathleen TOMSIN*, Tinne MESENS, Geert MOLENBERGHS, Wilfried GYSELAERS*

Clinical Physiology and Functional Imaging
Clin Physiol Funct Imaging 2011, 31 (2): 145-150

3.1.1 Summary

Cardiovascular parameters and their measurements are subject to variation. In this study, we evaluated the reproducibility of ICG measurements following orthostatic and diurnal challenges for a set of 22 cardiovascular parameters in ten randomly selected healthy non-pregnant women. A standard protocol was used to record a consecutive series of measurements for each parameter before and after three position changes. This series of measurements was performed twice (AM and PM sessions). For each parameter, measurement-shift following position change was evaluate at 5% cut-off and compared between sessions. Intra- and intersession ICC was calculated for individual measurements per position using repeated-measures analysis of variance. Intra- and intersession Pearson's correlation coefficient (PCC) was calculated for mean values per position. Intersession correlation for measurement-shift following position change was .42 (5/12) for pressure parameters, whereas this was .96 (52/54) for other parameters. Intra- and intersession ICC for individual measurements varied between .02 and 1.00 for all parameters, however intra- and intersession PCC for mean values was consistently $> .80$ for SV, stroke index (SI), CO, acceleration and velocity index (ACI and VI), thoracic fluid content (TFC), TFC index, and HPD. We conclude that in healthy subjects under standardized conditions, reproducibility of means of multiple ICG measurements is high for HPD, SV, SI, CO, ACI, VI, TFC, and TFCI. From our data, we cannot draw conclusions on trends in diseased subjects.

3.1.2 Introduction

ICG is a technique designed for non-invasive measurement and monitoring of cardiovascular parameters on a beat-to-beat basis. Cardiac activity induces changes in the thoracic impedance against a high frequency alternating current and these changes are registered through electrodes. The registered signals are filtered and processed via algorithms to calculate the cardiovascular parameters. ICG enables a continuous parallel registration of these multiple parameters in a single session [158, 159, 160]. For non-critically ill patients, ICG offers an alternative for invasive measurements, such as the Fick method and thermodilution [249].

Measurements by ICG were reported to be reliable as they correlate highly with clinical standard methods [250, 251, 252, 253, 254], however these results are debated by others [160, 251, 255, 256, 257]. After more than 40 years of comparative studies and improvements in hardware and software [258, 259], the third generation ICG has now been introduced for clinical use, allowing measurements of multiple cardiovascular parameters.

In this study, we evaluated for 22 of these cardiovascular parameters the reproducibility of ICG measurements from a third generation device after orthostatic challenge and between morning and afternoon sessions.

3.1.3 Methods

Impedance cardiography using NICCOMO^{TM}

The ICG system used in this study is NICCOMO^{TM} (Software version 2.0, Medis Medizinische Messtechnik GmbH, Ilmenau, Germany). This is a third generation ICG with a four electrode arrangement eliminating skin resistance. Two dual sensors are placed on the patient's neck, one to each side, and two dual sensors are placed on each side of the thorax along the midaxillary line. Each dual sensor has one current electrode (most distal to the heart) and one measuring electrode (most proximal to the heart). The current electrodes pass an alternating current with a high frequency (60-100 kHz) and a very low amplitude (1 mA). The voltage which is produced when the current flows through the thorax is measured by the measuring electrodes.

On the monitor two signals are depicted: the ECG and the ICG generated by this system (Figure 3.1). The Q- and R-wave of the ECG represent the systole, i.e. the initial start and the peak depolarization of the ventricles respectively. Point B and

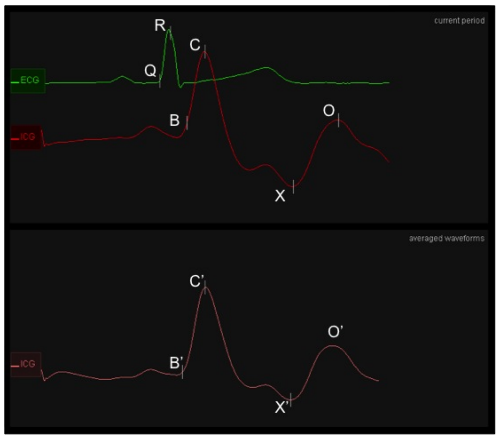

Figure 3.1: The ECG and the ICG of one cardiac cycle (upper), accompanied by the ICG of the averaged waveforms (lower), which is used as a reference. ICG (dZ/dt) is the first mathematical derivative of the change in impedance over time (Z) for an alternating current with high frequency (60-100 kHz) and very low amplitude (1 mA) transmitted through the thorax by a four electrode arrangement eliminating skin resistance. The Q and R wave of the ECG represent the systole, i.e. the initial start and the peak depolarization of the ventricles, respectively. Point B and point X of the ICG correspond respectively to the opening and closing of the aortic valve. The opening of the mitral valve is expressed as point O. The C-point of the ICG characterizes the maximal systolic flow. The location of the curve points on the present ICG are derived from the basic waveform averaged over 16 heart cycles (points B', C', X' and O').

point X of the ICG correspond respectively to the opening and closing of the aortic valve. The opening of the mitral valve is expressed as point O. The C-point of the ICG characterizes the maximal systolic flow. The location of the curve points on the ICG are derived from the basic waveform averaged over 16 heart cycles (points B', C', X', and O', Figure 3.1).

The monitor is equipped with a module for automated oscillometric blood pressure measurements. This allows selecting standardized time points for postexamination data-analyses.

Parameters

In this study the ICG parameters are classified into five subgroups, as enlisted in Tables 3.1, 3.2, and 3.3.

Pressure Mean arterial blood pressure (MAP = DBP + PP/3) and pulse pressure (PP = SBP - DBP) are calculated from the systolic and diastolic blood pressures (SBP and DBP, respectively), measured with the automated oscillometric blood pressure module.

Time period From the ECG-signal, HR and HPD are calculated. The time interval between the Q-wave of the ECG and the B-point of the ICG is the PEP: this is the period of isovolumetric ventricular contraction. The left ventricular ejection time (LVET) or the duration of the mechanical systole is the time interval between the B-point and the X-point of the ICG. The systolic time ratio (STR) is the ratio of the electrical and the mechanical systole. The mechanical systole related to the complete heart cycle is labelled the ejection time ratio (ETR). These ratios are calculated using the following formulas: $STR = \frac{PEP}{LVET}$ and $ETR = 100\% \times \frac{LVET}{HPD}$.

Volume SV is calculated using the Sramek-Bernstein formula [260] (see Equation 1.2). SI is SV normalized from body surface area, which is calculated from DuBois and DuBois's formula [261]. This allows for comparison between subjects with different BMI. The amount of blood pumped by the heart during one minute is the CO, this is calculated as $SV \times HR$. Cardiac index (CI) is CO normalized for body surface area.

Contractility The VI, equivalent to the amplitude of the systolic wave, and the ACI, equivalent of the maximum acceleration of blood flow in the aorta, are parameters of contractility derived from the normalized impedance waveform. When contractility increases, the amplitude of VI and ACI becomes larger. A more sensitive parameter of contractility is the Heather index (HI) in which the amplitude of the systolic ICG-wave is corrected for the time needed by the ventricle to reach maximum ejection. The O/C-ratio (O/C) is the ratio between the systolic (C-point) and diastolic (O-point) impedance wave.

Resistance The overall impedance of the thorax is defined as the base impedance (Z_0). This base impedance is influenced by the amount of conducting fluid in the thorax, and this fluid level is expressed as the TFC, related to the body surface area (TFCI). The total arterial compliance (TAC) is a value for the distensibility of the arterial vascular system and is calculated as $\frac{SV}{PP}$. When dividing SI by PP the TAC index (TACI) is calculated.

Study population

This study was performed in a population of ten randomly selected non-pregnant women, presenting at the Department of Obstetrics and Gynecology (ZOL). Approval of the local ethical committee was obtained before study onset (MEC ZOL reference: 09/050). Healthy women of reproductive age without history or symptoms of medical or cardiovascular diseases were included.

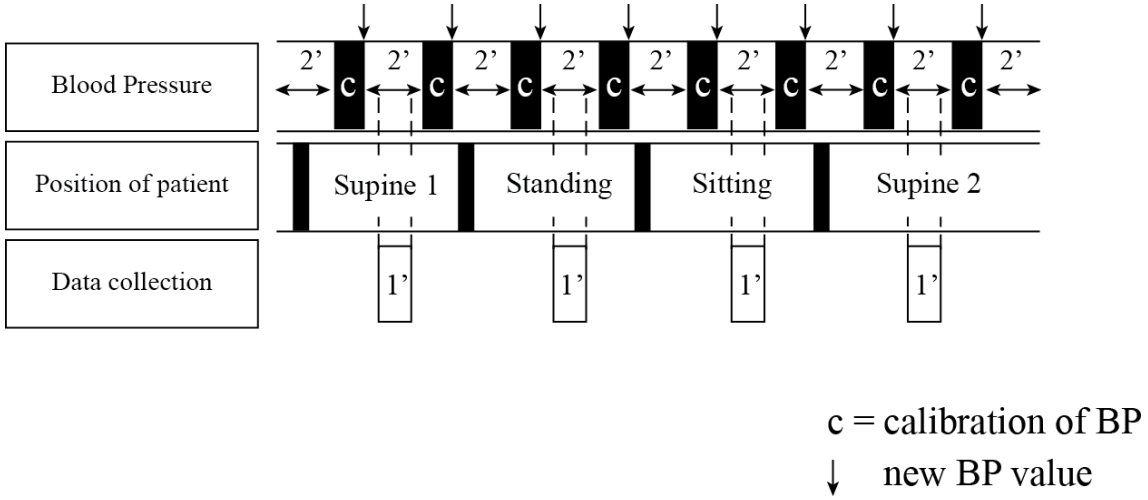

Figure 3.2: Measurement protocol in which blood pressure (BP) is taken every two minutes. A calibration period (c) is present before the new blood pressure value is depicted on the screen. The time period during position change is highlighted in black. Data are collected over a timespan of one minute.

Data collection

For each subject, a consecutive series of ICG-examinations in different positions were performed (Figure 3.2): *1*) supine 1, *2*) standing, *3*) sitting, and *4*) supine 2. To evaluate possible influences of the circadian rhythm, this series of measurements was performed twice, once in the morning (AM) and once in the afternoon (PM).

During the measurements, ICG values were recorded every two seconds, blood pressure was taken automatically every two minutes ([2'] in Figure 3.2). Per position, blood pressure was measured twice. Data were collected over a timespan of one minute after the first blood pressure was depicted on the screen ([1'] in Figure 3.2). These values were neither influenced by the blood pressure measurements itself ([c] in Figure) nor the movements during change in position (black boxes in Figure 3.2).

Data were exported from the monitor into a database: for every position during each session, one value for pressure parameters and 30 values of other parameters were eligible for analysis.

Statistical analyses

Measurement-shift after position changes were evaluated qualitatively for each parameter. In this study, a measured value of $< 95\%$ or $> 105\%$ relative to the value measured before orthostatic challenge was defined a relevant position-induced decrease or increase, respectively.

For each parameter, repeated-measures analysis of variance (SAS procedure NLMIXED) was used to calculate the ICC between 30 single measurements per position per session per woman, and PCC was calculated for mean values of 30 measurements per position per session per woman. Intrasession correlation was evaluated between positions supine 1 and supine 2 per AM or PM session, and intersession correlation was evaluated between supine 1 AM and supine 1 PM, between standing AM and standing PM, between sitting AM and sitting PM, and between supine 2 AM and supine 2 PM.

3.1.4 Results

Ten non-pregnant women were included, and 22 parameters were evaluated for each woman. Mean age of the total study population was 25.9 ± 4.3 years, the time interval between AM and PM sessions was 04:12:10$\pm$ 01:20:31 hours.

Table 3.1: Measurement-shift following position change for AM and PM sessions. A shift of 5% or more: i.e. a measured value of $< 95\%$ or $> 105\%$ relative to the value measured before position change is defined as a relevant position-induced decrease ($\searrow$) or increase ($\nearrow$), respectively. A shift of $< 5\%$ is indicated as no change (=).

Position change:		from supine 1 to standing		from standing to sitting		from sitting to supine 2	
		AM	PM	AM	PM	AM	PM
Pressure	SBP	=	=	=	=	=	=
	DBP	=	$\nearrow$	=	$\searrow$	=	=
	MAP	=	$\nearrow$	=	$\searrow$	=	=
	PP	=	$\searrow$	$\nearrow$	=	=	$\nearrow$
Time period	HR	$\nearrow$	$\nearrow$	$\searrow$	$\searrow$	$\searrow$	$\searrow$
	HPD	$\searrow$	$\searrow$	$\nearrow$	$\nearrow$	$\nearrow$	$\nearrow$
	PEP	$\nearrow$	$\nearrow$	=	=	$\searrow$	$\searrow$
	LVET	$\searrow$	$\searrow$	$\nearrow$	$\nearrow$	$\nearrow$	$\nearrow$
	STR	$\nearrow$	$\nearrow$	$\searrow$	$\searrow$	$\searrow$	$\searrow$
	ETR	=	=	=	=	=	=
Volume	SV	$\searrow$	$\searrow$	$\nearrow$	$\nearrow$	$\nearrow$	$\nearrow$
	SI	$\searrow$	$\searrow$	$\nearrow$	$\nearrow$	$\nearrow$	$\nearrow$
	CO	$\searrow$	$\searrow$	=	=	$\nearrow$	$\nearrow$
	CI	$\searrow$	$\searrow$	=	=	$\nearrow$	$\nearrow$
Contractility	ACI	=	$\searrow$	=	=	=	=
	VI	$\searrow$	$\searrow$	$\nearrow$	=	$\nearrow$	$\nearrow$
	HI	$\searrow$	$\searrow$	=	=	$\nearrow$	$\nearrow$
	O/C	$\searrow$	$\searrow$	$\nearrow$	$\nearrow$	$\nearrow$	$\nearrow$
Resistance	TFC	$\searrow$	$\searrow$	=	=	$\nearrow$	$\nearrow$
	TFCI	$\searrow$	$\searrow$	=	=	$\nearrow$	$\nearrow$
	TAC	$\searrow$	$\searrow$	$\nearrow$	$\nearrow$	$\nearrow$	$\nearrow$
	TACI	$\searrow$	$\searrow$	$\nearrow$	$\nearrow$	$\nearrow$	$\nearrow$

Measurement-shift of 5% or more after position change was consistent in both AM and PM sessions for 17 out of 22 parameters. Parameters of which at least one of three position-induced changes were inconsistent between AM and PM sessions were: DBP, MAP, PP, ACI, and VI (Table 3.1). Overall correlation between AM and PM session for measurement-shifts after position change was .86 ($\frac{57}{[22\times 3]}$). For pressure parameters only, this correlation was .42 (5/12) whereas this was .96 (52/54) for all other parameters.

Intra- and intersession ICC for 30 single ICG measurements per position per session per woman showed highly variable ICC, varying between .02 and 1.00 (Table 3.2).

Table 3.2: ICC calculated for individual measurements per position per session using repeated-measures analysis of variance.

ICC for multiple measurements		AM vs PM				supine 1 vs. supine 2	
		supine 1	standing	sitting	supine 2	AM	PM
Pressure	SBP	.53	.54	.42	.51	.50	.50
	DBP	.73	.66	.65	.51	.77	.60
	MAP	.54	.36	.57	.42	.68	.85
	PP	.76	.70	.37	.64	.59	.60
Time period	HR	.06	.72	.16	.29	.76	1.00
	HPD	.54	.58	.84	.55	.72	.34
	PEP	.47	.45	.46	.42	.50	.50
	LVET	.88	.58	.59	.70	.58	.63
	STR	.50	.63	.63	.50	.52	.51
	ETR	.52	.14	.17	.18	.83	.21
Volume	SV	.49	.88	.61	.49	.49	.49
	SI	.44	.02	.59	.17	.11	.66
	CO	.08	.70	.68	.59	.74	.65
	CI	.62	.61	.65	.61	.76	.73
Contractility	ACI	.62	.58	.36	.68	.06	.07
	VI	.64	.88	.68	.04	.49	.48
	HI	.35	.39	.63	.53	.27	.63
	O/C	.85	.75	.10	.14	.90	.29
Resistance	TFC	.68	.56	.72	.66	.90	.37
	TFCI	.35	.73	.66	.57	.27	.34
	TAC	.69	.69	.05	.85	.53	.20
	TACI	.11	.91	.59	.62	.48	.57

However, intra- and intersession PCC between mean values of 30 measurements per position and per session per woman consistently showed ICC $\geq .80$ for HPD, SV, SI, CO, ACI, VI, TFC, and TFCI (Table 3.3). ICC $\geq .60$ was found for HR, STR, ETR, CI, HI, and O/C (Table 3.3).

Table 3.3: PCC calculated for mean values of 30 measurements per parameter, except pressure parameters.

PCC for multiple measurements		AM vs PM				supine 1 vs. supine 2	
		supine 1	standing	sitting	supine 2	AM	PM
Pressure	SBP	.77	.67	.44	.69	.84	.72
	DBP	.80	.76	.67	.58	.79	.73
	MAP	.80	.77	.78	.58	.81	.79
	PP	.74	.43	-.58	.64	.85	.59
Time period	HR	.68	.93	.91	.78	.96	.79
	HPD	.81	.94	.95	.85	.96	.89
	PEP	.86	.48	.60	.74	.90	.87
	LVET	.58	.81	.89	.75	.96	.84
	STR	.78	.65	.92	.82	.95	.81
	ETR	.79	.65	.79	.85	.92	.80
Volume	SV	.88	.93	.95	.92	98	.93
	SI	.82	.90	.94	.88	.97	.88
	CO	.90	.90	.90	.93	.99	.97
	CI	.85	.80	.78	.87	.98	.97
Contractility	ACI	.86	.91	.91	.95	.97	.97
	VI	.90	.84	.84	.94	.97	.97
	HI	.87	.75	.78	.94	.97	.96
	O/C	.77	.75	.69	.83	.81	.86
Resistance	TFC	.99	.99	.99	.98	1.00	.99
	TFCI	.99	.99	1.00	.99	1.00	1.00
	TAC	.40	.66	.45	.67	.64	.51
	TACI	.37	.60	.40	.65	.57	.48

3.1.5 Discussion

The principle of impedance changes following physiological events in humans was first reported by Nyboer [158] and the concept of impedance waveform analysis allowing measurement of cardiovascular parameters non-invasively was introduced in 1966 [79]. In the last decades, many reports and reviews have been published on ICG with conflicting results and conclusions. Valuable ICG measurements have been reported [159, 160, 259], with values comparable to those obtained by conventional methods such as thermodilution or Fick method [250, 251, 252, 253, 256, 258], as well as inaccurate measurements with substantial variation between different algorithms [159, 257]. Due to this, ICG as an useful clinical device has not yet gained wide acceptance [127, 257, 262]. Recently, ICG devices of the third generation have been introduced. In this study, we have assessed the reproducibility of third generation ICG measurements under standardized resting conditions in healthy subjects.

Measurement of cardiovascular parameters is subject to variation, resulting from orthostasis, circadian rhythm, measurement error, and interindividual differences [263, 264, 265, 266]. Therefore, standardization of ICG methodology is mandatory for reproducibility studies. As explained schematically in Figure 3.2, a stringent protocol was used in our study allowing intra- and intersession comparison in and between AM and PM measurement sessions.

It is known that head-up tilting results in increased HR with decreased SV and CO [264, 267, 268, 269]. As shown in Table 3.1, we also observed these shifts during position change from supine to standing, together with an associated reduction of LVET, VI, HI, O/C, TFC(I), and TAC(I), and an increase of PEP and STR. The overall intersession correlation for position-induced changes of ICG measurements in our study was $> .80$, as these changes were consistent in AM and PM sessions for all parameters, except DBP, MAP, PP, ACI, and VI. For the pressure parameters DBP, MAP, and PP, correlation between AM and PM sessions for position-induced changes was $< .50$ (Table 3.1). It should be emphasized that in our protocol, only one blood pressure measurement per position was performed, which is much less than for other parameters. However, influence related to circadian rhythm on position-induced blood pressure shifts cannot be excluded. Patterns of diurnal blood pressure variations have been reported, which are attributed to variation in physical activity throughout the day [270, 271]. In our study, AM and PM measurements indeed were recorded from our subjects before and during or after working activities. From the data presented in Table 3.1, it can be concluded that position-induced changes of

ICG measurements are independent from the time of day for time period, volume, and resistance parameters, and this is not true for pressure parameter.

It is known that ICG measurements can be imprecise in severely ill patients [160, 127]. In healthy subjects, such as our study population, measurement error can occur following electrode placement [272]. As is shown in Table 3.2, we found a wide variation in the total of 30 individual ICG measurements per woman per position per session: the ICC varied between .02 and 1.00. Much better results were obtained when mean values of 30 individual measurements per woman per position per session were used for correlation between AM and PM sessions (intersession correlation) and between supine 1 and supine 2 sessions (intrasession correlation). Correlation coefficients $>.80$ were found for all volume parameters (except CI), TFC(I), HPD, ACI, and VI. For the latter two, the inconsistent position-induced shifts between AM and PM sessions (Table 3.1) demand further investigation into diurnal variations. Correlation coefficients $>.60$ were found for time periods HR, STR, and ETR, volume parameter CI, and for contractility parameters HI and O/C. From the data presented in Table 3.3, it can be concluded that ICG measurements in healthy subjects are highly reproducible for volume parameters as well as HPD, ACI, VI, and TFC(I). In our study, unsatisfactory reproducibility was found for TAC(I).

In summary, from the data presented in this study on ICG measurements in healthy subjects, we conclude that position-induced changes are independent from the time of day for time period, volume and resistance parameters, but this is not true for pressure parameters. Reproducibility is high for HPD, volume parameters, ACI, VI, and TFC(I), but unsatisfactory for TAC(I). Reproducibility of ICG measurements is much better when *mean values of multiple measurements* are used for each parameter, instead of individual measurements.

3.2 Feasibility of maternal impedance cardiography

Impedance cardiography in uncomplicated pregnancy and preeclampsia:

a reliability study

Kathleen TOMSIN*, Tinne MESENS, Geert MOLENBERGHS, Wilfried GYSELAERS*

Journal of Obstetrics and Gynaecology
J Obstet Gynaecol 2012, 32 (7): 630-634

3.2.1 Summary

It has been reported that cardiac contractility is altered in PE compared to UP. Because of the non-invasive nature of ICG, this method is gaining popularity in the obstetrics field. We assessed the reliability of ICG measurements in third trimester UP and PE. ICG measurements were recorded before and after three position changes, and this examination was done twice (session 1 and 2) per subject. For each of the 22 hemodynamic parameters, intra- and intersession PCC were calculated for mean values of 30 measurements per position per subject. PCC was consistently $\geq .80$ for contractility parameters ACI, VI, and HI in both UP and PE. These data illustrate that correlation between repeated ICG measurements of cardiac contractility is high under standardized conditions, and that ICG may be useful to study changes of cardiac contractility in pregnancy.

3.2.2 Introduction

Human pregnancy is characterized by major cardiovascular adaptations, such as plasma volume expansion, reduced vascular resistance, and increased HR [11]. Maladaptation of the cardiovascular system plays a significant role in the pathophysiology of PE, a disease associated with significant morbidity and mortality for both mother and child. It has been reported that cardiac contractility is altered in PE compared to UP [4, 6, 7, 8, 9]. Current methods to evaluate cardiovascular adaptation and maldaptation during pregnancy have not gained popularity because of their invasive nature [273, 274, 275] or the lack of required expertise [276].

ICG is designed for non-invasive measurement and monitoring of cardiovascular parameters on a beat-to-beat basis. ICG enables a continuous parallel registration of multiple parameters in a single session [158, 159, 160]. Good correlation (intra- and intersession) for position-challenged ICG measurements was reported in healthy non-pregnant subjects, especially when mean values of multiple measurements were used for each parameter (see Chapter 3.1) [161].

We evaluated intra- and intersession correlation of ICG measurements for 22 cardiovascular parameters with a third generation device after orthostatic challenge and between two independent sessions in women with third trimester UP and women with PE.

3.2.3 Methods

Approval of the local ethical committee was obtained before study onset (MEC ZOL reference: 09/050). Two populations of each ten randomly selected subjects were included: pregnant women in third trimester UP presenting during a time frame of two weeks at the antenatal clinic of the Department of Obstetrics and Gynecology (ZOL) and women with PE admitted during the following weeks to the maternal-fetal medicine unit (ZOL). PE was defined according to standard criteria [21]: gestation-induced hypertension $>140/90$ mmHg on at least two occasions six hours apart, in combination with >300 mg per 24 hours.

Data collection

The ICG system used in this study is NICCOMO^{TM} (Software version 2.0, SonoSite, Medis Medizinische Messtechnik GmbH, Ilmenau, Germany) with a four electrode arrangement eliminating skin resistance. This system allows for simultaneous measurement of 22 parameters in five categories: pressure, time period, volume, contrac-

tility, and resistance parameters [161, 277, 278]. The examination was performed according to the protocol as reported (Chapter 3.1) [161]. After informed consent, for each subject, a consecutive series of ICG examinations in different positions were performed during normal breathing (Figure 3.2): *1*) supine 1, *2*) standing, *3*) sitting, and *4*) supine 2. To evaluate the repeatability of this examination, the series of measurements was performed twice at two independent time periods during daytime, i.e. session 1 and session 2, with no more than eight hours apart to avoid influence of the circadian rhythm [279].

During the sessions, ICG values were recorded every two seconds, and blood pressure was taken automatically every two minutes. Per position, blood pressure was measured twice. Data were collected over a timespan of one minute after the first blood pressure value was depicted on the screen. These values were neither influenced by the blood pressure measurement itself nor the movements during change in position.

Data were exported from the monitor into a database: for every position during each session, one value for pressure parameters and 30 values of other parameters were eligible for analysis.

Statistical analyses

For each parameter, PCC was calculated for mean values of 30 measurements per position per session per subject. Intersession correlation was evaluated between supine 1 session 1 and supine 1 session 2, between standing session 1 and standing session 2, between sitting session 1 and sitting session 2, and between supine 2 session 1 and supine 2 session 2. Intra-session correlation was evaluated between positions supine 1 and supine 2 per session.

Statistical analyses on the numerical values of the 22 cardiovascular parameters after orthostatic challenge or on the differences between UP and PE were not included, as this was not the aim of this reliability study.

3.2.4 Results

Patient characteristics are enlisted in Table 3.4. Mean age was 32.70± 3.30 and 30.12± 6.05 years for UP and PE, respectively. The mean time interval between the two independent sessions was 06:15:23± 01:13:43 hours. Tables 3.5 and 3.6 represent inter- and intra-session PCC, respectively.

Table 3.4: Patient characteristics of the study populations: third trimester UP and women with PE.

				Gestational Age in weeks days		Pregnancy outcome	
Age (years)	BMI (kg/m^2)	Parity	Proteinuria (mg/24h)	Exam	Delivery	Birth weight (%)	Gender[1]
Uncomplicated pregnancy							
30	22	1	/	33 6	36 3	25	F
37	32	4	/	29 1	40 1	75-90	M
28	34	1	/	35 2	39 3	50-75	F
29	28	0	/	32 6	40 5	>90	M
38	38	2	/	28 3	39 1	50	F
32	47	1	/	29 1	38 2	75-90	M
32	26	2	/	27 2	35 2	75	M
35	32	1	/	31 6	38 3	25-50	M
34	44	1	/	36 5	40 6	50-75	F
30	32	0	/	33 3	36 6	>90	M
Preeclampsia							
21	21	0	2 543	30 4	31 1	10-25	F
25	33	0	838	31 5	32 1	10-25	M
30	31	0	7 823	34 0	34 1	10-25	F
25	33	0	7 053	32 1	32 3	25-50	M
36	28	1	336	24 6	26 4	<10	F
32	41	1	2 115	36 4	36 6	25	M
35	31	0	589	38 6	40 0	25-50	M
40	32	0	310	36 6	39 0	50-75	M
27	47	0	10 255	39 5	40 0	10-25	M
26	31	0	515	36 5	36 6	50	M

In UP, intersession PCC varied between -.02 and .91 for all pressure parameters, with significant correlations for DBP and MAP ($\geq .69$, $P < .03$). However, intrasession PCC was consistently more than .83 for all pressures ($P \leq .003$). This was not true for PE, which showed highly variable intra- and intersession PCC for pressures.

In both groups, the contractility parameters ACI, VI, and HI consistently showed PCC $\geq .80$ ($P \leq .003$). This was also true for TFC and TFCI (PCC$\geq .84$; $P \leq .002$). For all other parameters, intersession PCC was $\leq .63$ on at least one occasion, which was not significant.

[1]male (M) or female (F) infant

Intrasession PCC was also $>.80$ for heart rhythm (HR and HPD; $P \leq .005$) in both UP and PE. In UP, but not in PE, intrasession PCC was significant for TAC and TACI ($P \leq .01$). On top of this, intrasession PCC was $\geq .72$ for volume parameters in PE ($P < .02$), but not in UP. For all other parameters, intrasession PCC was not significant on at least one occasion.

Table 3.5: Intersession PCC between mean values of multiple measurements per position per session per subject. Significant correlations are labeled with ○ at the nominal level $\alpha = .05$, and with ● at the nominal level $\alpha = .01$.

Mean values		session 1 vs. session 2							
		UP				PE			
		supine 1	standing	sitting	supine 2	supine 1	standing	sitting	supine 2
Pressure	SBP	.72 ○	.41	.84 ●	.91 ●	.67 ○	.83 ●	.73 ○	.60
	DBP	.76 ○	.72 ○	.69 ○	.76 ○	.49	.37	.66 ○	.45
	MAP	.85 ●	.82 ●	.84 ●	.83 ●	.41	.66 ○	.69 ○	.48
	PP	.46	.25	-.02	.88 ●	.60	.71 ○	.82 ●	.60 ○
Time period	HR	.84 ●	.38	.51	.68 ○	.77 ●	.44	.72 ○	.61
	HPD	.83 ●	.47	.48	.72 ○	.74 ○	.42	.74 ○	.51
	PEP	.47	.65 ○	.69 ○	-.11	.94 ●	.88 ●	.57	.91 ●
	LVET	.18	.83 ●	.76 ○	-.02	.57	.00	.73 ○	.43
	STR	.46	.71 ○	.78 ●	-.22	.58	.47	.41	.51
	ETR	.52	.68 ○	.94 ●	-.26	.43	.48	.74 ○	.12
Volume	SV	.64 ○	.79 ●	.82 ●	.63	.85 ●	-.23	.74 ○	.56
	SI	.60	.84 ●	.86 ●	.67 ○	.82 ●	.09	.82 ●	.60
	CO	.74 ○	.70 ○	.93 ●	.34	.82 ●	.66 ○	.69 ○	.43
	CI	.68 ○	.67 ○	.94 ●	.36	.73 ○	.42	.67 ○	.41
Contractility	ACI	.91 ●	.84 ●	.97 ●	.93 ●	.85 ●	.92 ●	.89 ●	.83 ●
	VI	.94 ●	.96 ●	.98 ●	.95 ●	.95 ●	.96 ●	.95 ●	.95 ●
	HI	.85 ●	.86 ●	.92 ●	.88 ●	.93 ●	.90 ●	.93 ●	.94 ●
	O/C	.26	.52	.57	.60	.31	.71 ○	.54	.67 ○
Resistance	TFC	.84 ●	.97 ●	.97 ●	.92 ●	.97 ●	.95 ●	.96 ●	.95 ●
	TFCI	.90 ●	.98 ●	.98 ●	.94 ●	.97 ●	.94 ●	.96 ●	.96 ●
	TAC	.60	.74 ○	.29	.73 ○	.83 ●	.69 ○	.85 ●	.39
	TACI	.63	.74 ○	.46	.77 ○	.83 ●	.64 ○	.85 ●	.44

Table 3.6: Intrasession PCC between mean values of multiple measurements per subject in supine 1 and supine 2 positions within both sessions (session 1 and session 2). Significant correlations are labeled with ∘ at the nominal level $\alpha = .05$, and with • at the nominal level $\alpha = .01$.

Mean values		supine 1 vs. supine 2			
		UP		PE	
		session 1	session 2	session 1	session 2
Pressure	SBP	.94 •	.89 •	.60	.83 •
	DBP	.86 •	.86 •	.92 •	.40
	MAP	.88 •	.93 •	.93 •	.63 ∘
	PP	.85 •	.83 •	.29	.47
Time period	HR	.81 •	.88 •	.92 •	.92 •
	HPD	.83 •	.87 •	.94 •	.89 •
	PEP	.96 •	.23	.91 •	.94 •
	LVET	.41	.80 •	.70 ∘	.72 ∘
	STR	.79 •	.36	.56	.83 •
	ETR	.45	.63	.57	.58
Volume	SV	.47	.96 •	.79 •	.89 •
	SI	.47	.97 •	.84 •	.89 •
	CO	.42	.93 •	.76 ∘	.82 •
	CI	.38	.92 •	.72 ∘	.79 •
Contractility	ACI	.96 •	.93 •	.96 •	.98 •
	VI	.97 •	.95 •	.98 •	.99 •
	HI	.96 •	.95 •	.95 •	.96 •
	O/C	.51	.87 •	.84 •	.67 ∘
Resistance	TFC	.96 •	.98 •	.99 •	.98 •
	TFCI	.98 •	.99 •	.99 •	.99 •
	TAC	.76 ∘	.85 •	.66 ∘	.61
	TACI	.76 ∘	.87 •	.67 ∘	.60

3.2.5 Discussion

Non-invasive assessment of the cardiovascular system and cardiac contractility is relevant to explore maternal gestational adaptation mechanisms, as well as background mechanisms behind cardiovascular diseases. The aim of this study was to assess the reliability of ICG measurements in pregnant women. Measurements by ICG in non-pregnant subjects are reported to be reliable as they correlate highly under standardized conditions [249, 250, 251, 252, 253, 254], however imprecise ICG in severely ill patients was reported [160, 280]. In healthy non-pregnant subjects, we observed that position-induced changes of ICG measurements are independent from the time of day for time period, volume, contractility, and thoracic impedance [161]. We also found that reproducibility of ICG measurements was much better when mean values of multiple measurements were used for each parameter (see Chapter 3.1) [161]. We used the same study protocol as reported [161] to evaluate ICG measurements in UP and PE.

As is shown in Tables 3.5 and 3.6, intra- but even more intersession correlation for blood pressure parameters was variable. Diurnal variation for maternal blood pressure has been reported, together with diurnal variation of HR [281]. For time periods and volume parameters, intra- and intersession correlation coefficients were lower in pregnancies than in the healthy non-pregnant subjects of our former study [161] (Tables 3.5 and 3.6). This may relate to the pregnancy-associated inability to regulate HR and blood pressure in response to postural alterations [282, 283], and increased gestational variability of HR and blood pressure [284], which is even higher in pregnancy-induced hypertension [285].

Cardiac adaptation with altered contractility is an important feature of maternal cardiovascular changes during pregnancy [9]. In our study, intra- and intersesion correlation was high for contractility parameters, i.e. ACI, VI, and HI, in UP and PE (Tables 3.5 and 3.6). This can be explained partly by the nature of these parameters, i.e. ACI, VI, HI, and TFC are measured directly from the ICG-wave characteristics. Contrary to this, measurements from most other parameters are secondary calculations derived from both ECG- and ICG-waves and/or patient characteristics, and therefore they are more prone to variation. Highly consistent ICG measurements for contractility parameters indicate that ICG can be an appropriate tool to study cardiac contractility in UP and PE.

Thoracic resistance parameters TFC and TFCI also showed high intra- and inter-

session correlation coefficients in UP and PE (Tables 3.5 and 3.6). TFC is a measure of total thoracic fluid content, both intra- and extracellular, which can be measured directly and reliably with ICG [252]. This parameter is for detection of subclinical signs of congestive heart failure in the early stages of pulmonary edema [286, 287]. In PE, higher TFC values have been observed in severe and in mild disease [278, 288]. At values ≥ 65 kOhm^{-1}, the relative risk for development of pulmonary edema in peripartum was 18.2 relative to women with lower values [288]. Our results show that ICG may also be a valuable method to assess early stages of pulmonary edema in PE.

From the data presented in Tables 3.5 and 3.6, we conclude that ICG measurements of cardiac contractility and thoracic fluid content using a third generation device in UP and PE women correlate well after position-induced challenge. Because normal and pathologic change of cardiac contractility has been reported during pregnancy, our results open perspectives to implement ICG as a non-invasive method to study (mal)adaptation of *cardiac contractility* in UP and in PE.

3.2.6 Acknowledgements

The authors would like to thank Prof. Dr. Louis Peeters of the Maastricht University Medical Centre for his kind help and recommendations in our study.

3.3 Impedance cardiography throughout normal pregnancy

Cardiovascular hemodynamics throughout normal pregnancy and postpartum as measured by impedance cardiography

original paper

Kathleen TOMSIN, *Jolien OBEN, Anneleen STAELENS, Tinne MESENS, Geert MOLENBERGHS, Louis PEETERS, Wilfried GYSELAERS*

Submitted to Reproductive Sciences
Reprod Sci 2013

3.3.1 Abstract

ICG measurements were performed to evaluate the feasibility of the non-invasive assessment of maternal cardiac and arterial characteristics (left ventricular output, cardiac cycle time intervals, aortic flow characteristics, and total peripheral vascular resistance (TPVR)) throughout UP and postpartum (n=16). SAS procedure MIXED for linear mixed models was used, and fitted to the data - binned in four-weekly intervals - for each parameter separately. Differences (mean$\pm$ standard error of mean, SEM) between gestational and postpartum measurements were evaluated by One-Sample Wilcoxon Signed Rank Tests. Throughout UP, supine values of SV and CO differed from standing ($P \leq .008$) and sitting values ($P \leq .048$). As compared to early postpartum (7 weeks), all cardiovascular parameters remained unchanged after one year postpartum (n=12; $P \geq .074$). Gestational evolutions of left ventricular output were similar to the reported changes in literature, and were influenced by maternal position. Our study illustrates that ICG has the potential to become a useful tool in perinatal medicine.

3.3.2 Introduction

Normal pregnancy is characterized by a decrease in total peripheral resistance and increased plasma volume [11]. The use of non-invasive alternatives for the conventional methods to study these hemodynamics is becoming increasingly important [289, 80] to understand the cardiovascular maladaptation in pregnancy disorders such as PE [18, 21]. One of these popular non-invasive techniques, i.e. ICG, correlates well with the standard thermodilution technique for CO determination [80]. Moreover, we have recently shown that ICG is reproducible in pregnancy (see Chapter 3.2) [290].

In this prospective study, we aim to describe the hemodynamic changes observed using ICG throughout normal pregnancy to illustrate its usefulness in the study of maternal hemodynamics.

3.3.3 Methods

Approval of the local ethical committee was obtained before study onset (MEC ZOL reference: 09/050). We established a longitudinal observational study in pregnant women presenting at the antenatal outpatient clinic of ZOL in early gestation (November 2009 - March 2010). Singleton pregnancies of women without history or symptoms of medical or cardiovascular diseases were included. All women were included at six to eight weeks of gestation based on ultrasound dates and were evaluated monthly until term. The normal course and outcome of pregnancy was verified postpartum. Measurements were repeated at six to eight weeks postpartum and one year postpartum. Postpartum exclusion criteria were new-onset of pregnancy or symptoms of medical or cardiovascular diseases.

For all women, maternal age at inclusion (years), pregestational and postpartum BMI, nulliparity (yes or no), gestational age at delivery (weeks), and birth weight (g and percentiles) were registered.

After informed consent, all women underwent an ICG examination according to the protocol detailed previously (see Chapters 3.1 and 3.2) [161, 290] using NICCOMO^{TM} (Software version 2.0, SonoSite, Medis Medizinische Messtechnik GmbH, Ilmenau, Germany). The ICG (dZ/dt) is the first mathematical derivative of the thoracic impedance (Z) change over time for an alternating current with high frequency (60-100 kHz) and low amplitude (1 mA) transmitted through the thorax by a four electrode arrangement which eliminates skin resistance.

After ten minutes of adaptation to the supine position, all measurements were registered in three positions: supine, sitting, and standing. Hence, the effect of aortacaval compression can be visualized.

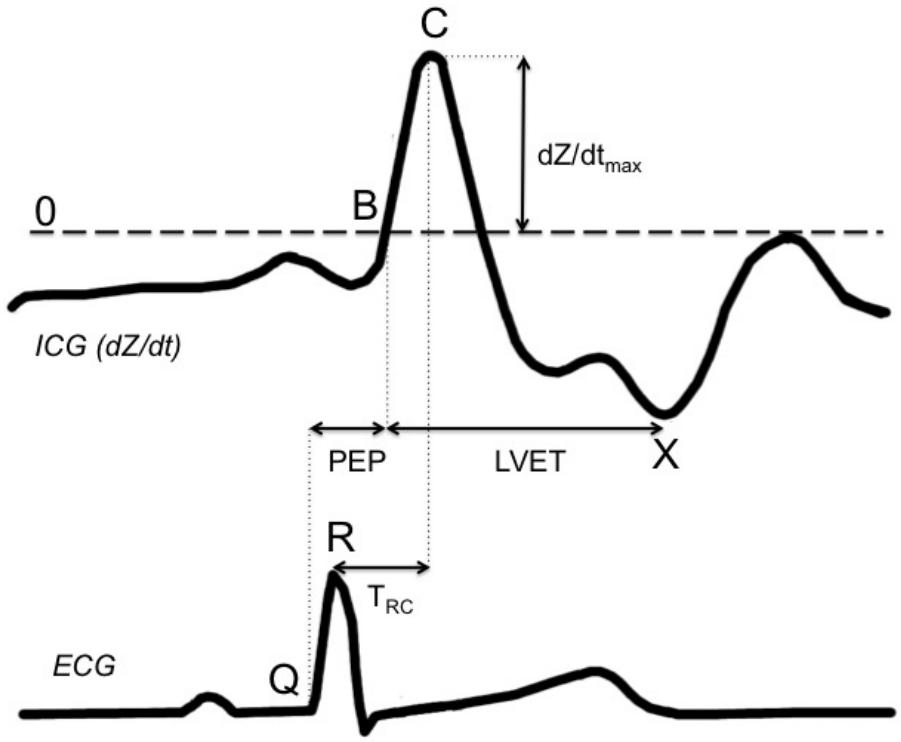

Figure 3.3: The corresponding signals of the ECG and the ICG. ICG (dZ/dt) is the first mathematical derivative of the change in impedance over time (Z) for an alternating current with high frequency (60-100 kHz) and very low amplitude (1 mA) transmitted through the maternal thorax by a four electrode arrangement eliminating skin resistance. Q: start of ventricular depolarization, R: peak ventricular depolarization, B: opening of aortic valve, C: peak systolic flow (dZ/dt_{max}), X: closure of aortic valve, O: opening of mitral valve, and T_{RC}: time from R to C.

Based on both ICG- and ECG-signals (Figure 3.3), all cardiovascular characteristics were assessed by applying third generation algorithms incorporating known electrophysiological and clinical principles [80], and were classified into six groups as follows:

Pressures

SBP and DBP (mmHg) are measured by the automated oscillometric module of the NICCOMO^{TM}-device, enabling the calculation of PP and MAP.

Left ventricular output

HR (beats/min) was calculated from the HPD (ms), measured as the RR-interval of the ECG-signal. SV (mL) was calculated using the Sramek-Bernstein formula (see Equation 1.2), which incorporates the electrically participating chest tissue estimated from patient's characteristics [260]. CO (L/min) represents the amount of blood pumped by the heart per minute, calculated from

$$CO = HR \times SV \tag{3.1}$$

Cardiac cycle time intervals

PEP (ms) is the period of isovolumetric ventricular contraction defined as the time interval between the ECG's Q-wave (start of ventricular depolarization) and the ICG's B-point (opening of the aortic valve), i.e. the time needed for the ventricle to exceed the aortic pressure and start ejection (electrical systole, Figure 3.1). LVET (ms) represents the duration of ejection (mechanical systole) [291] and is the time interval between the B- and X-point (opening and closing of the aortic valve, respectively) of the ICG (Figure 3.1). Together, PEP and LVET represent the electromechanical systole. Diastolic time (DT) (ms) [292] is calculated as $HPD - (PEP + LVET)$. Both LVET and DT are expressed as a percentage of HPD, i.e. LVET index (LVETi) and DT index (DTi) [293]. STR is calculated as the ratio of the electrical and the mechanical systole, that is

$$STR = \frac{PEP}{LVET} \tag{3.2}$$

Aortic flow

Characteristics of aortic flow were derived from the normalized Z waveform, i.e. ICG (dZ/dt) corrected for an individual's Z_0.

$$VI = 1000 \times \left(\frac{dZ}{dt_{max}} / Z_0\right) \text{ in } 1/1\ 000/\text{s} \tag{3.3}$$

is the equivalent of the amplitude or maximum velocity of the systolic wave (C-point).

$$ACI = 100 \times \left(\frac{d^2Z}{dt^2_{max}} / Z_0\right) \text{ in } 1/100/\text{s}^2 \tag{3.4}$$

is the equivalent of the maximum acceleration of blood flow in the aorta (d^2Z/dt^2), second mathematical derivative of the change in Z over time).

$$HI = \frac{dZ}{dt_{max}}/T_{RC} \text{ in Ohm/s}^2 \tag{3.5}$$

represents the amplitude of the systolic ICG-wave which is corrected for the time needed by the ventricle to reach maximum ejection (ECG R-wave to ICG C-wave; T^{RC}). The distensibility of the aorta is estimated by TAC (mL/mmHg) [294]. This is calculated as

$$TAC = \frac{SV}{PP} \tag{3.6}$$

Total peripheral vascular resistance

TPVR in mmHg/L/min was estimated as

$$TPVR = \frac{MAP}{CO} \tag{3.7}$$

Thoracic fluid

The base impedance (Z_0 in Ohm) represents the overall Z measured across the thorax, which is influenced by the amount of conducting fluid in the thorax. This fluid level is expressed as TFC (1/kOhm).

Orthostatic index

For every ICG-parameter, an orthostatic index (OI) [263, 267] was calculated as a percentage of change when moving from supine to standing position:

$$OI = \frac{\text{standing value}}{\text{supine value}} \times 100 - 100 \tag{3.8}$$

In order to establish reference curves, a linear mixed model was fitted to the data for each parameter separately [142]. As such, a random subject effect was included. To avoid imposing parametric structures on the curve, an unstructured profile was considered. To this end, the data were binned in four-weekly intervals between eight weeks of gestation and term. For each gestational age interval, the median value was calculated and plotted graphically. For this, SAS procedure MIXED (SAS Inc., software version 9.2, Chicago, IL, USA) was used.

Differences between gestational and postpartum measurements were evaluated by One-Sample Wilcoxon Signed Rank Tests. All data are represented as means (SEM) or numerical values (%).

3.3.4 Results

In 16 women with UP, nine consecutive ICG-examinations were performed at 8 ± 0, 12 ± 0, 16 ± 0, 20 ± 0, 24 ± 0, 28 ± 0, 32 ± 0, 36 ± 0, and 38 ± 0 weeks of gestation. Four women missed the last ICG-examination because they delivered between 37 and 38 weeks of gestation. Postpartum measurements were performed at 7 ± 0 weeks and at 53 ± 0 weeks postpartum. Four women were excluded at one year postpartum for new-onset medical disease (n=1), pregnancy (n=2), and drop-out (n=1). Demographic characteristics at inclusion and pregnancy outcome are listed in Table 3.7. Women's BMI was 1 ± 0 kg/m^2 lower one year postpartum (n=12) compared with their early postpartum value (P=.040).

Table 3.7: Demographic characteristics and pregnancy outcome of normal pregnant women. Data are represented as means (SEM) or numerical values (%).

	UP (n=16)
Demographic characteristics at inclusion	
Maternal age (years)	29 ± 1
BMI (kg/m^2)	23 ± 1
Nulliparity (%)	n=9 (56)
Pregnancy outcome characteristics	
Birth weight (g)	$3\,387\pm121$
Birth weight (percentile)	54 ± 6
Gestational age at delivery (weeks)	39 ± 0

Gestational evolution and postpartum values of ICG measurements are shown in Figure 3.4 and Table 3.8. All parameters changed significantly throughout pregnancy in all three positions ($P \leq .0001$).

In third trimester UP, SV and CO (Figure 3.4) tended to fall in supine position compared with standing or sitting positions ($P \leq .036$). Gestational evolution of HR differed between supine and standing positions ($P = .023$) as HR in supine position tended to rise towards term. Next to this, PEP and LVETi also showed a different gestational evolution between the supine and standing positions ($P \leq .047$). Throughout UP, no differences in left ventricular output characteristics were observed between standing and sitting positions ($P \geq .389$).

When comparing one year postpartum values (53 ± 0 weeks) to early postpartum, no significant differences were observed ($P \geq .074$), except for standing DBP which decreased with 5 ± 2 mmHg one year postpartum ($P = .037$).

When comparing early gestational measurements with postpartum values, CO was higher ($P = .016$) in supine position due to an increase in HR ($P = .011$), but not in SV ($P = .753$) (Table 3.8). Next to this, early gestational STR and PEP were significantly lower ($P \leq .006$), whereas LVETi was significantly higher ($P = .041$). Moreover, VI, ACI, and HI were higher ($P \leq .004$) at early gestation when compared with postpartum values. OI of all parameters were comparable between early gestation and early postpartum ($P \geq .090$).

As compared to term pregnancy, standing SBP and PP both decreased at early postpartum ($P \leq .049$). During standing position, early postpartum values for SV and CO were decreased compared with term gestational values ($P \leq .008$). STR was increased together with an increase in PEP ($P \leq .028$); LVETi was significantly lower in postpartum as compared with term pregnancy ($P = .012$). TFC was decreased at early postpartum compared with term pregnancy ($P = .013$).

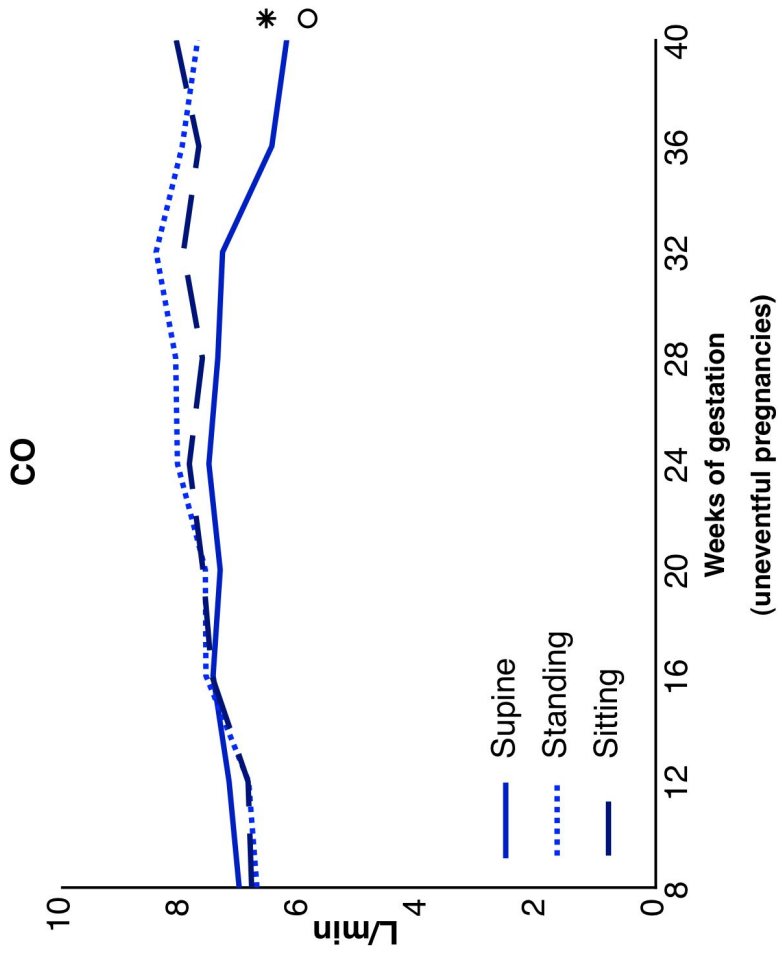

Figure 3.4: For each gestational age, medians of CO were calculated per position and presented graphically. Full, dotted and dashed lines are used for differentiation between supine, standing and sitting positions, respectively. Significant differences between supine and standing, and between supine and sitting positions are indicated with an asterisk and circle, respectively. There was no significant difference between standing and sitting positions.

Table 3.8: ICG-measurements at early gestation (supine: n=16; standing: n=14), term (supine and standing: n=12), early postpartum (supine and standing: n=16), and late postpartum (supine and standing:n=12). Data are presented as means (SEM).

		Pregnancy		Postpartum	
		8± 0 weeks	38± 0 weeks	7± 0 weeks	53± 0 weeks
Pressures					
SBP (mmHg)	supine	114± 2	119± 4	114± 2	111± 3
	standing	117± 2	123± 4	117± 3	112± 3
DBP (mmHg)	supine	72± 2	78± 2	73± 1	71± 2
	standing	78± 2	82± 3	81± 2	78± 2
MAP (mmHg)	supine	82± 2	87± 3	82± 2	81± 2
	standing	88± 2	93± 3	91± 2	88± 2
PP (mmHg)	supine	42± 1	41± 3	41± 2	39± 2
	standing	39± 2	40± 2	36± 2	34± 1
Left ventricular output					
CO (L/min)	supine	7.0± 0.4	6.5± 0.4	6.4± 0.4	6.5± 0.4
	standing	6.8± 0.3	7.9± 0.4	6.3± 0.3	6.0± 0.3
HR (1/min)	supine	77± 2	80± 2	70± 2	70± 2
	standing	93± 3	92± 3	88± 3	84± 3
SV (mL)	supine	92± 5	82± 5	92± 5	93± 6
	standing	73± 3	87± 4	72± 3	72± 3
Cardiac cycle time intervals					
PEP (ms)	supine	91± 3	124± 5	107± 3	103± 4
	standing	102± 4	113± 5	127± 3	122± 4
LVETi (%)	supine	37± 1	33± 1	35± 1	36± 1
	standing	38± 1	38± 1	36± 1	35± 1
DTi (%)	supine	52± 1	51± 2	53± 1	52± 2
	standing	47± 1	45± 1	46± 1	48± 1
STR	supine	0.32± 0.02	0.50± 0.03	0.36± 0.02	0.34± 0.01
	standing	0.42± 0.02	0.46± 0.02	0.52± 0.02	0.49± 0.01
Aortic flow					
VI (1/1 000/s)	supine	75± 3	58± 4	66± 4	67± 4
	standing	65± 3	67± 5	62± 3	62± 4
ACI ($1/100/s^2$)	supine	128± 7	93± 6	110± 7	111± 8
	standing	124± 8	123± 11	119± 6	116± 8
HI (Ohm/s^2)	supine	20.7± 1.4	12.7± 1.5	16.1± 1.3	16.3± 1.4
	standing	18.1± 1.2	16.3± 1.6	14.7± 0.8	14.7± 1.0
TAC (mL/mmHg)	supine	2.2± 0.1	2.1± 0.1	2.3± 0.1	2.4± 0.1
	standing	1.9± 0.1	2.2± 0.1	2.1± 0.1	2.2± 0.1
Total peripheral vascular resistance					
TPVR (mmHg/L/min)	supine	12.2± 0.6	14.1± 1.0	13.6± 0.8	13.0± 0.7
	standing	13.4± 0.8	12.2± 0.9	14.8± 0.6	14.9± 0.8
Fluid					
TFC (1/kOhm)	supine	31.6± 1.4	35.7± 2.4	31.3± 0.9	31.7± 1.0
	standing	28.7± 0.8	31.3± 1.8	27.6± 0.7	27.5± 0.7

3.3.5 Discussion

In the non-critically ill pregnant woman, the use of invasive techniques such as pulmonary artery catheterization are rarely justified as they are associated with significant intrinsic morbidity. ICG may offer a good alternative to these conventional invasive methods, allowing for the assessment of the cardiac and arterial system in pregnancy [290].

Specialists in hemodynamics often criticize ICG measurements because they are obtained from mathematical calculations. On top of this, their correct physiological nature is not always easily understood. Despite these limitations, a recent meta-analysis reported good correlation between ICG measurements and those obtained by invasive methods, specifically in non-critically ill patients [80]. Moreover, it has been reported that ICG measurements are reproducible under standardized conditions in non-pregnant individuals [161], in UP, and PE [290].

Our study illustrates that gestational and postpartum evolution of ICG-measurements of cardiovascular function is similar to reported observations using other methods [13, 16, 295]. Our study shows the relevance of maternal position during this examination: SV, CO, PEP, and LVETi were significantly different between supine and standing positions. These left ventricular characteristics are derived from the preload-dependent parameter LVET [291, 296]. These observations are likely to be related to the growing pregnant uterus which interferes with venous return [51, 89, 92] in the supine position. This phenomenon possibly troubles the interpretation of CO evolution near term, as is indicated by the reported presence of conflicting results of CO evolution from third trimester pregnancy to term [19]. On top of this, different filling states amongst the female population could also explain those inconsistent results: High variability in CO and plasma volume is observed in pregnancy disorders such as PE [135, 137]. This variability helped to explain the reoccurrence of PE in women with a low plasma volume [240], which is suggested to be linked to venous capacitance [238, 297].

Most hemodynamic parameters are suggested to return to preconception values within 8 to 12 weeks postpartum [298], which is also true in our study. Next to this, we found that early postpartum measurements around 7 weeks postpartum did not differ from one-year postpartum, except for a subclinical difference in DBP (Table 3.8). As compared to early postpartum values, we reported a higher HR in early pregnancy resulting in an increase in CO, together with an increase in the aortic flow

parameters VI, ACI, and HI, and lower STR and PEP values. This is in line with other observations, reporting an early augmentation of sympathetic activity [15] in reaction to the primary fall in systemic vascular tone [1].

Despite the small number of women included in this study, we conclude that our observations illustrate the feasibility of ICG in the observation and registration of cardiac and arterial adaptation mechanisms throughout human pregnancy, hereby emphasizing the importance of the position of the maternal body. This opens perspectives for ICG as a potentially useful method in the cardiovascular assessment of women with gestational complications, such as hypertension, PE, or FGR.

3.3.6 Acknowledgements

The authors would like to thank all the women included in this study and their husbands for their commitment to this project throughout and beyond their entire pregnancy.

Chapter 4

The cardiovascular profile

4.1 The feasibility of the cardiovascular profile

Non-invasive cardiovascular profiling using combined electrocardiogram-Doppler ultrasonography and impedance cardiography:

an experimental approach

Kathleen TOMSIN*, Annette VRIENS, Tinne MESENS, Wilfried GYSELAERS*

Clinical and Experimental Pharmacology and Physiology
In revision 2013

4.1.1 Summary

Aim In this experimental study, the feasibility of cardiovascular profiling using both combined ECG-Doppler ultrasonography and ICG is evaluated.

Methods 14 non-pregnant healthy women received 500 mL of saline solution (NaCl 0.9% at 999 mL/h) intravenously by steady-state infusion. Before and after this acute volume loading, we measured orthostatic-challenged cardiac and arterial characteristics using ICG, and assessed venous characteristics by combined ECG-Doppler before and during Valsalva manoeuvre. Changes are expressed as means ± SEM and evaluated by One-Sample Wilcoxon Signed Rank Tests.

Results After volume loading, the observed fall in SV after postural change from supine to standing decreased (-14± 3 versus -23± 2%; P=.011). Hepatic A-wave velocity increased 63± 28% after volume loading (P=.007), and decreased during the Valsalva manoeuvre (-205± 21%; P=.001). Volume loading raised the TFCI in both the supine and standing positions (7± 2% and 10± 1%, respectively; $P \leq .014$).

Discussion Combined ECG-Doppler ultrasonography and ICG enables the non-invasive identification of concomitant hemodynamic changes at the level of the heart, the arterial bed, and the venous compartment. Our data support the view that non-invasive cardiovascular profiling is feasible, which seems particularly useful to evaluate non-critically ill patients, such as pregnant women.

4.1.2 Introduction

Many common cardiovascular diseases, such as heart failure, include the malfunctioning of heart and arteries as well as the venous system [299]. This is also true for PE, a complex pregnancy disorder with high maternal and neonatal morbidity [181, 300]. Therefore, we define cardiovascular profiling as the assessment of cardiac function in combination with arterial and venous hemodynamics, thus allowing an integrated evaluation of an individual's cardiovascular state. However, the invasive nature of the conventional techniques limits their application in non-critically ill individuals such as pregnant women [273, 274, 275]. Therefore, non-invasive cardiovascular profiling has gained popularity in the field of risk stratification and personalized treatment strategy of several cardiovascular diseases [47]. Recent studies have shown high feasibility of combined ECG-Doppler ultrasonography in the assessment of venous characteristics in UP and PE [156, 301]. Additionally, ICG has been shown to reliably estimate cardiac and arterial characteristics in both non-pregnant [161] and pregnant subjects [290]. The combination of both techniques enables non-invasive maternal cardiovascular profiling, the performance of which has not been described yet. This methodology has potential *1*) to increase our fundamental knowledge of maternal hemodynamics in both normal and pathological pregnancies, and *2*) to expand the current clinical work-up, including prevention and treatment, of gestational disorders such as PE and IUGR.

In this experimental study, the feasibility of cardiovascular profiling using combined ECG-Doppler ultrasonography together with ICG is evaluated by changing one hemodynamic variable in a non-pregnant female population, i.e. an acute increase of the intravascular volume by a simple saline infusion. It has been reported in rats that isotonic blood volume expansion triggers an acute increase in ANP and a fall in vasopressin, inducing both natriuresis and water dissipation, thus eventually restoring the original volume status [302]. We hypothesize that our non-invasive, easily applicable, and highly accessible cardiovascular profiling test will be able to register these minor acute hemodynamic changes at different sites of the circulation, thus opening perspectives for non-invasive and integrated hemodynamics studies in obstetrics.

4.1.3 Methods

Protocol

After approval of the local ethical committee (MEC ZOL reference: 09/049), 14 healthy non-pregnant nulliparous women were included and informed consent was

obtained. In all women, we assessed the cardiovascular profile before and after a continuous steady-state saline infusion according to the following protocol:

1. ICG-examination in four positions (supine, standing, sitting, and supine)
2. ECG-Doppler examination in supine position
3. Intravenous administration of 500 mL saline solution (NaCl .9% at 999 mL/h)
4. ECG-Doppler examination in supine position
5. ICG-examination in four positions (supine, standing, sitting, and supine)

Participants were asked to limit water consumption in the four to five hours prior to the experiment to one glass of ± 225 mL and to present themselves with an empty bladder. We only wanted to induce modest changes in the hemodynamics, avoiding rapid non-physiologic changes in volume regulation, while also enabling the evaluation of the performance of the technique. Therefore, we performed volume loading with an isotonic instead of an iso-oncotic solution.

Combined ECG-Doppler examination

Combined ECG-Doppler examinations using a 3.5 MHz transabdominal probe (Toshiba Aplio Mx) were performed in a supine position at the level of the RIV and HV. Here, impedance indices (RIVI and HVI) were calculated as [(velocity X - velocity A)/velocity X] (see Equation 2.1), and VPTT as the time interval between the ECG P-wave and the corresponding venous Doppler A-wave corrected for HPD (Figure 2.9 (A and B)). The effect of increasing intra-abdominal pressure on the HV Doppler waveform characteristics was assessed by means of the Valsalva manoeuvre.

ICG examination

Cardiac and arterial changes were measured using the NICCOMO^{TM} (Software version 2.0, SonoSite, Medis Medizinische Messtechnik GmbH, Ilmenau, Germany - as presented in Chapter 3.3) [161], an ICG-device of the third generation [161, 290]. PP was measured using the automated oscillometric module of the device. ICG-parameters were assessed based on the corresponding signals of the ECG- and the ICG-waveforms (Figure 3.3), as explained in the next paragraph. In order to establish cardiac reflex responses, OI of these ICG-measurements were calculated as a percentage change induced by standing up from a supine position.

CO (L/min) was calculated as HR (in beats/min) $\times$ SV (in mL) (following the Sramek-Bernstein [260]). STR was measured as the ratio of the electrical systole and the mechanical systole: the electrical systole is defined as the time interval between Q-wave of ECG and opening of aortic valve (B-point of ICG, Figure 3.3), and the mechanical systole is defined as the time interval between opening and closing of the aortic valve (B- to X-point of ICG, Figure 3.3). VI (i.e. maximum aortic flow velocity), ACI (i.e. maximum aortic flow acceleration), and HI (i.e. maximum aortic flow velocity corrected for the time needed to reach this maximum ejection) were derived from the systolic wave (C-point of ICG, Figure 3.3), which reflect properties of cardiac contractility. TAC (mL/mmHg) was defined as the ratio of SV and PP. TFCI (1/kOhm/m^2) represented the overall impedance across the thorax corrected for body surface area, which is estimated by the Dubois and Dubois's formula [261].

Statistical analyses

For all parameters, we calculated the % change after volume loading relative to baseline values. For OI, we based the % change after volume loading on a so-called "difference-in-difference model", calculated as follows: [(standing value - supine value)$_{post}$ - (standing value - supine value)$_{pre}$] / (standing value - supine value)$_{pre}$ $\times$ 100.

Data are presented as means $\pm$ SEM. Relative changes were evaluated by a two-sided One-Sample Wilcoxon Signed Rank Test. This paired statistical approach reduces the effects of confounding factors arising from high inter-individual variability. Significant results were denoted as P-values at nominal level $\alpha = .05$. All statistical analyses were done using the SPSS package (SPSS Inc., Software version 19.0, Chicago, IL, USA).

4.1.4 Results

Table 4.1 lists the relative changes triggered by volume loading in the combined ECG-Doppler measurements in supine position. Volume loading shortened VPTT in kidneys and liver ($P \leq .042$), while also inducing a rise in the left RIVI ($P = .028$). The right RIVI and the HVI did not change appreciably in response to volume loading. The Valsalva manoeuvre flattened HV Doppler waveform irrespective of volume loading, obstructing the measurement of HVI and VPTT in over 30% of the cases. Figure 4.1 illustrates the effect of volume loading and the Valsalva manoeuvre on the HV flow pattern; volume loading induced a 63$\pm$ 28% rise in HV Doppler A-wave velocity

(Panel A to Panel B, Figure 4.1) (P=.007). The Valsalva manoeuvre reversed the HV Doppler A-wave from a positive (retrograde) to a negative (forward) flow, irrespective of volume loading (Panels C and D, Figure 4.1) (-205± 21% and -204± 56%; $P \leq .009$).

Table 4.1: The percentage change after acute volume loading of the combined ECG-Doppler ultrasonography measurements (supine position, during normal breathhold) presented as mean and SEM. A two-sided One-Sample Wilcoxon Signed Rank Test at nominal level α =.05 was used to evaluate the percentage change after acute volume loading and presented as P-values.

		Mean± SEM	P-value
Left RIV	RIVI	12± 5%	.028
	VPTT	-9± 4%	.042
Right RIV	RIVI	5± 5%	.552
	VPTT	-16± 4%	.007
HV	HVI	34± 19%	.209
	VPTT	-11± 4%	.041

Although volume loading in the supine position did not induce appreciable changes in left ventricular and aortic parameters (data not shown; $P \geq .054$), it did lead to a small but consistent rise in HI (1± 13%; P=.030). Table 4.2 lists the volume loading-induced response in the standing position of HR, SV, STR, and TAC ($P \leq .025$). All these variables had changed towards a more attenuated orthostatic stress response ($P \leq .033$; Table 4.3). Volume loading had induced a consistent rise in TFCI ($P \leq .014$) in the supine (7± 2%) as well as in the standing (10± 1%) position.

Table 4.2: The percentage change after acute volume loading of ICG measurements (standing position) presented as mean and SEM. A two-sided One-Sample Wilcoxon Signed Rank Test at nominal level α =.05 was used to evaluate the percentage change after acute volume loading and presented as P-values.

		Mean± SEM	P-value
Left ventricle	CO	9± 11%	.422
	HR	-4± 6%	.023
	SV	12± 4%	.001
	STR	-8± 3%	.023
Aorta	VI	13± 15%	.861
	ACI	10± 12%	.807
	HI	4± 12%	.148
	TAC	22± 10%	.025
Thorax	TFCI	10± 1%	.001

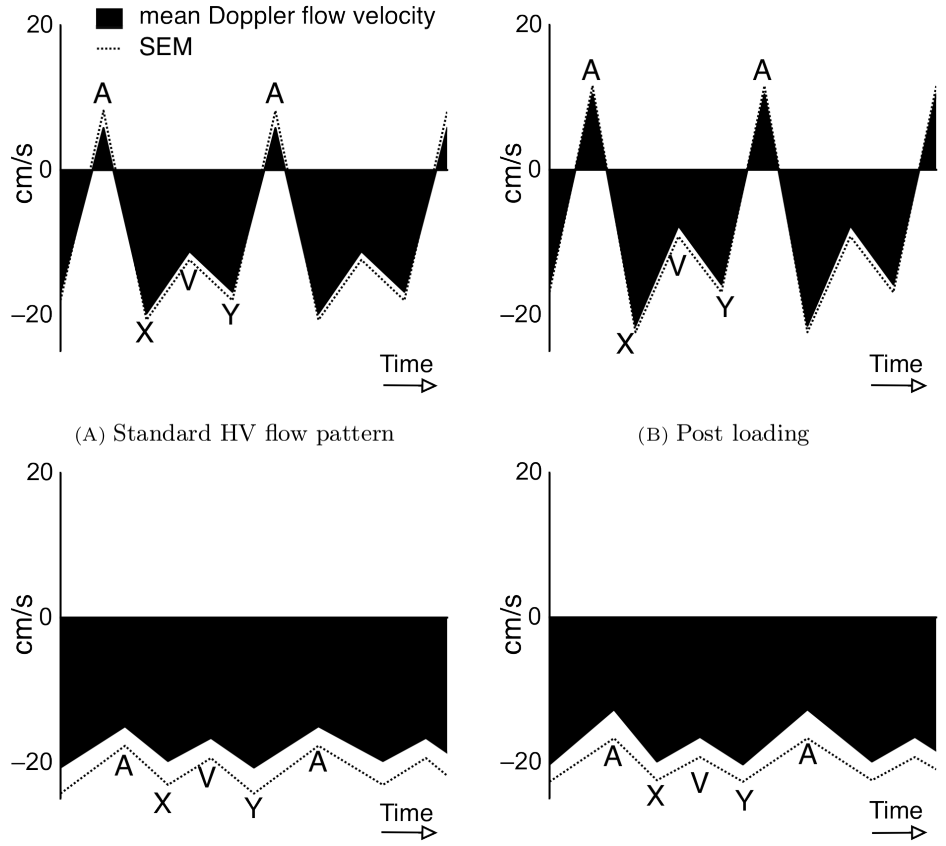

(A) Standard HV flow pattern

(B) Post loading

(C) Valsalva manoeuvre

(D) Post loading, Valsalva manoeuvre

Figure 4.1: Illustration of the effect of acute volume loading (panel B and D) and Valsalva manoeuvre (panel C and D) on standard non-pregnant hepatic venous flow (panel A). Doppler velocity measurements of the HV flow characteristics (A, X, V, and Y) in 14 healthy non-pregnant women are presented graphically as means (standard error of means).

Table 4.3: OI as measured by ICG when moving from supine to standing position, presented as mean and SEM, in both the pre- and post-acute volume loading condition. A two-sided One-Sample Wilcoxon Signed Rank Test at nominal level $\alpha = .05$ was used to evaluate the OI and significant P-values are marked with an $*$. The percentage change after acute volume loading of the OI as measured by ICG, presented as mean and SEM. A two-sided One-Sample Wilcoxon Signed Rank Test at nominal level $\alpha = .05$ was used to evaluate the percentage change after acute volume loading and presented as P-values

		OI		% change after acute volume loading of the OI	
		Pre acute volume loading	Post acute volume loading		
		Mean± SEM	Mean± SEM	Mean± SEM	P-value
Left ventricle	CO	-11± 3%*	-5± 3%	-40± 63%	.824
	HR	17± 4%*	11± 3%*	-34± 24%	.064
	SV	-23± 2%*	-14± 3%*	33± 11%	.011
	STR	48± 7%*	35± 4%*	85± 117%	.033
Aorta	VI	-13± 3%*	-7± 3%	67± 74%	.233
	ACI	3± 6%	7± 7%	91± 70%	.730
	HI	-5± 4%	-2± 4%	0± 48%	.777
	TAC	-17± 6%*	14± 16%	192± 130%	.003
Thorax	TFCI	-15± 2%*	-13± 1%*	-3± 10%	.706

4.1.5 Discussion

We define cardiovascular profiling as the integrated evaluation of heart, arteries, and veins. Non-invasive cardiovascular profiling would allow the study of hemodynamic changes in the non-critically ill patient, e.g. the pregnant woman suffering from an obstetrical cardiovascular complication such as PE [289, 80]. Here, the use of invasive techniques such as pulmonary artery catheterization is rarely justified as they are associated with an increased risk of morbidity [289, 80]. Moreover, techniques such as ICG are considered to be a cost-effective alternative to invasive monitoring by lowering both material- and complication-related costs [303]. In this experiment, we evaluated the feasibility of an easily applicable, non-invasive cardiovascular profile test to detect small changes in the hemodynamic function. We assessed the effect of acute volume loading on the venous functional characteristics in healthy non-pregnant women using combined ECG-Doppler ultrasonography together with ICG. The use of a paired statistical analysis reduces the high variability, as indicated by the large standard errors (Tables 4.1, 4.2, and 4.3), resulting from *1*) our indirect measurement approach of cardiovascular parameters, *2*) the small plasma volume expansion, and *3*) the inter-individual differences in e.g. the HV flow patterns [62] or the hemodynamic response to orthostatic challenge [265].

Our results indicate that an acutely administered volume load disperses over the extracellular space, which is seven times larger than the intravascular compartment. In the supine position, cardiac changes in response to volume loading consisted of a small but consistent rise in HI, suggesting a rise in cardiac contractility. As expected, volume loading also attenuated the response to orthostatic stress, as indicated by the blunted rise and fall in HR and SV, respectively, without an appreciable change in CO. The effect of volume loading on the venous system was most prominent, reflected in a shorter VPTT. Obviously, volume loading raised TFCI and was accompanied by accelerated urine production indicating activated volume dissipation. The latter stimulates the release of ANP [304]. Higher circulating levels of ANP accelerate natriuresis, thus dissipating excessive extracellular fluid [304].

In this study, we observed VPTT shortening after acute volume loading. This effect may relate to the increased venous filling state induced by volume loading. Besides the shortening of the VPTT, volume loading also raised the HV A-wave velocity, which indicates reversed flow from the right atrium into the inferior vena cava during atrial contraction [92]. A rise of HV A-wave velocity without a concomitant rise in CO may also relate to an increased venous filling state. The absence of this effect

in the RIV may indicate that the splanchnic bed is the primary site of venous storage.

Raising intra-abdominal pressure by the Valsalva manoeuvre transformed the standard triphasic- into a biphasic HV Doppler wave pattern (Figure 4.1 (C)). This pattern resembles the one observed in advanced pregnancy [91, 93].

The impact of volume loading on the cardiac and arterial parameters in our study was small. Nevertheless, volume loading did increase tolerance to orthostatic stress as indicated by a smaller post-loading rise in STR after standing up from a supine position. This observation is likely to result from a positive inotropic effect induced by the rise in venous return by volume loading [305, 306]. Meanwhile, other cardiac and arterial changes evaluated in the supine position were small and inconsistent. Our results are consistent with reports in basic animal studies stating that isotonic blood volume expansion induces physiological changes to eventually restore baseline volume status [302].

We realize that the results of our pilot study only consist of indirectly measured hemodynamic % changes in response to volume loading and orthostatic stress. Nevertheless, these observed changes are all in line with physiologic expectations. Therefore, we feel that our study illustrates the feasibility of our proposed non-invasive procedure to evaluate and monitor the cardiovascular function and to detect relevant hemodynamic changes at different sites in the cardiovascular system. Therefore, this study supports the application of this type of non-invasive cardiovascular profiling to study hemodynamics in non-critically ill individuals, such as pregnant women.

4.1.6 Acknowledgments

The authors would like to thank Geert Molenberghs (PhD), director of the Interuniversity Institute for Biostatistics and statistical Bioinformatics at the universities of Hasselt and Leuven (Belgium), for his recommendations on the statistical approach used in this study.

4.2 The cardiovascular profile in maternal hypertensive disorders

---

The cardiovascular profile of gestational hypertension and preeclampsia

original paper

Wilfried GYSELAERS, ***Kathleen TOMSIN****, Tinne MESENS, Jolien OBEN, Anneleen STAELENS, Geert MOLENBERGHS*

Submitted to British Journal of Obstetrics and Gynaecology
BJOG 2013

4.2.1 Abstract

Objective To identify differences of cardiac, arterial, and venous function between UP, non-proteinuric gestational hypertension (GH), and PE.

Design Observational cohort study.

Setting Secondary level referral centre for fetomaternal medicine in Belgium.

Methods A non-invasive standardized cardiovascular assessment with ICG and combined ECG-Doppler ultrasonography was performed in 13 women with UP, 21 with GH, 34 with LPE ($\geq$ 34 weeks) and 22 with EPE ($\leq$ 34 weeks). ICG parameters were aortic flow VI, ACI, and TFC. ECG-Doppler parameters at the level of arcuate UtArt were resistive index, pulsatility index, and arterial PTT, as well as VPTT and venous impedance index (see Equation 2.1) at the level of RIV and HV. Mann-Whitney *U*-test, Kruskall-Wallis test, and linear regression analysis with heteroskedastic variance was used for statistical analysis.

Results Compared to UP, $>30\%$ lower values for VI and ACI ($P \leq .029$), and $>15\%$ lower values for arterial PTT ($P \leq .012$) were found for GH, LPE, and EPE. Compared to GH, proteinuria of EPE and LPE was associated with $>15\%$ higher values for RIVI in both kidneys ($P \leq .010$).

Conclusion In comparison to UP, similar abnormalities of cardiac systolic dysfunction and arterial PTT were found in GH, EPE, and LPE. In EPE and LPE, proteinuria was associated with increased RIVI, which was not observed in GH.

4.2.2 Introduction

Cardiovascular profiling is defined as the integrated assessment of an individual's cardiac function, together with arterial and venous hemodynamics. In a recent review, it has been suggested that cardiovascular profiling may be useful in the assessment of women with UP and those with gestational complications such as PE or FGR [181]. Abnormal arterial tone and increased arterial stiffness in PE have been reported [2, 307]. This is reflected in abnormal notching and increased pulsatility index in duplex ultrasound assessment of the UtArt [2] and in abnormal serum analytes in pregnant women destined to develop PE [308]. It has also been reported that the maternal heart is subject to morphological and functional changes during UP [16], and that this cardiac adaptation is different in women with PE [309, 310] or destined to develop PE [311]. Finally, it has been reported that PE is associated with venous hemodynamic dysfunction [147], which is present weeks before clinical onset of disease [95, 181].

Combined ECG-Doppler ultrasonography [156, 301, 312] and ICG are non-invasive methods to study maternal hemodynamics, with acceptable reproducibility and repeatability when applied according to standardized protocols [161, 290]. In this study, we used combined ECG-Doppler evaluation of maternal arterial and venous hemodynamics, and ICG for assessment of cardiac and arterial function, to evaluate the cardiovascular profile of women with UP, non-proteinuric GH, EPE, or LPE.

4.2.3 Material and Methods

Women were considered for inclusion, when admitted to the Fetal Maternal Medicine Unit of ZOL (between 1/10/2009 and 31/10/2012) for gestational hypertensive disease. For this study, we excluded women with multiple gestation, EH, renal disease, history of organ transplantation, women with concomitant diseases as diabetes, thyroid dysfunction, cholestasis, or liver disease, and women with HELLP syndrome without proteinuria or with non-hypertensive proteinuria, leaving for inclusion only those women without known diseases and new onset hypertension $>$ 20 weeks. Definitions of GH and PE were used, according to the criteria of the National High Blood Pressure Education Program Working Group on High Blood Pressure in Pregnancy [313]: hypertension is defined as blood pressure $>$ 140/90 mmHg on at least two occasions at least six hours apart. New onset hypertension of more than 20 weeks with proteinuria less than 300 mg/24h is defined as GH, whereas hypertension with proteinuria $\geq$ 300 mg/24h is defined as PE. PE less than 34 weeks is defined as EPE,

whereas PE $\geq$ 34 weeks is defined as LPE.

All women had clinical observations for at least 24h, including blood pressure measurement ($3\times$ per day), fetal monitoring (once per day), 24h urine sampling for quantitative assessment of creatinine clearance and proteinuria, and serum analysis for hemoglobin level, hematocrit, blood platelet count and concentrations of ASAT, ALAT, and uric acid. After informed consent, all women had combined ECG-Doppler investigations in supine position at the level of HV, RIV of both kidneys, and left and right arcuate UtArt as reported [94, 93, 301], using a 3.5 MHz probe (Aplio Mx, Toshiba Medical Systems nv, Sint-Stevens-Woluwe, Belgium). Arcuate UtArt were preferred over UtArt for their intra-parenchymal localization, comparable with the localization of HV and RIV [156]. The Doppler ultrasound measurements of the arcuate UtArt were performed within a maximum of two cm distance from the bifurcation of the UtArt. None of the subjects were in labor at the time of the investigations. Doppler investigations were performed by two sonographers, with a known inter-observer and intra-observer correlations of $\geq .86$.

Immediately after the Doppler ultrasonography, all women had ICG-assessment in supine and standing position using the NICCOMO^{TM} (Software version 2.0, Medis Medizinische Messtechnik GmbH, Ilmenau, Germany) according to the reported methodology and protocol with known repeatability [161, 290]. This ICG technique is a non-invasive method of evaluating hemodynamic parameters, based on thoracic resistance changes measured during each heart cycle of a high frequent, low powered electrical current using a set of four skin-electrodes.

ICG-parameters were classified as pressure parameters, left ventricular output parameters, aortic flow parameters, and TFC (1/kOhm) [161, 290]. Pressure parameters were SBP, DBP, PP (= SBP - DBP), and MAP (= DBP + PP/3), all expressed in mmHg. Left ventricular output parameters were SV in mL, HR in beats/min, and CO in mL/min ($HR\times SV$). Aortic flow parameters were VI in 1/1 000/s which is equivalent to the amplitude of the systolic wave, ACI in 1/100/s^2 which stands for the maximum acceleration of blood flow in the aorta, HI in Ohm/s^2 in which the amplitude of the systolic ICG wave is corrected for the time needed by the ventricle to reach maximum ejection, and TAC in mL/mmHg which is calculated as SV/PP and is equivalent for distensibility of the arterial vascular system.

Maternal Doppler flow parameters were classified as RIVI, HVI or arterial resistive

index (see Equation 2.1). Arterial pulsatility index was defined as

$$\text{arterial pulsatility index} = \frac{(MxV - \text{mean velocity})}{MxV} \tag{4.1}$$

Maternal VPTT were defined as the time interval (ms) between the maternal ECG P-wave and corresponding Doppler A-wave [156], corrected for the duration of the corresponding cardiac cycle (time interval between 2 consecutive maternal ECG R-waves in ms). Maternal arterial PTT was defined as the time interval (ms) between the maternal ECG Q-wave and start of Doppler systole, again corrected for the duration of the corresponding cardiac cycle [312].

ICG and maternal Doppler flow parameters were also collected at 38 weeks of gestation in a total of 13 women with confirmed normal outcome of pregnancy.

All women delivered in ZOL and data on maternal and neonatal outcome were collected after delivery: maternal age and BMI (weight in kg/length in m^2) at admission, parity, gestational age at observation and delivery (weeks), birth weight (g) and birth weight percentiles according to population specific reference values [314].

Data were filled into a database and categorized as *1*) UP, *2*) GH, *3*) LPE, and *4*) EPE, and expressed as means and IQR. SPSS software version 20.0 was used for statistical comparison at nominal level $\alpha = .05$, using Mann-Whitney U-test for comparison between individual groups and Kruskall-Wallis test for combined comparison of groups. Significant linear dependence between clinical, laboratory, ICG, and ECG-Doppler variables was identified using PCC at nominal level $\alpha = .05$ (two-tailed), and goodness of fit of the resulting linear regression model was reported by R^2 and corresponding P-values. Correlations were calculated between VPTT and impedance indices for UP, GH, LPE, and EPE at the level of HV and RIV, and compared statistically using linear regression analysis with heteroskedastic variance (SAS software V9.2).

Approval of the local Committee for Medical Ethics was obtained before study onset (MEC ZOL reference 08/049 and 09/050).

4.2.4 Results

A total of 90 women were included: 13 with UP, 21 with GH, 34 with LPE, and 22 with EPE. Table 4.4 lists the demographic characteristics in the four patient groups. Maternal age, BMI, number of smokers, and nulliparity were not different between

the groups. The same was true for values of hemoglobin, hematocrit, platelet count, ASAT, ALAT, and creatinine clearance. Gestational age at delivery, birth weight and birth weight percentile were different between the groups, with lowest values for EPE. Concentrations of serum uric acid and proteinuria were highest for EPE and lowest for GH.

Table 4.5 shows the maternal ICG measurements in the four groups, which were measured at 38 weeks in UP, GH and LPE and at 32 weeks in EPE. In the gestational hypertension groups, blood pressures were higher than in UP as expected, but also aortic flow parameters ACI, VI, and TAC were lower than in UP. TFC was lower in GH than in other groups.

As shown in Table 4.6, combined ECG-Doppler renal VPTT and arcuate UtArt PTT, and RIV, resistive indices, and pulsatility indices were different between groups, with respectively lowest and highest values for EPE. Only HV PTT was not different between groups.

Figure 4.2 illustrates the comparison between UP and GH, between GH and LPE, and between LPE and EPE for left ventricular systolic function (aortic flow), venous hemodynamic function at the level of HV, right and left RIV and arterial hemodynamic function at right and left arcuate UtArt. Aortic flow parameters ACI and VI were lower in the hypertension groups than in UP, but were not different between GH, LPE and EPE (Figure 4.2 (A)). The same was true for HV PTT (Figure 4.2 (B)). HVI was higher in EPE than in the other three groups (Figure 4.2 (B)). RIVI were not different between UP and GH, or between hypertension groups. However, RIVI was higher in PE groups than in GH and UP (Figure 4.2 (C and D)). Arcuate UtArt PTT in GH was shorter than in UP and higher than in LPE, but not different between the PE groups (Figure 4.2 (E and F)). Arcuate UtArt resistive index was higher in EPE than in the other groups (Figure 4.2 (E and F)).

There was a negative correlation between venous impedance index (HVI and RIVI) and VPTT for all groups at the level of liver and right kidney. For the left kidney, however, the negative correlation between RIVI and VPTT was only true for EPE, but not for UP, GH, and LPE. The difference in slope and correlation between left kidney EPE and UP, GH, or LPE was significant ($P \leq .05$). Figure 4.3 shows the correlation between venous impedance index and VPTT for EPE, LPE, and GH at the level of liver (Figure 4.3 (A)), right (Figure 4.2 (B)) and left kidneys (Figure 4.2 (C)).

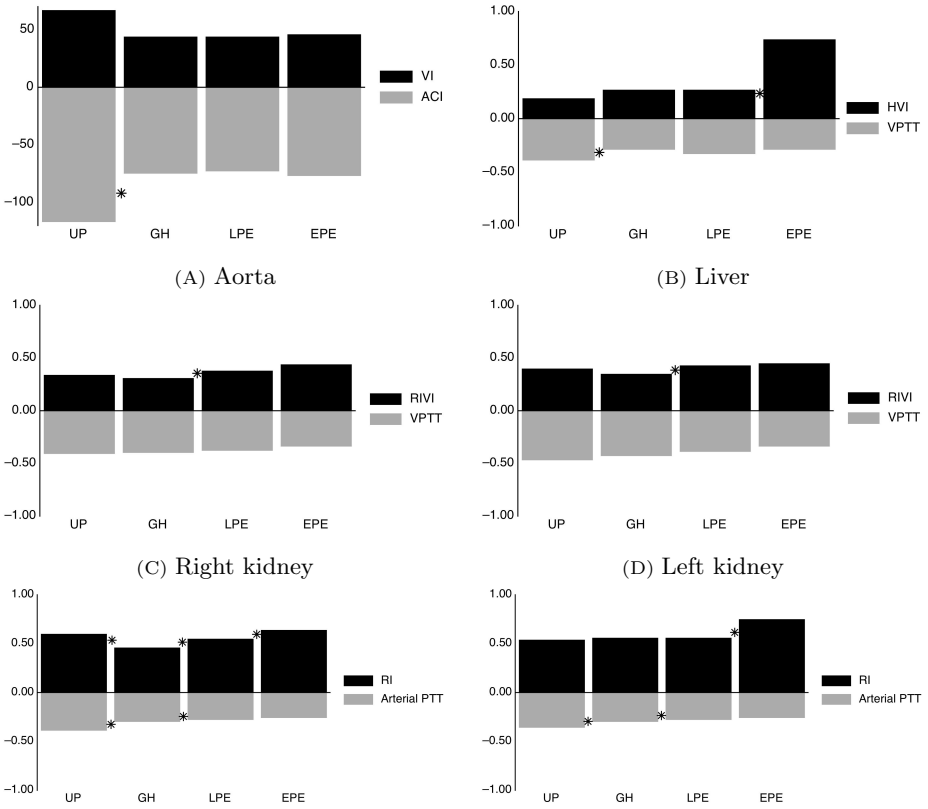

(A) Aorta

(B) Liver

(C) Right kidney

(D) Left kidney

(E) Right arcuate UtArt

(F) Left arcuate UtArt

Figure 4.2: Comparison of cardiac, arterial, and venous hemodynamic parameters between UP, GH, LPE, and EPE at the level of aorta (panel A), liver (L, panel B), right kidney (RK, panel C), left kidney (LK, panel D), right arcuate UtArt (Raut, panel E), and left arcuate UtArt (Laut, panel F). An asterisk indicates a statistically significant difference at nominal level $\alpha = .05$ with Mann-Whitney U-test between UP and GH, between GH and LPE, or between LPE and EPE.

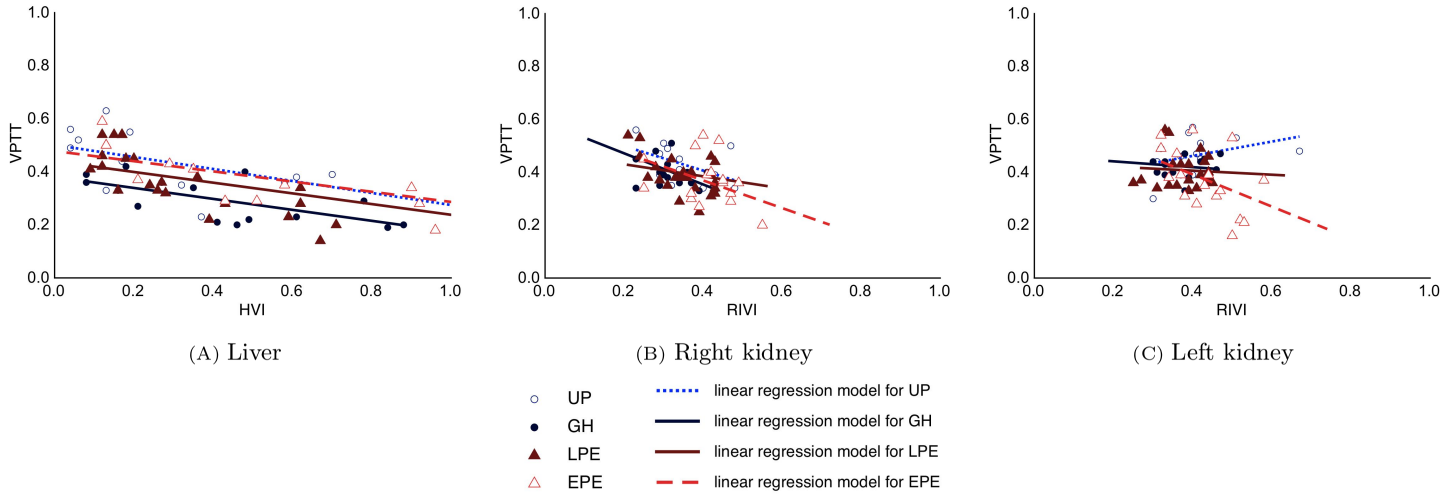

(A) Liver (B) Right kidney (C) Left kidney

Figure 4.3: Correlation between VPTT and venous impedance index (HVI for liver and RIVI for kidneys) for UP, GH, LPE, and EPE, at the level of the liver (panel A), right kidney (panel B), and left kidney (panel C).

Table 4.4: Demographic data and lab results in women with UP, GH, LPE, and EPE. Data are presented as medians (IQR). Kruskall-Wallis test was used to test group differences.

Demographics	UP	GH	LPE	EPE	P-value
	n=13	n=21	n=34	n=22	UP to EPE
Maternal characteristics					
Age (years)	31 (28;32)	32 (30;36)	29 (26;34)	29 (26;30)	.058
BMI	23 (21;26)	24 (22;29)	27 (23;34)	25 (24;31)	.103
Smokers (n,%)	0 (0)	2 (10)	3 (9)	3 (14)	.524
Nulliparity (n,%)	6 (46)	15 (71)	28 (82)	17 (77)	.088
Pregnancy outcome					
GA[1] at delivery (weeks)	40 (38;41)	39 (39;40)	38 (37;39)	32 (29;34)	$<.001$
Birth weight (g)	3455 (3180;3790)	3545 (3120;3743)	3030 (2749;3679)	1607 (1176;1933)	$<.001$
Birth weight (percentile)	50 (38;79)	63 (31;83)	38 (18;75)	31 (18;50)	.007
Lab results					
Hb[2] (g/dL)	n.a.	12.1 (11.4;13.3)	11.7 (10.6;12.5)	12.1 (11.2;13.2)	.248
Hct[3] (%)	n.a.	35.4 (33.6;38.4)	34.2 (31.9;36.4)	35;6 (33.1;36.9)	.317
Blood platelets(1 000/μ L)	n.a.	193 (152;227)	183 (165;256)	178 (142;218)	.632
ASAT (U/L)	n.a.	19 (16;22)	18 (15;25)	19 (16;32)	.326
ALAT (U/L)	n.a.	12 (10;14)	13 (10;20)	15 (10;34)	.205
Uric acid (mg/dL)	n.a.	5.0 (4.1;6.3)	6.0 (5.0;6.9)	6.6 (5.3;7.7)	.014
Proteins (mg/24h)	n.a.	174 (134;222)	858 (388;2273)	2254 (899;5345)	$<.001$
CreatCl[4] (mL/min)	n.a.	124 (92;149)	125 (97;155)	119 (91;152)	.898

[1] Gestational Age

[2] Hemoglobin

[3] Hematocrit

[4] Creatinine clearance

Table 4.5: Parameters of maternal cardiovascular function as measured by ICG in UP, GH, LPE, and EPE. Data are presented as medians (IQR). Kruskall-Wallis test was used to test group differences.

ICG	UP	GH	LPE	EPE	P-value
	n=13	n=21	n=34	n=22	UP to EPE
Gestational age	38 (38;39)	38 (37;39)	38 (36;39)	32 (30;34)	$<.001$
Pressures					
SBP (mmHg)	124 (117;132)	150 (138;161)	155 (141;168)	155 (145;172)	$<.001$
DBP (mmHg)	84 (81.88)	98 (92;104)	102 (96;109)	101 (92;109)	$<.001$
MAP (mmHg)	95 (92;99)	111 (102;117)	115 (108;120)	113 (107;123)	$<.001$
PP (mmHg)	38 (36;44)	53 (44;57)	53 (41;64)	57 (49;63)	$<.001$
Left ventricular output					
CO (L/min)	7.6 (6.5;8.9)	7.9 (7.0;9.4)	8.4 (7.1;10.3)	7.7 (6.6;9.1)	.359
HR (beats/min)	95 (81;100)	94 (92;102)	90 (82;101)	96 (79;105)	.634
SV (mL)	84 (77;96)	89 (69;98)	91 (79;114)	85 (68;95)	.352
Cardiac cycle time intervals					
PEP (ms)	109 (107;127)	117 (97;135)	110 (89;119)	105 (98;121)	.634
LVETi (%)	39 (36;41)	42 (38;46)	42 (37;45)	40 (36;42)	.079
DTi (%)	44 (42;49)	41 (37;44)	41 (39;47)	44 (40;48)	.144
STR	0.44 (0.43;0.48)	0.44 (0.37; 0.54)	0.41 (0.33;0.51)	0.42 (0.34;0.53)	.491
Aortic flow					
VI (1/1 000/s)	67 (50;69)	44 (41;61)	44 (36;54)	46 (34;61)	.018
ACI (1/100/s^2)	117 (76;142)	75 (60;100)	73 (56;87)	77 (56;111)	.043
HI (Ohm/s^2)	15.5 (10.6;20.7)	12.3 (10.4;16.6)	11.1 (7.6;13.9)	10.9 (6.4;15.4)	.066
TAC (mL/mmHg)	2.1 (1.9;2.6)	1.6 (1.3;2.3)	1.7 (1.4;2.4)	1.5 (1.2;1.8)	.019
Fluid					
TFC (1/kOhm)	31.9 (27.7;34.9)	27.5 (26.6;30.2)	32.3 (29.2;36.0)	34.9 (32.1;40.6)	$<.001$

Table 4.6: Combined ECG-Doppler assessment of arterial hemodynamics at left and right arcuate UtArt and of venous hemodynamic at left kidney, right kidney, and liver. Data are presented as medians (IQR). Kruskall-Wallis test was used to test group differences.

Combined ECG-Doppler	UP	GH	LPE	EPE	P-value
	n=13	n=19	n=31	n=20	UP to EPE
Gestational age	38 (38;39)	38 (37;39)	38 (36;39)	32 (28;33)	$<.001$
Arterial					
Resistivity and Pulsatility					
Left ArtUt RI[5]	0.54 (0.43,0.60)	0.56 (0.39;0.62)	0.56 (0.48;0.66)	0.75 (0.60;0.81)	.001
Left ArtUt PI[6]	0.75 (0.55;0.85)	0.82 (0.49;0.90)	0.79 (0.63;1.01)	1.19 (0.84;1.35)	.001
Right ArtUt RI	0.60 (0.51;0.68)	0.46 (0.39;0.56)	0.55 (0.46;0.61)	0.64 (0.51;0.78)	.005
Right ArtUt RI	0.87 (0.62;1.05)	0.58 (0.49;0.78)	0.77 (0.61;0.88)	0.94 (0.69;1.26)	.006
PTT					
Left ArtUt QD/RR	0.36 (0.31;0.40)	0.30 (0.28;0.34)	0.28 (0.23;0.30)	0.26 (0.22;0.30)	$<.001$
Left ArtUt QD/RR	0.39 (0.37;0.41)	0.30 (0.29;0.35)	0.28 (0.24;0.30)	0.26 (0.23;0.30)	$<.001$
Venous					
Impedance index					
LK[7] RIVI	0.40 (0.35;0.42)	0.35 (0.31;0.43)	0.43 (0.36;0.47)	0.45 (0.37;0.53)	.010
RK[8] RIVI	0.34 (0.30;0.42)	0.31 (0.27;0.36)	0.38 (0.32;0.43)	0.44 (0.38;0.49)	.001
L[9] HVI	0.19 (0.10;0.60)	0.27 (0.08;0.49)	0.27 (0.15;0.67)	0.74 (0.23;1.55)	.044
Sum	1.01 (0.83;1.23)	1.05 (0.73;1.38)	1.09 (0.94;1.50)	1.42 (1.08;2.49)	.025
PTT					
LK PA/RR	0.47 (0.42;0.52)	0.43 (0.39;0.45)	0.39 (0.36;0.45)	0.34 (0.24;0.45)	.003
RK PA/RR	0.41 (0.37;0.50)	0.40 (0.36;0.46)	0.38 (0.35;0.43)	0.34 (0.29;0.40)	.043
L PA/RR	0.39 (0.34;0.54)	0.29 (0.21;0.36)	0.33 (0.22;0.44)	0.29 (0.19;0.43)	.065
Sum	1.35 (1.13;1.42)	1.11 (1.05;1.18)	1.13 (0.94;1.25)	0.98 (0.77;1.34)	.027

[5] Resistivity index
[6] Pulsatility index
[7] Left kidney
[8] Right kidney
[9] Liver

4.2.5 Discussion

Main findings

From the results of this observational cohort study, some characteristics of cardiac, arterial, and venous function can be deduced for GH, LPE, and EPE. In this so-called cardiovascular profiling, it is illustrated that: *1*) gestational hypertensive diseases GH, LPE, and EPE show impaired cardiac systolic function as compared to UP, *2*) arterial vascular tone in LPE is higher than in GH, but lower than in EPE, *3*) compared to GH, PE exhibits higher RIVI in association with proteinuria.

Strengths

Our study is original because it evaluates the global maternal circulation, including heart, arteries, and veins. The non-invasive methods used have all been thoroughly evaluated, and reproducibility and repeatability have been reported. Finally, the patients included in each group strictly comply with all reported criteria for each disorder, and are free of interfering maternal or gestational diseases.

Limitations

Our study does not allow drawing definitive conclusions on the individual role of heart, arteries, and veins in the development or the clinical presentation of PE, nor on the role of the venous compartment in PE-related organ dysfunction. To evaluate this, more clinical and experimental research is needed.

Interpretation

Arterial hemodynamic dysfunction in gestational hypertensive disorders presents clinically as overt arterial hypertension, related to vasoconstriction of smaller peripheral arteries and increased systemic vascular resistance, which in PE is associated with increased stiffness of the larger arteries [176]. Reduced arterial compliance persists for years in women who had pregnancies complicated with PE [174] and predisposes to gestational hypertensive complications when present before conception [315]. Arterial hypertonia and serum concentrations of vasoactive agents are reported to be higher in EPE than LPE, both during as before clinical onset of the disease [88, 308, 316]. Our data correlate with this: as illustrated in Table 4.6, arcuate UtArt resistivity index is higher in EPE than in LPE, which in turn shows shorter arterial PTT than

in GH.

Aortic flow parameters VI and ACI directly relate to cardiac systolic function: the stronger the ventricular ejection, the higher maximum velocity and acceleration of blood flow in the aorta. Reduced VI and ACI in gestational hypertensive diseases, as measured by ICG (Table 4.5), can be considered the result of impaired cardiac systolic function. Impaired systolic function has been associated with atypical gestational morphologic remodeling of the heart [317] and is reported for GH [318], for preterm [319] and for term PE [7]. This dysfunction also persists for years after PE [320].

Venous hemodynamic dysfunction in PE was reported for the first time by Bateman *et al.* (2004) [109]. In former publications, we have reported that RIVI is higher in EPE than in LPE [147] and HVI is also increased in PE, as compared to UP [93]. Current data add to these reports that both EPE and LPE differ from GH in increased RIVI (Table 4.6). Increase of RIVI for both kidneys correlates significantly with proteinuria in 24h urine collections and is also associated with increased serum uric acid concentrations (Table 4.4). RIVI is defined as $\frac{(MxV-MnV)}{MxV}$ (see Equation 2.1). Venous MnV has been linked to a sudden deceleration of forward flow due to the counteractive force of the right atrial systole, which causes intravenous backflow into the venous system by lack of a valve between the atrium and the vena cava [92]. At the level of HV, this counteraction is responsible for reversal of the venous A-wave, leading to a triphasic pattern of HV Doppler waves in PE [93]. At the level of RIV, this counteraction is responsible for the so-called VPAN in PE, which is rarely seen in UP or in non-pregnant condition [92]. As such, these observations illustrate that intravenous backflow from atrial systole in PE is transported in retrograde direction up to the level of the renal parenchym. Our current data illustrate that RIVI values in EPE and LPE are higher than in GH, implying that this intrarenal backflow is an intrinsic feature for PE but not for GH (Figure 4.2 and Table 4.6).

An inverse correlation between venous impedance index and VPTT is illustrated in Figure 4.3. PTT is considered a measure for vascular tone: in conditions of increased vascular tone or stiffness, the propulsion wave is transported faster through the circulation than in conditions of low vascular tone, and this is responsible for a shorter time interval between the ECG and pulse or Doppler wave [321, 322, 323]. During PE, shorter PTT have been measured at both the arterial [324] and venous sides of the circulation [312]. We reported an increase of VPTT in UP and a reduction in PE, which correspond to a reduction or increase of venous tone in UP and PE,

respectively [312]. Figure 4.3 illustrates the negative correlation between VPTT and venous impedance index, which accounts for UP, GH, LPE, and EPE in liver and right kidney, but only for EPE in the left kidney. It is likely that increased venous tone in PE is associated with a faster and more distant rebound of atrial contraction throughout the venous circulation up to the level of the kidneys. Figure 4.3 suggests that only in EPE, this rebound reaches the left kidney, which is more distant from the heart than the liver and right kidney [92]. As such, increased RIVI, with or without VPAN, can be considered a reflection of pulsatile counteraction of forward venous flow from the kidneys, which intermittently (sub)obstructs renal outflow during each atrial contraction [147]. Obstruction to renal venous efflux is known to induce proteinuria, both under experimental conditions [200] as in clinical syndromes such as RV thrombosis [325], the nutcracker syndrome [326], and the cardiorenal syndrome [229]. Whether this pulsatile rebound of atrial contraction is the trigger for renal dysfunction with increase of serum uric acid and occurrence of proteinuria $>$ 300 mg/24h should be evaluated in further experimental and clinical research.

4.2.6 Conclusion

The results of this study confirm those of other publications that cardiac and arterial function is different between gestational hypertensive diseases and UP. Our study adds to this knowledge that venous hemodynamic dysfunction in PE is more pronounced than in GH. This venous dysfunction may perhaps be much more important in the clinical presentation of PE than currently considered today.

4.2.7 Acknowledgments

We acknowledge Prof. Dr. M. Ameloot from the Physiology department at Hasselt University, for his evaluation and constructive comments on the physiological background mechanisms of our observations.

4.3 The cardiovascular profile in preeclampsia

Characteristics of heart, arteries, and veins in low and high cardiac output preeclampsia

original paper

Kathleen TOMSIN*, Tinne MESENS, Geert MOLENBERGHS, Louis PEETERS, Wilfried GYSELAERS*

European Journal of Obstetrics & Gynecology and Reproductive Biology
Eur J Obstet Gynecol Reprod Biol 2013 - in press

4.3.1 Abstract

Objective To assess the feasibility of non-invasive measurements of maternal CO in relation to birth weight percentile and cardiovascular physiology in PE.

Method In a cohort of 62 women with PE, ICG was used to measure CO and to evaluate heart and arteries. Venous characteristics were assessed by combined ECG-Doppler ultrasonography. Statistical differences were evaluated by Mann-Whitney U-tests.

Results CO correlated with birth weight percentile ($P = .002$) with more SGA newborns in low CO (< 7.5 L/min) PE (lPE) than in high CO (≥ 8.9 L/min) PE (hPE) (12/29 vs. 2/16, $P = .044$). This was associated with lower aortic flow indices and shorter VPTT in lPE than in hPE.

Conclusion Non-invasive ICG measurements of maternal CO correlate with birth weight percentile and are associated with different functionality of heart, arteries, and veins in lPE and hPE.

4.3.2 Introduction

PE has been reported to exist with low or high maternal CO suggesting several types of PE [135, 136]. We hypothesize that these different CO states relate to different characteristics of maternal heart, arteries, and veins, in parallel with the clinical manifestation of PE.

In the assessment of maternal hemodynamics, the use of non-invasive alternatives for conventional invasive methods is of particular interest as they are eligible for a worldwide application in maternal health services. ICG is reproducible in pregnancy (see Chapter 3.2) [290], and high correlations are reported with the standard thermodilution technique for CO determination [80]. Furthermore, changes in maternal venous functional characteristics can be assessed using combined ECG-Doppler ultrasonography (see Chapters 2.4 and 2.5) [312].

Because of the reported correlation between maternal CO and neonatal birth weight [327, 328] we aimed at analyzing an observational cohort of women with PE, stratified according to maternal CO in order to evaluate the functionality of heart, arteries, and veins parallel to its clinical presentation. For this, we used both ICG and combined ECG-Doppler ultrasonography.

4.3.3 Methods

Approval of the local ethical committee was obtained before study onset (MEC ZOL reference: 08/049 and 09/050). Women with PE, admitted to the maternal-fetal medicine unit (ZOL) (November 2009 - December 2011), were included and assessed once at hospital admission. PE was defined as gestational hypertension ($\geq$ 140/90 mmHg), measured on at least two occasions $\geq$ six hours apart, associated with *de novo* proteinuria of $\geq$ 300 mg per 24 hours [329]. Only singleton pregnancies of women without history or symptoms of medical or cardiovascular diseases were included.

For all women, maternal age at inclusion (years), pregestational BMI, nulliparity (yes or no), gestational age at delivery (weeks), birth weight (g and percentiles) were registered, together with lab results: proteinuria (g/24h), serum uric acid (mg/dL), creatinine clearance (mL/min), blood platelets (1000/mm^3), aspartate and alanine aminotransferases (ASAT and ALAT, respectively) (U/L), and lactate dehydrogenase (LDH) (U/L). The Chi-Square test for the categorical variable "nulliparity" and the Kruskall-Wallis test for continuous data were used to test group differences.

After informed consent, all women underwent an ICG examination according to a reproducible protocol as reported elsewhere (see Chapters 3.1 , 3.2 , and 3.3) [290] using NICCOMO^{TM} (Software version 2.0, SonoSite, Medis Medizinische Messtechnik GmbH, Ilmenau, Germany). Here, parameters were classified as measurements of pressures (measured with the automated sphygomanometer), left ventricular output (i.e. HR, SV [260], and CO), systolic time intervals, aortic flow, total peripheral vascular resistance (TPVR), and thoracic fluid (i.e. the overall impedance across the thorax) [290]. Systolic time intervals include *a*) the PEP or the electrical systole, *b*) the LVETi or the mechanical systole corrected for HR, *c*) the DT corrected for HR, and *d*) STR as the ratio between the electrical and mechanical systole. Aortic flow parameters are divided into *a*) the maximum systolic flow velocity (VI), *b*) the maximum acceleration of aortic flow (ACI), *c*) the HI which represents the maximum velocity corrected for the time needed to reach this maximum ejection, and *d*) the TAC measured as the ratio of SV and PP. All measurements were taken in both supine and standing position. Hence, an OI could be calculated as a percentage of change when moving form supine to standing position, to visualize the regulation of hemodynamics in response to postural challenge, which is altered in human pregnancy [283].

We also performed combined ECG-Doppler examination as reported elsewhere [312] at the level of RIV, HV, and arcuate branches of UtArt measuring both PTT and indices of impedance. All examinations were performed by two ultrasonographers (Wilfried Gyselaers; Kathleen Tomsin) using a 3.5 MHz transabdominal probe (Aplio Mx, Toshiba Medical Systems nv, Sint-Stevens-Woluwe, Belgium).

Significant linear relations between pregnancy outcome variables and cardiovascular characteristics were quantified using PCC at nominal level $\alpha = .05$ (two-tailed). Locally weighted scatter plot smoothing was applied to the significant correlations using a Gaussian kernel with 95% bandwidth. This non-parametric regression analysis allows for the detection of cut-off points to define types of PE. Comparison between different types of PE was done by Mann-Whitney U-test for continuous variables and the Fisher's exact test for categorical data.

Data are represented as medians (IQR) and statistical differences at nominal level $\alpha = .05$ (two-tailed) were denoted as P-values. Statistical analyses were performed using the SPSS package (SPSS Inc., software version 19.0, Chicago, IL, USA).

4.3.4 Results

We found a significant correlation between birth weight percentiles and both CO and SV (PCC: .363 and .297, $P \leq .008$). Locally weighted scatter plot smoothing curves were fitted for PE. This allowed defining clinically useful cut-off values for the definition of lPE (< 7.5 L/min), mPE (7.5 to 8.8 L/min), or hPE (≥ 8.9 L/min) (Figure 4.4).

As presented in Table 4.7, maternal characteristics were comparable between lPE (n=29), mPE (n=17), and hPE (n=16) ($P \geq .411$). Following the classification of PE types based on CO, birth weight percentiles were lower in women presenting with lPE (17.5 (5.0;25.0), $P \leq .040$) compared with those with mPE (25.0 (17.5;43.8)) and hPE (43.8 (17.5;82.5)), when separately compared using a Mann-Whitney U-test. SGA newborns were significantly more frequent in lPE compared with hPE (12/29 vs. 2/16, P=.044); LGA newborns were significantly more frequent in hPE compared with those presented with lPE (3/16 vs. 0/29, P=.039). Neither birth weight percentiles nor the incidence of SGA or LGA differed significantly between newborns from mPE and hPE (3 SGA and 0 LGA in 17 newborns from mPE, $P \geq .103$). Proteinuria was more severe in participants with lPE (2.7 (0.8;6.7) g/24h) compared with those with hPE (1.2 (0.6;2.5) g/24h, P=.046). All other lab results were not different between the three PE groups ($P \geq .053$) (Table 4.7).

The PE groups differed from each other for many cardiovascular parameters as presented in Table 4.8. In lPE, aortic flow parameters, except ACI (Table 4.8), and all VPTT (Table 4.9) were lower compared with hPE. TPVR was higher in lPE compared to mPE and hPE (Table 4.8).

PEP increased more ($P \leq .042$) in response to orthostatic stress in both lPE (21 (7;34)%) and mPE (11 (6;21)%) compared with hPE (6 (-5;13)%). On top of this, the fall in TFC after orthostatic stress was higher in women with lPE compared with those presenting with hPE (-12 (-14;-9) vs. -8 (-10;-6)%, P=.005). All other OI were not different between the three PE groups ($P \geq .068$).

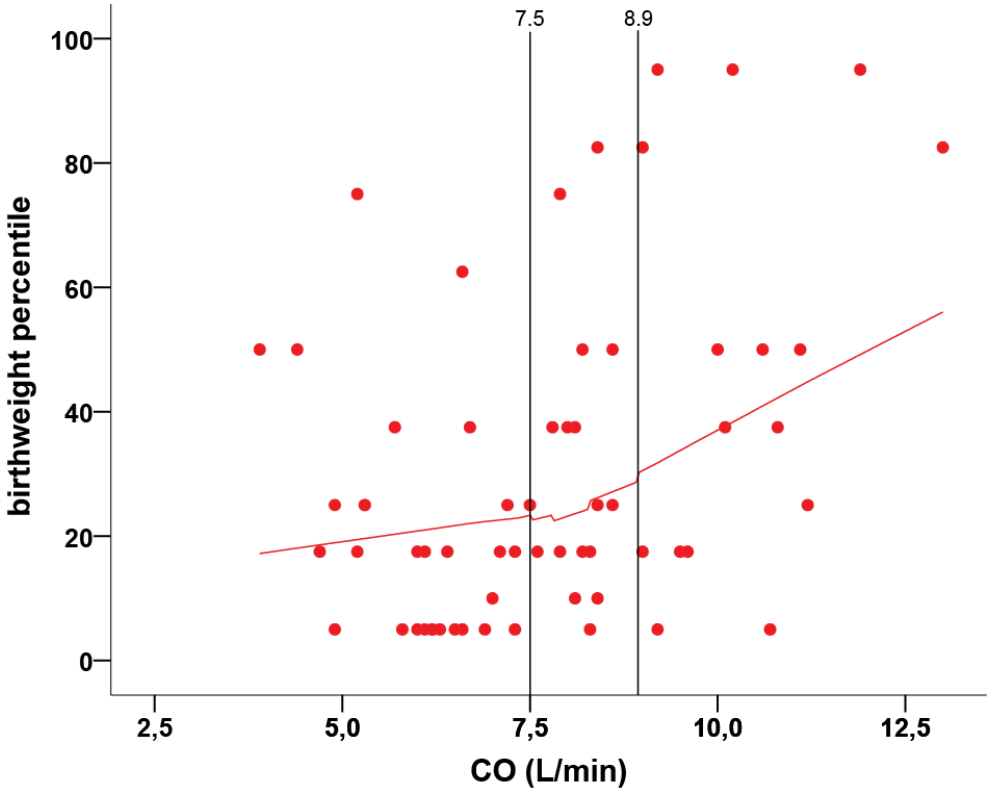

Figure 4.4: Scatter plot of birth weight percentile versus CO measured during standing position in PE (open circles). Locally weighted scatter plot smoothing (LOESS) curves were fitted (Gaussian kernels with 95% bandwidth). Cut-off values were identified for the PE cohort, indicated by the vertical full lines at 7.5 and 8.9 L/min.

Table 4.7: Demographic data and lab results in women with lPE, mPE, and hPE. Data are presented as medians (IQR) for continuous data or as n (%) for categorical data. Kruskall-Wallis test or Chi-Square test were used to test group differences at nominal level $\alpha = .05$. Significant differences (at nominal level $\alpha = .05$) between lPE and hPE using a Mann-Whitney U-test for continuous variables or Fisher's exact test for categorical data are marked in bold.

Demographics	lPE	mPE	hPE	P-value
	n=13	n=21	n=34	lPE to hPE
Maternal characteristics				
Age (years)	29 (25;33)	29 (27;33)	28 (26;33)	.857
BMI	24 (22;30)	27 (23;33)	25 (24;32)	.411
Nulliparity (n,%)	23 (80)	15 (88)	13 (81)	.741
Pregnancy outcome				
GA[10] at delivery (weeks)	34 (29;37)	37 (34;39)	36 (32;39)	.154
Birth weight (g)	**1610 (1163;2738)**	2620 (1825;3030)	**2803 (1480;3636)**	.020
Birth weight (percentile)	**17.5 (5.0;25.0)**	25.0 (17.5;43.8)	**43.8 (17.5;82.5)**	.007
SGA (n,%)	**12 (41)**	3 (18)	**2 (13)**	.066
LGA (n,%)	**0 (0)**	0 (0)	**3 (19)**	.011
Lab results				
Blood platelets(1 000/μ L)	183 (146;225)	177 (136;240)	183 (147;238)	976
ASAT (U/L)	23 (17;45)	18 (15;29)	18 (16;38)	.295
ALAT (U/L)	21 (12;42)	13 (10;26)	15 (11;25)	.374
Uric acid (mg/dL)	6.1 (5.3;6.8)	7.0 (5.5;7.5)	6.0 (5.2;7.0)	.263
Proteins (mg/24h)	**2659 (847;6745)**	753 (373;3977)	**1175 (595;2500)**	.062
CreatCl[11] (mL/min)	121 (95;141)	116 (89;156)	139 (107;173)	.275
LDH (U/L)	229 (215;257)	207 (185;253)	208 (194;226)	.158

[10] Gestational Age

[11] Creatinine clearance

Table 4.8: ICG measurements in three PE groups divided based on CO measured while standing, i.e. lPE (< 7.5 L/min), mPE (7.5-8.8 L/min), and hPE (≥ 8.9 L/min). Data are represented as medians (IQR). Differences between PE groups were calculated using Mann-Whitney U-test and presented as P-values (bold when significant at nominal level $\alpha = .05$).

	ICG (standing)					
	lPE (n=29)	P-value[12]	mPE (n=17)	P-value[13]	hPE (n=16)	P-value[14]
Pressures						
SBP (mmHg)	152 (135;163)	.759	150 (137;172)	1.000	142 (151;168)	.991
DBP (mmHg)	100 (93;109)	.616	103 (93;112)	.330	100 (92;107)	.514
MAP (mmHg)	112 (104;121)	.802	114 (103;124)	.652	115 (106;119)	.731
PP (mmHg)	49 (41;58)	.991	51 (42;57)	.505	54 (41;64)	.514
Left ventricular output						
CO (L/min)	6.1 (5.3;6.7)	< **.001**	8.2 (7.9;8.4)	< **.001**	10.2 (9.3;11.0)	< **.001**
HR (1/min)	88 (79;95)	.846	87 (78;98)	.063	93 (89;106)	**.041**
SV (mL)	68 (61;81)	< **.001**	91 (85;104)	**.021**	108 (92;126)	< **.001**
Cardiac cycle time intervals						
PEP	118 (111;129)	.179	114 (101;133)	.121	101 (86;117)	**.001**
LVETi (%)	37 (36;42)	.408	38 (36;43)	**.009**	43 (40;46)	< **.001**
DTi (%)	46 (41;48)	.982	47 (39;49)	.053	41 (39;43)	**.008**
STR	0.46 (0.42;0.52)	.264	0.44 (0.36;0.50)	.160	0.36 (0.30;0.45)	**.005**
Aortic flow						
VI (1/1 000/s)	41 (33;49)	.176	49 (32;60)	.900	49 (42;56)	**.012**
ACI (1/100/s^2)	63 (51;92)	.387	65 (54;115)	.460	80 (71;88)	.138
HI (Ohm/s^2)	7.6 (6.3;9.1)	**.030**	11.9 (8.3;13.8)	.358	12.9 (11.6;14.9)	< **.001**
TAC (mL/mmHg)	1.4 (1.2;1.8)	**.006**	1.8 (1.6;2.4)	.339	2.3 (1.5;2.9)	**.001**
Resistance						
TPVR (mmHg/L/min)	18.5 (17.1;21.8)	< **.001**	14.4 (12.8;15.4)	< **.001**	11.0 (9.9;11.7)	< **.001**
Fluid						
TFC (1/kOhm)	34.3 (32.4;41.3)	.187	35.1 (30.4;37.6)	.418	32.5 (30.6;35.4)	**.049**

[12] lPE vs. mPE
[13] mPE vs. hPE
[14] lPE vs. hPE

Table 4.9: Combined ECG-Doppler ultrasonography measurements in three PE groups divided based on CO measured while standing, i.e. lPE (<7.5 L/min), mPE (7.5-8.8 L/min), and hPE (≥ 8.9 L/min). Data are represented as medianc (IQR). Differences between UP and PE were calculated using Mann-Whitney U-test and presented as P-values (bold when significant at nominal level $\alpha=.05$).

			Combined ECG-Doppler ultrasonography					
			lPE ($n=29$)	P-value[15]	mPE ($n=17$)	P-value[16]	hPE ($n=16$)	P-value[17]
Kidneys	left	RIVI	0.49 (0.41;0.46)	.098	0.44 (0.38;0.49)	.589	0.43 (0.37;0.60)	.330
		PA/RR	0.34 (0.28;0.40)	.284	0.37 (0.32;0.41)	.119	0.43 (0.36,0.46)	**.022**
	right	RIVI	0.45 (0.42;0.60)	**.023**	0.40 (0.35;0.47)	.843	0.39 (0.34,0.51)	.057
		PA/RR	0.33 (0.25;0.40)	.335	0.37 (0.33;0.39)	.078	0.39 (0.36;0.45)	**.045**
Liver		HVI	1.14 (0.20;1.69)	.162	0.61 (0.16;0.95)	.514	0.28 (0.15;0.92)	**.046**
		PA/RR	0.22 (0.15;0.35)	.224	0.31 (0.20;0.40)	.329	0.33 (0.27,0.40)	**.034**
Uterus	left	Resistive index	0.69 (0.61;0.75)	.640	0.67 (0.50;0.80)	.332	0.60 (0.48;0.70)	.093
		Pulsatility index	1.03 (0.88;1.20)	.698	1.01 (0.66;1.35)	.384	0.86 (0.65;1.09)	.088
		QD/RR	0.23 (0.21;0.31)	.658	0.24 (0.23;0.28)	**.032**	0.28 (0.26;0.32)	.063
	right	Resistive index	0.74 (0.61;0.79)	.053	0.59 (0.50;0.70)	.905	0.58 (0.51;0.66)	**.011**
		Pulsatility index	1.16 (0.87;1.29)	.060	0.85 (0.67;1.08)	.843	0.82 (0.69;0.98)	**.014**
		QD/RR	0.24 (0.21;0.30)	.936	0.24 (0.23;0.27)	**.002**	0.30 (0.26;0.33)	**.021**

[15] lPE vs. mPE
[16] mPE vs. hPE
[17] lPE vs. hPE

4.3.5 Discussion

In this study, we assessed maternal cardiovascular function using non-invasive methods eligible for worldwide application in prenatal care. We found that maternal CO measured by ICG correlates with birth weight percentiles and is associated with more pronounced dysfunction of heart and veins in lPE than in hPE.

It is well known in cardiovascular physiology that the heart and veins cooperate as one functional unit in the control and regulation of CO [131]. The correlation between maternal CO and birth weight percentiles in our study (Figure 4.4) is in line with other reports [327, 328]. We defined subgroups of PE according to the level of correlation: PE with *1*) low, *2*) medium, or *3*) high CO. SGA and LGA neonates were predominantly present in the lPE and hPE groups respectively, and birth weight percentiles of lPE were significantly lower compared with other subgroups.

PE is associated with impaired cardiac function [309] and increased arterial tone [324]. Next to this, we found that lPE is more associated with reduced aortic compliance and right arcuate UtArt PTT compared to hPE, which are both markers of increased arterial tone or stiffness. Bamfo *et al* suggested that parameters of fetal growth were associated with systolic dysfunction and assigned the manifestation of hypertension and PE to a diastolic impairment [6]. We also found shorter PTT at the level of the maternal veins in lPE, indicating increased venous tone or stiffness in lPE compared to hPE. This correlates with other reports: PE is frequently accompanied by a raised venous tone and reduced venous capacitance [18, 297].

In this study, both the observed cardiac and vascular hemodynamic dysfunction at diagnosis seem to be more pronounced in lPE than in hPE (Tables 4.8 and 4.9). Our study illustrates that this level of maternal venous dysfunction is inversely related to CO, i.e. VPTTs decrease from hPE to lPE (Table 4.9). From the clinical point of view, this observation is very interesting. To date, the mechanisms of some of the severe complications of PE are not fully understood. One of the hypothetical pathways of PE-related organ dysfunction might be venous congestion following hampered venous drainage from several organs as part of the PE-related venous dysfunction [144, 147, 330]. This hypothesis requires experimental and clinical research. Exploring maternal venous hemodynamics might also contribute to a better understanding of some of the beneficial effects of magnesium sulphate ($MgSO_4$), commonly used in PE. With $MgSO_4$-administration, CO and cardiac function improved in animal experiments [331, 332]. $MgSO_4$ in humans was found to induce dorsal hand

venous dilatation [333] and forearm blood flow improvement [334]. Finally, our CO-based classification of PE opens perspectives to rethink today′s standard therapy of all women presenting with PE symptoms towards an individualized type of clinical management: e.g. selective application of venodilators such as nitrates [39], CO enhancers such as Continuous Positive Airway Pressure (CPAP) breathing at night [335], plasma volume expansion, etc.

Many of the described abnormalities have been reported to occur weeks or even months prior to the clinical onset of PE [95, 336, 337]. Our data only provide relevant information on the cardiac, arterial, and venous characteristics of pregnant women at the time of diagnosis. Another limitation of our study is situated in the statistical interpretation. The different levels of comparison suggest the possible need for a statistical correction at the α-level, which will render our observations insignificant. However, we have opted for an observational approach to explore possible changes in parameters, as the level of association between the different cardiovascular parameters is still unknown. The current observations should therefore be interpreted with some caution, but the existence of previous studies with similar results indicates the importance of including the venous characteristics in gestational hemodynamic studies. Therefore, from our limited dataset, it remains unclear whether the heart, arteries, or veins are the primary trigger for the observed global cardiovascular dysfunction in PE. Nevertheless, our results indicate that abnormal venous hemodynamics is an integral part of the pathophysiology of PE, being more pronounced in lPE than in hPE. More research is needed to elucidate the sequence of cardiovascular events in the preclinical stages of PE, and for this the combined use of ICG with maternal venous Doppler assessment seems a useful approach.

4.3.6 Acknowledgements

The authors would like to thank Jolien Oben for her assistance with the data analysis.

Chapter 5

General discussion

Studying the cascade of maternal cardiovascular changes throughout pregnancy using non-invasive, easily applicable, and highly accessible methods has become increasingly important because a single derangement in the gestation-induced adaptation process can lead to maternal or fetal disease. The possibility of an *early discrimination* between low and high risk patients and the *classification* of different pregnancy disorders based on a maternal cardiovascular profile will help us guide the *clinical work-up* of our pregnant population regarding both *prevention* and *treatment*, as well as *follow-up*. We defined maternal cardiovascular profiling as the combined evaluation of heart, arteries, and veins.

From the introduction (see Chapter 1), it is clear that the venous system has two important functions: *1*) it returns deoxygenated blood from the periphery back to the right atrium to be transported to the pulmonary circulation for oxygenation and *2*) it serves as the main blood reservoir of the human body, and is a key player in the distribution of blood between the circulating (active) volume and the stored (passive) blood. Today, this activity is largely underappreciated in obstetrics, where maintenance of a constant low-fluctuating blood flow to the uterus is mandatory for normal fetal development. As such, the venous system can be considered the "ugly duckling of obstetrics".

In this thesis, we aimed to highlight the importance of including the assessment of *the maternal venous system* in the maternal cardiovascular profile.

To this end, we divided our study into three main research questions:

1. The venous system in pregnancy and preeclampsia: what do we already know and how can we study it?
2. How can we non-invasively study the heart and arterial system parallel to our venous Doppler evaluation?
3. Does the venous system contribute to the maternal cardiovascular profile in pregnancy?

We addressed these three research questions using three methodological strategies:

1. Doppler ultrasonography (Chapter 2),
2. impedance cardiography (Chapter 3), and
3. a maternal cardiovascular profile based on both Doppler ultrasonography and impedance cardiography (Chapter 4).

5.1 The maternal venous system: the ugly duckling of obstetrics!

5.1.1 Strategy 1: Doppler ultrasonography

Doppler ultrasonography has been shown to be an appropriate tool to study the circulatory system. Moreover, its use is widely accepted in obstetrics as it is non-invasive and safe in pregnancy, enabling to visualize both maternal and fetal circulation. However, most gestational Doppler studies focus either on the fetal [85] or the uteroplacental circulation, especially on the UtArt waveforms [86, 87, 88], whereas Doppler studies on the veins are scarce [89, 90, 91, 92, 93, 94]. In this thesis, the application of Doppler ultrasonography to study the maternal venous system was explored.

In our research group, venous compliance was studied by use of the venous Doppler equivalent of the arterial RI, i.e. the venous impedance index (see Equation 2.1) derived from the venous Doppler waveform velocities at the level of both RIV and HV. As explained in Chapter 1, both kidneys and liver play important roles in the volume homeostasis, and thus, the regulation of CO in the gestational physiology. As such, RIVI turned out to be increased in PE when compared to UP, which can be linked to known features of gestational cardiovascular physiology (see Chapter 2.1), i.e. they mimic changes in SV and renal GFR. On top of this, it became clear that RIVI might also be associated with fetal growth and renal function; RIVI was higher in EPE than in LPE in which EPE presented with lower birth weight percentiles and higher proteinuria (see Chapter 2.3). However, Doppler velocimetry in the HV seemed to be much more variable than that in the RIV, which showed good reproducibility in pregnancy (see Chapter 2.2). This can be explained by the morphology of the HV tree and thus the appearance of atypical waves troubling the interpretation of its velocity characteristics. Therefore, we introduced the maternal ECG as part of the venous Doppler wave analysis. Next to the improved reproducibility [338], the maternal ECG enabled the correct identification of the different venous Doppler flow characteristics, as they indirectly reflect the right cardiac atrial function (see Chapter 2.4). From this, it became clear that the time interval between the corresponding ECG- and Doppler waves was subject to change throughout UP and could be used to study characteristics of venous tone. Our results indicated that the assessment of this PTT, at both the arterial (QD time interval) and the venous side (PA time interval), is an easily and highly accessible measure for vascular reactivity. Again, our observations correlated well with known gestational cardiovascular adaptation mechanisms (see Chapter 2.5). Next to this, we considered the use of 3D ultrasonography to visualize

changes in hepatic vascularity as it is becoming a popular method in obstetrics. We concluded that this technique might be feasible in gestational hepatic hemodynamics. In our pilot study (see Chapter 2.6), a reference point (e.g. a clear bifurcation of the hepatic venous branches) was identified by the ultrasonographer during the first exam, and location of the ultrasound probe and several device settings were manually recorded in a subject-specific scientific record. A 3D-PDU image was stored and volume analyses were performed around this user-defined reference point. Relocation of this anatomical reference point during the second sonographic exam failed in 30% of the cases when using the subhepatic approach, but was successful when using the intrahepatic approach, although this only resulted in moderate reproducibility for the corresponding volume analyses. Therefore, one should keep in mind that this protocol is prone to error originating from both the sonographer's use of the probe and the device settings, as the calculated vascularity indices are dependent on multiple factors such as the angle and depth of the Doppler wave. More research is needed to optimize this type of HV evaluation in pregnancy.

From our studies, we concluded that the venous system is indeed a crucial determinant of CO (as highlighted in Chapter 1), and that this can possibly be translated into measurable objective changes in venous Doppler waveforms, and thus impedance indices and VPTT. On top of this, these parameters are subject to changes in UP and PE enabling their use in gestational hemodynamic studies (see Chapter 2.7).

5.1.2 Strategy 2: Impedance cardiography

The invasive standard approaches to obtain information on the heart and arteries are not justified in non-critically ill pregnant women. Therefore, ICG is proposed to be a good non-invasive and safe alternative for invasive methods [249, 289], as it correlates highly with the invasive standard methods, such as thermodilution [80]. However, results of ICG-measurements are often debated by others [160, 251, 255, 256, 257]. Therefore, we conducted two reliability studies to ensure that our measurements could be reproduced in our specific population. As cardiovascular measurements are subject to variation caused by orthostasis, our protocol included changes in position. We concluded that the reproducibility of such ICG-measurements is much better when mean values of multiple measurements over time are used for each ICG-parameter, instead of individual beat-to-beat measurements (see Chapter 3.1). Even though postural challenges in pregnancy have a significant influence on cardiovascular parameters, e.g. the vena cava syndrome, good correlation was found for the ICG-measurements under our standardized conditions, and this was especially true for the aortic flow parameters ACI, VI, and HI (see Chapter 3.2).

From our longitudinal study (see Chapter 3.3), it became clear that our ICG-observations throughout UP are comparable with known gestational changes in heart and arteries. Therefore, it is considered a good technique to study these characteristics in pregnancy. We learned that measurements during the standing position were the most accurate and remained stable throughout gestation, as in this position the vena cava syndrome is likely to be absent.

In a single session [158, 159, 160], parameters of pressure, left ventricular output, cardiac cycle time intervals, thoracic fluid, and aortic flow are continuously registered (see Chapters 3.1 and 3.2). Therefore, ICG allows for a global impression of cardiac and arterial function, which together with our combined ECG-Doppler ultrasonographic evaluation of venous function, enables us to create a generalized maternal cardiovascular profile based on non-invasive, easily applicable, and highly accessible methods.

5.1.3 Strategy 3: Maternal cardiovascular profile

As both combined ECG-Doppler and ICG are proven to be feasible in the study of gestational hemodynamics, we wondered whether the combination of both could give us valuable information on the global maternal cardiovascular state. To this end, this cardiovascular profiling was tested in an experimental setting in which one hemodynamic parameter was changed in a non-pregnant healthy female population, i.e. an acute increase of the intravenous volume by a simple saline infusion. From this, one can conclude that minor changes can be registered with our methodology for cardiovascular profiling, which is based on both the combined ECG-Doppler and the ICG examinations (see Chapter 4.1).

Following this observation, the maternal cardiovascular profile was compared between UP and maternal hypertensive disorders revealing differences in a large set of cardiovascular parameters including all three entities, i.e. the heart, arteries, and veins. From this, the development of proteinuria in PE was found to be related to an increase in RIVI, discriminating PE from GH in terms of degree in venous dysfunction (see Chapter 4.2). Next to this, a correlation between birth weight percentiles and maternal CO state was observed in our pregnant population (see Figure 4.4), confirming former observations of other research groups [136, 327, 339]. From this correlation, a stratification of our PE population based on the maternal CO state revealed different maternal cardiovascular profiles. Here, the venous dysfunction was inversely correlated to the CO state, and thus correlated to maternal and fetal outcome; PE women with aggravated venous dysfunction presented with higher proteinuria and delivered neonates with lower birth weight percentiles compared to PE women with high CO and thus milder venous dysfunction (see Chapter 4.3). This, again, confirms the role of the venous system in the regulation of CO, which seems directly related to fetal growth.

5.2 Future perspectives

All three strategies helped us answer our main research question (Chapter 1): i.e.

We can include the venous system in a clinically useful maternal cardiovascular profile in pregnancy, and this inclusion seems to be valuable in the study of maternal physiology and pathophysiology.

Our maternal cardiovascular profile combines the heart, arteries, and veins into one functional unit, and minor changes in these different compartments are able to influence its global functionality. The methodology presented in this thesis enabled us to classify our women with PE according to their individual cardiovascular state and this might open perspectives to change today's standard clinical work-up, including prevention, treatment, and follow-up, towards an individualized type of clinical management for each patient.

Future research is needed to shed more light on the hypothesis that our maternal cardiovascular profiling, as presented in this thesis, might enable us to define a type-specific risk profile for many gestational diseases, which may guide the clinical work-up of and screening for this high-risk population.

5.2.1 Fundamental research

Although our results indicate a possible clinical use of the presented maternal cardiovascular profile in the obstetric field, the functional interpretation of several output parameters of this profile remains incomplete. Future research should be aimed at determining the physiological nature of the obtained cardiovascular parameters generated by the techniques presented in this thesis.

For instance, investigating the fundamental role of the different combined ECG-Doppler parameters to the vascular function curve (Figure 1.2) presented in Chapter 1.3.2 is important to understand its relation to CO and venous return. Also, the understanding of the interdependence of all our presented cardiovascular parameters is relevant in the statistical interpretation of our observations as well as the physiological meaning of the observed gestational evolutions in both the maternal physiology and pathophysiology. In addition, the technical influence of pregnancy-related changes (e.g. weight gain and possible changes in thorax-related diameters) on the ICG-waveform algorithm should be considered when constructing reference ranges in pregnancy. Moreover, the etiology of the atypical presentation of PE, e.g. early-onset versus late-onset or mild versus severe disease, and its relation to our maternal cardiovascular profile should be studied into more detail. Finally, the maternal venous drainage at the level of the uteroplacental circulation in early gestation seems to be of particular interest to elucidate its possible role in placental development, and thus in placental abnormalities leading to pregnancy disorders such as PE [340].

This knowledge, however, can be explored simultaneously with the clinical introduction of this profile to enable early discrimination (Chapter 5.2.2), classification (Chapter 5.2.3), and clinical work-up (Chapter 5.2.4).

5.2.2 Early discrimination

The first trimester is the most relevant target period to apply this maternal cardiovascular profiling, enabling the exploration of the maternal (mal)adaptation to pregnancy, eventually offering the possibility to early identify abnormal pregnancy development. Discriminating high from low risk patients will enable prevention, and thus, risk management. However, the atypical presentation of PE and IUGR supports the hypothesis of different origins for these disorders. Depending on the primary, still unknown, cause of these gestational disorders, i.e. either an abnormal maternal uterine vascular remodeling [341, 242, 342] or a preexisting maternal cardiovascular disease [343], will open perspectives to primary or secondary prevention, respectively.

Preliminary results of our research group revealed the early presentation of significantly decreased aortic flow (low ACI, VI, and HI) around 12 weeks of gestation in women who subsequently developed gestational hypertension or preeclampsia (n=13). These patients showed no clinical signs of hypertension or cardiovascular disease at the time of examination. On top of this, significantly decreased SV and CO at 12 weeks of gestation was present in normotensive women who delivered SGA (n=11) infants, defined as a birth weight percentile of five or less. Signs of venous dysfunction, however, were not significantly detectable in both of these small groups [344]. Parallel studies using biochemical markers of placental dysfunction, such as Placental Growth Factor, revealed minor differences in this early stage of pregnancy [344].

These observations open perspectives to identify the high risk patients for gestational disorders, such as PE and IUGR, at an early stage of gestation. Next to these cardiovascular parameters, it is, however, advised to take into account *a priori* risk factors, e.g. BMI and maternal age, when screening for gestational disorders in order to achieve high sensitivity and specificity for this heterogeneous population [242].

5.2.3 Classification

To date, the definition of PE is merely based on two maternal symptoms, i.e. gestational hypertension and proteinuria. However, the clinical presentation of this maternal disease is often heterogeneous and atypical, increasing the need to define subtypes of PE and other gestational hypertensive diseases. Examples of such classifications are based on

- the severity of maternal disease (mild vs. severe) [345],
- the clinical onset of maternal disease (early vs. late) [135],
- the presence of another preexisting maternal disease (gestational vs. superimposed) [346], or
- the presence of coexisting fetal disease (with vs. without IUGR) [347].

Many of these classifications are based on simple fine-tuning of the existing diagnostic criteria of PE and IUGR [329]. However, the observed wide range of maternal dysfunction suggests the need to further discriminate pregnant women based on their individual health state, including her cardiovascular health, as illustrated in Chapter 4.2.

When comparing these groups based on our maternal cardiovascular profiling approach, it became clear that these several types of gestational disorders have different cardiovascular profiles. Nonetheless, our current treatment protocols are uniform between gestational hypertension, essential hypertension, and PE, as they are directed to their common symptom, i.e. hypertension. Our observations on the different maternal cardiovascular profiles, however, suggest that the origin of hypertension in each of these groups is different and may need another clinical work-up and therapeutic approach. In the future, it is necessary to attempt a more personalized classification of our pregnant women using an approach which includes a maternal cardiovascular profile.

5.2.4 Clinical work-up

The Doppler assessment, as presented in this thesis, reveals dysfunctional venous characteristics in certain women, directly influencing the functionality of the maternal venous system, which could be part of a personalized clinical work-up and treatment. This novel approach could include the selective application of venodilators such as nitrates [39], CPAP breathing at night [335], and plasma volume expansion which might enhance both the cardiovascular state of the mother and her clinical outcome, together with an improved fetal outcome. In order to obtain this information, a clinical work-up protocol should include monitoring of both

1. the maternal cardiovascular profile (as presented in this thesis) and
2. the fetal state (standard cardiotocography and ultrasound evaluation of amniotic fluid, fetal growth, umbilical artery, and middle cerebral artery flow)

in parallel with the standard clinical tests. In this way, determination of which parameters are influenced by this personalized treatment protocol, and which cardiovascular variables actively influence maternal and fetal outcome, can be achieved. This in turn will help us to understand the pathophysiological mechanisms behind gestational disorders such as PE and IUGR.

5.3 Conclusion

The aforementioned challenges for the future obstetrical field (early discrimination, classification, and clinical work-up) are all included in current projects of our research group, of which preliminary results are very promising towards highlighting the relevance of the venous compartment in the etiology and clinical presentation of gestational diseases, such as hypertension and fetal growth restriction.

To conclude this thesis, we would like to state that our *"ugly duckling": the maternal venous system* is evolving into the "beautiful swan" in the story of preeclampsia and many other gestational disorders. We hope that the reader of this thesis is as confident as its author that this is the beginning of many other studies regarding maternal venous hemodynamics as an important piece of the gestational physiology puzzle.

Bibliography

[1] Duvekot JJ, Cheriex EC, Pieters FA, Menheere PP, Peeters LH. Early pregnancy changes in hemodynamics and volume homeostasis are consecutive adjustments triggered by a primary fall in systemic vascular tone. Am J Obstet Gynecol. 1993;169(6):1382–92.

[2] Carbillon L, Uzan M, Uzan S. Pregnancy, vascular tone, and maternal hemodynamics: a crucial adaptation. Obstet Gynecol Surv. 2000;55(9):574–81.

[3] Hibbard JU, Shroff SG, Lang RM. Cardiovascular changes in preeclampsia. Semin Nephrol. 2004;24(6):580–7.

[4] Andrietti S, Kruse AJ, Bekkers SC, Sep S, Spaanderman M, Peeters LL. Cardiac adaptation to pregnancy in women with a history of preeclampsia and a subnormal plasma volume. Reprod Sci. 2008;15(10):1059–65.

[5] Bamfo JE, Kametas NA, Chambers JB, Nicolaides KH. Maternal cardiac function in fetal growth-restricted and non-growth-restricted small-for-gestational age pregnancies. Ultrasound Obstet Gynecol. 2007;29(1):51–7.

[6] Bamfo JE, Kametas NA, Chambers JB, Nicolaides KH. Maternal cardiac function in normotensive and pre-eclamptic intrauterine growth restriction. Ultrasound Obstet Gynecol. 2008;32(5):682–6.

[7] Melchiorre K, Sutherland GR, Baltabaeva A, Liberati M, Thilaganathan B. Maternal cardiac dysfunction and remodeling in women with preeclampsia at term. Hypertension. 2011;57(1):85–93.

[8] Novelli GP, Valensise H, Vasapollo B, Larciprete G, Altomare F, Di Pierro G, et al. Left ventricular concentric geometry as a risk factor in gestational hypertension. Hypertension. 2003;41(3):469–75.

[9] Simmons LA, Gillin AG, Jeremy RW. Structural and functional changes in left ventricle during normotensive and preeclamptic pregnancy. Am J Physiol Heart Circ Physiol. 2002;283(4):H1627–33.

[10] Schrier RW, Briner VA. Peripheral arterial vasodilation hypothesis of sodium and water retention in pregnancy: implications for pathogenesis of preeclampsia-eclampsia. Obstet Gynecol. 1991;77(4):632–9.

[11] Duvekot JJ, Peeters LL. Maternal cardiovascular hemodynamic adaptation to pregnancy. Obstet Gynecol Surv. 1994;49(12 Suppl):S1–14.

[12] Hagedorn KA, Cooke CL, Falck JR, Mitchell BF, Davidge ST. Regulation of vascular tone during pregnancy: a novel role for the pregnane X receptor. Hypertension. 2007;49(2):328–33.

[13] Duvekot JJ, Peeters LL. Renal hemodynamics and volume homeostasis in pregnancy. Obstet Gynecol Surv. 1994;49(12):830–9.

[14] Fu Q, Levine BD. Autonomic circulatory control during pregnancy in humans. Semin Reprod Med. 2009;27(4):330–7.

[15] Ekholm EM, Erkkola RU. Autonomic cardiovascular control in pregnancy. Eur J Obstet Gynecol Reprod Biol. 1996;64(1):29–36.

[16] Melchiorre K, Sharma R, Thilaganathan B. Cardiac structure and function in normal pregnancy. Curr Opin Obstet Gynecol. 2012;24(6):413–21.

[17] Krabbendam I, Spaanderman ME. Venous adjustments in healthy and hypertensive pregnancy. Expert Rev Obstet Gynecol. 2007;2:671–679.

[18] Sakai K, Imaizumi T, Maeda H, Nagata H, Tsukimori K, Takeshita A, et al. Venous distensibility during pregnancy. Comparisons between normal pregnancy and preeclampsia. Hypertension. 1994;24(4):461–6.

[19] van Oppen AC, Stigter RH, Bruinse HW. Cardiac output in normal pregnancy: a critical review. Obstet Gynecol. 1996;87(2):310–8.

[20] van Oppen AC, van der Tweel I, Alsbach GP, Heethaar RM, Bruinse HW. A longitudinal study of maternal hemodynamics during normal pregnancy. Obstet Gynecol. 1996;88(1):40–6.

[21] Davey DA, MacGillivray I. The classification and definition of the hypertensive disorders of pregnancy. Am J Obstet Gynecol. 1988;158(4):892–8.

[22] Walfisch A, Hallak M. Hypertension. In: James D, Steer P, Weiner C, Gonik B, editors. High risk pregnancy: Management options. Philadelphia: Elsevier Inc; 2006. p. 772–789.

[23] Reece EA. Pre-eclampsia-eclampsia syndrome. In: Reece EA, Barbieri RL, editors. Obstetrics and Gynecology: The essentials of clinical care. Stuttgart - New York: Thieme; 2010. p. 149–158.

[24] Bernstein IM, Meyer MC, Osol G, Ward K. Intolerance to volume expansion: a theorized mechanism for the development of preeclampsia. Obstet Gynecol. 1998;92(2):306–8.

[25] Baumwell S, Karumanchi SA. Pre-eclampsia: clinical manifestations and molecular mechanisms. Nephron Clin Pract. 2007;106(2):c72–81.

[26] Ritchie A, Brown MA. Proteinuria in preeclampsia: from bench to bedside. Fetal and Maternal Medicine Review. 2010;21(1):1–23.

[27] James JL, Whitley GS, Cartwright JE. Pre-eclampsia: fitting together the placental, immune and cardiovascular pieces. J Pathol. 2010;221(4):363–78.

[28] Wolf M, Kettyle E, Sandler L, Ecker JL, Roberts J, Thadhani R. Obesity and preeclampsia: the potential role of inflammation. Obstet Gynecol. 2001;98(5 Pt 1):757–62.

[29] de Groot CJ, Taylor RN. New insights into the etiology of pre-eclampsia. Ann Med. 1993;25(3):243–9.

[30] Hays PM, Cruikshank DP, Dunn LJ. Plasma volume determination in normal and preeclamptic pregnancies. Am J Obstet Gynecol. 1985;151(7):958–66.

[31] Shah DM. Role of the renin-angiotensin system in the pathogenesis of preeclampsia. Am J Physiol Renal Physiol. 2005;288(4):F614–25.

[32] Schobel HP, Fischer T, Heuszer K, Geiger H, Schmieder RE. Preeclampsia – a state of sympathetic overactivity. N Engl J Med. 1996;335(20):1480–5.

[33] Fischer T, Schobel HP, Frank H, Andreae M, Schneider KT, Heusser K. Pregnancy-induced sympathetic overactivity: a precursor of preeclampsia. Eur J Clin Invest. 2004;34(6):443–8.

[34] Salas SP, Marshall G, Gutierrez BL, Rosso P. Time course of maternal plasma volume and hormonal changes in women with preeclampsia or fetal growth restriction. Hypertension. 2006;47(2):203–8.

[35] Goodlin RC. Venous reactivity and pregnancy abnormalities. Acta Obstet Gynecol Scand. 1986;65(4):345–8.

[36] Boulpaep EL. Organization of the cardiovascular system. In: Boron WF, Boulpaep EL, editors. Medical physiology. Philadelphia: Elsevier Inc.; 2003. p. 423–446.

[37] Boulpaep EL. Arteries and veins. In: Boron WF, Boulpaep EL, editors. Medical physiology. Philadelphia: Elsevier Inc.; 2003. p. 447–462.

[38] Sandoo A, van Zanten JJ, Metsios GS, Carroll D, Kitas GD. The endothelium and its role in regulating vascular tone. Open Cardiovasc Med J. 2010;4:302–12.

[39] Pang CC. Autonomic control of the venous system in health and disease: effects of drugs. Pharmacol Ther. 2001;90(2-3):179–230.

[40] Gelman S. Venous function and central venous pressure: a physiologic story. Anesthesiology. 2008;108(4):735–48.

[41] Segal SS. Special circulations. In: Boron WF, Boulpaep EL, editors. Medical physiology. Philadelphia: Elsevier Inc.; 2003. p. 558–573.

[42] Boulpaep EL. Integrated control of the cardiovascular system. In: Boron WF, Boulpaep EL, editors. Medical physiology. Philadelphia: Elsevier Inc.; 2003. p. 574–590.

[43] Berne MN R M ; Levy. Cardiovascular physiology. 4th ed. London: The C.V. Mosby Company; 1981.

[44] Dora KA. Coordination of vasomotor responses by the endothelium. Circ J. 2010;74(2):226–32.

[45] Khalil RA. Regulation of Vascular Smooth Muscle Function. San Rafael (CA): Morgan and Claypool Life Sciences; 2010.

[46] Bank AJ, Kaiser DR. Smooth muscle relaxation: effects on arterial compliance, distensibility, elastic modulus, and pulse wave velocity. Hypertension. 1998;32(2):356–9.

[47] Tomiyama H, Yamashina A. Non-invasive vascular function tests: their pathophysiological background and clinical application. Circ J. 2010;74(1):24–33.

[48] Greenway CV, Lautt WW. Blood volume, the venous system, preload, and cardiac output. Can J Physiol Pharmacol. 1986;64(4):383–7.

[49] Lu D, Kassab GS. Role of shear stress and stretch in vascular mechanobiology. J R Soc Interface. 2011;8(63):1379–85.

[50] Collins C, Tzima E. Hemodynamic forces in endothelial dysfunction and vascular aging. Exp Gerontol. 2011;46(2-3):185–8.

[51] Berne R, Levy M. Control of cardiac output: coupling of heart and blood vessels. In: Berne R, Levy M, editors. Cardiovascular physiology. London: The C.V. Mosby Company; 2001. p. 199–226.

[52] Boulpaep EL. Regulation of arterial pressure and cardiac output. In: Boron WF, Boulpaep EL, editors. Medical physiology. Philadelphia: Elsevier Inc.; 2003. p. 534–557.

[53] Boulpaep EL. The heart as a pump. In: Boron WF, Boulpaep EL, editors. Medical physiology. Philadelphia: Elsevier Inc.; 2003. p. 508–533.

[54] Lewis B. The peripheral veins. In: Rumack CM, Wilson RD, Charboneau JW, Johnson JM, editors. Diagnostic ultrasound. Philadelphia: Elsevier Mosby; 2005. p. 1019–1035.

[55] Teichgraber UK, Gebel M, Benter T, Manns MP. Effect of respiration, exercise, and food intake on hepatic vein circulation. J Ultrasound Med. 1997;16(8):549–54.

[56] de Swiet M. The cardiovascular system. In: Chamberlain G, Pipkin F, editors. Clinical physiology in obstetrics. Oxford, UK: Blackwell Science Ltd; 1998. p. 33–70.

[57] Roderick P, Ferris G, Wilson K, Halls H, Jackson D, Collins R, et al. Towards evidence-based guidelines for the prevention of venous thromboembolism: systematic reviews of mechanical methods, oral anticoagulation, dextran and regional anaesthesia as thromboprophylaxis. Health Technol Assess. 2005;9(49):iii–iv, ix–x, 1–78.

[58] Pang CC. Measurement of body venous tone. J Pharmacol Toxicol Methods. 2000;44(2):341–60.

[59] Berne R, Levy M. Special circulations. In: Berne R, Levy M, editors. Cardiovascular physiology. London: The C.V. Mosby Company; 2001. p. 241–270.

[60] Hickie JB. The valve of the inferior vena cava. Br Heart J. 1956;18(3):320–6.

[61] Magder S. Central venous pressure: A useful but not so simple measurement. Crit Care Med. 2006;34(8):2224–7.

[62] Pedersen JF, Dakhil AZ, Jensen DB, Sondergaard B, Bytzer P. Abnormal hepatic vein Doppler waveform in patients without liver disease. Br J Radiol. 2005;78(927):242–4.

[63] Pannier BM, Avolio AP, Hoeks A, Mancia G, Takazawa K. Methods and devices for measuring arterial compliance in humans. Am J Hypertens. 2002;15(8):743–53.

[64] Smith SA, Morris JM, Gallery ED. Methods of assessment of the arterial pulse wave in normal human pregnancy. Am J Obstet Gynecol. 2004;190(2):472–6.

[65] Nichols WW, Denardo SJ, Wilkinson IB, McEniery CM, Cockcroft J, O'Rourke MF. Effects of arterial stiffness, pulse wave velocity, and wave reflections on the central aortic pressure waveform. J Clin Hypertens (Greenwich). 2008;10(4):295–303.

[66] Foo JY, Lim CS. Pulse transit time as an indirect marker for variations in cardiovascular related reactivity. Technol Health Care. 2006;14(2):97–108.

[67] Sharwood-Smith G, Bruce J, Drummond G. Assessment of pulse transit time to indicate cardiovascular changes during obstetric spinal anaesthesia. Br J Anaesth. 2006;96(1):100–5.

[68] Patrianakos AP, Parthenakis FI, Karakitsos D, Nyktari E, Vardas PE. Proximal aortic stiffness is related to left ventricular function and exercise capacity in patients with dilated cardiomyopathy. Eur J Echocardiogr. 2009;10(3):425–32.

[69] Hon EH, Fukushima T. R-pulse wave timing in cardiovascular monitoring: further observations. Obstet Gynecol. 1992;79(4):597–600.

[70] Savage MT, Ferro CJ, Pinder SJ, Tomson CR. Reproducibility of derived central arterial waveforms in patients with chronic renal failure. Clin Sci (Lond). 2002;103(1):59–65.

[71] Bradlow WM, Gatehouse PD, Hughes RL, O'Brien AB, Gibbs JS, Firmin DN, et al. Assessing normal pulse wave velocity in the proximal pulmonary arteries using transit time: a feasibility, repeatability, and observer reproducibility study by cardiovascular magnetic resonance. J Magn Reson Imaging. 2007;25(5):974–81.

[72] Nichols WW, Singh BM. Augmentation index as a measure of peripheral vascular disease state. Curr Opin Cardiol. 2002;17(5):543–51.

[73] Nichols WW. Clinical measurement of arterial stiffness obtained from noninvasive pressure waveforms. Am J Hypertens. 2005;18(1 Pt 2):3S–10S.

[74] Allen J, Murray A. Age-related changes in peripheral pulse timing characteristics at the ears, fingers and toes. J Hum Hypertens. 2002;16(10):711–7.

[75] Bukachi F, Waldenstrom A, Morner S, Lindqvist P, Henein MY, Kazzam E. Pulmonary venous flow reversal and its relationship to atrial mechanical function in normal subjects–Umea General Population Heart Study. Eur J Echocardiogr. 2005;6(2):107–16.

[76] Nelson TR, Pretorius DH. The Doppler signal: where does it come from and what does it mean? AJR Am J Roentgenol. 1988;151(3):439–47.

[77] Martin N, Lilly LS. The cardiac cycle: Mechanisms of heart sounds and murmurs. In: Lilly LS, editor. Pathophysiology of heart disease. Philadelphia: Lippincott Williams & Wilkins; 2007. p. 29–44.

[78] Lederer JW. Cardiac electrophysiology and the electrocardiogram. In: Boron WF, Boulpaep EL, editors. Medical physiology. Philadelphia: Elsevier Inc.; 2003. p. 483–507.

[79] Kubicek WG, Karnegis JN, Patterson RP, Witsoe DA, Mattson RH. Development and evaluation of an impedance cardiac output system. Aerosp Med. 1966;37(12):1208–12.

[80] Summers RL, Shoemaker WC, Peacock WF, Ander DS, Coleman TG. Bench to bedside: electrophysiologic and clinical principles of noninvasive hemodynamic monitoring using impedance cardiography. Acad Emerg Med. 2003;10(6):669–80.

[81] Bernstein DP. A new stroke volume equation for thoracic electrical bioimpedance: theory and rationale. Crit Care Med. 1986;14(10):904–9.

[82] Sramek BB. Cardiac output by electrical impedance. Med Electron. 1982;13(2):93–7.

[83] Flo K, Wilsgaard T, Acharya G. A new non-invasive method for measuring uterine vascular resistance and its relationship to uterine artery Doppler indices: a longitudinal study. Ultrasound Obstet Gynecol. 2011;37(5):538–42.

[84] Napolitano R, Rajakulasingam R, Memmo A, Bhide A, Thilaganathan B. Uterine artery Doppler screening for pre-eclampsia: comparison of the lower, mean and higher first-trimester pulsatility indices. Ultrasound Obstet Gynecol. 2011;37(5):534–7.

[85] Malcus P. Antenatal fetal surveillance. Curr Opin Obstet Gynecol. 2004;16(2):123–8.

[86] Abramowicz JS, Sheiner E. Ultrasound of the placenta: a systematic approach. Part II: functional assessment (Doppler). Placenta. 2008;29(11):921–9.

[87] Papageorghiou AT, Leslie K. Uterine artery Doppler in the prediction of adverse pregnancy outcome. Curr Opin Obstet Gynecol. 2007;19(2):103–9.

[88] Cnossen JS, Morris RK, ter Riet G, Mol BW, van der Post JA, Coomarasamy A, et al. Use of uterine artery Doppler ultrasonography to predict pre-eclampsia and intrauterine growth restriction: a systematic review and bivariable meta-analysis. CMAJ. 2008;178(6):701–11.

[89] Karabulut N, Baki Yagci A, Karabulut A. Renal vein Doppler ultrasound of maternal kidneys in normal second and third trimester pregnancy. Br J Radiol. 2003;76(907):444–7.

[90] Bateman GA, Cuganesan R. Renal vein Doppler sonography of obstructive uropathy. AJR Am J Roentgenol. 2002;178(4):921–5.

[91] Roobottom CA, Hunter JD, Weston MJ, Dubbins PA. Hepatic venous Doppler waveforms: changes in pregnancy. J Clin Ultrasound. 1995;23(8):477–82.

[92] Gyselaers W. Hemodynamics of the maternal venous compartment: a new area to explore in obstetric ultrasound imaging. Ultrasound Obstet Gynecol. 2008;32(5):716–7.

[93] Gyselaers W, Molenberghs G, Mesens T, Peeters L. Maternal hepatic vein Doppler velocimetry during uncomplicated pregnancy and pre-eclampsia. Ultrasound Med Biol. 2009;35(8):1278–83.

[94] Gyselaers W, Molenberghs G, Van Mieghem W, Ombelet W. Doppler measurement of renal interlobar vein impedance index in uncomplicated and preeclamptic pregnancies. Hypertens Pregnancy. 2009;28(1):23–33.

[95] Gyselaers W, Mesens T. Renal interlobar vein impedance index: a potential new Doppler parameter in the prediction of preeclampsia? J Matern Fetal Neonatal Med. 2009;22(12):1219–21.

[96] Carty DM, Delles C, Dominiczak AF. Novel biomarkers for predicting preeclampsia. Trends Cardiovasc Med. 2008;18(5):186–94.

[97] Neumann JO, Thorn M, Fischer L, Schobinger M, Heimann T, Radeleff B, et al. Branching patterns and drainage territories of the middle hepatic vein in computer-simulated right living-donor hepatectomies. Am J Transplant. 2006;6(6):1407–15.

[98] Grant EG, Schiller VL, Millener P, Tessler FN, Perrella RR, Ragavendra N, et al. Color Doppler imaging of the hepatic vasculature. AJR Am J Roentgenol. 1992;159(5):943–50.

[99] Ahmed K, Sampath R, Khan MS. Current trends in the diagnosis and management of renal nutcracker syndrome: a review. Eur J Vasc Endovasc Surg. 2006;31(4):410–6.

[100] Itoh S, Yoshida K, Nakamura Y, Mitsuhashi N. Aggravation of the nutcracker syndrome during pregnancy. Obstet Gynecol. 1997;90(4 Pt 2):661–3.

[101] Satyapal KS, Rambiritch V, Pillai G. Additional renal veins: incidence and morphometry. Clin Anat. 1995;8(1):51–5.

[102] Satyapal KS, Rambiritch V, Pillai G. Morphometric analysis of the renal veins. Anat Rec. 1995;241(2):268–72.

[103] Fernandez-Cuadrado J, Alonso-Torres A, Baudraxler F, Sanchez-Almaraz C. Three-dimensional contrast-enhanced magnetic resonance angiography of congenital inferior vena cava anomalies. Semin Pediatr Surg. 2005;14(4):226–32.

[104] Mathews R, Smith PA, Fishman EK, Marshall FF. Anomalies of the inferior vena cava and renal veins: embryologic and surgical considerations. Urology. 1999;53(5):873–80.

[105] Pannu HK, Maley WR, Fishman EK. Liver transplantation: preoperative CT evaluation. Radiographics. 2001;21 Spec No:S133–46.

[106] Gallego C, Miralles M, Marin C, Muyor P, Gonzalez G, Garcia-Hidalgo E. Congenital hepatic shunts. Radiographics. 2004;24(3):755–72.

[107] Juncquiera L, Carneiro J. The circulatory system. In: Juncquiera L, Carneiro J, editors. Basic histology: text and atlas. New York: McGraw-Hill Professional; 2005. p. 205–222.

[108] Downey DB. The retroperitoneum and the great vessels. In: Rumack CM, Wilson RD, Charboneau JW, Johnson JM, editors. Diagnostic ultrasound. Philadelphia: Mosby, Inc; 2005. p. 443–488.

[109] Bateman GA, Giles W, England SL. Renal venous Doppler sonography in preeclampsia. J Ultrasound Med. 2004;23(12):1607–11.

[110] Lui EY, Steinman AH, Cobbold RS, Johnston KW. Human factors as a source of error in peak Doppler velocity measurement. J Vasc Surg. 2005;42(5):972–9.

[111] Nakai A, Oya A. Accuracy and reproducibility of ultrasound measurements in obstetric management. Gynecol Obstet Invest. 2002;54(1):31–6.

[112] Oktar SO, Yucel C, Ozdemir H, Karaosmanoglu D. Doppler sonography of renal obstruction: value of venous impedance index measurements. J Ultrasound Med. 2004;23(7):929–36.

[113] Hecher K, Campbell S. Characteristics of fetal venous blood flow under normal circumstances and during fetal disease. Ultrasound Obstet Gynecol. 1996;7(1):68–83.

[114] Moll W. Venous return in the fetal-placental cardiovascular system. Eur J Obstet Gynecol Reprod Biol. 1999;84(2):133–7.

[115] Oh JK, Seward JB, Tajik AJ. Assessment of diastolic function and diastolic heart failure. In: Oh JK, Seward JB, Tajik AJ, editors. The echo manual. Philadelphia: Lippincott Williams & Wilkins; 2007. p. 121–142.

[116] Schneider AR, Teuber G, Kriener S, Caspary WF. Noninvasive assessment of liver steatosis, fibrosis and inflammation in chronic hepatitis C virus infection. Liver Int. 2005;25(6):1150–5.

[117] Colli A, Cocciolo M, Riva C, Martinez E, Prisco A, Pirola M, et al. Abnormalities of Doppler waveform of the hepatic veins in patients with chronic liver disease: correlation with histologic findings. AJR Am J Roentgenol. 1994;162(4):833–7.

[118] Dietrich CF, Lee JH, Gottschalk R, Herrmann G, Sarrazin C, Caspary WF, et al. Hepatic and portal vein flow pattern in correlation with intrahepatic fat deposition and liver histology in patients with chronic hepatitis C. AJR Am J Roentgenol. 1998;171(2):437–43.

[119] Bolondi L, Li Bassi S, Gaiani S, Zironi G, Benzi G, Santi V, et al. Liver cirrhosis: changes of Doppler waveform of hepatic veins. Radiology. 1991;178(2):513–6.

[120] Ohta M, Hashizume M, Tomikawa M, Ueno K, Tanoue K, Sugimachi K. Analysis of hepatic vein waveform by Doppler ultrasonography in 100 patients with portal hypertension. Am J Gastroenterol. 1994;89(2):170–5.

[121] Salgado O, Garcia R, Henriquez C, Rosales B, Sulbaran P. Severely elevated intrarenal arterial impedance and abnormal venous flow pattern in a normal functioning kidney graft. Transplant Proc. 2003;35(5):1772–4.

[122] Zubarev AV. Ultrasound of renal vessels. Eur Radiol. 2001;11(10):1902–15.

[123] Witz M, Kantarovsky A, Morag B, Shifrin EG. Renal vein occlusion: a review. J Urol. 1996;155(4):1173–9.

[124] Pekindil G, Varol FG, Yuce MA, Yardim T. Evaluation of hepatic venous pulsatility and portal venous velocity with Doppler ultrasonography during the puerperium. Eur J Radiol. 1999;29(3):266–9.

[125] Nakai A, Sekiya I, Oya A, Koshino T, Araki T. Assessment of the hepatic arterial and portal venous blood flows during pregnancy with Doppler ultrasonography. Arch Gynecol Obstet. 2002;266(1):25–9.

[126] Satyapal KS. Classification of the drainage patterns of the renal veins. J Anat. 1995;186 (Pt 2):329–33.

[127] Wang JJ, Flewitt JA, Shrive NG, Parker KH, Tyberg JV. Systemic venous circulation. Waves propagating on a windkessel: relation of arterial and venous windkessels to systemic vascular resistance. Am J Physiol Heart Circ Physiol. 2006;290(1):H154–62.

[128] Dhawan V, Brookes ZL, Kaufman S. Repeated pregnancies (multiparity) increases venous tone and reduces compliance. Am J Physiol Regul Integr Comp Physiol. 2005;289(1):R23–8.

[129] Hohmann M, Zoltan D, Kunzel W. Age and reproductive status affect basal venous tone in the rat. Eur J Obstet Gynecol Reprod Biol. 1996;68(1-2):185–9.

[130] Skudder J P A, Farrington DT, Weld E, Putman C. Venous dysfunction of late pregnancy persists after delivery. J Cardiovasc Surg (Torino). 1990;31(6):748–52.

[131] Tyberg JV. How changes in venous capacitance modulate cardiac output. Pflugers Arch. 2002;445(1):10–7.

[132] Kiserud T. Fetal venous circulation–an update on hemodynamics. J Perinat Med. 2000;28(2):90–6.

[133] Kiserud T. Physiology of the fetal circulation. Semin Fetal Neonatal Med. 2005;10(6):493–503.

[134] Verbeke G, Molenberghs G. Linear Mixed Models for Longitudinal Data. 2nd ed. New York: Springer; 2001.

[135] Valensise H, Vasapollo B, Gagliardi G, Novelli GP. Early and late preeclampsia: two different maternal hemodynamic states in the latent phase of the disease. Hypertension. 2008;52(5):873–80.

[136] Easterling TR, Benedetti TJ, Carlson KC, Brateng DA, Wilson J, Schmucker BS. The effect of maternal hemodynamics on fetal growth in hypertensive pregnancies. Am J Obstet Gynecol. 1991;165(4 Pt 1):902–6.

[137] Easterling TR, Benedetti TJ, Schmucker BC, Millard SP. Maternal hemodynamics in normal and preeclamptic pregnancies: a longitudinal study. Obstet Gynecol. 1990;76(6):1061–9.

[138] Crispi F, Llurba E, Dominguez C, Martin-Gallan P, Cabero L, Gratacos E. Predictive value of angiogenic factors and uterine artery Doppler for early- versus late-onset pre-eclampsia and intrauterine growth restriction. Ultrasound Obstet Gynecol. 2008;31(3):303–9.

[139] Yu CK, Khouri O, Onwudiwe N, Spiliopoulos Y, Nicolaides KH. Prediction of pre-eclampsia by uterine artery Doppler imaging: relationship to gestational age at delivery and small-for-gestational age. Ultrasound Obstet Gynecol. 2008;31(3):310–3.

[140] Khaw A, Kametas NA, Turan OM, Bamfo JE, Nicolaides KH. Maternal cardiac function and uterine artery Doppler at 11-14 weeks in the prediction of pre-eclampsia in nulliparous women. BJOG. 2008;115(3):369–76.

[141] Gyselaers W, Verswijvel G, Molenberghs G, Ombelet W. Interlobar venous flow is different between left and right kidney in uncomplicated third trimester pregnancy. Gynecol Obstet Invest. 2008;65(1):6–11.

[142] Laenen A, Vangeneugden T, Geys H, Molenberghs G. Generalized reliability estimation using repeated measurements. Br J Math Stat Psychol. 2006;59(Pt 1):113–31.

[143] Devlieger H, Martens G, Bekaert A, Eeckels R, Vlietinck R. Standaarden van geboortegewicht-voor-zwangerschapsduur voor de Vlaamse boreling. In: Bekaert A, Martens G, Devlieger H, editors. Perinatale activiteiten in Vlaanderen 1996. Brussels: Studiecentrum voor Perinatale Epidemiologie (SPE); 1997. p. 94–116.

[144] Houben AJ, de Leeuw PW, Peeters LL. Configuration of the microcirculation in pre-eclampsia: possible role of the venular system. J Hypertens. 2007;25(8):1665–70.

[145] de Cleva R, Silva FP, Zilberstein B, Machado DJ. Acute renal failure due to abdominal compartment syndrome: report on four cases and literature review. Rev Hosp Clin Fac Med Sao Paulo. 2001;56(4):123–30.

[146] Doty JM, Saggi BH, Sugerman HJ, Blocher CR, Pin R, Fakhry I, et al. Effect of increased renal venous pressure on renal function. J Trauma. 1999;47(6):1000–3.

[147] Gyselaers W, Mesens T, Tomsin K, Molenberghs G, Peeters L. Maternal renal interlobar vein impedance index is higher in early- than in late-onset preeclampsia. Ultrasound Obstet Gynecol. 2010;36(1):69–75.

[148] Appleton CP, Hatle LK, Popp RL. Superior vena cava and hepatic vein Doppler echocardiography in healthy adults. J Am Coll Cardiol. 1987;10(5):1032–9.

[149] Ommen SR, Nishimura RA, Hurrell DG, Klarich KW. Assessment of right atrial pressure with 2-dimensional and Doppler echocardiography: a simultaneous catheterization and echocardiographic study. Mayo Clin Proc. 2000;75(1):24–9.

[150] Ommen SR, Nishimura RA, Appleton CP, Miller FA, Oh JK, Redfield MM, et al. Clinical utility of Doppler echocardiography and tissue Doppler imaging in the estimation of left ventricular filling pressures: A comparative simultaneous Doppler-catheterization study. Circulation. 2000;102(15):1788–94.

[151] Haendl T, Strobel D, Steinebrunner N, Frieser M, Hahn EG, Bernatik T. Hepatic transit time in benign liver lesions. Ultraschall Med. 2008;29(2):184–9.

[152] Galderisi M, Cattaneo F, Mondillo S. Doppler echocardiography and myocardial dyssynchrony: a practical update of old and new ultrasound technologies. Cardiovasc Ultrasound. 2007;5:28.

[153] Berzigotti A, Castaldini N, Rossi V, Magalotti D, Tiani C, Zappoli P, et al. Age dependency of regional impedance indices regardless of clinical stage in patients with cirrhosis of the liver. Ultraschall Med. 2009;30(3):277–85.

[154] Khalil AA, Cooper DJ, Harrington KF. Pulse wave analysis: a preliminary study of a novel technique for the prediction of pre-eclampsia. BJOG. 2009;116(2):268–76; discussion 276–7.

[155] Spaanderman ME, Willekes C, Hoeks AP, Ekhart TH, Peeters LL. The effect of pregnancy on the compliance of large arteries and veins in healthy parous control subjects and women with a history of preeclampsia. Am J Obstet Gynecol. 2000;183(5):1278–86.

[156] Tomsin K, Mesens T, Molenberghs G, Peeters L, Gyselaers W. Time Interval Between Maternal Electrocardiogram and Venous Doppler Waves in Normal Pregnancy and Preeclampsia: A Pilot Study. Ultraschall Med. 2012;33(7):E119–25.

[157] Grab D, Hutter W, Sterzik K, Terinde R. Reference values for resistance index and pulsatility index of uteroplacental Doppler flow velocity waveforms based on 612 uneventful pregnancies. Gynecol Obstet Invest. 1992;34(2):82–7.

[158] Kim DW. Detection of physiological events by impedance. Yonsei Med J. 1989;30(1):1–11.

[159] Woltjer HH, Bogaard HJ, de Vries PM. The technique of impedance cardiography. Eur Heart J. 1997;18(9):1396–403.

[160] Sodolski T, Kutarski A. Impedance cardiography: A valuable method of evaluating haemodynamic parameters. Cardiol J. 2007;14(2):115–26.

[161] Tomsin K, Mesens T, Molenberghs G, Gyselaers W. Diurnal and position-induced variability of impedance cardiography measurements in healthy subjects. Clin Physiol Funct Imaging. 2011;31(2):145–50.

[162] Naschitz JE, Bezobchuk S, Mussafia-Priselac R, Sundick S, Dreyfuss D, Khorshidi I, et al. Pulse transit time by R-wave-gated infrared photoplethysmography: review of the literature and personal experience. J Clin Monit Comput. 2004;18(5-6):333–42.

[163] Benetos A, Waeber B, Izzo J, Mitchell G, Resnick L, Asmar R, et al. Influence of age, risk factors, and cardiovascular and renal disease on arterial stiffness: clinical applications. Am J Hypertens. 2002;15(12):1101–8.

[164] Wang YX, Fitch RM. Vascular stiffness: measurements, mechanisms and implications. Curr Vasc Pharmacol. 2004;2(4):379–84.

[165] Nurnberger J, Kribben A, Philipp T, Erbel R. [Arterial compliance (stiffness) as a marker of subclinical atherosclerosis]. Herz. 2007;32(5):379–86.

[166] Jani B, Rajkumar C. Ageing and vascular ageing. Postgrad Med J. 2006;82(968):357–62.

[167] Wang X, Keith J J C, Struthers AD, Feuerstein GZ. Assessment of arterial stiffness, a translational medicine biomarker system for evaluation of vascular risk. Cardiovasc Ther. 2008;26(3):214–23.

[168] Asmar R. Effect of antihypertensive agents on arterial stiffness as evaluated by pulse wave velocity: clinical implications. Am J Cardiovasc Drugs. 2001;1(5):387–97.

[169] Ronnback M, Lampinen K, Groop PH, Kaaja R. Pulse wave reflection in currently and previously preeclamptic women. Hypertens Pregnancy. 2005;24(2):171–80.

[170] Elvan-Taspinar A, Franx A, Bots ML, Koomans HA, Bruinse HW. Arterial stiffness and fetal growth in normotensive pregnancy. Am J Hypertens. 2005;18(3):337–41.

[171] Avni B, Frenkel G, Shahar L, Golik A, Sherman D, Dishy V. Aortic stiffness in normal and hypertensive pregnancy. Blood Press. 2010;19(1):11–5.

[172] Macedo ML, Luminoso D, Savvidou MD, McEniery CM, Nicolaides KH. Maternal wave reflections and arterial stiffness in normal pregnancy as assessed by applanation tonometry. Hypertension. 2008;51(4):1047–51.

[173] Allen J. Photoplethysmography and its application in clinical physiological measurement. Physiol Meas. 2007;28(3):R1–39.

[174] Lampinen KH, Ronnback M, Kaaja RJ, Groop PH. Impaired vascular dilatation in women with a history of pre-eclampsia. J Hypertens. 2006;24(4):751–6.

[175] Edouard DA, Pannier BM, London GM, Cuche JL, Safar ME. Venous and arterial behavior during normal pregnancy. Am J Physiol. 1998;274(5 Pt 2):H1605–12.

[176] Tihtonen KM, Koobi T, Uotila JT. Arterial stiffness in preeclamptic and chronic hypertensive pregnancies. Eur J Obstet Gynecol Reprod Biol. 2006;128(1-2):180–6.

[177] Robb AO, Mills NL, Din JN, Smith IB, Paterson F, Newby DE, et al. Influence of the menstrual cycle, pregnancy, and preeclampsia on arterial stiffness. Hypertension. 2009;53(6):952–8.

[178] Poppas A, Shroff SG, Korcarz CE, Hibbard JU, Berger DS, Lindheimer MD, et al. Serial assessment of the cardiovascular system in normal pregnancy. Role of arterial compliance and pulsatile arterial load. Circulation. 1997;95(10):2407–15.

[179] Mersich B, Rigo J J, Besenyei C, Lenard Z, Studinger P, Kollai M. Opposite changes in carotid versus aortic stiffness during healthy human pregnancy. Clin Sci (Lond). 2005;109(1):103–7.

[180] Krabbendam I, Courtar DA, Janssen BJ, Aardenburg R, Peeters LL, Spaanderman ME. Blunted autonomic response to volume expansion in formerly preeclamptic women with low plasma volume. Reprod Sci. 2009;16(1):105–12.

[181] Gyselaers W, Mullens W, Tomsin K, Mesens T, Peeters L. Role of dysfunctional maternal venous hemodynamics in the pathophysiology of pre-eclampsia: a review. Ultrasound Obstet Gynecol. 2011;38(2):123–9.

[182] Riccabona M, Nelson TR, Pretorius DH. Three-dimensional ultrasound: accuracy of distance and volume measurements. Ultrasound Obstet Gynecol. 1996;7(6):429–34.

[183] Lazebnik RS, Desser TS. Clinical 3D ultrasound imaging: beyond obstetrical applications. Diagnostic Imaging. 2007;1:1–6.

[184] Lee W. Quantitative approaches for volume sonography during pregnancy. Ultrasound Clin. 2007;2:203–215.

[185] Pairleitner H, Steiner H, Hasenoehrl G, Staudach A. Three-dimensional power Doppler sonography: imaging and quantifying blood flow and vascularization. Ultrasound Obstet Gynecol. 1999;14(2):139–43.

[186] Costa J, Rice H, Cardwell C, Hunter A, Ong S. An assessment of vascularity and flow intensity of the placenta in normal pregnancy and pre-eclampsia using three-dimensional ultrasound. J Matern Fetal Neonatal Med. 2010;23(8):894–9.

[187] Jones NW, Raine-Fenning N, Mousa H, Bradley E, Bugg G. Evaluation of the intraobserver and interobserver reliability of data acquisition for three-dimensional power Doppler angiography of the whole placenta at 12 weeks gestation. Ultrasound Med Biol. 2010;36(9):1405–11.

[188] Lai PK, Wang YA, Welsh AW. Reproducibility of regional placental vascularity/perfusion measurement using 3D power Doppler. Ultrasound Obstet Gynecol. 2010;36(2):202–9.

[189] Merce LT, Barco MJ, Bau S. Reproducibility of the study of placental vascularization by three-dimensional power Doppler. J Perinat Med. 2004;32(3):228–33.

[190] Jokubkiene L, Sladkevicius P, Rovas L, Valentin L. Assessment of changes in volume and vascularity of the ovaries during the normal menstrual cycle using three-dimensional power Doppler ultrasound. Hum Reprod. 2006;21(10):2661–8.

[191] Raine-Fenning NJ, Campbell BK, Clewes JS, Kendall NR, Johnson IR. The reliability of virtual organ computer-aided analysis (VOCAL) for the semiquantification of ovarian, endometrial and subendometrial perfusion. Ultrasound Obstet Gynecol. 2003;22(6):633–9.

[192] Moron AF, Milani HJF, Barreto EQS, Junior EA, Haratz KK, Rolo LC, et al. Analysis of three-dimensional power Doppler sonography reproducibility in the assessment of fetal brain circulation. Radiol Bras. 2010;43:369–374.

[193] Raine-Fenning NJ, Nordin NM, Ramnarine KV, Campbell BK, Clewes JS, Perkins A, et al. Evaluation of the effect of machine settings on quantitative three-dimensional power Doppler angiography: an in-vitro flow phantom experiment. Ultrasound Obstet Gynecol. 2008;32(4):551–9.

[194] Verbeke G, Molenberghs G. Longitudinal and incomplete clinical studies (with discussion). International Journal of Statistics. 2005;63:143–176.

[195] Raine-Fenning NJ, Campbell BK, Clewes JS, Johnson IR. The interobserver reliability of ovarian volume measurement is improved with three-dimensional ultrasound, but dependent upon technique. Ultrasound Med Biol. 2003;29(12):1685–90.

[196] Bude RO, Rubin JM, Adler RS. Power versus conventional color Doppler sonography: comparison in the depiction of normal intrarenal vasculature. Radiology. 1994;192(3):777–80.

[197] Rubin JM, Bude RO, Carson PL, Bree RL, Adler RS. Power Doppler US: a potentially useful alternative to mean frequency-based color Doppler US. Radiology. 1994;190(3):853–6.

[198] Janssens U, Graf J. [Volume status and central venous pressure]. Anaesthesist. 2009;58(5):513–9.

[199] Duvekot JJ, Cheriex EC, Tan WD, Heidendal GA, Peeters LL. Measurement of anterior-posterior diameter of inferior vena cava by ultrasonography: a new non-invasive method to assess acute changes in vascular filling state. Cardiovasc Res. 1994;28(8):1269–72.

[200] Doty JM, Saggi BH, Blocher CR, Fakhry I, Gehr T, Sica D, et al. Effects of increased renal parenchymal pressure on renal function. J Trauma. 2000;48(5):874–7.

[201] Dilley JR, Corradi A, Arendshorst WJ. Glomerular ultrafiltration dynamics during increased renal venous pressure. Am J Physiol. 1983;244(6):F650–8.

[202] Corradi A, Arendshorst WJ. Rat renal hemodynamics during venous compression: roles of nerves and prostaglandins. Am J Physiol. 1985;248(6 Pt 2):F810–20.

[203] Lotgering FK, Wallenburg HC. Hemodynamic effects of caval and uterine venous occlusion in pregnant sheep. Am J Obstet Gynecol. 1986;155(6):1164–70.

[204] Zigman A, Yazbeck S, Emil S, Nguyen L. Renal vein thrombosis: a 10-year review. J Pediatr Surg. 2000;35(11):1540–2.

[205] Naschitz JE, Slobodin G, Lewis RJ, Zuckerman E, Yeshurun D. Heart diseases affecting the liver and liver diseases affecting the heart. Am Heart J. 2000;140(1):111–20.

[206] Ronco C, Haapio M, House AA, Anavekar N, Bellomo R. Cardiorenal syndrome. J Am Coll Cardiol. 2008;52(19):1527–39.

[207] Tang WH, Mullens W. Cardiorenal syndrome in decompensated heart failure. Heart. 2010;96(4):255–60.

[208] Firth JD, Raine AE, Ledingham JG. Raised venous pressure: a direct cause of renal sodium retention in oedema? Lancet. 1988;1(8593):1033–5.

[209] Winton FR. The influence of venous pressure on the isolated mammalian kidney. J Physiol. 1931;72(1):49–61.

[210] Burnett J J C, Knox FG. Renal interstitial pressure and sodium excretion during renal vein constriction. Am J Physiol. 1980;238(4):F279–82.

[211] Burnett J J C, Haas JA, Knox FG. Segmental analysis of sodium reabsorption during renal vein constriction. Am J Physiol. 1982;243(1):F19–22.

[212] Wathen RL, Selkurt EE. Intrarenal regulatory factors of salt excretion during renal venous pressure elevation. Am J Physiol. 1969;216(6):1517–24.

[213] Maxwell MH, Breed ES, Schwartz IL. Renal Venous Pressure in Chronic Congestive Heart Failure. J Clin Invest. 1950;29(3):342–8.

[214] Fiksen-Olsen MJ, Romero JC. Renal effects of prostaglandin inhibition during increases in renal venous pressure. Am J Physiol. 1991;260(4 Pt 2):F525–9.

[215] Fiksen-Olsen MJ, Strick DM, Hawley H, Romero JC. Renal effects of angiotensin II inhibition during increases in renal venous pressure. Hypertension. 1992;19(2 Suppl):II137–41.

[216] Seeto RK, Fenn B, Rockey DC. Ischemic hepatitis: clinical presentation and pathogenesis. Am J Med. 2000;109(2):109–13.

[217] Badalamenti S, Graziani G, Salerno F, Ponticelli C. Hepatorenal syndrome. New perspectives in pathogenesis and treatment. Arch Intern Med. 1993;153(17):1957–67.

[218] Castells A, Salo J, Planas R, Quer JC, Gines A, Boix J, et al. Impact of shunt surgery for variceal bleeding in the natural history of ascites in cirrhosis: a retrospective study. Hepatology. 1994;20(3):584–91.

[219] Hamza SM, Kaufman S. Effect of mesenteric vascular congestion on reflex control of renal blood flow. Am J Physiol Regul Integr Comp Physiol. 2007;293(5):R1917–22.

[220] Kastner PR, Hall JE, Guyton AC. Renal hemodynamic responses to increased renal venous pressure: role of angiotensin II. Am J Physiol. 1982;243(3):F260–4.

[221] DiBona GF, Kopp UC. Neural control of renal function. Physiol Rev. 1997;77(1):75–197.

[222] Kon V, Yared A, Ichikawa I. Role of renal sympathetic nerves in mediating hypoperfusion of renal cortical microcirculation in experimental congestive heart failure and acute extracellular fluid volume depletion. J Clin Invest. 1985;76(5):1913–20.

[223] Charkoudian N, Martin EA, Dinenno FA, Eisenach JH, Dietz NM, Joyner MJ. Influence of increased central venous pressure on baroreflex control of sympathetic activity in humans. Am J Physiol Heart Circ Physiol. 2004;287(4):H1658–62.

[224] Creager MA, Creager SJ. Arterial baroreflex regulation of blood pressure in patients with congestive heart failure. J Am Coll Cardiol. 1994;23(2):401–5.

[225] Shi X, Foresman BH, Raven PB. Interaction of central venous pressure, intramuscular pressure, and carotid baroreflex function. Am J Physiol. 1997;272(3 Pt 2):H1359–63.

[226] Gauer OH, Henry JP. Neurohormonal control of plasma volume. Int Rev Physiol. 1976;9:145–90.

[227] Mullens W, Abrahams Z, Skouri HN, Francis GS, Taylor DO, Starling RC, et al. Elevated intra-abdominal pressure in acute decompensated heart failure: a potential contributor to worsening renal function? J Am Coll Cardiol. 2008;51(3):300–6.

[228] Malbrain ML, Deeren D, De Potter TJ. Intra-abdominal hypertension in the critically ill: it is time to pay attention. Curr Opin Crit Care. 2005;11(2):156–71.

[229] Mullens W, Abrahams Z, Francis GS, Sokos G, Taylor DO, Starling RC, et al. Importance of venous congestion for worsening of renal function in advanced decompensated heart failure. J Am Coll Cardiol. 2009;53(7):589–96.

[230] Damman K, Navis G, Smilde TD, Voors AA, van der Bij W, van Veldhuisen DJ, et al. Decreased cardiac output, venous congestion and the association with renal impairment in patients with cardiac dysfunction. Eur J Heart Fail. 2007;9(9):872–8.

[231] Mullens W, Abrahams Z, Francis GS, Taylor DO, Starling RC, Tang WH. Prompt reduction in intra-abdominal pressure following large-volume mechanical fluid removal improves renal insufficiency in refractory decompensated heart failure. J Card Fail. 2008;14(6):508–14.

[232] Duvekot JJ, Peeters L. Very early changes in cardiovascular physiology. In: Chamberlain G, Pipkin F, editors. Clinical physiology in obstetrics. Oxford, UK: Blackwell Science; 1998. p. 3–32.

[233] Spaanderman M, Ekhart T, van Eyck J, de Leeuw P, Peeters L. Preeclampsia and maladaptation to pregnancy: a role for atrial natriuretic peptide? Kidney Int. 2001;60(4):1397–406.

[234] Hohmann M, McLaughlin MK, Kunzel W. [Direct assessment of mesenteric vein compliance in the rat during pregnancy]. Z Geburtshilfe Perinatol. 1992;196(1):33–40.

[235] Ganzevoort W, Rep A, Bonsel GJ, de Vries JI, Wolf H. Plasma volume and blood pressure regulation in hypertensive pregnancy. J Hypertens. 2004;22(7):1235–42.

[236] Rang S, van Montfrans GA, Wolf H. Serial hemodynamic measurement in normal pregnancy, preeclampsia, and intrauterine growth restriction. Am J Obstet Gynecol. 2008;198(5):519 e1–9.

[237] Spaanderman ME, Ekhart TH, van Eyck J, Cheriex EC, de Leeuw PW, Peeters LL. Latent hemodynamic abnormalities in symptom-free women with a history of preeclampsia. Am J Obstet Gynecol. 2000;182(1 Pt 1):101–7.

[238] Aardenburg R, Spaanderman ME, Courtar DA, van Eijndhoven HW, de Leeuw PW, Peeters LL. A subnormal plasma volume in formerly preeclamptic women is associated with a low venous capacitance. J Soc Gynecol Investig. 2005;12(2):107–11.

[239] Aardenburg R, Spaanderman ME, van Eijndhoven HW, de Leeuw PW, Peeters LL. Formerly preeclamptic women with a subnormal plasma volume are unable to maintain a rise in stroke volume during moderate exercise. J Soc Gynecol Investig. 2005;12(8):599–603.

[240] Aardenburg R, Spaanderman ME, Ekhart TH, van Eijndhoven HW, van der Heijden OW, Peeters LL. Low plasma volume following pregnancy complicated by pre-eclampsia predisposes for hypertensive disease in a next pregnancy. BJOG. 2003;110(11):1001–6.

[241] De Paco C, Kametas N, Rencoret G, Strobl I, Nicolaides KH. Maternal cardiac output between 11 and 13 weeks of gestation in the prediction of preeclampsia and small for gestational age. Obstet Gynecol. 2008;111(2 Pt 1):292–300.

[242] Steegers EA, von Dadelszen P, Duvekot JJ, Pijnenborg R. Pre-eclampsia. Lancet. 2010;376(9741):631–44.

[243] Redman CW, Sargent IL. Latest advances in understanding preeclampsia. Science. 2005;308(5728):1592–4.

[244] Zavorsky GS. Cardiopulmonary aspects of obesity in women. Obstet Gynecol Clin North Am. 2009;36(2):267–84, viii.

[245] Nasr A, Nafeh H. Decreased hepatic perfusion in patients with HELLP syndrome. J Obstet Gynaecol. 2009;29(7):624–7.

[246] Kawabata I, Nakai A, Takeshita T. Prediction of HELLP syndrome with assessment of maternal dual hepatic blood supply by using Doppler ultrasound. Arch Gynecol Obstet. 2006;274(5):303–9.

[247] Oosterhof H, Voorhoeve PG, Aarnoudse JG. Enhancement of hepatic artery resistance to blood flow in preeclampsia in presence or absence of HELLP syndrome (hemolysis, elevated liver enzymes, and low platelets). Am J Obstet Gynecol. 1994;171(2):526–30.

[248] Tokunaga N, Kanayama N, Sugimura M, Kobayashi T, Terao T. Dilatation of the left renal vein in preeclampsia. J Matern Fetal Med. 2000;9(6):356–9.

[249] Mitchell JE, Palta S. New diagnostic modalities in the diagnosis of heart failure. J Natl Med Assoc. 2004;96(11):1424–30.

[250] Spiess BD, Patel MA, Soltow LO, Wright IH. Comparison of bioimpedance versus thermodilution cardiac output during cardiac surgery: evaluation of a second-generation bioimpedance device. J Cardiothorac Vasc Anesth. 2001;15(5):567–73.

[251] Drazner MH, Thompson B, Rosenberg PB, Kaiser PA, Boehrer JD, Baldwin BJ, et al. Comparison of impedance cardiography with invasive hemodynamic measurements in patients with heart failure secondary to ischemic or nonischemic cardiomyopathy. Am J Cardiol. 2002;89(8):993–5.

[252] Van De Water JM, Miller TW, Vogel RL, Mount BE, Dalton ML. Impedance cardiography: the next vital sign technology? Chest. 2003;123(6):2028–33.

[253] Albert NM, Hail MD, Li J, Young JB. Equivalence of the bioimpedance and thermodilution methods in measuring cardiac output in hospitalized patients with advanced, decompensated chronic heart failure. Am J Crit Care. 2004;13(6):469–79.

[254] Cotter G, Moshkovitz Y, Kaluski E, Cohen AJ, Miller H, Goor D, et al. Accurate, noninvasive continuous monitoring of cardiac output by whole-body electrical bioimpedance. Chest. 2004;125(4):1431–40.

[255] Mathews L, Singh RK. Cardiac output monitoring. Ann Card Anaesth. 2008;11(1):56–68.

[256] Engoren M, Barbee D. Comparison of cardiac output determined by bioimpedance, thermodilution, and the Fick method. Am J Crit Care. 2005;14(1):40–5.

[257] de Waal EE, Konings MK, Kalkman CJ, Buhre WF. Assessment of stroke volume index with three different bioimpedance algorithms: lack of agreement compared to thermodilution. Intensive Care Med. 2008;34(4):735–9.

[258] Woltjer HH, Bogaard HJ, Scheffer GJ, van der Spoel HI, Huybregts MA, de Vries PM. Standardization of non-invasive impedance cardiography for assessment of stroke volume: comparison with thermodilution. Br J Anaesth. 1996;77(6):748–52.

[259] Ono T, Yasuda Y, Ito T, Barros AK, Ishida K, Miyamura M, et al. Validity of the adaptive filter for accurate measurement of cardiac output in impedance cardiography. Tohoku J Exp Med. 2004;202(3):181–91.

[260] Thomas SH. Impedance cardiography using the Sramek-Bernstein method: accuracy and variability at rest and during exercise. Br J Clin Pharmacol. 1992;34(6):467–76.

[261] Dubois D, Dubois EF. A formula to estimate the approximate surface area if height and weight be known. Arch Intern Med. 1916;17:863–871.

[262] Donovan KD, Dobb GJ, Woods WP, Hockings BE. Comparison of transthoracic electrical impedance and thermodilution methods for measuring cardiac output. Crit Care Med. 1986;14(12):1038–44.

[263] Weissler AM, Leonard JJ, Warren JV. Effects of posture and atropine on the cardiac output. J Clin Invest. 1957;36(12):1656–62.

[264] Olufsen MS, Ottesen JT, Tran HT, Ellwein LM, Lipsitz LA, Novak V. Blood pressure and blood flow variation during postural change from sitting to standing: model development and validation. J Appl Physiol. 2005;99(4):1523–37.

[265] Ramirez-Marrero FA, Charkoudian N, Hart EC, Schroeder D, Zhong L, Eisenach JH, et al. Cardiovascular dynamics in healthy subjects with differing heart rate responses to tilt. J Appl Physiol. 2008;105(5):1448–53.

[266] Bau PF, Bau CH, Naujorks AA, Rosito GA, Fuchs FD. Diurnal variation of vascular diameter and reactivity in healthy young men. Braz J Med Biol Res. 2008;41(6):500–3.

[267] Tuckman J, Shillingford J. Effect of different degrees of tilt on cardiac output, heart rate, and blood pressure in normal man. Br Heart J. 1966;28(1):32–9.

[268] Zambrano SS, Spodick DH. Comparative responses to orthostatic stress in normal and abnormal subjects. Evaluation by impedance cardiography. Chest. 1974;65(4):394–6.

[269] Lance VQ, Spodick DH. Heart rate–left ventricular ejection time relations. Variations during postural change and cardiovascular challenges. Br Heart J. 1976;38(12):1332–8.

[270] Kario K, Schwartz JE, Pickering TG. Ambulatory physical activity as a determinant of diurnal blood pressure variation. Hypertension. 1999;34(4 Pt 1):685–91.

[271] Shaw JA, Chin-Dusting JP, Kingwell BA, Dart AM. Diurnal variation in endothelium-dependent vasodilatation is not apparent in coronary artery disease. Circulation. 2001;103(6):806–12.

[272] Hett DA, Jonas MM. Non-invasive cardiac output monitoring. Intensive Crit Care Nurs. 2004;20(2):103–8.

[273] Maragiannis D, Lazaros G, Aloizos S, Vavouranakis E, Stefanadis C. Pulmonary artery catheter (PAC) under attack? Hellenic J Cardiol. 2010;51(1):49–54.

[274] Nolan TE, Wakefield ML, Devoe LD. Invasive hemodynamic monitoring in obstetrics. A critical review of its indications, benefits, complications, and alternatives. Chest. 1992;101(5):1429–33.

[275] Young P, Johanson R. Haemodynamic, invasive and echocardiographic monitoring in the hypertensive parturient. Best Pract Res Clin Obstet Gynaecol. 2001;15(4):605–22.

[276] Nihoyannopoulos P. Echocardiography in 2009: the future of clinical diagnosis. Future Cardiol. 2010;6(1):37–49.

[277] Chaffin DG, Webb DG. Outcomes of pregnancies at risk for hypertensive complications managed using impedance cardiography. Am J Perinatol. 2009;26(10):717–21.

[278] Parrish MR, Laye MR, Wood T, Keiser SD, Owens MY, May WL, et al. Impedance cardiography facilitates differentiation of severe and superimposed preeclampsia from other hypertensive disorders. Hypertens Pregnancy. 2012;31(3):327–40.

[279] Kuller R. The influence of light on circarhythms in humans. J Physiol Anthropol Appl Human Sci. 2002;21(2):87–91.

[280] Wang DJ, Gottlieb SS. Impedance cardiography: more questions than answers. Curr Cardiol Rep. 2006;8(3):180–6.

[281] Koenen SV, Franx A, Mulder EJ, Bruinse HW, Visser GH. Fetal and maternal cardiovascular diurnal rhythms in pregnancies complicated by pre-eclampsia and intrauterine growth restriction. J Matern Fetal Neonatal Med. 2002;11(5):313–20.

[282] Airaksinen KE, Kirkinen P, Takkunen JT. Autonomic nervous dysfunction in severe pre-eclampsia. Eur J Obstet Gynecol Reprod Biol. 1985;19(5):269–76.

[283] Heiskanen N, Saarelainen H, Valtonen P, Lyyra-Laitinen T, Laitinen T, Vanninen E, et al. Blood pressure and heart rate variability analysis of orthostatic challenge in normal human pregnancies. Clin Physiol Funct Imaging. 2008;28(6):384–90.

[284] Ayala DE, Hermida RC, Cornelissen G, Brockway B, Halberg F. Heart rate and blood pressure chronomes during and after pregnancy. Chronobiologia. 1994;21(3-4):215–25.

[285] Ekholm EM, Tahvanainen KU, Metsala T. Heart rate and blood pressure variabilities are increased in pregnancy-induced hypertension. Am J Obstet Gynecol. 1997;177(5):1208–12.

[286] Folan L, Funk M. Measurement of thoracic fluid content in heart failure: the role of impedance cardiography. AACN Adv Crit Care. 2008;19(1):47–55.

[287] Tang WH, Tong W. Measuring impedance in congestive heart failure: current options and clinical applications. Am Heart J. 2009;157(3):402–11.

[288] Newman RB, Pierre H, Scardo J. Thoracic-fluid conductivity in peripartum women with pulmonary edema. Obstet Gynecol. 1999;94(1):48–51.

[289] Critchley LA. Impedance cardiography. The impact of new technology. Anaesthesia. 1998;53(7):677–84.

[290] Tomsin K, Mesens T, Molenberghs G, Gyselaers W. Impedance cardiography in uncomplicated pregnancy and pre-eclampsia: A reliability study. J Obstet Gynaecol. 2012;32(7):630–4.

[291] Weissler AM, Harris WS, Schoenfeld CD. Systolic time intervals in heart failure in man. Circulation. 1968;37(2):149–59.

[292] Ferro G, Piscione F, Carella G, Betocchi S, Spinelli L, Chiariello M. Systolic and diastolic time intervals during spontaneous angina. Clin Cardiol. 1984;7(11):588–92.

[293] Sundberg S. Influence of heart rate on systolic time intervals. Am J Cardiol. 1986;58(11):1144–5.

[294] Randall OS, Westerhof N, van den Bos GC, Alexander B. Reliability of stroke volume to pulse pressure ratio for estimating and detecting changes in arterial compliance. J Hypertens Suppl. 1986;4(5):S293–6.

[295] R DB, G B, G M, C L, F M, E P, et al. Cardiovascular function in pregnancy: effects of posture. BJOG. 2001;108(4):344–52.

[296] Newlin DB, Levenson RW. Pre-ejection period: measuring beta-adrenergic influences upon the heart. Psychophysiology. 1979;16(6):546–53.

[297] Krabbendam I, Janssen BJ, Van Dijk AP, Jongsma HW, Oyen WJ, Lotgering FK, et al. The relation between venous reserve capacity and low plasma volume. Reprod Sci. 2008;15(6):604–12.

[298] Robson SC, Hunter S, Moore M, Dunlop W. Haemodynamic changes during the puerperium: a Doppler and M-mode echocardiographic study. Br J Obstet Gynaecol. 1987;94(11):1028–39.

[299] Kemp CD, Conte JV. The pathophysiology of heart failure. Cardiovasc Pathol. 2012;21(5):365–71.

[300] Melchiorre K, Sutherland G, Sharma R, Nanni M, Thilaganathan B. Mid-gestational maternal cardiovascular profile in preterm and term pre-eclampsia: a prospective study. BJOG. 2013;120(4):496–504.

[301] Mesens T, Tomsin K, Molenberghs G, Gyselaers W. Reproducibility and repeatability of maternal venous Doppler flow measurements in renal interlobar and hepatic veins. Ultrasound Obstet Gynecol. 2010;36(1):120–1.

[302] Ruginsk SG, Oliveira FR, Margatho LO, Vivas L, Elias LL, Antunes-Rodrigues J. Glucocorticoid modulation of neuronal activity and hormone secretion induced by blood volume expansion. Exp Neurol. 2007;206(2):192–200.

[303] Hendrickson K. Cost-effectiveness of noninvasive hemodynamic monitoring. AACN Clin Issues. 1999;10(3):419–24.

[304] Maack T. Role of atrial natriuretic factor in volume control. Kidney Int. 1996;49(6):1732–7.

[305] Lewis RP, Boudoulas H, Welch TG, Forester WF. Usefulness of systolic time intervals in coronary artery disease. Am J Cardiol. 1976;37(5):787–96.

[306] Thompson B, Drazner MH, Dries DL, Yancy CW. Systolic time ratio by impedance cardiography to distinguish preserved vs impaired left ventricular systolic function in heart failure. Congest Heart Fail. 2008;14(5):261–5.

[307] Hausvater A, Giannone T, Sandoval YH, Doonan RJ, Antonopoulos CN, Matsoukis IL, et al. The association between preeclampsia and arterial stiffness. J Hypertens. 2012;30(1):17–33.

[308] Grill S, Rusterholz C, Zanetti-Dallenbach R, Tercanli S, Holzgreve W, Hahn S, et al. Potential markers of preeclampsia–a review. Reprod Biol Endocrinol. 2009;7:70.

[309] Melchiorre K, Thilaganathan B. Maternal cardiac function in preeclampsia. Curr Opin Obstet Gynecol. 2011;23(6):440–7.

[310] Solanki R, Maitra N. Echocardiographic assessment of cardiovascular hemodynamics in preeclampsia. J Obstet Gynaecol India. 2011;61(5):519–22.

[311] Vasapollo B, Novelli GP, Valensise H. Total vascular resistance and left ventricular morphology as screening tools for complications in pregnancy. Hypertension. 2008;51(4):1020–6.

[312] Tomsin K, Mesens T, Molenberghs G, Gyselaers W. Venous pulse transit time in normal pregnancy and preeclampsia. Reprod Sci. 2012;19(4):431–6.

[313] on High Blood Pressure in Pregnancy NHBPEPWG. Report of the National High Blood Pressure Education Program Working Group on High Blood Pressure in Pregnancy. Am J Obstet Gynecol. 2000;183(1):S1–S22.

[314] Martens E, Doom E, Martens G. SPE-Gewichtscurven. Brussels, Belgium. 2009;.

[315] Hale S, Choate M, Schonberg A, Shapiro R, Badger G, Bernstein IM. Pulse pressure and arterial compliance prior to pregnancy and the development of complicated hypertension during pregnancy. Reprod Sci. 2010;17(9):871–7.

[316] Raymond D, Peterson E. A critical review of early-onset and late-onset preeclampsia. Obstet Gynecol Surv. 2011;66(8):497–506.

[317] Li J, Umar S, Amjedi M, Iorga A, Sharma S, Nadadur RD, et al. New frontiers in heart hypertrophy during pregnancy. Am J Cardiovasc Dis. 2012;2(3):192–207.

[318] Valensise H, Novelli GP, Vasapollo B, Di Ruzza G, Romanini ME, Marchei M, et al. Maternal diastolic dysfunction and left ventricular geometry in gestational hypertension. Hypertension. 2001;37(5):1209–15.

[319] Melchiorre K, Sutherland GR, Watt-Coote I, Liberati M, Thilaganathan B. Severe myocardial impairment and chamber dysfunction in preterm preeclampsia. Hypertens Pregnancy. 2012;31(4):454–71.

[320] Strobl I, Windbichler G, Strasak A, Weiskopf-Schwendinger V, Schweigmann U, Ramoni A, et al. Left ventricular function many years after recovery from pre-eclampsia. BJOG. 2011;118(1):76–83.

[321] Vaschillo EG, Vaschillo B, Buckman JF, Pandina RJ, Bates ME. Measurement of vascular tone and stroke volume baroreflex gain. Psychophysiology. 2012;49(2):193–7.

[322] Naka KK, Tweddel AC, Doshi SN, Goodfellow J, Henderson AH. Flow-mediated changes in pulse wave velocity: a new clinical measure of endothelial function. Eur Heart J. 2006;27(3):302–9.

[323] Smith RP, Argod J, Pepin JL, Levy PA. Pulse transit time: an appraisal of potential clinical applications. Thorax. 1999;54(5):452–7.

[324] Kaihura C, Savvidou MD, Anderson JM, McEniery CM, Nicolaides KH. Maternal arterial stiffness in pregnancies affected by preeclampsia. Am J Physiol Heart Circ Physiol. 2009;297(2):H759–64.

[325] Asghar M, Ahmed K, Shah SS, Siddique MK, Dasgupta P, Khan MS. Renal vein thrombosis. Eur J Vasc Endovasc Surg. 2007;34(2):217–23.

[326] Ozcakar ZB, Yalcinkaya F, Fitoz S, Cipe G, Soygur T, Ozdemir H, et al. Nutcracker syndrome manifesting with severe proteinuria: a challenging scenario in a single-kidney patient. Pediatr Nephrol. 2011;26(6):987–90.

[327] Desai DK, Moodley J, Naidoo DP. Echocardiographic assessment of cardiovascular hemodynamics in normal pregnancy. Obstet Gynecol. 2004;104(1):20–9.

[328] Jia RZ, Liu XM, Wang X, Wu HQ. Relationship between cardiovascular function and fetal growth restriction in women with pre-eclampsia. Int J Gynaecol Obstet. 2010;110(1):61–3.

[329] Sibai BM, Stella CL. Diagnosis and management of atypical preeclampsia-eclampsia. Am J Obstet Gynecol. 2009;200(5):481 e1–7.

[330] Sugerman HJ. Hypothesis: preeclampsia is a venous disease secondary to an increased intra-abdominal pressure. Med Hypotheses. 2011;77(5):841–9.

[331] James MF, Cork RC, Dennett JE. Cardiovascular effects of magnesium sulphate in the baboon. Magnesium. 1987;6(6):314–24.

[332] Coates BJ, Broderick TL, Batia LM, Standley CA. MgSO4 prevents left ventricular dysfunction in an animal model of preeclampsia. Am J Obstet Gynecol. 2006;195(5):1398–403.

[333] Landau R, Scott JA, Smiley RM. Magnesium-induced vasodilation in the dorsal hand vein. BJOG. 2004;111(5):446–51.

[334] Dawes M, Ritter JM. Mg(2+)-induced vasodilation in human forearm vasculature is inhibited by N(G)-monomethyl-L-arginine but not by indometacin. J Vasc Res. 2000;37(4):276–81.

[335] Blyton DM, Sullivan CE, Edwards N. Reduced nocturnal cardiac output associated with preeclampsia is minimized with the use of nocturnal nasal CPAP. Sleep. 2004;27(1):79–84.

[336] Sep SJ, Schreurs MP, Bekkers SC, Kruse AJ, Smits LJ, Peeters LL. Early-pregnancy changes in cardiac diastolic function in women with recurrent pre-eclampsia and in previously pre-eclamptic women without recurrent disease. BJOG. 2011;118(9):1112–9.

[337] Carbillon L. First trimester uterine artery Doppler for the prediction of preeclampsia and foetal growth restriction. J Matern Fetal Neonatal Med. 2011;.

[338] Tomsin K, Staelens A, Mesens T, Molenberghs G, Gyselaers W. Improving reliability of venous Doppler flow measurements: relevance of an additional ECG and training. Submitted. 2013;.

[339] Nisell H, Lunell NO, Linde B. Maternal hemodynamics and impaired fetal growth in pregnancy-induced hypertension. Obstet Gynecol. 1988;71(2):163–6.

[340] Gyselaers W, Peeters L. Physiological implications of arteriovenous anastomoses and venous hemodynamic dysfunction in early gestational uterine circulation: a review. J Matern Fetal Neonatal Med. 2013;.

[341] Brosens JJ, Pijnenborg R, Brosens IA. The myometrial junctional zone spiral arteries in normal and abnormal pregnancies: a review of the literature. Am J Obstet Gynecol. 2002;187(5):1416–23.

[342] Pennington KA, Schlitt JM, Jackson DL, Schulz LC, Schust DJ. Preeclampsia: multiple approaches for a multifactorial disease. Dis Model Mech. 2012;5(1):9–18.

[343] Hall ME, George EM, Granger JP. [The heart during pregnancy]. Rev Esp Cardiol. 2011;64(11):1045–50.

[344] Oben J, Tomsin K, Staelens A, Mesens T, Molenberghs G, Gyselaers W. Maternal cardiovascular profiling in the first trimester of pregnancies destined to develop hypertension or fetal growth retardation. Submitted. 2013;.

[345] Uzan J, Carbonnel M, Piconne O, Asmar R, Ayoubi JM. Pre-eclampsia: pathophysiology, diagnosis, and management. Vasc Health Risk Manag. 2011;7:467–74.

[346] Leeman L, Fontaine P. Hypertensive disorders of pregnancy. Am Fam Physician. 2008;78(1):93–100.

[347] Vatten LJ, Skjaerven R. Is pre-eclampsia more than one disease? BJOG. 2004;111(4):298–302.

List of Figures

List of Tables

List of Abbreviations

Δ V	delta Doppler velocity
2D	two-dimensional
3D	three-dimensional
3D-PDU	three-dimensional power Doppler ultrasonography
ACI	acceleration index
ALAT	alanine aminotransferase
AM	morning
ANP	atrial natriuretic peptide
ASAT	aspartate aminotransferase
B-D mode	brightness-Doppler mode
BMI	body mass index
CI	cardiac index
CO	cardiac output
CPAP	continuous positive airway pressure
DBP	diastolic blood pressure
DT	diastolic time
DTi	diastolic time index
ECG	electrocardiogram
EH	essential hypertension
EPE	early-onset preeclampsia
ETR	ejection time ratio
FGR	fetal growth restriction
fi	flow index
GFR	glomerular filtration rate
GH	gestational hypertension
HELLP	hemolysis elevated liver enzymes and low platelets
HI	Heather index
HPD	heart period duration

hPE	high cardiac output preeclampsia
HR	heart rate
HV	hepatic vein
HVI	hepatic venous impedance index
ICC	intraclass correlation
ICG	impedance cardiography
IQR	interquartile range
IUGR	intra-uterine growth retardation
LDH	lactate dehydrogenase
LGA	large-for-gestational age
LPE	late-onset preeclampsia
lPE	low cardiac output preeclampsia
LVET	left ventricular ejection time
LVETi	left ventricular ejection time index
MAP	mean arterial blood pressure
$MgSO_4$	magnesium sulphate
MnV	minimum Doppler velocity
mPE	medium cardiac output preeclampsia
MxV	maximum Doppler velocity
NICCOMO^{TM}	non-invase continuous cardiac output monitor
NO	nitric oxide
O/C	O/C ratio
OI	orthostatic index
PA	time interval between ECG P-wave and Doppler A-wave
PCC	Pearson's correlation coefficient
PE	preeclampsia
PEP	pre-ejection period
PM	afternoon
PP	pulse pressure
PTT	pulse transit time
PWV	pulse wave velocity
RIV	renal interlobar vein
RIVI	renal interlobar venous impedance index
RR	duration of one cardiac cycle
RV	renal vein
SBP	systolic blood pressure
SEM	standard error of mean
SGA	small-for-gestational age

SI	stroke index
STR	systolic time ratio
SV	stroke volume
TAC	total arterial compliance
TACI	total arterial compliance index
TFC	thoracic fluid content
TFCI	thoracic fluid content index
TPVR	total peripheral vascular resistance
UP	uncomplicated pregnancy
UtArt	uterine artery
vfi	vascularization-flow index
vi	vascularization index
VI	velocity index
VOCAL	virtual organ computer-aided analysis
VPTT	venous pulse transit time
VPAN	venous pre-acceleration nadir
Z	impedance
Z_0	base impedance
ZOL	Ziekenhuis Oost-Limburg, Genk, Belgium

List of Equations

Equation 1.1 (Chapter 1.4) - Kubicek's stroke volume equation

$$SV = \rho \times (\frac{L^2}{Z_0^2}) \times (\frac{dZ}{dt_{max}}) \times \text{LVET in mL}$$

ρ: a constant; L: the distance between the receiving electrodes; dZ/dt_{max}: peak systolic flow.

Equation 1.2 (Chapter 1.4) - Sramek and Bernstein's stroke volume equation

$$SV = \delta \times \frac{(0.17 \times H)^3}{4.25} \times (\frac{dZ}{dt_{max}} / Z_0) \times \text{LVET in mL}$$

δ: patient's weight; H: patient's height.

Equation 2.1 (Chapter 2.1) - venous impedance or arterial resistive index equation

$$\text{RIVI or HVI or arterial resistive index} = \frac{MxV - MnV}{MxV}$$

Equation 3.1 (Chapter 3.3) - cardiac output equation

$$CO = HR \times SV \text{ in L/min}$$

Equation 3.2 (Chapter 3.3) - systolic time ratio equation

$$STR = \frac{PEP}{LVET}$$

Equation 3.3 (Chapter 3.3) - velocity index equation

$$VI = 1000 \times (\frac{dZ}{dt_{max}} /Z_0) \text{ in } 1/1\ 000/\text{s}$$

Equation 3.4 (Chapter 3.3) - acceleration index equation

$$ACI = 100 \times (\frac{d^2Z}{dt^2_{max}} /Z_0) \text{ in } 1/100/\text{s}^2$$

d^2Z/dt^2_{max}: maximum acceleration of blood flow in the aorta.

Equation 3.5 (Chapter 3.3) - Heather index equation

$$HI = \frac{dZ}{dt_{max}}/T_{RC} \text{ in Ohm/s}^2$$

T^{RC}: time needed by the ventricle to reach maximum ejection.

Equation 3.6 (Chapter 3.3) - total arterial compliance equation

$$TAC = \frac{SV}{PP} \text{ in mL/mmHg}$$

Equation 3.7 (Chapter 3.3) - total peripheral vascular resistance equation

$$TPVR = \frac{MAP}{CO} \text{ in mmHg/L/min}$$

Equation 3.8 (Chapter 3.3) - orthostatic index equation

$$OI = \frac{\text{standing value}}{\text{supine value}} \times 100 - 100 \text{ in } \%$$

Equation 4.1 (Chapter 4.3) - arterial pulsatility index equation

$$\text{arterial pulsatility index} = \frac{(MxV - \text{mean velocity})}{MxV}$$

Scientific contributions

The following list of scientific contributions contains work that is part of this dissertation. Specific co-author contributions of Kathleen Tomsin (KT) are described for each publication. Ranking and impact factors are shown as published in the Journal Citation Reports (JCR)® of the corresponding publication year.

Publications

1. Gyselaers Wilfried, Mesens Tinne, **Tomsin Kathleen**, Peeters Louis: Doppler assessment of maternal central venous hemodynamics in uncomplicated pregnancy: a comprehensive review. Facts, views & vision in ObGyn, 1(3):171-181 (**2009**)

   KT assisted in the literature searches and performed the clinical data management of the examples and illustrations presented in this review.

2. Gyselaers Wilfried, Mesens Tinne, **Tomsin Kathleen**, Molenberghs Geert, Peeters Louis: Maternal renal interlobar vein impedance index is higher in early- than in late-onset pre-eclampsia. Ultrasound in Obstetrics and Gynecology, 36(1):69-75 (**2010**) - IF: 3.163 (10 out of 77 in Obstetrics and Gynecology; 3 out of 30 in Acoustics)

   KT created a clinical database and handled the management of the datasets presented in this article.

3. Mesens Tinne, **Tomsin Kathleen**, Molenberghs Geert, Gyselaers Wilfried: Reproducibility and repeatability of maternal venous Doppler flow measurements in renal interlobar and hepatic veins. Ultrasound in Obstetrics and Gynecology, 36(1):120-121 (**2010**) - IF: 3.163 (10 out of 77 in Obstetrics and Gynecology; 3 out of 30 in Acoustics)

   KT managed the datasets and helped in the preparation of this letter to the editor.

4. **Tomsin Kathleen**, Mesens Tinne, Molenberghs Geert, Peeters Louis, Gyselaers Wilfried: Time-interval between maternal electrocardiogram and venous Doppler waves in normal pregnancy and pre-eclampsia: a pilot study. Ultraschall in der Medizin / European Journal of Ultrasound, 33(7):E119-25 (2012). (ePub Oct 11, **2010**) - IF: 3.260 (1 out of 30 in Acoustics)

   KT performed the ultrasonographic analyses, managed the data, interpreted the results, and prepared the manuscript.

5. **Tomsin Kathleen**, Mesens Tinne, Molenberghs Geert, Gyselaers Wilfried: Diurnal and position-induced variability of Impedance Cardiography measurements in healthy subjects. Clinical Physiology and Functional Imaging, 31(2):145-150 (**2011**) - IF: 1.213 (66 out of 79 in Physiology)

   KT performed the ICG-measurements, managed the data, interpreted the results, and prepared the manuscript.

6. Gyselaers Wilfried, Mullens Wilfried, **Tomsin Kathleen**, Mesens Tinne, Peeters Louis: Role of dysfunctional maternal venous hemodynamics in the pathophysiology of pre-eclampsia: a review. Ultrasound in Obstetrics and Gynecology, 38(2):123-129 (**2011**) - IF: 3.007 (11 out of 78 in Obstetrics and Gynecology; 2 out of 30 in Acoustics)

   KT assisted in the literature searches and performed the clinical data management of the examples presented in this review.

7. **Tomsin Kathleen**, Mesens Tinne, Molenberghs Geert, Gyselaers Wilfried: Venous pulse transit time in normal pregnancy and preeclampsia. Reproductive Sciences, 19(4) 431-436 (**2012**) - IF: 2.444 (18 out of 78 in Obstetrics and Gynecology)

   KT performed the ultrasonographic analyses, managed the data, interpreted the results, and prepared the manuscript.

8. **Tomsin Kathleen**, Mesens Tinne, Molenberghs Geert, Gyselaers Wilfried: Impedance cardiography in uncomplicated pregnancy and pre-eclampsia: a reliability study. Journal of Obstetrics and Gynaecology, 32 (7): 630-634 (**2012**) - IF: 0.542 (67 out of 78 in Obstetrics and Gynecology)

   KT performed the ICG-measurements, managed the data, interpreted the results, and prepared the manuscript.

9. Claeskens Jorien, **Tomsin Kathleen**, Molenberghs Geert, Van Holsbeke Caroline, Mesens Tinne, Meylaerts Liesbeth, Gyselaers Wilfried: Validation of 3D power Doppler and VOCAL software in the sonographic assessment of hepatic venous flow. Facts, views & vision in ObGyn, (**2013**). In press.

   KT performed the ultrasonographic examinations.

10. **Tomsin Kathleen**, Mesens Tinne, Molenberghs Geert, Peeters Louis, Gyselaers Wilfried: Characteristics of heart, arteries, and veins in low and high cardiac output preeclampsia. European Journal of Obstetrics & Gynecology and Reproductive Biology, (**2013**). In press. - IF: 1.974 (27 out of 78 in Obstetrics and Gynecology; 18 out of 28 in Reproductive Biology)

    KT performed both the examinations and analyses, managed the data, interpreted the results, and prepared the manuscript.

Submitted publications

1. **Tomsin Kathleen**, Oben Jolien, Staelens Anneleen, Mesens Tinne, Molenberghs Geert, Gyselaers Wilfried: Cardiovascular hemodynamics throughout normal pregnancy and postpartum using impedance cardiography.

    KT performed both the examinations and analyses, managed the data, interpreted the results, and prepared the manuscript.

2. **Tomsin Kathleen**, Vriens Annette, Mesens Tinne, Molenberghs Geert, Gyselaers Wilfried: Non-invasive cardiovascular profiling using combined ECG-Doppler ultrasonography and impedance cardiography: an experimental approach. In revision.

    KT performed both the examinations and analyses, managed the data, interpreted the results, and prepared the manuscript.

3. Gyselaers Wilfried, **Tomsin Kathleen**, Mesens Tinne, Oben Jolien, Staelens Anneleen, Molenberghs Geert: The cardiovascular profile of gestational hypertension and preeclampsia

    KT performed both the examinations and analyses, and managed the data.

4. Oben Jolien & **Tomsin Kathleen**, Staelens Anneleen, Mesens Tinne, Molenberghs Geert, Gyselaers Wilfried: Maternal cardiovascular profiling in the first trimester of pregnancies destined to develop hypertension or fetal growth retardation.

    KT (together with Oben J.) performed both the examinations and analyses, and managed the data.

5. Mesens Tinne, **Tomsin Kathleen**, Molenberghs Geert, Peeters Louis, Gyselaers Wilfried: Maternal venous Doppler impedance index of preeclampsia correlates with birth weight percentile and proteinuria. In revision.

   KT performed both the examinations and analyses, and managed the data.

6. **Tomsin Kathleen** & Staelens Anneleen, Mesens Tinne, Molenberghs Geert, Gyselaers Wilfried: Improving reliability of venous Doppler flow measurements: relevance of an additional ECG and training.

   KT (together with Staelens A.) performed both the ultrasonographic examinations and analyses, managed the data, interpreted the results, and prepared the manuscript.

7. Staelens Anneleen, **Tomsin Kathleen**, Oben Jolien, Mesens, Tinne, Spaanderman Marc, Jacquemyn Yves, Gyselaers Wilfried: Impedance cardiography and invasive procedures for hemodynamics assessment in non-critically ill subjects.

   KT assisted in the literature searches for the preparation of the manuscript.

Presentations

Oral presentations

1. **Tomsin Kathleen**, Mesens Tinne, Molenberghs Geert, Peeters Louis, Gyselaers Wilfried: Time-interval between maternal hepatic vein Doppler and ECG is shorter in pre-eclampsia than in normal third trimester pregnancy. 21^{st} European Congress of Obstetrics and Gynaecology, Antwerp, Belgium, May 5-8 (**2010**)

2. **Tomsin Kathleen**, Mesens Tinne, Oben Jolien, Molenberghs Geert, Peeters Louis, Gyselaers Wilfried: Impedance Cardiography: a straightforward and reliable tool to evaluate differences of cardiac reflex response between normal pregnancy and pre-eclampsia. 18^{th} World Congress of International Society for the Study of Hypertension in Pregnancy, Geneva, Switzerland, July 9-12 (**2012**)

Posters

1. **Tomsin Kathleen**, Mesens Tinne, Molenberghs Geert, Peeters Louis, Gyselaers Wilfried: The time-interval between corresponding characteristics of maternal electrocardiogram and venous Doppler waves is shorter in pre-eclampsia than in normal third trimester pregnancy. 13^{th} Maastricht Medical Students Research Conference, Maastricht, The Netherlands, April 29 (**2009**)

2. **Tomsin Kathleen**, Mesens Tinne, Molenberghs Geert, Peeters Louis, Gyselaers Wilfried: Hepatic vein cardio-venous communication time is longer in late than in early pregnancy. 9^{th} World Congress of Perinatal Medicine, Berlin, Germany, October 24-28 (**2009**)

3. **Tomsin Kathleen**, Mesens Tinne, Molenberghs Geert, Peeters Louis, Gyselaers Wilfried: Organ-specific cardio-venous communication time is gestation-dependent. 9^{th} World Congress of Perinatal Medicine, Berlin, Germany, October 24-28 (**2009**)

4. **Tomsin Kathleen**, Mesens Tinne, Molenberghs Geert, Peeters Louis, Gyselaers Wilfried: Cardio-venous communication time is shorter in pre-eclampsia than in normal third trimester pregnancy. 9^{th} World Congress of Perinatal Medicine, Berlin, Germany, October 24-28 (**2009**)

5. **Tomsin Kathleen**, Mesens Tinne, Molenberghs Geert, Peeters Louis, Gyselaers Wilfried: Hepatic venous wave protraction time is longer in late than in early pregnancy. The life sciences summit - Biomedica, Aachen, Germany, March 17-18 (**2010**)

6. **Tomsin Kathleen**, Mesens Tinne, Molenberghs Geert, Peeters Louis, Gyselaers Wilfried: Venous wave protraction time is shorter in pre-eclampsia than in normal third trimester pregnancy. The life sciences summit - Biomedica, Aachen, Germany, March 17-18 (**2010**)

7. **Tomsin Kathleen**, Mesens Tinne, Molenberghs Geert, Peeters Louis, Gyselaers Wilfried: Time-interval between maternal hepatic vein Doppler and ECG is longer in late than in early pregnancy. 21^{th} European Congress of Obstetrics and Gynaecology, Antwerp, Belgium, May 5-8 (**2010**)

8. **Tomsin Kathleen**, Mesens Tinne, Molenberghs Geert, Gyselaers Wilfried: Orthostatic challenged cardiac contractility in pre-eclampsia, as measured by impedance cardiography. Fetus as a patient, Taormina, Italy, May 26-28 (**2011**)

9. **Tomsin Kathleen**, Mesens Tinne, Molenberghs Geert, Gyselaers Wilfried: Vascular pulse transit time in normal pregnancy and pre-eclampsia: a new parameter for measurement of vascular tone? Fetus as a patient, Taormina, Italy, May 26-28 (**2011**)

10. **Tomsin Kathleen**, Oben Jolien, Mesens Tinne, Molenberghs Geert, Peeters Louis, Gyselaers Wilfried: Cardiac reflex responses measured by impedance cardiography are different between low and high cardiac output pre-eclampsia. 18^{th} World Congress of International Society for the Study of Hypertension in Pregnancy, Geneva, Switzerland, July 9-12 (**2012**)

11. **Tomsin Kathleen**, Oben Jolien, Staelens Anneleen, Molenberghs Geert, Mesens Tinne, Peeters Louis, Gyselaers Wilfried: The influence of maternal position on gestational hemodynamics. 19^{th} World Congress of International Society for the Study of Hypertension in Pregnancy, Tromsø, Norway, June 12-14 (**2013**)

12. Oben Jolien, **Tomsin Kathleen**, Staelens Anneleen, Mesens Tinne, Molenberghs Geert, Gyselaers Wilfried: Maternal cardiovascular profiling in the first trimester of pregnancies complicated with gestation-induced hypertension or fetal growth restriction. 19^{th} World Congress of International Society for the Study of Hypertension in Pregnancy, Tromsø, Norway, June 12-14 (**2013**)

Competitions

1. **Tomsin Kathleen**: Candidate for "Prize of the Academy for Clinical Scientific Research in Medicine (period 2009-2012)". - Title: "The maternal venous system: the ugly duckling of obstetrics?" (**2012**)

Dankwoord

Then he felt quite ashamed, and hid his head under his wing; for he did not know what to do, he was so happy, and yet not at all proud. He had been persecuted and despised for his ugliness, and now he heard them say he was the most beautiful of all the birds. Even the elder-tree bent down its bows into the water before him, and the sun shone warm and bright. Then he rustled his feathers, curved his slender neck, and cried joyfully from the depths of his heart, "I never dreamed of such happiness as this, while I was an ugly duckling."

Toen ik mijn doctoraatsproject startte op de gynaeco in 2009, voelde ik me soms wel het lelijke eendje uit het sprookje van Hans Christian Andersen. Ik hoorde nergens thuis; al waren de dokters zeer vriendelijk, ik zag hen als mijn bazen. Maar nét omdat ik steun en vrijheid kreeg van de dokters om mijn weg te vinden als wetenschapper in hun dienst, hoorde ik ook niet thuis bij de vroedvrouwen en de secretaressen: zij moesten dingen voor mij en de studie doen en vervolgens zagen ze mij dus als één van hun bazen die hen opzadelde met extra werk. En ook al voel ik me uiteindelijk gerespecteerd voor hetgeen ik doe, ik beschouw mezelf nog steeds als een buitenbeentje in deze klinische omgeving. Desalniettemin veranderde dit concept stilaan over de jaren heen, en meer en meer biomedische wetenschappers deden hun intrede in de kliniek: Het Limburg Clinical Research Program werd geboren, en ik was niet meer alleen.

My doctoral Committee

First of all, I would like to thank my jury for this nice opportunity and their time and thoughts on my work: Ivo Lambrichts, DDS PhD (Hasselt University), Emmy Van Kerkhove, MSc PhD (Hasselt University), Veerle Somers, MSc PhD (Hasselt University), Eric de Jonge, MD PhD (ZOL Genk), Jan Nijhuis, MD PhD (Maastricht Medical Center), Christoph Lees, MD MRCOG (Cambridge University Hospitals), and Olivier Morel, MD PhD (Maternité Régionale Universitaire de Nancy).

Dr. Gyselaers, bedankt voor jouw onuitputtelijke geduld en tijd die je voor me hebt genomen de afgelopen jaren. Ik ben jou (en de hele maatschap Verloskunde en Gynaecologie o.l.v. Dr. Willem Ombelet) zeer dankbaar voor het geloven in mijn kunnen en dus het creëren van deze onderzoeksplaats, van onze eigen moestuin als het ware. Bedankt om mij steeds weer iets bij te leren: van de ideale manier om koffie te zetten tot de werking van de veneuze tonnetjes, die meermaals samen tot een eureka moment hebben geleid. Jouw enthousiasme en plezier in wetenschap doen, je lachwekkende vergelijkingen opdat ik het maar zou begrijpen (cfr. de verwarmingsbuizen), waren steeds weer een drijfveer om gemotiveerd en met een glimlach te komen werken: het moet tot slot plezant blijven! Ik ben tevreden en ook terecht fier dat we dit werk samen tot een mooi eind (of is het niet eerder een begin?) hebben gebracht. Wilfried, ik hoop dat je nog vele jaren mag genieten van je favoriete hobby!

Dr. Peeters, bedankt voor de leerrijke begeleiding in het bekomen van dit mooie proefschrift. De eerste keer dat ik je ontmoette werd ik overdonderd door jouw uitgebreide kennis omtrent de zwangerschap: ik begreep er helemaal niets van! Die ervaring heeft me geprikkeld om steeds weer wat bij te leren over deze ingewikkelde, doch interessante, materie. Je hebt me ook veel bijgebracht over het belang van netwerken, en dankzij jou en Wilfried heb ik dan ook heel wat belangrijke figuren in het gebied van de maternale fysiologie mogen ontmoeten. Louis, bedankt voor alle steun en ik hoop dat ik mag blijven van je leren; want al is mijn kennis nu al stukken uitgebreider sinds onze eerste ontmoeting, er valt nog veel te ontdekken over de magie van de zwangerschapsfysiologie.

Onze onderzoeksgroep

Ik voelde me in het begin misschien wel het lelijke eendje, of beter, de vreemde eend in de bijt, maar gelukkig is onze onderzoeksgroep over de jaren heen sterk uitgebouwd.

Tinne en Inge, dankzij jullie voelde ik me niet alleen in het leerproces van de veneuze Dopplers en het (soms wat té trage en frustrerende) publicatie-leven. Ik denk dat we alledrie mogen tevreden zijn over de vooruitgang die we samen als wetenschappers hebben geboekt. Tinne, ook Sicilië was gezellig en hierdoor voelde onze wetenschapsuitstap soms wat meer aan als een welverdiende vakantie. Bedankt voor jullie collegiale vriendschap. Ik wens jullie allebei nog veel succes met jullie verdere carrière, zowel als gynaecologen, als wetenschappers, maar ook als mama's!

Jolien, ik wil je graag bedanken voor de vele manieren waarop je mij hebt doen verbazen. Vooreerst, je was een uitstekende student: je gedrevenheid en leergierigheid tijdens je masterstage waren aanstekelijk, en al snel werden we goede vrienden. Samen naar Genève was voor ons allebei een hele ervaring; het ontmoeten van de grote figuren (soms kleiner dan verwacht) waarvan we allebei zo goed als alles hadden gelezen, was als de kers op de taart van ons jaar hard werken (meer dan 300 screeningen, goed voor zo'n 600 uurtjes werk). Vervolgens werd je bij ons aangesteld als halftijdse wetenschappelijk medewerker, en je verminderde aanwezigheid is niet onopgemerkt aan me voorbijgegaan. Telkens als ik een koffietje ga drinken, blijft de andere helft van mijn suikertje onaangeroerd. Maar toch, bedankt voor de vlotte overname van mijn 3-D echo's, de leuke gesprekken, de vele koffie-momentjes, de nachtelijke McDo uitstappen, de mooie "ugly duckling"-tekening, en de fijne samenwerking. Jolien, alles komt op z'n pootjes terecht, en dus ook jij als wetenschapper!

Anneleen, jouw komst was voor mij een verrassing en het heeft even geduurd om aan je (Antwaarpse) aanwezigheid te wennen: ik moest mijn territorium 'achter de kast' delen met een nieuweling. Maar dat je een zelfstandige werker bent, werd me al snel duidelijk: in minder dan een maand kon ik, zonder vrees, mijn 'eerste kind' bij je achterlaten toen ik voor 4 weekjes naar Nottingham ging. En alsof dat al niet genoeg was, liet ik je weer een maandje aan je lot over terwijl ik in Nancy zat. Na mijn terugkomst besefte ik dat mijn 'eerste kind' opgegroeid was tot een heuse tiener die volop aan het puberen was: de opstartfase van je project liep niet van een leien dakje, maar je hebt dit geweldig aangepakt en je gaat hier zeker en vast de vruchten van plukken. Anneleen, nog veel succes met je carrière!

Geert, ik wil jou oprecht bedanken voor jouw statistisch inzicht en steun doorheen mijn doctoraatsproject. Ik heb erg veel geleerd tijdens onze korte (telefonische) gesprekken - nét als tijdens de hoorcolleges in mijn opleiding - door jouw enthousiaste manier van lesgeven en jouw vele plezante en illustratieve voorbeeldjes. Bedankt voor al je tijd en energie, maar vooral ook voor je interesse in ons onderzoeksproject. Mede dankzij jou is ons lelijk eendje uitgegroeid tot een mooie zwaan.

Ook wil ik alle andere studenten geneeskunde en biomedische wetenschappen die meegewerkt hebben aan dit doctoraatsproject oprecht bedanken, en dit in het bijzonder naar Jorien, Annette, Jolien en Stefan. Jullie bijdrage en inspanningen zijn als kleine stukjes puzzel op hun plaats gevallen. Ik hoop dat jullie weten dat de extra inspanningen die jullie geleverd hebben in jullie vrije tijd sterk geapprecieerd worden door zowel mezelf als de rest van onze onderzoeksgroep.

De vroedvrouwen en secretaressen

Een groot deel van mijn dank gaat uit naar alle vroedvrouwen en secretaressen van onze dienst.

De periode op de echo, toen ik nog rondliep als enige PhD-studente in het ZOL, was een zeer leerrijke en aangename tijd. Jullie leerden mij (misschien soms onbewust) de kneepjes van het vak: afspraken maken in UltraGenda, omgaan met patiënten en dokters, de telefoontjes, de vele elektronische en papieren dossiers, ProGyn, MediWeb, enzovoort. Aan iedereen op de raadpleging, bedankt om mij zo hartelijk te ontvangen.

Liesje, ook al hoor je niet meer bij de gynaeco, voor mij blijf je onlosmakelijk verbonden met mijn tijd in het ZOL: de vele gesprekken (in het dossierkot, de keuken, achter de kast op de echo, op de bloedafname, op de oftalmologie,... Kortom overal waar ik je moest komen zoeken) met een tas koffie, maar soms ook met een doos tissues op de schoot, zitten voor eeuwig in mijn geheugen gegriefd. Veel succes met je vervolgcarrière als diensthoofd op de recovery.

Maar vooral bedankt aan alle vroedvrouwen van de MIC, de VK en de raadpleging, die me dag in dag uit geholpen hebben met de studie: voor het tijdig verwittigen, voor jullie collegiale omgang en jullie respect voor mijn drukke schema, maar ook voor het aanleggen van vele NICCOMO's en voor het transporteren van patiënten, wil ik jullie bedanken. Zonder jullie inzet, jullie harde werk, jullie vertrouwen in de studie en jullie lieve glimlach, had ik dit eindresultaat nooit durven dromen.

De patiënten

Bedankt aan alle studie-patiënten en hun partners voor hun deelname aan de studie en hun vertrouwen in mij en onze dienst. In ieder kind geboren, begint de wereld opnieuw. Geniet samen en maak er het beste van!

De bureau, oftewel de 'visbokaal'

Lieve ZOL-doctorandi, samen doctoreren betekent samen SPSS'en, samen lunchen, samen lachen maar vooral samen ongestoord ons beklag doen over wat er op onze lever, maar ook wel op onze nieren, longen, hart, hersenen en voortplantingsorganen ligt - voor spijsvertering moet je bij het JESSA zijn.

Ingrid, met jou deel ik al het langste de bureau, en voor ons betekent samen doctoreren samen discussiëren over het verschil tussen flow en perfusie met de Boron op de schoot, samen artikels sorteren, kasten opruimen en publicaties schrijven in het weekend, samen roddelblaadjes lezen onder de Andalusische zon, samen ontelbare pogingen wagen om mij te leren balletjes gooien en samen pauzeren wanneer we het echt nog eens nodig hadden. Bedankt Ingrid, je bent een geweldige collega, maar nog meer een geweldige vriendin.

Onze groep groeide exponentieel over de afgelopen twee jaar, maar desalniettemin blijft de sfeer er ten alle tijden in zitten. Enkel het 'vrijdageffect' maakt nu steevast al zijn intrede tegen woensdagnamiddag dankzij het tropische klimaat van onze visbokaal, hetgeen leidt tot hoogstaande conversaties en wetenschappelijke grapjes op maat. Maar bij ons is er niks dat een boksbal, een quizvraag hier of daar, een bureaustoel op wieltjes, iPod-oortjes, magneten, stress-balletjes, een extra computerscherm of twee, een verhoogd pixelgehalte en een SPSS-boek voor dummies niet kan oplossen. Mother Duck bedankt jullie voor de dagelijkse portie steun en toeverlaat. Hopelijk redden jullie het zo zonder mijn connecties met de IT en de technische diensten. Ik ga jullie in ieder geval missen en ik kijk dus ook stiekem uit naar de volgende doctoraatsverdedigingen van het beste feestcomité van het ZOL... Het ga jullie goed!

Mijn vrienden

Patricia, Miriam en Sandra: onze 'dates' staan in mijn top 3 van momenten waar ik het meest naar verlang in drukke tijden zoals deze. Onze ietwat vreemde combinatie bleek meer dan een spontane ingeving te zijn en groeide uit tot een hechte vriendschap die gebaseerd is op wederzijds vertrouwen, een gemeenschappelijke liefde voor lekker eten en drinken, gekenmerkt door spontane afspraakjes om gewoon gezellig bij te

kletsen getint met een goeie portie roddels, kortom een leuk gezelschap vol girlpower! Iets wat elke doctorandus nodig heeft om energie uit te putten als het even tegenzit, maar ook om een glas (of twee, drie) te heffen op de goede momenten (en doelen).

De meisjes van Sweet Chili, de mannen van LaPoire en de Koninklijke Harmonie Concordia voor mijn vrije tijd op te vullen met mijn favoriete inspannende ontspanning, namelijk de muziek. Steven, Roland en Marleen, Rina, Karen, mijn sportmaatjes Veronique en Angy, en alle lieve mensen die ik onderweg heb mogen ontmoeten voor alle fijne momenten waar we lief en leed kunnen delen. De BMW'ers en aanhang voor de traditiegetrouwe kerstdates en etentjes. Dank je wel, allemaal!

Thank you to everyone from Nurture (Nottingham, UK), especially Lukasz for helping me with the Doppler studies and making me laugh a lot for things we always seem to forget. Merci beaucoup à tout le monde de Nancy (France), j'ai rencontré des amis pour la vie: Jie avec la stéréologie (c'était amusant), et Ale, Lyda & Jeka: les "superwomen" de la Sud. Olivier et Cécile, merci beaucoup pour votre accueil chaleureux. I promise I'll visit you all soon!

Mijn familie

Last but not least, wil ik mijn familie bedanken: mijn broers en schoonzussen voor de maandelijkse familie-etentjes en de sporadische spelletjesavonden, mijn oma voor haar goede raad en onuitputtelijke interesse, mijn tantes en nonkels voor hun aanwezigheid op alle belangrijke momenten, mijn grote nichtjes voor de avondjes stappen, en mijn kleine nichtjes en metekindjes voor hun oprechte liefde en vele knuffels wanneer ik ze nodig had. Bij jullie voel ik me altijd thuis en nooit alleen.

Mama en papa, zonder jullie zou ik dit doel nooit hebben bereikt. Bedankt voor alle kansen en mogelijkheden die jullie me altijd hebben gegeven, en blijven geven opdat ik mij onbezorgd kan verder ontplooien op eender welk gebied. Jullie staan op elk moment voor me klaar ongeacht waar of wat ik ook wil, en ik bewonder jullie geduld voor mijn soms wat onbedwingbare energie waarmee ik mijn activiteiten uitvoer. Mijn leergierigheid wordt gevoed door jullie vele schouderklopjes en ik ben blij dat jullie altijd het beste met mij voorhebben. Bedankt voor de tijd die jullie mij geven opdat ik mijn dromen kan blijven waarmaken.

Ik wil dit werk dan ook graag opdragen aan mijn ouders als dank voor hun zorgzaamheid en hun vertrouwen in mij!